II
Interactions dans les structures
Wechselwirkung in Tragwerken
Interaction Problems in Structures

II a
Interaction de matériaux différents
Wechselwirkung zwischen verschiedenen Materialien
Interaction of different Materials

Leere Seite
Blank page
Page vide

Continuous Composite Beams for Bridges

Poutres mixtes continues pour des ponts

Durchlaufende Verbundträger für Brücken

JOHN W. FISHER J. HARTLEY DANIELS ROGER G. SLUTTER
Fritz Engineering Laboratory
Department of Civil Engineering
Lehigh University
Bethlehem, Pennsylvania, USA

1. INTRODUCTION

Composite steel and concrete beams for bridges have been used extensively in the United States for a number of years. The popularity of composite bridge construction led to the adoption in 1944 of general specifications covering this type of construction. Extensive research leading to practical design rules for shear connectors and the introduction of stud shear connectors resulted in the widespread use of composite design in bridges by the end of the 1950's. Today composite construction is used in bridges primarily for medium span overpass structures. A report outlining the present worldwide state of the art is contained in Ref. 1.

Composite design for bridges in the United States has been limited primarily to simple spans or to the positive moment (slab in compression) regions of continuous spans. In the latter case, even though the steel beam and the concrete deck are continuous, connectors are usually omitted from the negative moment (slab in tension) regions over interior supports for basically two reasons: (a) the allowable live load stress range in the top (tension) flange of the steel beam considering fatigue requirements for connectors in this region is substantially reduced(2) and (b) there are presently no simple design rules which consider important factors such as connector strength, influence of slab cracking, optimum reinforcement, effective width and time effects (creep and shrinkage). As a result, most designs ignore any contribution of the slab and reinforcement in the negative moment regions.

Continuous composite designs with discontinuous shear connection are permitted by the 1969 AASHO bridge specifications providing that additional connectors are placed in the vicinity of the dead load inflection points to prevent overstressing of the shear connectors in the positive moment regions. The AASHO specifications therefore provide an interim means of improving designs of this type. There are no provisions which consider the influence of, or control of slab cracking.

A full scale fatigue test of a two-span continuous composite tee beam designed according to the 1969 AASHO specifications and employing discontinuous shear connection did in fact result in fatigue failures in the top layer of longitudinal reinforcement over the interior support at about half the design life based on the fatigue requirements of the connectors.(3) Bridges in service are experiencing deterioration of the slabs over the interior supports due in part to the presence of cracks resulting from shrinkage of the concrete as well as from live load stresses.

The balance of this paper will be devoted to a more detailed discussion of some of the points just raised. Emphasis will be given to the results of recent research at Fritz Engineering Laboratory concerning continuous composite beams for bridges.

2. PRESENT STATUS IN THE UNITED STATES

The basic design criteria and method of proportioning shear connectors for simple span composite bridge members were developed from recent studies at Fritz Engineering Laboratory.(4) These studies suggested that the same criteria are also applicable to the design of shear connectors for continuous composite bridge beams. This was confirmed in a subsequent investigation.(5,6) However, this investigation indicated that for beams in which connectors were omitted from the negative moment regions, overstressing and premature fatigue failures of connectors can occur in the positive moment regions well before the design life of the member has been reached.

On the basis of these findings, the 1969 AASHO Specifications now require that additional anchorage connectors be placed in the vicinity of the dead load inflection points. The purpose of these anchorage connectors is to develop the tension force in the continuous longitudinal slab reinforcement in the negative moment region. The number of connectors required by AASHO is based on both the static and fatigue requirements. To satisfy the fatigue requirements, the range of shear taken by the connectors is computed using the area of longitudinal reinforcement associated with the tee-beam over the interior support and the computed range of stress in the reinforcement due to live loads plus impact.

The value of 10,000 psi suggested by AASHO for the reinforcement in lieu of more accurate computations of stress range was based on the investigation reported in Ref. 6. This permitted a rapid evaluation of the additional shear connectors. In Ref. 6 a two-span continuous composite tee-beam was fatigue tested using a single concentrated pulsating load in each span. The maximum stress range measured in the reinforcement over the center support was about 20,000 psi, which was also equal to the maximum and allowable stress. The probability of attainment of a stress range of this magnitude in an actual bridge was believed to be low and corresponds to the occurrence of a design truck in each of two adjacent spans. It is more likely that the design stress range will correspond to the required number of passages of a single design truck. On this basis the reduced stress range was adopted by AASHO. The number of connectors required is also based on the assumption that the range of shear is uniformly distributed within the group of anchorage connectors.

3. PARAMETERS INFLUENCING BEAM BEHAVIOR IN THE NEGATIVE MOMENT REGION

Based on the research results reported in Refs. 5 and 6 a further analytical and experimental research program was initiated at Fritz Engineering Laboratory. The objective of this research program was to develop a comprehensive design procedure for continuous composite beams. The program had four general objectives which were treated as four phases of study. They were: (I) to evaluate the extent to which connectors can be omitted in the negative moment region; (II) to determine the necessary requirements for longitudinal reinforcement in the negative moment region; (III) evaluation of effective width in the negative moment region; and (IV) to examine the feasibility of utilizing prestressing in the negative moment region to improve slab behavior as well as overall composite beam behavior. Some of the significant results of the first three phases will be discussed in this paper.

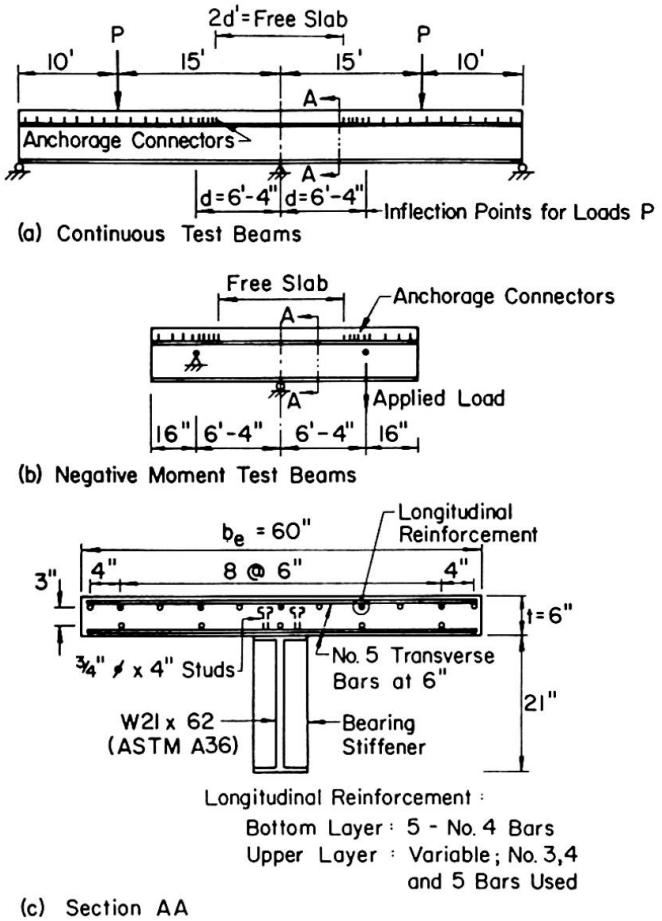

FIGURE 1

In the detailed Investigation of Phases I and II, three parameters were isolated for study and evaluation: (1) Ratio of the length 2d' over which connectors are omitted (called the free slab length) to the length 2d defined by the live load inflection points (Fig. 1a) (2) Reinforcement ratio p, or the ratio of the total area of the longitudinal reinforcement in the negative moment region to the area of the slab cross section ($b_e$xt) expressed in percentage where b_e is the effective width (Fig. 1c) and, (3) Perimeter ratio r, or the ratio of the total perimeter of the longitudinal reinforcement in the negative moment region to the area of the slab cross section.

4. THEORETICAL STUDIES

Two methods of analyses were developed for investigating the continuous composite beams. The first analysis considered the composite beam as a series of one-dimensional discrete elements.(7) Nodal points were assumed at each shear connector location and at intermediate points when connectors were omitted from portions of the negative moment region.

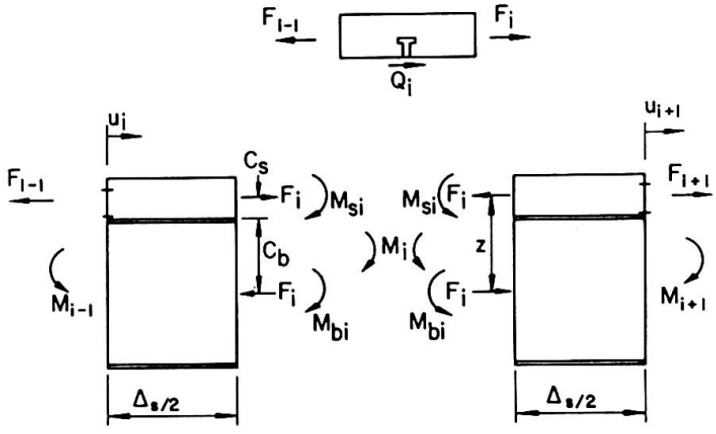

FIGURE 2

The analysis considered both elastic and inelastic behavior of all components; i.e. the steel section, concrete slab, reinforcement, and shear connectors. The analysis provided the distribution of stress resultants at any arbitrary cross section in both the positive and negative moment regions. From the stress resultants on an element such as element i in Fig. 2, equilibrium of the element can be established. Since the elongation of the slab relative to the steel beam is $\int_i(\epsilon_s-\epsilon_b)ds$ and is equal to the slip that occurs in element i, this yields

$$\int_i(\epsilon_s-\epsilon_b)ds = u_{i+1} - u_i \qquad (1)$$

For a linear load-slip relationship, a system of equations in terms of the unknown element forces is therefore obtained as follows:

$$\frac{1}{K} F_{i-1} - \left(\frac{1}{K_i} + \frac{1}{K_{i+1}} + \alpha_i \Delta s_i\right) F_i + \frac{1}{K_{i+1}} F_{i+1} = - M_i \beta_i \Delta s_i \qquad (2)$$

where $\alpha_i = \frac{1}{E_s A_s} + \frac{1}{E_b A_b} + \frac{1}{E_s I_s + E_b I_b}$, $\beta_i = \frac{Z}{E_s I_s + E_b I_b}$

Equation 2 is identical to the simultaneous equations that result from Newmark's differential equation(8) for incomplete interaction when expressed in finite difference form.

An incremental load procedure was used to obtain solutions in the inelastic region of various components. Different stiffnesses were assigned to each element by determining the tangent modulus for the concrete and steel at each increment of load as illustrated in Fig. 3a. Incremental strains and stresses were determined for each load increment and were used to approximate the tangent modulus for successive load increments.

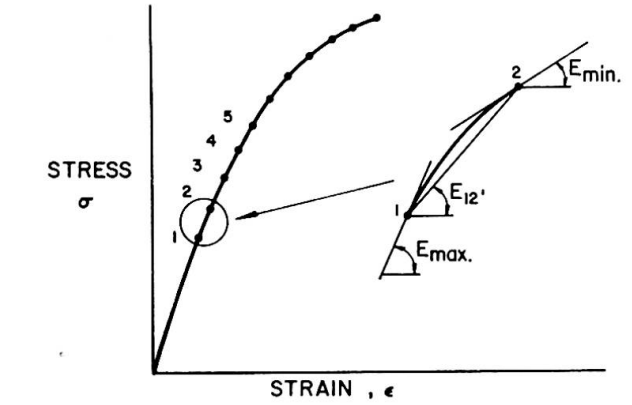

(a) Stress-Strain Relationship of Steel or Concrete

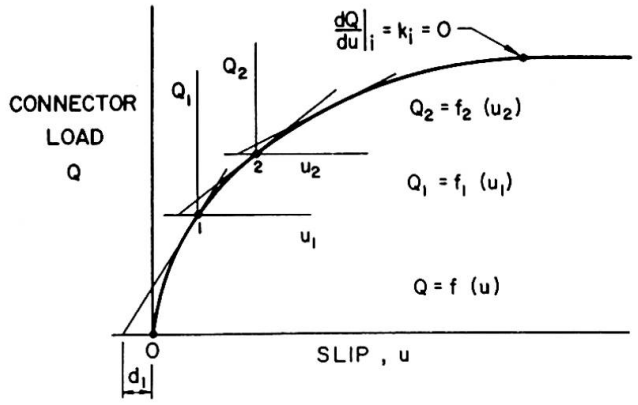

(b) Load-Slip Relationship For Shear Connectors

FIGURE 3

The non-linear load-slip behavior of the connectors was also accounted for by the incremental load method. For the load-slip relationship given in Fig.3b, an incremental connector stiffness K_i can be determined for each point on the curve. The displacement u_i can be expressed as

$$u_i = \frac{Q_i}{K_i} - d_i \qquad (3)$$

This value can be readily incorporated into Eq. 1 and results in a correction$(d_{i+1} - d_i)$ that must be added to the right side of Eq. 2.

To account for the cracked slab that existed in the negative moment region, an equivalent uncracked slab with decreased stiffness was assumed. The magnitude of this stiffness was evaluated by the second analysis.

The second analysis considered the stress resultants in the negative moment region of a continuous beam having a length of free slab.(9) It provided a means of estimating the cracked slab stiffness and was more suited to developing a simplified design procedure for continuous composite tee-beams.

The composite tee beam used in this analysis is shown in Fig. 4a. This beam represents a symmetrical two-span continuous beam with symmetrically placed live loads P equi-distant from the exterior supports. The negative moment region of this beam which contains the free slab is shown in Fig. 4b. The beam in this figure is subjected to a live load shear force Q at the inflection point where Q is a function of P. The corresponding stress resultants at the end of the free slab are shear q,

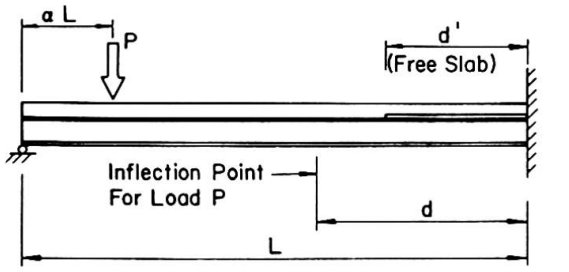

(a) Composite Tee Beam For Second Method of Analysis

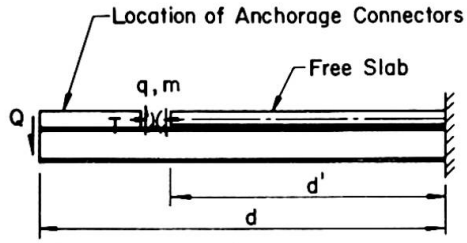

(b) Negative Moment Region

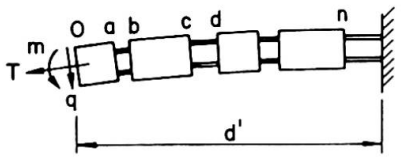

(c) Free Slab

FIGURE 4

moment m, and axial force T as shown in Fig. 4.

A first-order flexibility (force) analysis is used in this analysis and expressions derived relating Q (or P) to q, m and T within three domains defined by location of inflection point which are described by the variable α (Fig. 4) which can vary between 0 and 1. The free slab stress resultants cause random transverse cracking of the free slab. For analysis purposes, the free slab is idealized by a series of uncracked slab elements and reinforcing bar segments of random lengths as shown in Fig. 4c. The flexibility of the free slab therefore is a function of the flexibilities of the slab elements o-a, b-c, etc. and reinforcing segments a-b, c-d, etc.

The axial flexibility of the cracked free slab can be expressed in terms of a coefficient of participation, designated C_1. This coefficient is the ratio of the total length of uncracked slab elements (o-a+b-c+...etc.) to the length d' of the free slab, Fig. 4c. This coefficient is unity for an uncracked slab and zero for a fully cracked slab. The latter case corresponds to the assumption normally used in a simple tie-bar analysis. The evaluation of the coefficient C_1 which is a function of magnitude and position of the load P as well as other factors such as the existence of shrinkage cracks, the length of free slab, the reinforcement and perimeter ratios, and the concrete strength requires experimental evaluation. It is expected that further studies will enable a simple closed form expression for C_1 to be formulated.

5. EXPERIMENTAL STUDIES

The experimental phase of this investigation extended the work reported in Refs. 5 and 6. The purpose was to (1) evaluate the assumptions used in the analyses previously discussed, (2) determine the magnitudes of the several stress resultants in the negative moment region, (3)evaluate the coefficient C_1, and (4) compare actual and predicted behavior. Two two-span tee beams were tested. Details of these beams are shown in Fig. 1a. These beams were similar to the beams reported in Refs. 5 and 6 except for variations in the three parameters previously mentioned.

In addition, six shorter test beams consisting only of the negative moment regions of the two-span beams were tested. Details of these beams are shown in Fig. 1b. Cross-section details for all test beams are shown in Fig.1c. Two of the shorter beams were made identical to the negative moment regions of the continuous beams. The remaining four beams differed in the length of the free slab, the number of anchorage connectors and the reinforcement ratio for the longitudinal bars.

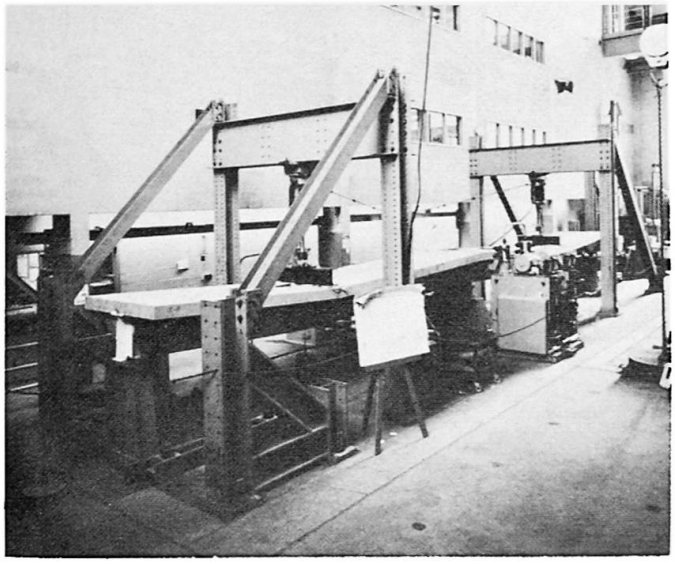

(a) Continuous Beam

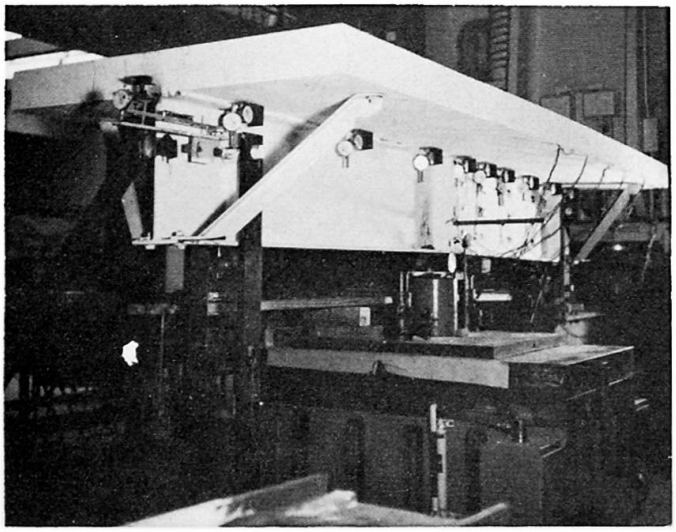

(b) Negative Moment Test

FIGURE 5

The two-span beams were first tested to 2,000,000 cycles of load application that subjected the shear connection to the average allowable values permitted by AASHO for the loading condition. Connectors were also placed so that the nominal tensile stresses in the beam flange would not be critical for fatigue of the base metal adjacent to the connectors. The beams were also tested statically to their maximum load carrying capacity. The shorter beams were also loaded statically to their maximum load. The loads were applied to produce negative bending moment (slab in tension) as shown in Fig. 1b. The beams under test are shown in Fig. 5.

The complete results of this investigation are presented in Refs. 3, 7, 9, 10, 13 and 14. The more significant results will be discussed with emphasis on the parameters affecting the behavior of the negative moment region.

6. INFLUENCE OF REINFORCEMENT AND PERIMETER RATIOS

The cracking behavior of the free slab for the six negative moment test beams is shown schematically in Fig. 6 for the working load level which was defined previously. Also shown are the values of d'/d, p and r used in the investigation and the average measured crack widths. The crack patterns in the negative moment regions of comparable continuous beams are similar. It is apparent that the average observed crack width decreases with an increase in both the reinforcement and perimeter ratios. The greatest reduction, however, was associated with increases in reinforcement ratio. Reinforced concrete research has also established the effectiveness of a larger number of smaller bars in minimizing crack widths.(11)

A rule of thumb often used by designers is that for concrete in tension, the yield strength of the reinforcement should not be less than the cracking strength of the concrete. Applying this rule to the test beams would require a reinforcement ratio of about 1.0 percent. This is based on f'_c = 4,000 psi for the concrete and f_y = 40,000 psi for the reinforcement. The test result showing a sharp reduction in crack width for p = 1.02 support the validity of such a rule. On the basis of this and previous investigations, a minimum reinforcement ratio not less than 1.0 to 1.5 percent is recommended in the negative moment region for

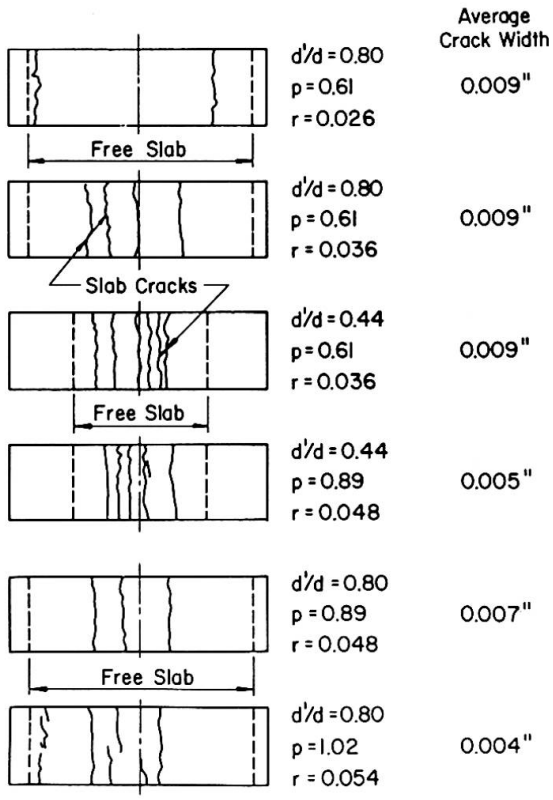

FIGURE 6

effective crack control. A larger proportion (say two-thirds) of this longitudinal reinforcement should be near the top of the slab. It is of interest to note that in the United States the Federal Highway Administration recommends somewhat higher reinforcement ratios for slabs in the negative moment regions of typical continuous concrete T-beam and box girder bridges.(12) The recommended ratios are about 2.5 percent for the T-beam and about 4 percent for the box girder bridges. The respective ratios for top slab reinforcement alone are about 2 percent and 3.5 percent.

7. INFLUENCE OF THE FREE SLAB

In the investigation reported in Ref. 6, the ratio d'/d varied from 0.28 to 1.0. For this investigation, the ratio d'/d was chosen as 0.44 or 0.80 for all test beams. The smaller value corresponds to placing connectors approximately at the point where the allowable stress in the base metal is governed by the AASHO fatigue requirements.(2) The larger value corresponds to placing the required anchorage connectors within the limits specified by AASHO. (All anchorage connectors are assumed to be placed on the negative moment side of the inflection point.) Examination of Fig. 6 shows that the effect of the reduced free slab length is to reduce the average crack widths. These beams also exhibit a larger number of narrower cracks compared with beams with the longer free slabs.

One of the purposes of the experimental phase of the investigation was to evaluate the coefficient of participation of the free slab C_1. The value of C_1 was influenced considerably by the level of axial force T carried by the free slab which is a function of the applied loads P. For loads close to zero, C_1 varied from about 0.80 to 0.90 for all test beams. As the loads increased, the values of C_1 decreased nearly linearly. For most of the beams, C_1 varied from 0.25 to 0.60 when the maximum load carrying capacity was reached. The minimum value of C_1 was 0.25 for all tests. At the assumed working load level, C_1 varied from 0.40 to 0.77 with an average value of 0.60 for those beams with reinforcement ratios of 0.89 and 1.02.

These studies indicate that the behavior of the free slab at working loads can be adequately represented by a tie bar whose length is about 60 percent uncracked concrete and 40 percent reinforcing steel. Such a simplified model can be used to calculate the average stress range in the longitudinal reinforcement. A similar calculation was performed for the continuous test beams. The allowable stress range for the reinforcement in these two beams for 2,000,000 cycles of load application is about 20 ksi.(9) The predicted stress range for the continuous beam with a longitudinal reinforcement ratio of 0.6% and a calculated

value of C_1 equal to 0.59 was approximately 25 ksi. On this basis fatigue failure of reinforcing bars could be expected and was observed at about 1,000,000 cycles. On the other hand, the predicted stress range for the continuous composite beam with a longitudinal reinforcement ratio of 1.02% and a calculated value of C_1 equal to 0.46 was about 17 ksi. No fatigue failures of the reinforcement in this beam occurred prior to reaching 2,000,000 cycles of load application.

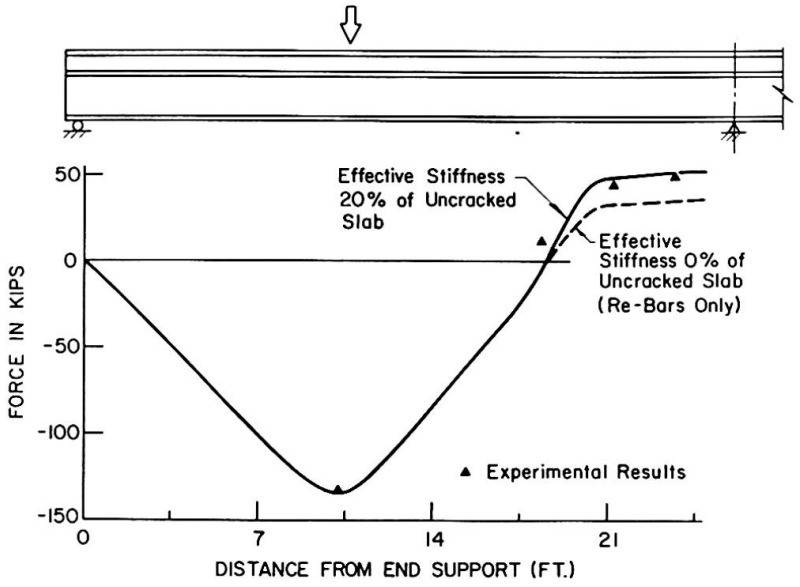

FIGURE 7

The above results were confirmed using the one-dimensional discrete element analysis previously described. A coefficient of participation $C_1 = 0.6$ is equivalent to a free slab with an effective axial stiffness equal to about 20% of the uncracked slab. The discrete element analysis predicted a variation in slab force throughout the length of the two-span composite beam with 1.02% longitudinal reinforcement which is shown in Fig. 7. In the negative moment region two conditions were evaluated. One considered the stiffness of the reinforcement alone (the dashed line) and the second used the effective stiffness. The predicted slab forces are compared with the experimental results and show good agreement when the effective stiffness was considered.

The simplified model mentioned above was used to calculate the stress range in the free slab reinforcement for several typical three span bridges considering the passage of an AASHO HS20-44 truck or equivalent lane loading.(9) Main spans were varied from 50 to 240 ft. and C_1 was varied from 0.4 to 0.8. The reinforcement ratio P was taken equal to 1.0. The resulting stress ranges varied from about 7.8 ksi for the 240 ft. main span with $C_1 = 0.80$, and lane loading to about 6 ksi for the 50 ft. main span with $C_1 = 0.80$ and truck loading. The AASHO stress range provision of 10,000 psi based on test results reported in Ref. 6 for a 25 ft. span thus appears to be conservative for most practical bridge beams when used to proportion anchorage shear connectors.

8. INFLUENCE OF CONNECTOR CONCENTRATION

The influence of the degree to which connectors are concentrated or spread out in the negative moment region on the free slab behavior, and the individual connector behavior, is quite complex. Although additional analytical studies are needed, some tentative comments are possible based on the investigations reported in Refs. 7 and 9. These investigations indicate that as the free slab length decreases, the total shear taken by the anchorage connectors may increase or decrease depending in

part on the reinforcement ratio. A decrease in free slab length tends to increase the axial force carried by the free slab because of the increased stiffness of the negative moment region. However, this results in a greater degree of cracking of the free slab (Fig. 6) which has the effect of reducing the value of C_1. A decrease in C_1 will in turn result in a decrease in the axial force in the free slab.

The predicted distribution of force acting on individual connectors confirmed that connectors adjacent to the free slab were more highly stressed than expected if the concrete slab were neglected altogether. Design procedures must account for this force if satisfactory connector behavior is to be provided.

Investigations also indicate that the assumption of uniform distribution of stress range to connectors within the anchorage connector group is fairly realistic. This appears to result from the redistribution of forces which occur within the connector group during cyclic loading.

9. DESIGN RECOMMENDATIONS

These studies have confirmed the desirability of increasing the amount of longitudinal reinforcing steel in the slab over the negative moment region to at least 1% of the cross-section area of the concrete. It is desirable for most of this reinforcement to be placed near the top surface of the slab. This will assist with controlling the cracking behavior of the negative moment region and provide a more favorable stress state in the longitudinal reinforcement.

The magnitude of slab force was greater than predicted from the steel reinforcement alone when shear connectors were omitted from the negative moment region. The connectors placed near the points of contraflexure and the reinforcement were overloaded. This condition was partially corrected with an increase in the amount of longitudinal reinforcement to 1% of the cross-section area of the concrete.

If it is desired to make a more accurate estimate of the stress f_r in the longitudinal reinforcement, methods for making these estimates have been developed. These studies indicate that the longitudinal slab force can be reasonably approximated from 20% of the uncracked area of the concrete slab in the negative moment region when the percentage of reinforcement is 1%. Alternately, the free slab can be represented by a tie bar whose length is composed of 60% of the uncracked concrete slab and the remaining 40% the longitudinal reinforcement.

The study has confirmed the suitability of other provisions of the AASHO specifications. Applying the same effective width provisions to both the positive and negative moment regions appears reasonable.

10. ACKNOWLEDGMENTS

The research described in this paper was conducted at Fritz Engineering Laboratory, Lehigh University, Bethlehem, Pennsylvania. The Pennsylvania Department of Transportation (PennDOT) and the Federal Highway Administration sponsored this program. The authors are indebted to Y. C. Wu, I. Garcia and F. W. Sarnes who worked as research assistants on this program.

11. REFERENCES

1. McDEVITT, C. F. and VIEST, I. M., - Interaction of Different Materials. Introductory Report, Ninth Congress, International Association of Bridge and Structural Engineering (IABSE), 1971, pp. 55-79

(Prepared for the 9th Congress, May 8-13, 1972).

2. AMERICAN ASSOCIATION OF STATE HIGHWAY OFFICIALS - Standard Specifications for Highway Bridges. AASHO, Tenth Ed., Washington, D.C., 1969.

3. WU, Y. C. and SLUTTER, R. G., - Continuous Composite Beams under Fatigue Loading. Fritz Engineering Laboratory Report No. 359.2, Lehigh University, Bethlehem, Pa., 1971.

4. SLUTTER, R. G. and FISHER, J. W., - Fatigue Strength of Shear Connectors. Highway Research Record No. 147, Highway Research Board, Washington, D.C., 1966.

5. DANIELS, J. H. and FISHER, J. W., - Static Behavior of Continuous Composite Beams. Fritz Engineering Laboratory Report No. 324.2, Lehigh University, Bethlehem, Pa., 1967.

6. DANIELS, J. H. and FISHER, J. W., - Fatigue Behavior of Continuous Composite Beams. Highway Research Record No. 253, Highway Research Board, Washington, D.C., 1968.

7. WU, Y. C., SLUTTER, R. G., and FISHER, J. W., - Analysis of Continuous Composite Beams. Fritz Engineering Laboratory Report No. 359.5, Lehigh University, Bethlehem, Pa., 1971.

8. NEWMARK, N. M., SIESS, C. P. and VIEST, I. M., - Test and Analysis of Composite Beams with Incomplete Interaction, Proc. Society for Experimental Stress Analysis, Vol. 9, No. 1, 1951.

9. GARCIA, I. and DANIELS, J. H., - Negative Moment Behavior of Composite Beams. Fritz Engineering Laboratory Report No. 359.4, Lehigh University, Bethlehem, Pa., 1971.

10. GARCIA, I. and DANIELS, J. H., - Tests of Composite Beams under Negative Moment. Fritz Engineering Laboratory Report No. 359.1, Lehigh University, Bethlehem, Pa. 1971.

11. GERGELY, P. and LUTZ, L. A., - Maximum Crack Width in Reinforced Concrete Flexural Members; Causes, Mechanisms, and Control of Cracking in Concrete. SP-20, American Concrete Institute, ACI, 1968.

12. U. S. DEPARTMENT OF TRANSPORTATION - FEDERAL HIGHWAY ADMINISTRATION - Standard Plans for Highway Bridges. Volume IV, Typical Continuous Bridges, Washington, D.C., 1969.

13. SARNES, F. C. and DANIELS, J. H., - Prestressing the Negative Moment Region of Composite Beams. Fritz Engineering Laboratory Report No. 359.7, Lehigh University, Bethlehem, Pa., 1971.

14. GARCIA, I. and DANIELS, J. H., - Variables Affecting the Negative Moment Behavior of Composite Beams, Fritz Engineering Laboratory Report No. 359.3, Lehigh University, Bethlehem, Pa., 1971.

12. SUMMARY

This paper describes analytical and experimental studies that were undertaken to evaluate the extent to which shear connectors can be

omitted in the negative moment (slab in tension) regions of continuous composite steel-concrete bridge beams. In addition, the necessary requirements for continuous longitudinal reinforcement in the negative moment region was examined.

The major parameters examined include the free slab length (length of negative moment region over which shear connectors are omitted), the area and perimeter of the longitudinal reinforcement, and the influence of connector concentration at the ends of the free slab.

These studies have indicated that satisfactory performance results if the continuous longitudinal reinforcing steel is at least 1 to 1.5% of the cross-section area of the free slab and sufficient anchorage connectors are placed near the points of contraflexure to develop the longitudinal reinforcement.

Leere Seite
Blank page
Page vide

Développement des recherches concernant les constructions mixtes exécutées par le C.R.I.F. à l'Université de Liège

Entwicklung der Forschung über Verbundkonstruktionen am C.R.I.F. der Universität Lüttich

Development in Research Regarding Mixed Structures carried out by the C.R.I.F. at the University of Liège

J. JANSS
Ingénieur
Chef de Travaux au C.R.I.F.
Université de Liège, Belgique

Depuis de nombreuses années, le Centre de Recherches Scientifiques et Techniques de l'Industrie des Fabrications Métalliques (C.R.I.F.) s'intéresse tout particulièrement aux constructions mixtes.

Le présent compte-rendu relate les principaux résultats des recherches exécutées dernièrement par le C.R.I.F. dans les laboratoires de l'Institut du Génie Civil de l'Université de LIEGE (Professeurs BAUS et MASSONNET).

I. LES POUTRES MIXTES ACIER-BETON LEGER

Le béton léger présente un intérêt de plus en plus croissant dans le domaine de la construction en béton grâce à ses propriétés intéressantes de légèreté, d'isolation et à ses qualités mécaniques satisfaisantes.

Dans les constructions mixtes, ce matériau nouveau a également d'importantes possibilités d'avenir et c'est dans l'intention de mieux connaître ce produit mixte que le C.R.I.F. a entrepris quelques essais. Ces essais sont de trois types :

1) essai du type "push-out"
2) et 3) essai statique de courte ou longue durée sur poutre mixte bi-appuyée

A. Le béton léger

Le granulat choisi pour la fabrication du béton léger est l'argile expansée (Argex) utilisée et produite en BELGIQUE. La composition pour 1 m^3 de béton est la suivante :

Argex S 3/16	900 l
Argex S 0/3	250 l
Sable 0/2	200 l
Ciment PHR	400 kg

Ce béton a comme propriétés mécaniques moyennes :

- Résistance à la compression sur cube (20 cm de coté) après 28 jours : 410 kg/cm^2.

- Résistance à la rupture sur prisme (16 x 16 x 50 cm) après 28 jours : 360 kg/cm^2
- Module d'élasticité en compression pour une contrainte de 100 kg/cm^2 : 140000 kg/cm^2
- Poids volumique : 1700 kg/m^3

B. Les essais du type "Push-out"

Les essais du type "push-out" (figure 1) donnent des résultats très satisfaisants concernant le comportement du béton léger au droit des connecteurs.

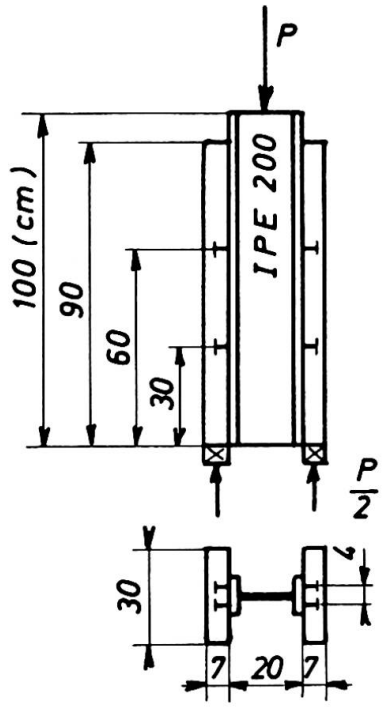

Figure 1

(connecteurs : goujons soudés - h = 50 mm
d = 12,7 mm)

Les formules classiques de dimensionnement ultime des goujons connecteurs adoptées pour le béton à granulats normaux donnent des résultats similaires dans le cas du béton léger.

Ces formules ont pour expression :

$$Q_u = 80\, d^2 \sqrt{R'_{br}} \quad \text{si} \quad \frac{h}{d} \geq 4{,}2$$

$$Q_u = 20\, hd \sqrt{R'_{br}} \quad \text{si} \quad \frac{h}{d} < 4{,}2$$

avec Q_u, l'effort rasant par goujon connecteur provoquant un glissement résiduel permanent égal à 0,08 mm

R'_{br}, la résistance à la compression du béton sur cube

h et d, respectivement la hauteur et le diamètre du goujon connecteur

C. Essai statique de courte durée sur poutre bi-appuyée

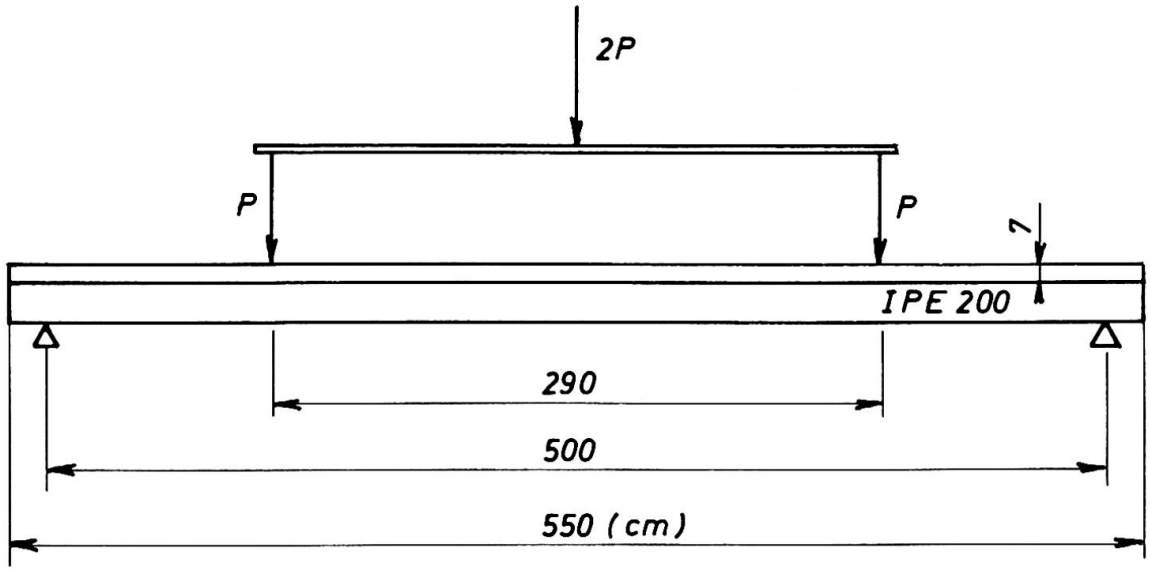

Figure 2

Les essais de flexion de courte durée (figure 2) montrent que les poutres mixtes avec béton léger ont un comportement comparable à celui des poutres mixtes avec béton à granulats normaux :

- la loi de HOOKE reste valable dans un domaine suffisant ;
- le dimensionnement dans le domaine élastique peut s'effectuer à partir de la valeur du coefficient d'équivalence m égal au rapport des modules d'élasticité de l'acier et du béton léger ;
- le calcul au stade ultime des poutres mixtes fléchies s'effectue d'une manière simple en envisageant l'état plastique complet des deux matériaux acier et béton léger à l'exclusion du béton tendu (tableau I)

TABLEAU I

COMPARAISON DES CHARGES ULTIMES MESUREES ET CALCULEES DE POUTRES MIXTES AVEC BETON LEGER

Type de poutre	Numéro de la poutre	Charge ultime calculée P_u (kg)	Charge ultime mesurée P_r (kg)	$\frac{P_r}{P_u}$
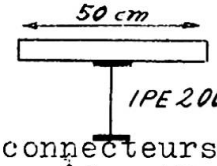 connecteurs: idem IB	1	9135	9500	1,040
	2	9219	9690	1,051
	3	9352	9440	1,009
	4	9225	9642	1,045

D. Essai statique de longue durée sur poutre bi-appuyée

Les essais de longue durée sont exécutés dans des dispositifs semblables à celui schématisé à la figure 2 et situés dans une salle thermostatique (20° C et 60 % d'humidité relative). Les charges P sont maintenues constantes grâce à un dispositif spécial (1). Les mesures des déformations et des flèches additionnelles dues au fluage du béton léger ont permis de déterminer la valeur du coefficient de fluage ψ après 18 mois de mise en charge. Ces valeurs sont comprises entre 3,2 et 5 soit de 30 à 60 % supérieures aux valeurs de ψ proposées pour les poutres mixtes avec béton à agrégats normaux utilisées dans les mêmes conditions.

II. REDUCTION DU NOMBRE DE CONNECTEURS PAR L'EMPLOI DE TOLE A ADHERENCE RENFORCEE

Lors du calcul de l'exécution des poutres mixtes, une attention toute particulière est donnée à la liaison acier-béton. Lorsque la dalle est bétonnée sur la semelle des poutrelles en acier, l'adhérence naturelle entre l'acier et le béton n'est pas prise en considération. En effet, cette liaison peut être diminuée ou même annulée par différents facteurs tels que retrait, chocs, sollicitations dynamiques, différence de température, etc... Dès lors, la totalité de l'effort rasant existant à la liaison acier-béton doit être reprise par des connecteurs. Toutefois, le prix des connecteurs représente un pourcentage important du coût de fabrication que l'on souhaite réduire.

Les quelques essais qui sont effectués ont pour but de déterminer jusqu'à quel point il est possible de réduire le nombre de connecteurs en ayant recours à des surfaces de contact acier-béton à plus haute adhérence, par analogie aux barres à béton à adhérence renforcée.

Des essais statiques du type "push-out" (figure 1) sont exécutés sur des poutres mixtes dont le profil métallique (analogue à l'IPE 200) est composé par soudure ; les semelles de contact acier-béton sont des tôles striées classiques (stries en losange, hauteur et largeur de la strie : 2 et 6 mm) et la liaison est assurée par deux goujons connecteurs soudés sur chaque semelle (h = 50 mm, d = 12,7 mm).

Lors des essais, on a mesuré le glissement relatif entre l'acier et le béton à leur jonction en fonction de l'effort extérieur appliqué ainsi que le glissement résiduel pour le même effort. Pour chaque essai, on a relevé l'effort provoquant un glissement résiduel conventionnel de 0,08 mm.

Au tableau II, on peut comparer cet effort à l'effort rasant provoquant le même glissement résiduel dans le cas de poutres avec semelles lisses et calculé à partir des formules classiques ($Q_u = 20\ hd\ \sqrt{R'_{br}}$ - voir paragraphe I-B)

TABLEAU II

COMPARAISON DES EFFORTS RASANTS PROVOQUANT UN GLISSEMENT RESIDUEL DE 0,08 mm

Numéro de l'essai	Effort en kg provoquant un glissement résiduel de 0,08 mm		$\frac{Q_r}{Q_c}$
	Effort mesuré Q_r semelles striées	Effort calculé Q_c semelles lisses	
1	20.800	9.260	2,25
2	21.600	10.525	2,05
3	18.700	9.040	2,07
4	18.800	10.185	1,85
5	23.000	8.860	2,60
6	21.600	9.220	2,34
7	18.000	8.320	2,15
8	17.600	8.470	2,08

Pour les huit essais, le rapport de ces deux valeurs est compris entre 1,85 et 2,60 avec une valeur moyenne égale à 2,17.

A la figure 3, on peut voir l'évolution des glissement résiduels à la liaison acier-béton pour la pièce d'essai 3 ainsi que la courbe de glissements résiduels obtenue à partir d'un essai du même type avec une poutre à semelles lisses et un béton de même qualité.

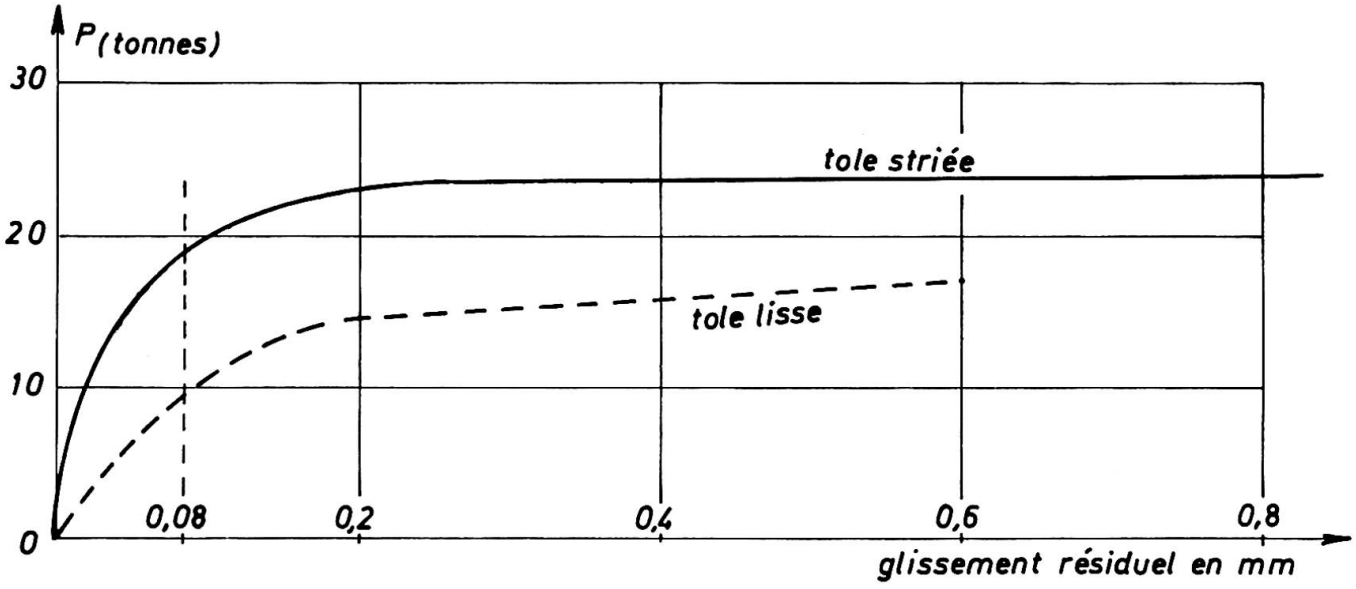

Figure 3

Ces premiers résultats sont très intéressants et semblent indiquer que l'emploi de semelles de contact acier-béton en tôle à adhérence renforcée permet de diminuer de moitié le nombre de connecteurs.

Des essais de contrôle sur poutres ainsi que quelques essais dynamiques sont encore nécessaires pour confirmer cette intéressante constatation.

Si, comme il est à prévoir, ces derniers essais sont concluants, il y aura lieu, dans la phase suivante, de chercher la meilleure forme de stries et même d'examiner la possibilité de laminage de poutres en double té (éventuellement dissymétrique) dont une semelle présenterait une face striée.

III. LE COMPORTEMENT AU FLAMBEMENT DE COLONNES CONSTITUEES DE TUBES EN ACIER REMPLIS DE BETON

L'étude théorique de ces colonnes est basée d'une part sur le comportement de l'acier soumis à un état de contrainte mono- ou biaxial, et d'autre part, sur le comportement du béton soumis à un état de contrainte mono- ou triaxial.

Pour définir le comportement de l'acier soumis à un état de contrainte monoaxial, on se base sur la courbe de flambement ($\bar{N}$, $\bar{\lambda}$) adoptée pour les tubes par la Convention Européenne de la Construction Métallique (C.E.C.M.) (2). Le critère de plastification de VON MISES est utilisé pour étudier le comportement de l'acier soumis à un état de contrainte biaxial.

La courbe contrainte-déformation du béton dans l'état de contrainte monoaxial est représentée par la relation

$$\frac{\sigma}{\sigma_m} = \frac{\varepsilon}{\varepsilon_m}\left(2 - \frac{\varepsilon}{\varepsilon_m}\right)$$

le sommet de la courbe ayant comme coordonnées (σ_m, ε_m) et σ_m étant la résistance à la compression sur cylindre du béton. Enfin, en ce qui concerne le béton soumis à un état de contrainte triaxial, on a adopté le critère suivant tiré d'une étude importante relative aux états de contraintes du béton (3)

$$(\sigma_{b,1} - \sigma_{b,r})^2 - R_c\,(\sigma_{b,1} + 2\sigma_{b,r}) = 0$$

avec $\sigma_{b,1}$ et $\sigma_{b,r}$ respectivement la contrainte longitudinale et radiale du béton et R_c la contrainte de rupture du béton en compression.

Pour les colonnes élancées dont le rapport $\frac{l}{d}$ de la longueur au diamètre est supérieur à 15, la détermination des charges ultimes est basée sur l'état de contrainte monoaxial de l'acier et du béton. Pour des valeurs de $\frac{l}{d}$ inférieures à 15 - ce qui est fréquent - l'effet du frettage se fait sentir et il y a lieu de prendre en considération l'état de contrainte triaxial du béton et biaxial de l'acier.

Les hypothèses générales formulées lors de l'étude théorique sont les suivantes :

1. le tube d'acier et le noyau de béton sont homogènes et isotropes ;
2. il y a interaction intégrale longitudinale entre l'acier et le béton ;
3. il y a interaction intégrale circonférencielle entre le tube et le noyau à partir du moment où la dilatation latérale du béton atteint celle de l'acier ;

4. la courbe contrainte-déformation du béton est identique en compression simple et en flexion, le béton ne possède aucune résistance en traction ;
5. les contraintes circonférencielles sont constantes sur l'épaisseur de la paroi d'acier.

L'effet des excentricités des charges est pris en considération par l'emploi de la formule d'interaction

$$\frac{P}{P_u} + \frac{M}{M_u} = 1 \qquad (3)$$

L'étude théorique (4) prédit d'une manière précise le comportement à la ruine de colonnes tubulaires remplies de béton chargées centriquement ou non, quel que soit leur élancement. La confrontation de la théorie avec les résultats expérimentaux est très satisfaisante ; la valeur moyenne, pour 23 essais sur tubes circulaires de diamètre maximal égal à 220 mm, du rapport de la charge ultime mesurée à la charge ultime calculée, est égale à 0,979 avec un écart standard de 0,054.

Afin de faciliter au maximum le calcul de ce type de colonne, qui normalement se fait par itération à l'aide d'une calculatrice électronique, on a établi à l'aide d'une table traçante, quelques abaques non dimensionnels (figure 4) permettant de déterminer avec

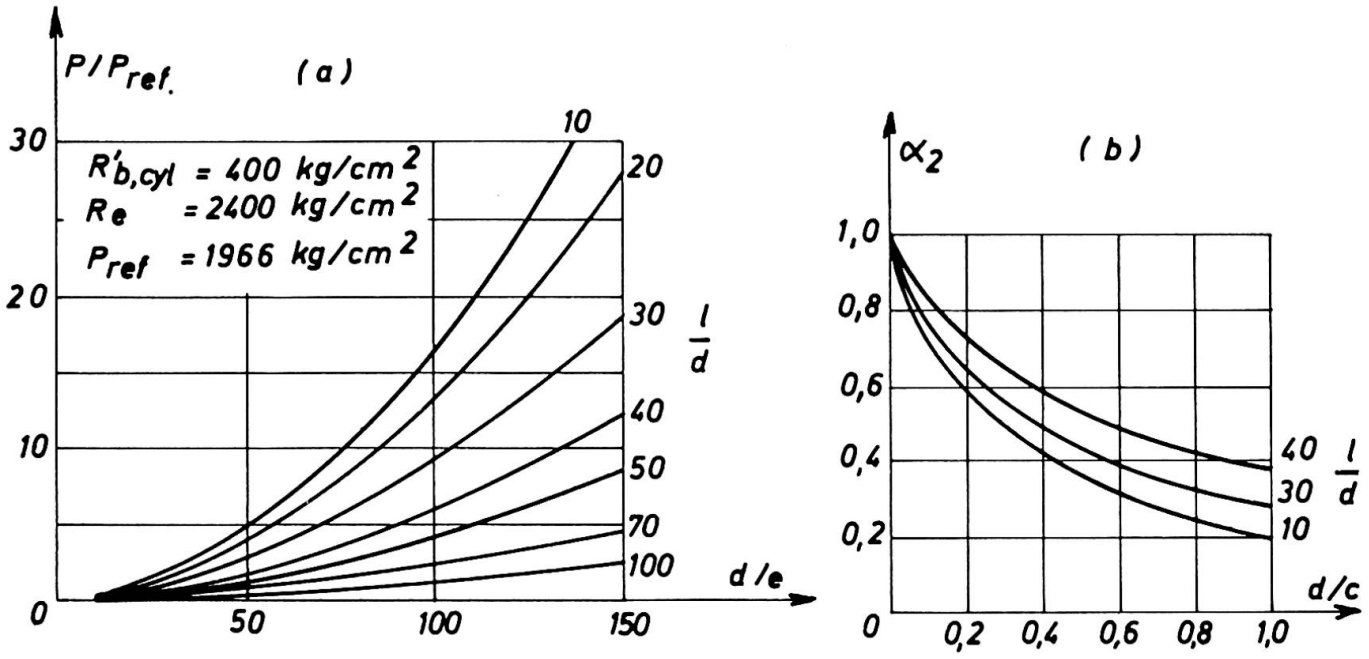

Figure 4

une très bonne précision, la charge ultime des colonnes quels que soient les élancements, les caractéristiques mécaniques ou géométriques de l'acier et du béton et les excentricités des charges (c).

Pour des valeurs données des caractéristiques mécaniques, du diamètre (d) et de l'épaisseur (e) du tube, on lit sur l'abaque du type (a) : $P/P_{réf}$

- Si la charge est centrée $P_{ult} = P_{réf} \times \frac{P}{P_{réf}} \times e^2$
- Si la charge a une excentricité (c) l'abaque (b) donne α et

$$P_{ult} = P_{réf} \times \frac{P}{P_{réf}} \times e^2 \times \alpha$$

BIBLIOGRAPHIE

(1) J. JANSS, G. VIATOUR
Mesures des propriétés globales des poutres mixtes fléchies
Publication MT-31 - novembre 1967 - CRIF (FABRIMETAL BRUXELLES)

(2) H. BEER, G. SCHULTZ
Bases nouvelles des courbes de flambement
Construction Métallique n° 3 - 1970

(3) TADEUSZ, GODYCKI et CWIRKO
Scinanie w Zelbecie
Arkady Warscawa 1969

(4) F. CAMPUS, Ch. MASSONNET
Comptes rendus de recherches
IRSIA - avril 1956

(5) P. GUIAUX, J. JANSS
Comportement au flambement de colonnes constituées de tubes en acier remplis de béton
Publication MT-65 - novembre 1970 - CRIF (FABRIMETAL BRUXELLES)

RESUME

Cette communication relate les principaux résultats des récents essais sur éléments mixtes exécutés par le C.R.I.F. à l'Université de LIEGE.

- essais statiques de courte ou longue durée sur poutres mixtes avec béton léger
- diminution sensible du nombre de connecteurs à la liaison acier-béton par l'emploi de tôle à adhérence renforcée
- établissement d'abaques simples permettant le calcul rapide de la charge ultime des colonnes tubulaires en acier remplies de béton quelles que soient les caractéristiques géométriques ou mécaniques.

Semi-Rigid Joints in Composite Frames

Joints semi-rigides dans les constructions en portique composées

Halbstarre Verbindungen in Verbund-Rahmen

R.P. JOHNSON
University of Warwick, Coventry, England

M. HOPE-GILL
University of Cambridge, England

Introduction

When composite beams are used in buildings, they often form part of a framed structure, the behaviour of which is influenced by the detailing of the beam-column joints. In no-sway frames, beam-column interaction can safely be neglected in the design of beams, if these are assumed to be simply-supported; but the corresponding assumption that loads are transferred to the columns at small eccentricities may be unsafe for column design, if floor slabs are continuous or if beam-column joints have appreciable rigidity. The column moments are likely to be under-estimated, particularly when the beams have unequal spans or loadings. Experience has shown that premature failure of columns designed by the existing 'simple' method does not occur in non-composite frames; but its implications for the design of columns in composite frames and at lower load factors remain unexplored.

Extensive research on composite beams continuous over simple supports[1,2] has shown that simple plastic theory gives reliable values for moments of resistance in both positive and negative bending and for the collapse load of a continuous beam, provided that premature buckling is avoided and that secondary failures are prevented by correct detailing.

The behaviour of individual lengths of composite columns has also received much attention, and a design method is available[3]. But little work on beam-column interaction in rigid jointed frames has been reported, apart from a study of the transfer of wind moments in sway frames from composite beams to steel columns[4].

Possible design methods for composite frames are now discussed. It is shown that neither 'simple' nor 'rigid' beam-column joints are ideal. An account is given of tests on a new type of semi-rigid joint, first proposed by Barnard[5], which combines some of the best features of the other types of joint.

Design of composite frames

We consider a no-sway multi-storey frame with uncased beams, composite for positive moments, and steel or composite columns. It is assumed that design is

governed by the limit states of Collapse and Unserviceability. Ultimate-strength analysis is appropriate at the Collapse limit state. Local damage or vibration may have to be considered at the Unserviceability limit state, but the usual design criterion is excessive deflection. Yield of steel at service loads need not be avoided for its own sake; it has long been accepted in joints and in light crack-control reinforcement in slabs.

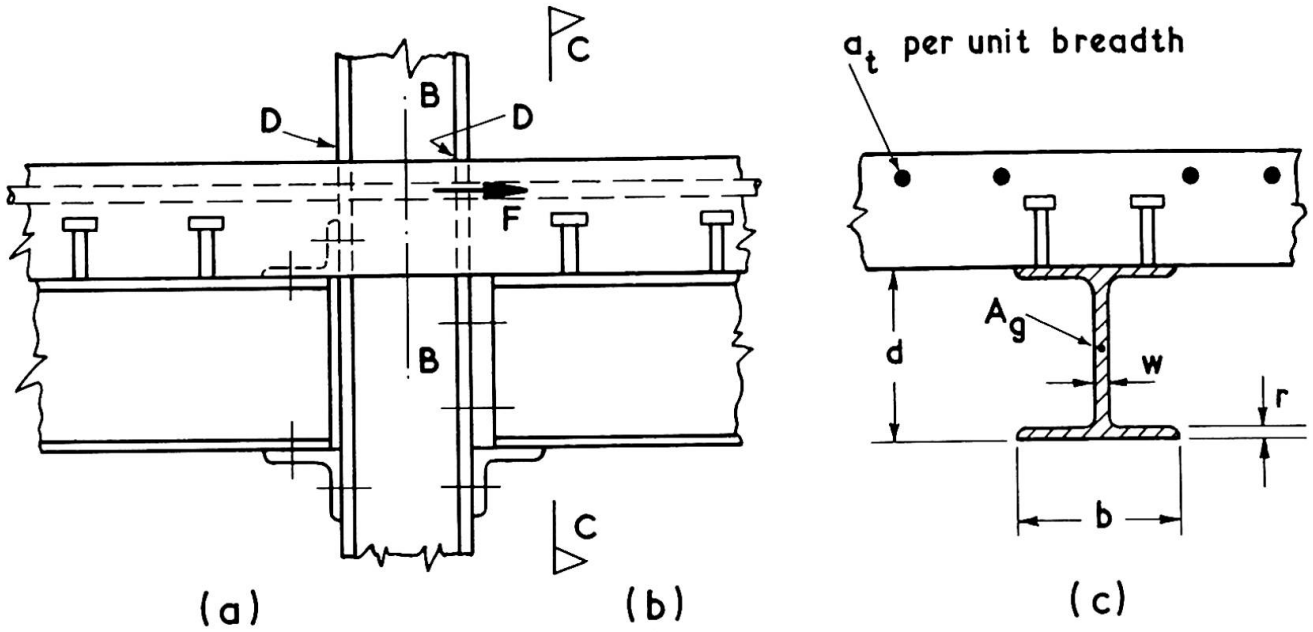

Fig. 1 Typical bolted joints between composite beam and steel stanchion

'Simple' design. This implies discontinuity of slope between two beams supported on an internal column, and that the moment transferred to the column is small, even when the beams are at flexural failure. If conventional black-bolted joints of the type shown in Figs. 1(a) and (b) are used, then bolt slip and deformation of the thin angles in (a) or end plate in (b) will ensure that end moments are small, provided that the concrete slab is jointed or unreinforced across line B-B. 'Simple' design of columns by the established methods is then acceptable.

However, if a two-way floor system is used, reinforcement crossing B-B is essential, as this is the plane of maximum longitudinal shear in a beam framing into the minor axis of the column. Even in a one-way system, crack-control reinforcement (dashed line in Fig. 1) is often preferable to a joint in the slab.

The beams, being designed as simply-supported, have shear connectors throughout their length. The crack-control reinforcement over a certain breadth of slab therefore acts compositely with the joist. If F (Fig. 1) is the resultant tensile force in the slab at the collapse limit state, the effective breadth B_e may be defined by

$$F = a_t B_e f_r \qquad (1)$$

where a_t is the area of reinforcement per unit width of slab, and f_r is its yield stress. The force F depends on the balance between several conflicting factors. It is increased by strain-hardening in the highly-strained reinforcement adjacent to the column, and by tensile stress in any uncracked concrete. It is reduced by loss of interaction due to slip at the shear connectors, and also by shear lag in the plane of the slab. The bending moment that can be transferred to the column is also difficult to predict. When both beams are at flexural failure, cracking of the slab will ensure that little, if any, of the force F is transferred to the column by compression on the faces D (Fig. 1). But the 'worst case' for the column is likely to be when one of the beams is unloaded. The force F will be balanced by an equal compressive force in the bottom flange of the loaded beam, giving a bending moment Fkd (Fig. 2), a large proportion of which may be resisted by the column, particularly if the beams are of unequal depth.

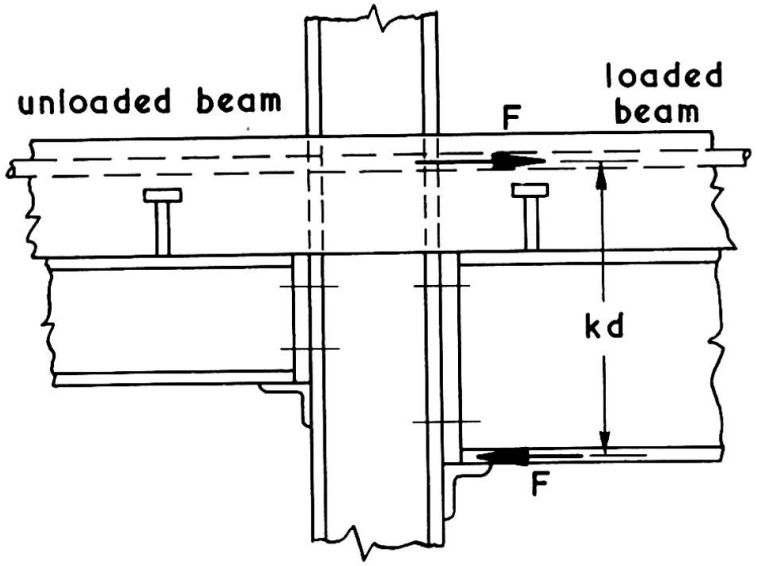

Fig. 2 Beams of unequal depth

If B_e in Eq. (1) is taken as equal to the effective breadth at midspan of the beam in question, it is found that in composite beams having relatively thick slabs, the moment Fkd could be as great as the plastic moment of resistance of the steel joist. It is obviously uneconomic to proportion all columns to resist moments of this magnitude, and yet to take no account of them in designing the beams. A possible solution is to limit the stiffness of the beam-column joints that may be used and the amount of crack-control reinforcement that may be placed in the slab, when 'simple' design is used for the beams, and to take account of these limits when specifying the eccentricities at which the load is assumed to be applied to the columns.

'Rigid' design. Another alternative is to make beam-column joints rigid, by welding or friction-grip bolting, to design the beams as continuous, using simple plastic theory, and to determine the moments in columns by analysis of a limited

frame, as recommended in a recent report (6) on the design of steel frames. This method only works well at the collapse limit state for beams having joists of compact cross-section, and may not give the most economical structure, as rigid joints are expensive, both in materials and in labour.

There is also a problem at the unserviceability limit state. The positive moment of resistance of a symmetrical I-section composite with a concrete slab is much greater than that of the joist alone. Thus the distribution of strength in a fixed-ended beam under uniform load (taken as a simple example) differs greatly from the distribution of moments at working load given by elastic analysis, even if allowance is made for the reduction of flexural rigidity due to cracking of the slab (Fig. 3). When this is not done (as is likely in practice), the disparity is worse. Thus if the present British limit of $0.9f_y$ for working-load stress in steel in composite beams is applied to continuous beams of uniform section, it will almost always govern design, and make it impossible to take full advantage of the large positive moment of resistance available at midspan. The problem is partly apparent, due to neglect in the elastic analysis of the redistribution of moment due to cracking of concrete, and partly real, for more accurate analysis of a particular composite frame showed (7) that yield would indeed occur at working load in regions of negative moment. This increases deflexions by an amount that is difficult to calculate, and should be avoided in practice for this reason.

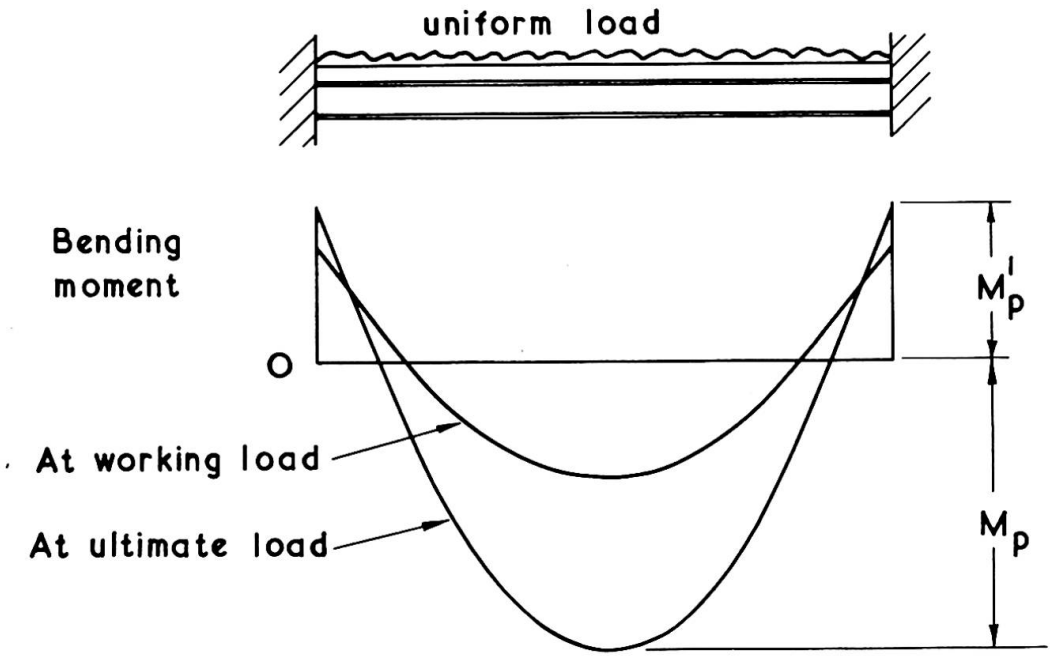

Fig. 3 Bending-moment distributions in a fixed-ended beam

The problem arises from the disparity between M_p and M'_p (Fig. 3) and can be mitigated, if not solved, by placing more top longitudinal reinforcement in the slab, and so increasing M'_p . But there is a limit to this process. At flexural failure, the joist must resist at cross-section C-C (Fig. 1b) a net compressive force F in addition to the vertical shear, and undergo without loss of strength

through buckling sufficient rotation to develop the midspan hinge moment. But the limiting web depth-thickness ratio of joists having adequate rotation capacity for this purpose falls as F increases (8), so that this design method is attractive only for the more compact rolled sections.

Semi-rigid joints

It has been shown that 'simple' design may be uneconomical because no use can be made in the beams of the end moments that may be developed by composite action of slab reinforcement in the negative moment region. If rigid joints are used, negative moment regions have inadequate rotation capacity unless joist cross-sections are compact, and reach yield at a load which is too low a proportion of the plastic collapse load for the beam as a whole. In brief, 'simple' joints are too unpredictable; 'rigid' joints are often too stiff in relation to their strength, and are expensive.

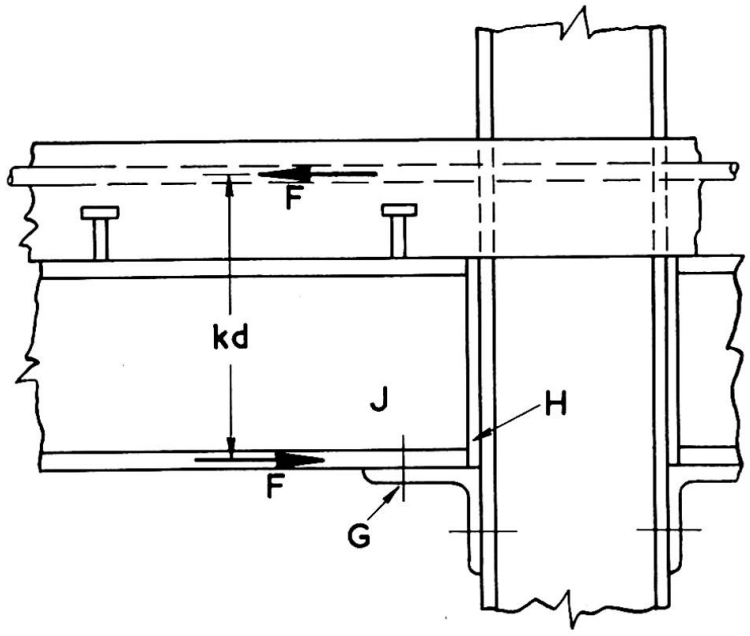

Fig. 4 A semi-rigid joint

Thus there is a need for a semi-rigid joint with a large rotation capacity and a predictable flexural strength, that does not require site welding or accurate fitting. These requirements are met by the joint shown in Fig. 4. It differs from that of Fig. 1(a) in three ways:

(i) The reinforcement A_t is heavier than the minimum required for crack control, and is placed close to the column, so that the force F may be taken as $A_t f_r$.

(ii) Friction-grip bolts are used in the joint at G, which has an ultimate strength in longitudinal compression not less than $A_t f_r$.

(iii) The beam is designed as continuous, using simple plastic theory, with M_p' taken as $A_t f_r kd$. Shear connectors are provided to transfer the force F from the

slab to the joist, using a method (9) derived from research on negative moment regions.

Research on such joints at Cambridge University began in 1969. The success of the first test led to a more comprehensive study, and four more specimens have been tested. In order to expose any limitations of the joint, web cleats and top brackets were omitted, even though they may be provided in practice, and quite large forces F were used. A non-dimensional measure of F is the Force Ratio, Φ , given by

$$\Phi = A_t f_r / A_g f_y \qquad (2)$$

where A_g and f_y refer to the whole cross-section of the rolled steel section. So far, force ratios from 0.16 to 0.44 have been used.

The suitability of a joint for plastic design is best indicated by its moment-rotation (M-θ) curve. The available rotation at maximum moment must be sufficient for a midspan hinge to develop when the specimen forms part of a continuous beam. Cost may be reduced if the design does not require a tight fit between joist and column at H (Fig. 4). Any slip of the bolts at C closes the gap at H and increases the rotation capacity of the joint; so the ultimate-strength behaviour may be improved if there is a gap.

The joint at G must be designed not to slip at working load. This may be done by using black bolts at G and packing at H, or friction-grip bolts at G. In the present work, friction-grip bolts were used, and a gap was left at H so that the load at bolt slip could be determined. At the larger forces F, the joint detail becomes clumsy if the bolts are loaded in single shear, so the double-angle detail shown in Fig. 5 was evolved. This and the use of a web stiffener in the column eliminates local bending of the column flange at this point. The relatively long angles required in a joint of this type help to stabilize the bottom flange of the joist. Moment gradient is so high in this region that the help is significant.

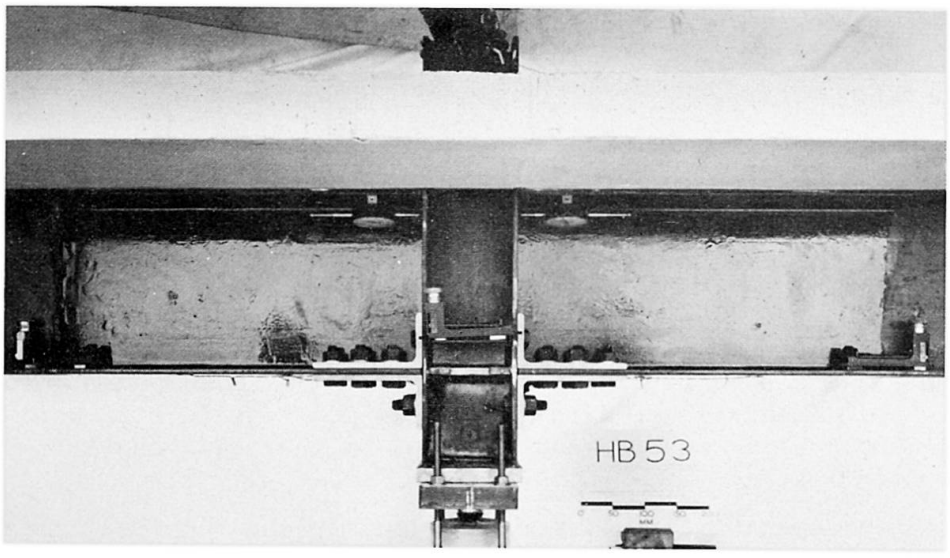

Fig. 5 The joint in specimen HB 53

The bolts through the column flange are designed for the whole of the vertical shear in the usual way. Friction-grip bolts were used in the test specimens, but black bolts should be equally suitable.

The results of the tests

The test specimens were numbered HB 50 to 54. Each consisted of a stub column connected by semi-rigid joints to short lengths of composite beam, which simulated the negative moment region of a continuous beam. Equal point loads were applied to the free ends of these beams (Fig. 5) and were increased in steps until failure occurred. Each test extended over two or three days. The bending moment at the face of the column, M, was calculated for each load stage. The results are given as curves of M/M'_p against the rotation, θ, in Figs. 6 and 7.

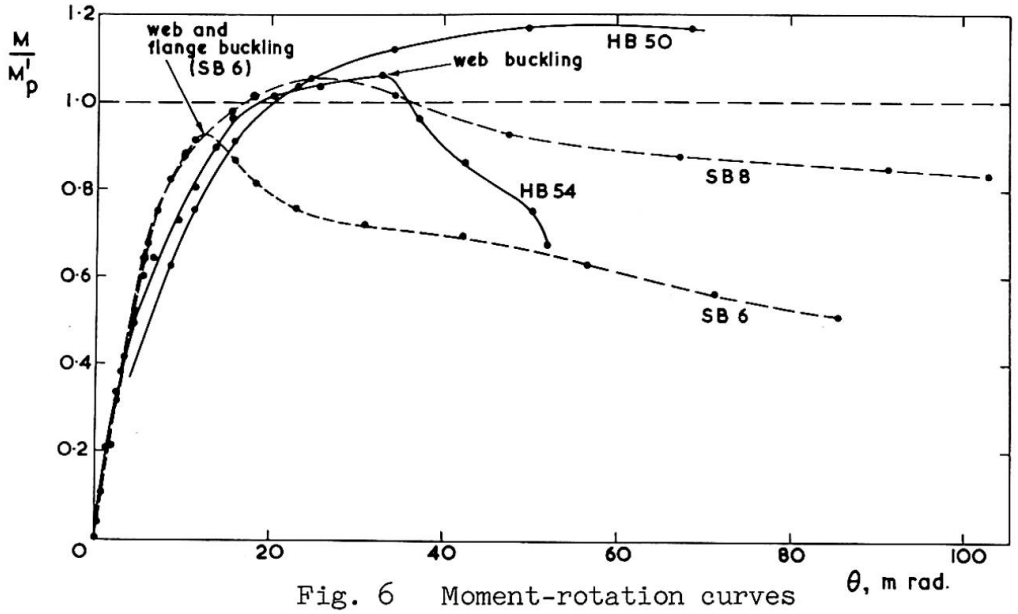

Fig. 6 Moment-rotation curves

The five specimens fall into three groups, according to the size of the steel joist. The Figures also give curves for the three rigid-jointed beams, tested by Climenhaga (8), that are most similar to the specimens of these groups. All three were continuous over their central support, and were heavily stiffened there to provide a rigid column-like support region. A composite concrete slab was provided in HB 41, as in the present tests, but in SB 6 and SB 8 the slab and its reinforcement were simulated by welding a plate to the top flange of the joist. Climenhaga's beams buckled on one side of the column, but not on the other. Buckling also occurred in HB 54, and slab failure in HB 53. The rotations given for these five specimens are therefore those of the free end on the side that failed, relative to the centre-line of the column. Results for beams HB 50 to 52 are averages of the rotations of the two beam lengths.

Table 1 gives the following data for these eight specimens: the joist dimensions b and d and the web and flange slendernesses (with notation as in Fig. 1(c)), and values of A_g, f_y, Φ and M'_p, as defined earlier.

The load at which slip first occurred in the bolted joints, W_s, is given by the ratio W_s/W_p, where W_p is the load at which the bending moment at the face of the columns is M'_p.

The flexibility of the joint at working load is indicated by θ/θ_e, where θ is the observed mean rotation when the bending moment at the column face is $0.5\ M'_p$, and θ_e is the mean rotation calculated by full-interaction elastic theory for the composite cross-section, assumed continuous over the whole length of the test specimen, and neglecting the stiffness of concrete in tension.

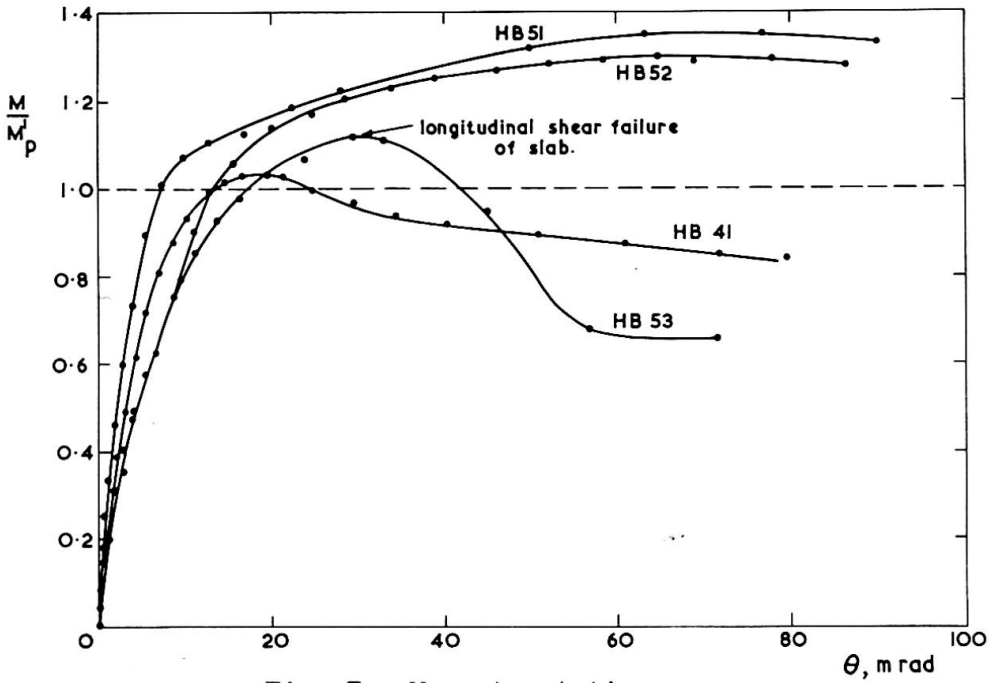

Fig. 7 Moment-rotation curves

Discussion

It has been found (8) that the parameters that most influence the rotation capacity of negative moment regions having rigid beam-column joints are the yield strength and web and flange slendernesses of the steel joist and the Force Ratio of the composite cross-section. The flange slendernesses (b/r) of seven of the sections considered here lay between 16.4 and 17.1; that of the eighth (HB 41) was 15.2. The rotation capacity of the three rigid-jointed beams was influenced by flange buckling, and none of the eight sections would normally be considered as suitable for use in plastic design. But in the beams with semi-rigid joints, little flange buckling occurred, due to the restraint provided by the angles used for the bolted joints.

The other three parameters all appear in the rule given in the current A.I.S.C. Specification for the limiting web slenderness of sections that can be used in plastic design. Climenhaga has concluded (8) that the rule should be applicable to rigid-jointed composite beams in the form:

$$\left.\begin{aligned} (d - 2r)/w &\leq 2.44(1 - 1.4\Phi)/\sqrt{\epsilon}_o \quad \text{for} \quad 0 \leq \Phi \leq 0.28, \\ (d - 2r)/w &\leq 1.48/\sqrt{\epsilon}_o \quad \text{for} \quad \Phi > 0.28 \end{aligned}\right\} \qquad (3)$$

where ϵ_o is the elastic strain of the steel at its yield stress. The ratio of the measured web slenderness of each beam to the limiting slenderness as given by Eq. (3) is given in Table 1 under the heading 'Web ratio'. Five of the eight beams were 'slender' as here defined; the others are described as 'compact'.

The Authors' study of rotation requirements in continuous composite beams is not yet complete; but it is known that a necessary condition for the applicability of simple plastic design is that the maximum negative moment reached in a test must exceed M'_p and that an important parameter is the 'available rotation', θ_a, defined as the maximum rotation at which $M/M'_p \geq 1.0$.

The results of the three groups of tests are now discussed in turn. The joists in specimens HB 50 and SB 8 were of the same 'compact' cross-section, and the force ratios were similar. Buckling of the rigid-jointed beam, SB 8, limited θ_a to 37 mrad (radians x 10^{-3}). The test on HB 50 was terminated by failure of the shear connectors at 68 mrad. The mean load per connector at M'_p was 75 per cent of the push-out strength. If '64 per cent' design had been used, as now recommended (9), the available rotation would have been even greater.

Some reduction in available rotation with increasing force ratio is indicated by the curves for specimens HB 51, 52, and 53 (Fig. 7). The tests on HB 51 and 52 were terminated at large rotations by failures of the shear connection in HB 51 and limitations of the test rig in HB 52. The transverse reinforcement in the slab of HB 53 was designed by a proposed ultimate-strength method (10) to be just sufficient at a bending moment of M'_p. Longitudinal shear failure occurred at 1.11 M'_p, and is the reason for the steep falling branch of the curve for this beam.

It does not follow from these failures in cantilever specimens that the shear connectors and transverse reinforcement in continuous composite beams will be inadequate if designed for shear flows calculated from simple plastic theory. The compatibility requirements in such beams are sometimes such that negative moments of resistance ten or twenty per cent above M'_p are reached (due to strain-hardening) at the design ultimate load. But the coexisting positive moments are less than M_p, and the total shear flow between locations of hogging and sagging hinges is similar to that given by the simple theory; whereas in a cantilever it is roughly proportional to the negative moment of resistance.

The web ratio of the rigid-jointed beam HB 41 was similar to those of HB 52 and 53, but it had a lower ultimate strength and a much lower available rotation. Plastic design could not be used for this beam, if Eq. (3) is followed. It is likely that it could be used for the three beams with semi-rigid joints, if the secondary failures were prevented.

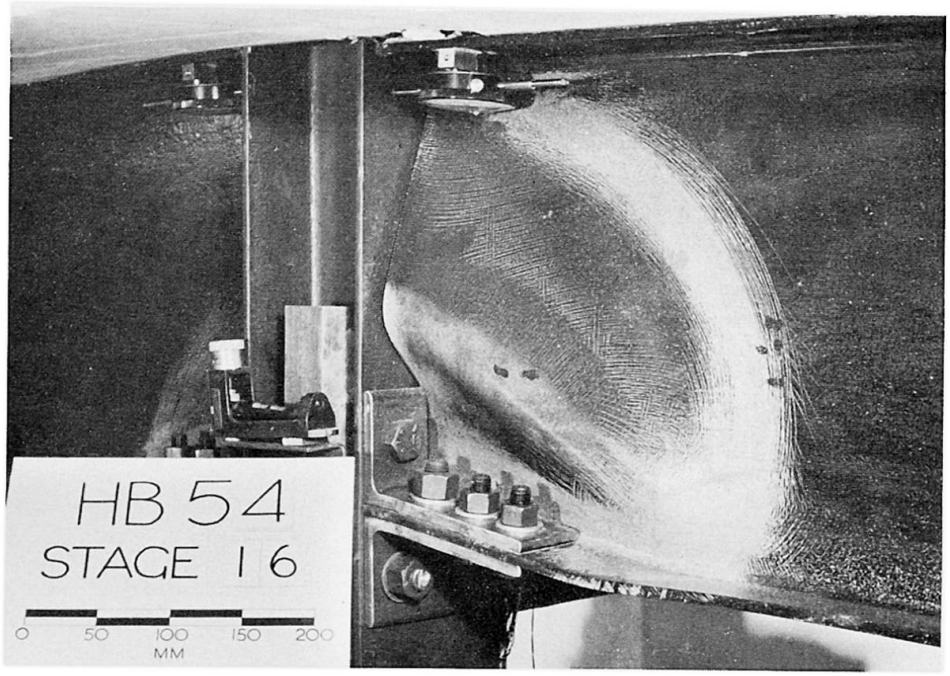

Fig. 8 Web buckling in specimen HB 54

The last comparison is between beams HB 54 and SB 6, both of which had very slender webs. Severe web and flange buckling occurred in the rigid-jointed beam, which failed at a maximum moment of $0.92M'_p$. In beam HB 54, buckling in vertical compression occurred at the free edge of the web at $1.06\ M'_p$, as shown in Fig. 8, and led to a local failure of the slab above. This mode of failure could easily be prevented by the use of a bolted web cleat, which would in any event be required to stabilize so slender a beam prior to the casting of the slab. These results show that even in a very slender beam, the semi-rigid joint gives a greater relative strength and available rotation than does a rigid joint. It is not suggested that either beam, without stiffening, is suitable for plastic design.

The preceding comparisons of strength have been made on a non-dimensional basis. For a given force ratio and joist cross-section, the calculated M'_p is of course reduced when a rigid joint is replaced by a semi-rigid joint. A relevant parameter is the ratio of M'_p to M'_{pj}, the plastic moment of the joist section alone. Values for the eight beams are given in Table 1. The plated joists of the SB series are not directly comparable with the HB series of beams, but the figures for HB 50 and 52 show that a semi-rigid joint can develop the strength of the joist section alone with a force ratio of about 0.35. The plastic moment at midspan is likely to exceed that of the joist alone by between 50 and 150 per cent. Thus is 'simple' supports at both ends of a beam are replaced by semi-rigid joints with $M'_p/M'_{pj} = 1$, the carrying capacity (for distributed load) is increased by between 67 and 40 per cent, which should easily pay for the additional connectors and the extra cost of the joints.

Beam	d mm	b mm	A_g cm^2	f_y N/mm^2	Φ	M'_p kN-m	$\frac{M'_p}{M_{pj}}$	$\frac{d-2r}{w}$	Web ratio	θ/θ_e at $M'_p/2$	$\frac{W_s}{W_p}$
HB 50	206	132	32.1	310	0.34	86	1.07	32.4	0.86	-	-
SB 8	201	135	32.5	320	0.42	108	1.31	32.6	0.87	-	-
HB 51	305	166	50.7	277	0.16	78	0.42	46.4	0.90	1.15	1.01
HB 52	305	166	50.7	277	0.35	171	0.93	46.0	1.14	1.26	0.76
HB 53	304	165	50.6	293	0.44	229	1.31	43.4	1.11	1.04	0.70
HB 41	260	102	27.9	330	0.27	126	1.46	40.5	1.08	-	-
HB 54	395	145	50.5	315	0.41	286	1.27	56.4	1.50	1.22	0.65
SB 6	398	141	47.5	320	0.38	317	1.38	61.5	1.64	-	-

Table 1

Behaviour at working load. When design is governed by deflexion, it is most advantageous to provide continuity at supports. The midspan deflexion of a uniform elastic fixed-ended beam is only 20 per cent of that of a similar simply-supported beam, for the same span and distributed load. If, in a composite beam, the flexural rigidity of the negative moment regions is half that

of the midspan region, the ratio is still only 29 per cent. The ratios θ/θ_e in Table 1 show that when a semi-rigid joint is used, the end rotation of the negative moment region may exceed that given by elastic theory by about 20 per cent. The increase in the deflexion due to this is offset in a continuous beam by a slight reduction in the length of the negative moment regions, and the ratio (29 per cent) increases only to 30 per cent. Even if the design load for the beam is 50 per cent greater than that of the simply-supported beam, its deflexion is still much less.

In these simple calculations, other factors influencing deflexion, such as shrinkage and creep of concrete, have been neglected. But even here, the continuous beam has an advantage. Shortening of the slab relative to the steel joist causes additional deflexion in a simply-supported beam, but not in an interior span of a continuous beam.

Finally, the longitudinal slip of the bolted joints is considered. The ratios W_s/W_p (Table 1) show that slip was first detected at $1.04M_p'$ in HB 51 and at about $0.7M_p'$ in HB 52 to 54. The negative moment at working load depends on the redistribution of moment due to cracking of the slab and on the safety factors used. It may be necessary to design for first slip at a higher proportion of M_p' than 0.7.

The loads at first slip given above are lower than was intended. The joints were designed using a slip factor of 0.45, and the nuts were tightened by the part-turn method. Slip first occurred at loads corresponding to apparent coefficients of friction (based on a nominal bolt tension of the proof load) ranging from 0.32 to 0.36. It has been shown (11) that the true coefficient of friction (slip load/bolt tension at slip) is dependent on the condition of the faying surfaces and the bolt tension at slip. The steel angles used in the joints tested had a slightly pitted surface. This would cause higher local stresses (as also does the use of the part-turn method of tightening) resulting in premature local yielding and increased relaxation of the bolt. It is believed that both these effects reduce the slip factor. Further study of this behaviour is in progress.

Conclusions

1. Semi-rigid joints of the type shown in Fig. 4 can be made with strengths exceeding the plastic moment of resistance of the steel joist. They provide a well-defined stiffness and moment of resistance at a support, of which advantage can be taken in the design of the beams; and yet should be much cheaper than a fully-rigid joint.

2. Tests on five specimens, covering the whole range of web slendernesses available in Universal beams, showed that negative moment regions with semi-rigid joints have greater resistance to buckling and much greater rotation capacity than rigid-jointed members of similar cross-section. Thus the limiting slendernesses of rolled sections that can be used in plastic design are increased when semi-rigid joints are used.

3. Appreciable strain hardening can occur in negative moment regions before the design collapse load of a continuous beam is reached, but is should not be necessary to design shear connectors and transverse reinforcement in a negative moment region to resist a longitudinal shear exceeding that at M_p'.

Acknowledgements

The authors acknowledge with thanks the assistance of two undergraduates, A.H. Davis and A.M. Neal, who conducted the first test as a third-year project; and are most grateful to the British Constructional Steelwork Association for its support of the research at the Universities of Cambridge and Warwick, of which this work forms a part.

References

1. Garcia, I., and Daniels, J.H., 'Tests of composite beams under negative moment'. Fritz Eng. Lab. Report No. 359.1, Lehigh University, Feb. 1971.

2. Johnson, R.P., 'Research on steel-concrete composite beams'. Proc. Amer. Soc. Civ. Engrs., Vol. 96, No. ST3, March 1970, pp. 445-459.

3. Basu, A.K. and Sommerville, W., 'Derivation of formulae for the design of rectangular composite columns', Proc. Instn. Civ. Engrs., Supp. Vol., 1969, pp. 233-280.

4. Daniels, J.H. et al., 'Behaviour of composite-beam to column joints'. Proc. Amer. Soc. Civ. Engrs., Vol. 96, No. ST3, March 1970, pp. 671-685.

5. Barnard, P.R., 'Innovations in composite floor systems'. Paper presented to Canadian Structural Engineering Conference, 1970. Canadian Steel Industries Construction Council, 1970, pp. 13.

6. Joint Committee on fully rigid multi-storey welded steel frames. Second Report. Institution of Structural Engineers, 1971. pp. 12.

7. Johnson, R.P., et al., 'A plastic composite design'. Proc. Instn. Civ. Engrs. Vol. 32, Oct. 1965, pp. 198-209.

8. Climenhaga, J.J., Local buckling in composite beams. Ph.D. thesis, University of Cambridge, 1970.

9. Johnson, R.P. et al., 'Stud shear-connectors in hogging moment regions of composite beams. Struct. Engr., Vol. 47, Sept. 1969, pp. 345-350.

10. Johnson, R.P., 'Longitudinal shear strength of composite beams'. Proc. Amer. Conc. Inst., Vol. 67, June 1970, pp. 464-6.

11. Cullimore, M.S.G. et al., 'The use of friction-grip bolts in structural steelwork'. Report on CIRIA Project 4/5/50, University of Bristol, Nov. 1969.

Summary

It is shown that neither 'simple' nor 'rigid' beam-column joints are ideal for use in steel-concrete composite framed structures for buildings. A new type of semi-rigid joint is described, and is shown by tests to have a well-defined flexural strength and a much greater rotation capacity than a rigid joint. It should also be cheaper. Its use should enable frames having joists of slender cross-section to be designed by simple plastic theory.

Fatigue Strength of Steel Plates with a Stud Shear Connector for Application to Continuous Composite Beams

Résistance à la fatigue de plaques d'acier avec goujons de cisaillement employées dans la construction de ponts mixtes continus

Ermüdungsfestigkeit von Stahlplatten mit Schubdübeln bei der Anwendung durchlaufender Verbundträger

YUKIO MAEDA
Dr. Eng., Professor
Department of Civil Eng.

YASUHARU KAJIKAWA
Master of Eng.
Graduate School

Oska University, SUITA
Osaka, Japan

1. Introduction

The static and fatigue behaviors of non-prestressed continuous composite beams, which are steel and concrete composite constructions along the entire length of structure without prestressing into concrete slab in negative moment regions, have been nearly clarified by the several experimental studies[1),2),3)]. However, a question in connection with the fatigue resistance of the tension flange in the regions where the beam passes over an interior support and which is subjected to repeated negative moments, has not completely been solved yet.

With respect to this problem, two types of fatigue tests have been conducted until now. Namely, one is a flat plate test by using specimens which consist of a flat plate and of one or more studs welded to it, and the other is a beam test for model composite beams subjected to negative moment. However, there were some defects in both of the test methods to obtain the S-N relationships on fatigue resistances of plates with a stud shear connector. First, in all of the flat plate tests which were conducted in the past, the fatigue strength of the plate was obtained under the condition where the stud was not subjected to any shear force, against the fact that the studs in composite beams act as shear connectors between steel beam and concrete slab. On the other hand, in the beam tests, a S-N relationship for any shear stress level could not be obtained, since it was not easy to vary arbitrarily the combination of flexural tensile stress in a tension flange with shear stress on a stud shear connector.

Now, in order to improve the above-mentioned defects in both tests and to obtain exact S-N relationships on fatigue resistances of plates with a stud shear connector, the authors have carried out the flat plate fatigue tests by using a new testing device which could make a pulsating shear force act on a stud in the same phase as a cyclic extensions applied to a plate. Moreover, static and fatigue tests were conducted with other three types of specimens, which were plain plates, plates with a stud removed and plates with a bare stud, in order to estimate the influences of welding and geometrical discontinuity caused by a stud upon static and fatigue resistances of plates.

In this paper, an outline of these experiments is described and the test results are provided and compared with the results[3)] of beam tests done by the authors.

2. Description of Specimens and Test Procedure

2.1 Description of test specimens

Structural carbon steel SS41 by JIS (the Japanese Industrial Standards) designation and high-strength quenched and tempered low alloy structural steel SM58Q by JIS were used in the fabrication of plates for test specimens, and the steel material of the studs corresponded to SS41 grade. Chemical composition and mechanical properties of these base materials indicated in mill sheet, are given in Table 1.

The whole test program for SS41 and SM58Q steels was broken down into seven different test series including three static tests, respectively. The dimensions of each specimen for these test series are shown in Fig. 1. Cross-sectional dimensions in parallel portion of plates were the same through all of the test series, and the shape and length of plates were identical in each of the SA through SC, A through C, and D series.

The fatigue tests were as follows:

A Series: The purpose of this series of tests was to obtain a basic S-N curve for plain plate of base material with mill scale under pulsating tension stress cycles.

B Series: In order to estimate the effect of welding on the base materials, the geometrical discontinuity caused by the upset around the root of stud was made to disappear by cutting off the stud and grinding down to the surrounding plate surface.

C Series: The function of this series was to determine a S-N curve for plates under the condition that a stud was not subjected to any shear forces, namely the state of a bare stud.

D Series: This series were intended to find out the effect of transmission of shear force through the stud shear connector at the same time when the plate is being subjected to a primary tension.

The static tensile strength of A through C series was checked by means of three static tests, SA, SB and SC series, respectively.

The authors have to mention that the experiments for SS41 steel have been carried out as planned, but for SM58Q steel, only the tests of SA, SB, SC and C series have been finished until now and the remains are being continued.

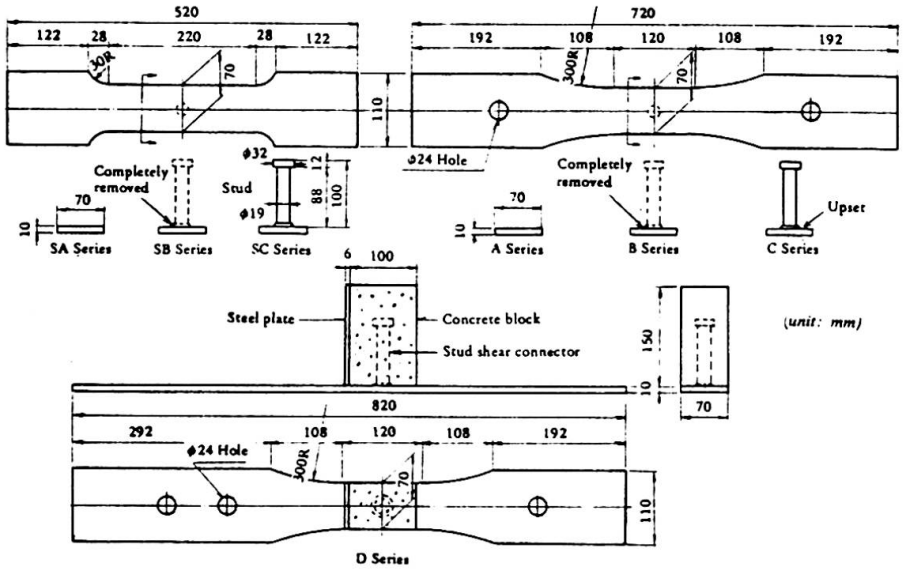

Fig.1 Dimensions of test specimens.

Table 1. Chemical composition and mechanical properties of base materials

Material	Chemical Composition (wt.%)						Mechanical Properties		
	C	Si	Mn	P	S	Cu	Y. P. (kg/mm^2)	T. S. (kg/mm^2)	Elong. (%)
SS41 Plate	0.17	0.04	0.77	0.009	0.031	——	30	45	32
SM58Q Plate	0.14	0.36	1.21	0.019	0.012	0.03	63	66	26
Stud	0.17	0.01	0.69	0.011	0.033	——	28	43	30

All of the plates for test specimens were fabricated from a large steel plate (10 x 1600 x 4100 mm) of which surface condition was as-received with mill scale. After the both sides of all plates were machined to specified dimensions, each specimen for SB, SC, and B through D series was provided with a single stud (ϕ 19 x 100 mm) at the center of plate by the same welding procedure that the weld current was 2,000 amps. and arc time 32/60 cycles for SS41 steels, and 1,700 amps. and 36/60 cycles for SM58Q steels.

For specimens of SB and B series, after stud welding, the studs were completely removed and ground down to approximately the same thickness as the surrounding plate.

In the case of specimens for D series, the stud was encased in a concrete block of 70 x 150 x 100 mm, as shown in Fig. 1, in order to secure similar stress conditions as observed in actual composite beams. After a grease had been placed on the plate surface in order to remove steel-concrete bond, the high-early-strength concrete, of which mean compressive strength at a week was about 320 kg/cm^2, was cast around the stud. In this way, it was expected that all of the applied shear force could be transmitted through the stud to the plate.

2.2 Test procedure

All of the fatigue tests were conducted with a Losenhausen-type fatigue testing machine of a maximum capacity of 40 tons for dynamic load, and all of the static tests were carried out with an Amsler-type universal testing machine of a maximum load capacity of 200 tons.

2.2.1 A, B and C Series

The fatigue tests for these series were conducted under the conditions of partial tension-to-tension stress cycles with the minimum load of 1 ton and with a constant loading speed of 500 cycles per minute for SS41 steels and 340 cycles per minute for SM58Q steels.

2.2.2 D Series

In this test series, a new shear loading device with a fatigue testing oil jack (maximum dynamic load capacity = 10 tons) was attached to a primary Losenhausen-type fatigue testing machine, so that the pulsating shear force could be acted on a stud which was welded to a plate, in the same phase as the pulsating tension of the plate.

A schematic diagram for this loading method for combined stress is shown in Fig. 2. A tensile force was applied to the plate with the Losenhausen-type fatigue testing machine in the same manner as an ordinary tensile fatigue test, and moreover, simultaneously the stud was

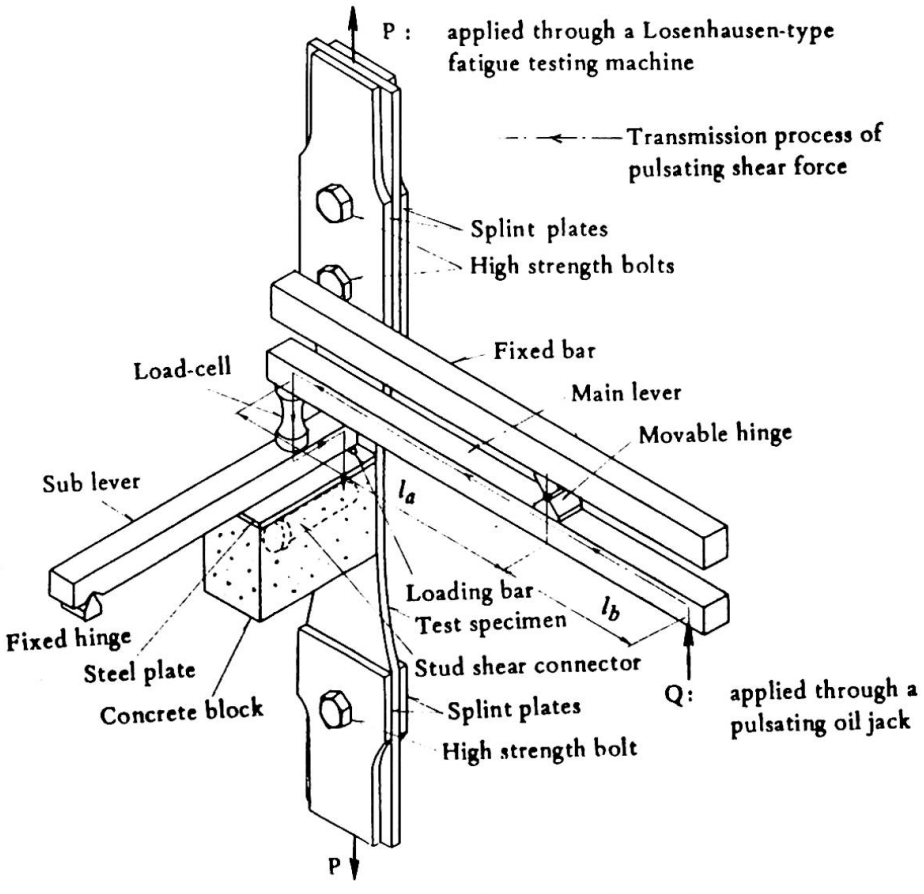

Fig. 2 Schematic diagram for combined stress loading method.

loaded through two levers of a shear loading device with an another oil jack through which pulsating loads were applied with a pulsator belonging to a primary testing machine. Fig. 3 shows a view of testing in progress.

The fatigue tests were conducted in combined pulsating stress cycles with the minimum tensile load of 1 ton for the plate, and with the constant shear stress range for the stud, which was about 2 or 4 kg/mm^2 in this test program. The loading speed was held approximately 340 cycles per minute through all of the specimens.

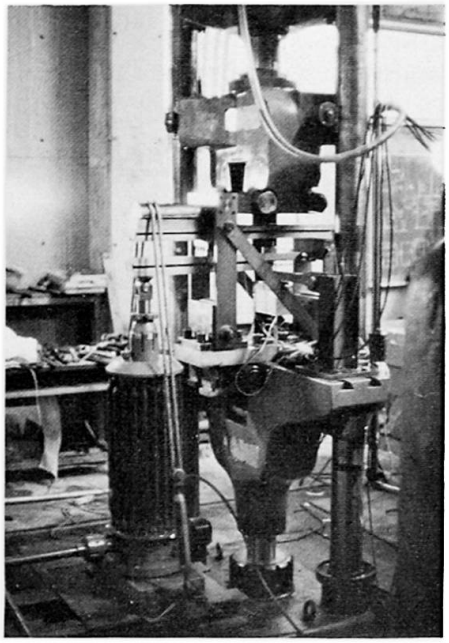

(a) Setup of fatigue testing machine

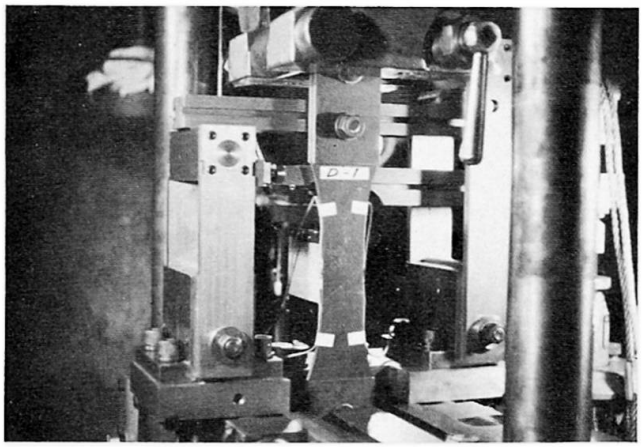

Fig. 3 Fatigue test of D series in progress.

3. Test Results and Discussions

3.1 Static tests

The results of static tests which are presented in Table 2, indicate that the stud welding and the geometrical variation of plate surface did not so much influence either on the stress at the yield point or on the ultimate tensile strength of a base material. The fractures in SB and SC series occurred in the base material at about 5 cm apart from the stud welding point.

The above-mentioned facts held true for the both of mild steel SS41 and high-strength steel SM58Q.

Table 2. Results of static tension tests

Test Series	SS 41			SM 58Q		
	Y. P. (kg/mm^2)	T. S. (kg/mm^2)	Elong. (%)	Y. P. (kg/mm^2)	T. S. (kg/mm^2)	Elong. (%)
SA	27.7	46.2	30.7	56.2	63.9	19.9
SB	27.1	45.2	30.7	55.9	64.6	20.8
SC	26.3	44.8	29.1	56.8	65.0	20.3

3.2 Fatigue tests

The results of fatigue tests are presented in the form of S-N diagram in Fig. 4, on the basis of log-log relationships between a nominal applied tensile

stress range in the smallest cross-section of plate and a number of cycles to failure. The figure indicates that the results showed amazingly little scatter, so that a relatively small number of tests were able to give a remarkable indication of the fatigue resistance for each test series.

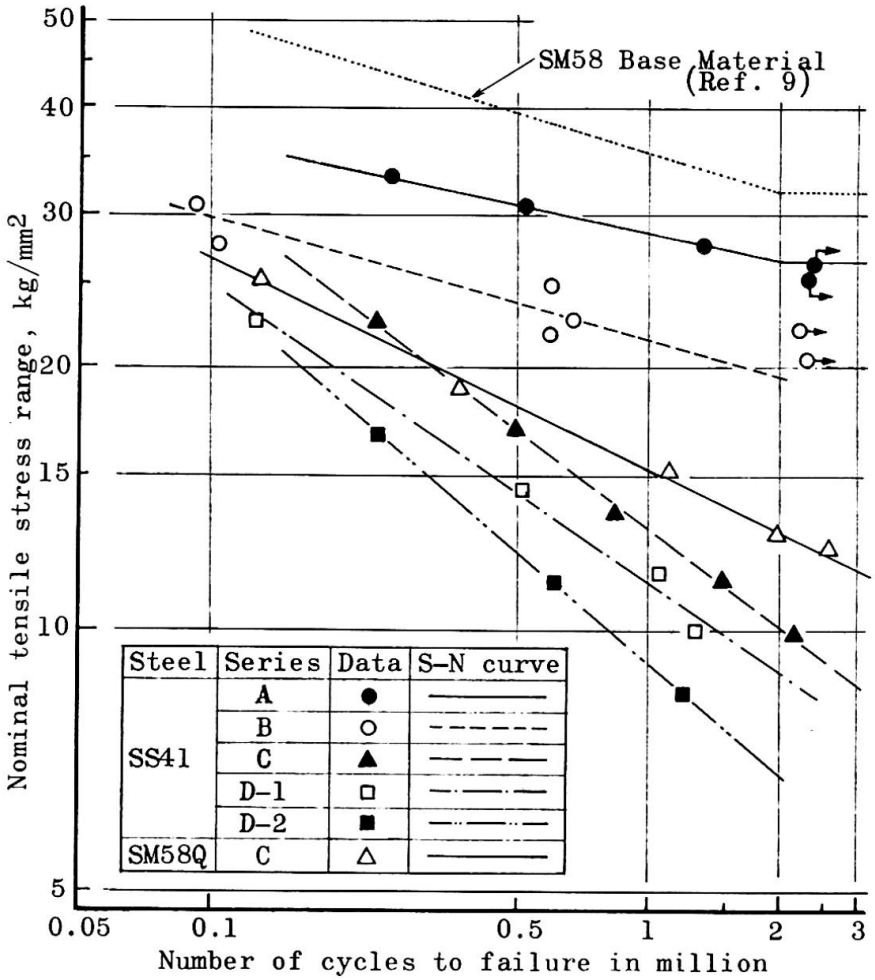

Fig. 4 Fatigue test data on S-N diagram.

3.2.1 A Series

From the results of A series for SS41 steels shown in Fig. 4, as the fatigue strength 36.4 and 26.3 kg/mm^2 at 10^5 and 2 x 10^6 cycles, respectively, could be obtained by an extrapolation of the data on a straight line. Although a few number of specimens in this series were tested, these values coincide fairly well with the results reported in Ref. 8), namely the values of 33.8 kg/mm^2 at 10^5cycles and 26.8 kg/mm^2 at 2 x 10^6 cycles for 50 % survival.

3.2.2 B Series

An indication of the effect of welding may be obtained by comparing the results of the A and B series for SS41 steels. In Fig. 4, it is observed that the S-N curve for B series is situated about 5 to 6 kg/mm^2 in terms of the fatigue strength below that for A series, and this difference would be caused by some effects of welding--- for example, stress concentration produced by weld defects which will occur in a welded part during the welding process, residual stress, change of materials in heat-affected zone and so on. In this test series, however, it may be considered that the stress concentration due to weld defects had a larger influence on fatigue strength compared with the other factors. Because, in visual inspection of fracture surface for B series specimens after the fatigue tests, it was observed that the fatigue fracture had initiated at the location of so-called blow-hole for two among five fractured specimens (see Fig. 5(a)), and at a part of lack of fusion for the rest.

And besides, from this fact, it is considered that the results for B series have somewhat scattered, since the degree of stress concentrations produced by the weld defects may delicately depend upon the type or nature of such defects as their shape, orientation and size, etc.

3.2.3 C Series

(a) SS41 Steels

From the results of C series as shown in Fig. 4, it is clear that the geometrical discontinuity at the root of stud has a large influence on the fatigue resistance of plates with a stud. In other words, the slope of S-N curve for C series is more steeper than that for A or B series, and the fatigue strength

decreases rapidly as the cycles increase, resulting in about 40 % of that for A series and about 50 % of that for B series, at 2 x 10^6 cycles.

In all of the specimens for C series, a fatigue crack initiated at either one of the upset edges closest to the ends of plate, and propagated more rapidly toward the both sides of plate. In visual inspection of fracture surface after the fatigue tests, such internal defects as observed in B series, were not found out at all. From these matters, it is clear that the influence of internal defects is not so great as the geometrical effect of stud. In the case of the presence of a stud, accordingly, it can be concluded that the fatigue strengths of plate with a stud will depend upon mainly the degree of stress concentrations at the root of stud, and properties of the base metal in heat-affected zone including residual stresses. In this test program, unfortunately the individual effect of these factors upon fatigue strength of plate could not be studied in detail, but would be investigated in future.

(b) SM58Q Steels

In Fig. 4, the S-N curve given in Ref. 9) for the plain plate fatigue tests of JIS SM58 steels with mill scale, is also drawn for comparing with the results of this series, since the tests of A series for this steel have not been conducted until now.

It is seen that the fatigue strengths of C series for SM58Q steels at any cycle lives drop down equally by about 40 % of those for plain plate, resulting in nearly the same value as for SS41 steels, while a large difference in static tensile strength between both steels is indicated in Table 2. This may be caused by a fatigue characteristic of high-strength steel, that is, a high notch sensitivity for stress concentrations.

From the fact that the conditions of initiation and propagation of a fatigue crack was nearly the same as the case of SS41 steels, it may be slso persisted that this reduction in fatigue strength would be caused by the reason above-mentioned for SS41 steels with a stud.

(c) Comparisons with other investigations

In Table 3, the fatigue strengths obtained from the S-N curve for C series of SS41 and SM58Q steels are compared with those obtained from the flat plate tests made by other investigators[4),5),6)]. It is indicated that, in spite of the differences in materials, number of stud attached to a plate, shape and size of specimens and so on, there is an excellent agreement among the results, although the present results for SM58Q steels were somewhat larger than the others.

Typical fracture surfaces after the fatigue tests for each of the test series are shown in Fig. 5. Fig. 5(a) for B series shows a typical fracture surface with a blow-hole at which the fatigue crack initiated. In Fig. 5(b) for C series, it is seen that the fatigue crack initiated just close at the edge of upset and propagated uniformly and approximately perpendicular to the plate surface.

Table 3. Comparisons of fatigue strength of plate with studs

Name	Material	Fatigue Strength, kg/mm^2		Number of stud welded to a plate
		N=500,000	N=2,000,000	
Authors	JIS SS41	16.8	10.1	one stud
	JIS SM58Q	18.2	13.0	
T. Wakabayashi et al.[5)]	JIS SS41	18.0	11.0	one stud
	JIS SM58	15.5	10.0	
K.A.Selby et al.[4)]	ASTM A7F A441	16.6～20.4	10.0～12.5	one or more studs, transversely
W. Roshardt[6)]	DIN St37	16.0	11.0	three studs, longitudinally
	DIN St60 St70	17.5	10.0	

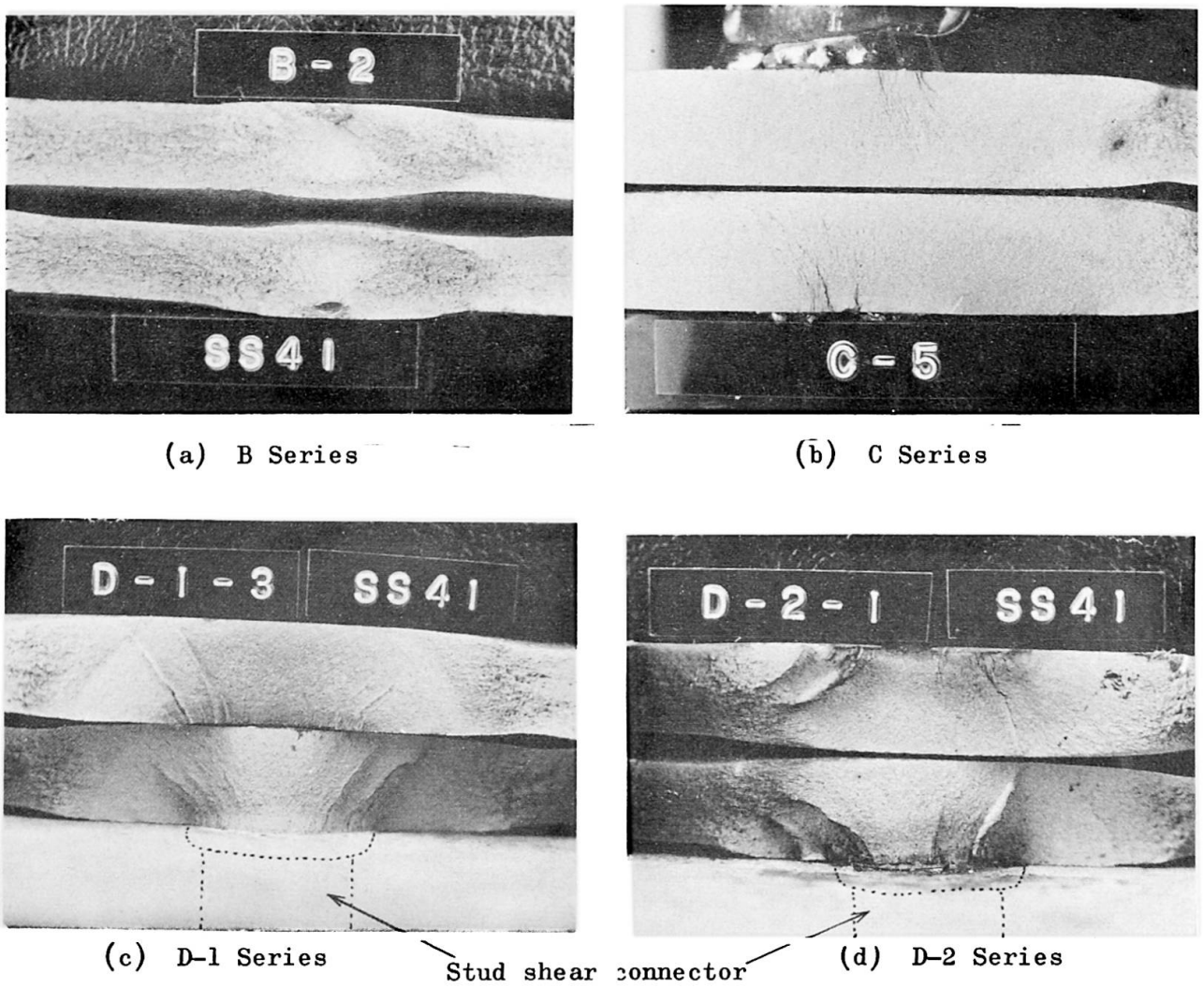

(a) B Series (b) C Series

(c) D-1 Series (d) D-2 Series

Fig. 5 Typical fatigue fracture surfaces in each test series.

3.2.4 D Series

In order to estimate the influence of shear force acting on a stud shear connector upon a tensile fatigue resistance of plate under combined stress conditions, a number of S-N curves must be obtained at various different levels of constant shear stress range. In this test program for SS41 steels, the fatigue tests were carried out under two different stress levels, that was, approximately 2 kg/mm^2 and 4 kg/mm^2 with a maximum deviation of $\pm$ 5 % in the average shear stress range acting on a nominal cross-section of stud, and each test series was distinguished as D-1 or D-2, respectively. The test results are plotted in Fig. 4 with the shear stress range as a parameter.

All of the specimen in this series failed due to propagation of a fatigue crack which had initiated at the upset edge closest to the side of applied shear force. A typical fracture surface is shown in Figs. 5(c) and (d). As compared with Fig. 5(b), it is seen that the fracture surface in D series includes a narrow region where a crack has propagated along the fusion line on account of the presence of shear force acting on the stud, while the fatigue crack in C series has propagated approximately perpendicular to the plate surface and formed a relatively flat fracture surface.

By comparing three S-N curves for C, D-1 and D-2 series as shown in Fig. 4, it is noticed that the fatigue strength of plate at any cycle life reduces gradually as the shear stress range increases, and it can be considered that this phenomenon may be reasonable. Then, in order to clarify how the tensile fatigue strength of plate would be influenced by a shear force acting on a stud, the authors tried to apply the test results to various criteria of failure that are generally used in the case of combined alternating bending and torsion in the

same phase.

The fatigue strengths at 2 x 10^6 cycles for C, D-1 and D-2 series, which were obtained from the S-N curves shown in Fig. 4, and the result of push-out tests, which were primarily conducted to determine the shearing strength of shear connectors under pure shears, reported in Ref. 7) are plotted on the so-called fatigue limit diagram under combined stresses in Fig. 6, in which the curves calculated corresponding to various theoretical criteria of failure[10] are also indicated. As seen in Fig. 6, the present test results including those for push-out test are not applicable to any curves, and accordingly the phenomenon of reduction in the fatigue strength of plate could not be interpreted fully and satisfactorily with the usual criteria of failure. The following factors may be considered as the main reasons for this: the difference in combined loading conditions of normal and shear stress, for example, the one is bending and torsion, and the other is tension and shearing; the difference in the estimation of fatigue strength, namely, the one is an endurance limit and the other is a fatigue strength at 2 x 10^6 cycles; the effect of stud welding and stress concentration at the root of stud in the present specimens; and so forth. Therefore, a definite experimental hypothesis for fatigue failure of plate with a stud under combined stress cycles, could not be obtained within a limit of the present test program lacking sufficient informations. Supplementary fatigue tests for other shear stress levels are being continued to make clear this phenomenon.

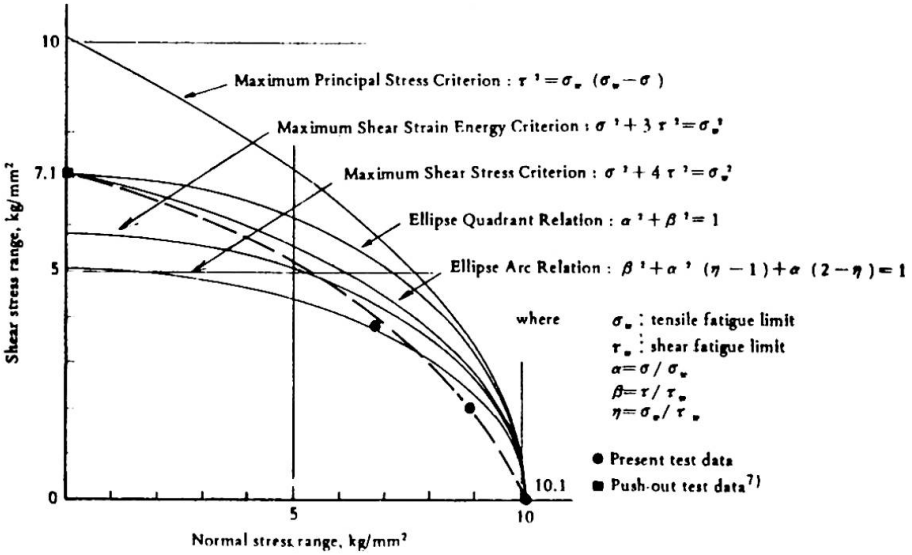

Fig. 6 Comparison of test data with various criteria of failure.

4. Comparison with the Results for Beam Tests

4.1 Summary of the beam tests

The experimental study on composite beams subjected to repeated negative moment was conducted as a part of investigations to clarify the fatigue behavior in negative moment regions of non-prestressed continuous composite beams, and its results were reported in Ref. 3) by the authors.

The test program was carried out on sixteen beam specimens which were divided into seven types, as shown in Table 4, according to location of loading, diameter of longitudinal reinforcing bar, and spacing and type of shear connectors. Cross-sectional dimensions, details of shear connectors, span length and location of applied load are shown in Fig. 7.

Table 4. Summary of test beams

Beam	No.	Diameter of longitudinal reinforcements	Spacing and type of shear connectors (cm)		Loading condition
E 1	2	D 13 mm	40	Stud	Two points
E 2-1	2	D 16	30		
E 2-2	2	D 16	60		
E 2-3	2	D 16	10		
E 3	2	D 19	20		
H 1	3	D 16	30	Stud	One point
H 2	3	D 16	45	Block	

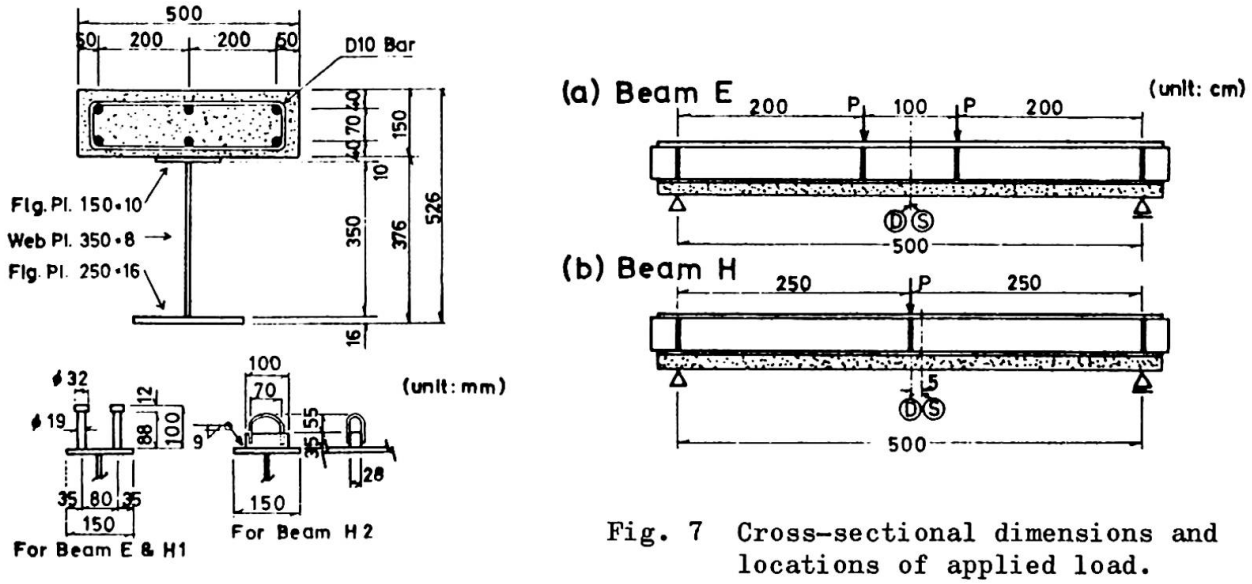

Fig. 7 Cross-sectional dimensions and locations of applied load.

Steel materials of all test specimens were structural carbon steels of JIS SS41 grade for steel beams and for stud shear connectors, deformed bars of SD30 at JIS for longitudinal reinforcements. At these fatigue tests, such phenomena were observed that a fatigue crack initiated at the upset edge of shear connectors and then propagated through the tension flange to which the shear connectors were attached.

In the present paper, the authors have rearranged the test data of beam tests by taking into account the so-called dynamic effects of repeated load due to an interaction of the applied dynamic load and inertia force of the beam, in calculating flexural fiber or shear stresses which occurred in the beams. Because, the effects were not considered for the arrangements of beam test results at the time when the Ref. 3) was published, resulting in a large underestimation for calculating the stresses.

The modified results for beam tests are plotted in Fig. 8 and compared with those for C and D series of SS41 steels.

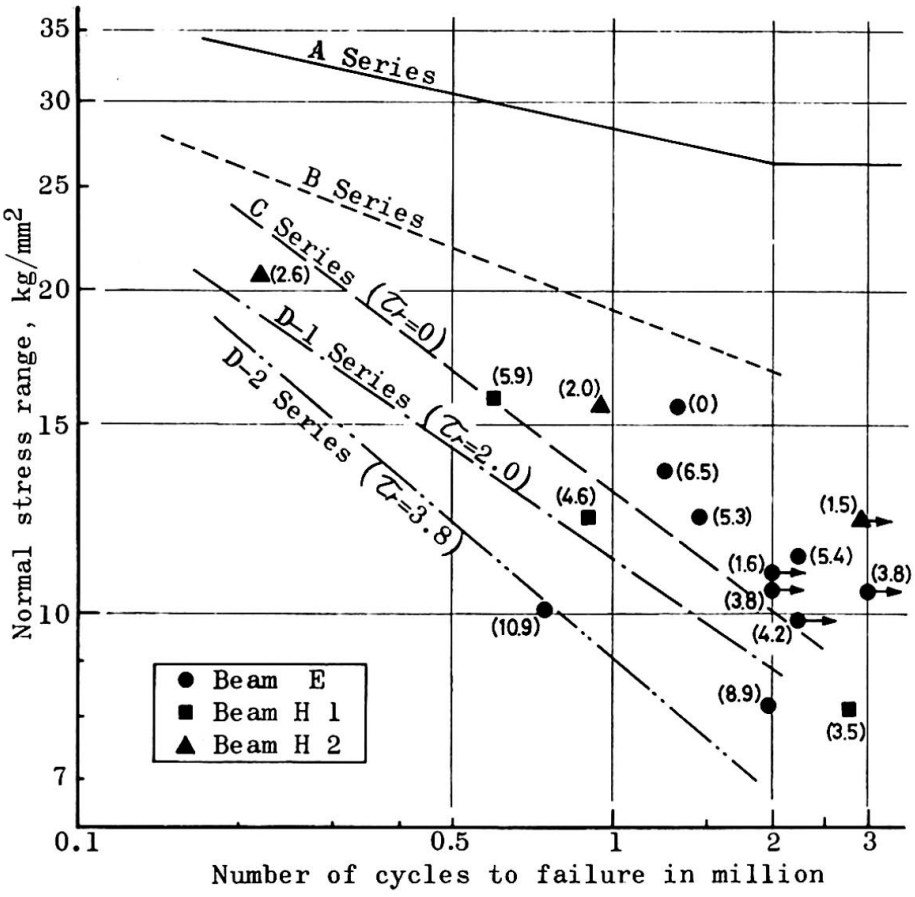

Fig. 8 Comparisons of the results for beam and plate tests in terms of normal tensile stress range.

4.2 Comparisons with the results of beam tests

In Fig. 8, the results for flat plate tests of SS41 steels are indicated in the forms of S-N curve, and these for beam tests are plotted by means of three kinds of marks. The numerals in parentheses express the shear stress range τ_r in kg/mm^2, which acted on a shear connector in each beam specimen. While shear connectors for H2 specimens were different from those for E and H1 specimens, the results for H2 beams were dealt with, for reference, together with those for E and H1 beams in the following discussions.

As shown in this figure, the most of the results for beam tests scatter widely on the right of S-N curves for C, D-1 and D-2 series. When paying attension to the value of τ_r which was indicated in the parentheses, such a tendency is observed that, with a few exceptions, at any normal stress range, the fatigue life for the data for smaller τ_r becomes longer than that for those for larger τ_r. From this fact, it would be understood at least qualitatively that, as seen in the flat plate tests, the fatigue strength of tension flange to which the shear connectors were attached is not a little influenced by the shear force which acted on shear connectors.

Next, the authors have tried to evaluate the both test results by means of the plane principal stress occurred at the base of stud. A principal stress σ_p consisting of normal stress σ_x, namely, a flexural fiber stress in tension flange for beam specimens or a nominal tensile stress in the cross-section for plate specimens, and of an average shear stress in the stud τ_{xy}, as shown in Fig. 9, were considered for the evaluation. A flexural stress in the root of the stud σ_y was excluded out of this principal stress, since its exact estimation had not been made yet.

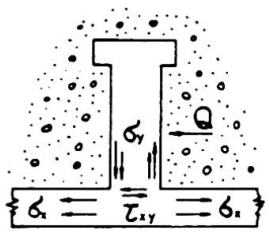

Fig. 9 Stress condition at base of stud.

The data for C, D-1 and D-2 series of plate tests and those for beam tests are plotted in Fig. 10 with the marks of black square and dot, respectively, and further, two scatter bands including the most part of each group are indicated by vertical or horizontal hatchings. As seen in the figure, all of the both test results are included in either comparatively nallow scatter band with the exception of a few data.

The breadth of scatter band for plate tests are somewhat wider than that for beam tests. This may be explained by the following two reasons. First, such a difficulty of shear loading method existed that the plate would be subjected to not only an axial tensile force, but a slight additional bending moment in the plane due to an eccentricity of shear loading, although the

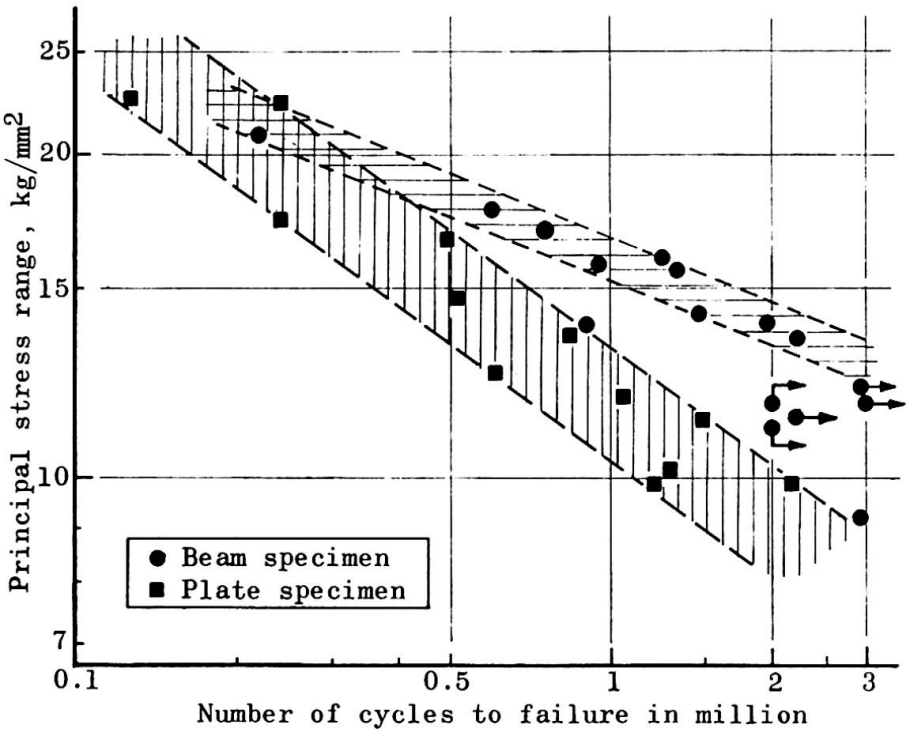

Fig. 10 Comparisons of the results for beam and plate tests in terms of principal stress.

loading point of shear force was kept as close as possible to the plate surface, about 4 mm. Second, the test results for C, D-1 and D-2 series were not applicable to the maximum principal stress criterion, as seen in Fig. 6.

Besides, the interpretation on a few exceptions which appeared in the results for beam tests, has not been completed yet.

In Fig. 10, it is observed that the scatter band for beam tests is located above that for the plate tests, and the differences of fatigue strength between the both bands become larger as the cycle life increases, while they nearly coincide with together at about 200,000 cycles. In the beam specimens, the stress in a tension flange is redistributed to longitudinal reinforcements which were embeded in concrete slab and acted fully effectively after the fatigue crack propagated through the tension flange, and also the shear stress on the stud is redistributed to adjacent studs even if the fatigue crack occurred in the tension flange at some studs. Hence, the speed of propagation of fatigue crack was very slow, especially when the load was smaller, and the fatigue cycle life of beam specimens will become longer. Against this fact, in the flat plate tests, the condition of the tests was very severe, compared with that of the beam tests on account of no redistribution of any stresses. Therefore, there is no doubt that the results for flat plate tests are on the safe side for an actual design of tension flange in negative moment regions of non-prestressed continuous composite beams.

In this manner, the both results for beam and flat plate tests may be interpreted fairly well by considering the principal stress, but, it is still in question why the fatigue failure of a plate in tension with stud shear connectors did not satisfy the maximum principal stress criterion.

5. Conclusions

The main conclusions of this investigation may be summarized as follows:

(1) In the static tensile tests, the stud welding and the geometrical variation of plate surface did not so much influence on either the yield point or the ultimate tensile strength of the base material of either SS41 and SM58Q steels.

(2) The fatigue strength of plate with a stud shear connector was influenced mainly by the stress concentration caused by a geometrical discontinuity at the root of stud, and accordingly the fatigue failure occurred at the edge of the upset.

(3) The fatigue strength of plates with a bare stud reduced remarkably compared with that of the base material, resulting in less than about 40 % at 2×10^6 cycles, namely, approximately 10.1 kg/mm^2 in the stress range for SS41 steels, and about 40 %, 13.0 kg/mm^2 for SM58Q steels.

(4) The fatigue tests conducted by using a new testing device, have produced very reasonable results relating with the tensile fatigue strength of plate. Namely, the pulsating shear force reduced the fatigue strength of plate below that for the plate with a bare stud, and as the result, the nominal tensile stress range at 2×10^6 cycles was lowered down to about 8.9 kg/mm^2 for the shear stress range of 2.0 kg/mm^2 and about 6.8 kg/mm^2 for that of 3.8 kg/mm^2.

(5) The informations which were obtained from the combined stress fatigue tests of flat plate with a stud shear connector, would be applicable to the evaluation of fatigue tests for the beam specimens.

(6) When the results for flat plate tests were compared with those for beam tests in terms of plane principal stress consisting of normal and shear stresses, the fatigue cycle life for the latter was longer than that for the former in general. This may be mainly due to the redistribution of stresses in beam specimens after a fatigue crack was initiated.

References

1) J.H. Daniels and J.W. Fisher, "Fatigue Behavior of Continuous Composite Beams," Fritz Eng. Lab. Rept. No.324.1, Dec. (1966).

2) Y. Tachibana, T. Mukaiyama and K. Minato, "Static Tests on Non-prestressed Continuous Composite Beams," Jour. of the Japan Society of Civil Engineers (JSCE), 53,10(1968), (in Japanese).
3) Y. Maeda and Y. Kajikawa, "Fatigue Behavior of Composite Beams Subjected to Negative Moment," Proceedings of the Symposium on Ultimate Strength of Structures and Their Components, Japan Society for the Promotion of Sience, Tokyo, Sept. (1971).
4) K.A. Selby, J.E. Stallmeyer and W.H. Munse, "Fatigue Tests of Plates and Beams with Stud Shear Connectors," Structural Research Series No.270, Univ. of Illinois, July (1963).
5) T. Wakabayashi, K. Sawano and M. Naruoka, "Tensile Fatigue Tests of Plates with a Stud Shear Connector," The Bridge and Foundation Engineering, Vol.5 No.4 (1971), (in Japanese).
6) W. Roshardt, "Einfluss des Aufschweissens von Bolzen auf das Grundmaterial," Schweiz. Bauzeitung, 84 Jahrgang Heft 51, (1966).
7) R.G. Slutter and J.W. Fisher, "Fatigue Strength of Shear Connectors," Highway Research Record No.147, Highway Research Board, (1966).
8) "Commentary on Standard Specification for Steel Railway Bridges," JSCE, (1970) (in Japanese).
9) KANSAI Investigation Group on the Fatigue of High Strength Steel, "Experimental Studies on the Fatigue Strength of High Strength Steel," Jour. of JSCE, 54, 11(1969), (in Japanese).
10) J.A. Pope, "Metal Fatigue," Chapman and Hall Ltd., London, (1959).

SUMMARY

The experiments are described primarily in order to study the influence of stud welding upon fatigue resistance of a plate in tension, and also to obtain information on the S-N relationship for the plate to which a stud-type shear connector is attached, under such a stress condition as tension in the plate and shear on the stud. Then, the test results are discussed in relation with the fatigue behavior of steel and concrete composite constructions in a negative moment.

Further Studies of Composite Steel and Concrete Structures

Etudes ultérieures de structures mixtes acier-béton

Weitere Studien über Verbundkonstruktionen aus Stahl und Beton

J.W. RODERICK
University of Sydney
Sydney, N.S.W., Australia

Much of the work over the last twenty years on composite steel and concrete structures has been devoted to the behaviour of simple composite beams and pin-ended columns. Limited use of this knowledge has been made in the design of concrete encased rigid steel frame structures by permitting some account to be taken of the stiffening effect of the concrete in proportioning members. But full advantage of the composite form will not accrue until such frames are designed to make greater use of the concrete in transmitting moment and shear force from beam to column. When the moment rotation characteristics of these truly composite connections can be reliably forecast, it should be possible to develop plastic design methods for the rigid frame composite steel and concrete structure which could lead to significant savings.

Over the last eight years considerable progress has been made at Sydney University towards the development of analytical methods of this nature. Both experimental and theoretical studies have been undertaken and include the topics: shear force transmission in composite T-beams; the effects of slip and other variables in these beams in both the linear and non-linear loading ranges; the characteristics of the negative moment region in continuous beams; eccentrically loaded pin-ended columns bent about any centroidal axis; and the behaviour of composite beam-to-column connections. In addition repeated loading tests have been made on simple and continuous beams; creep of eccentrically loaded pin-ended columns under sustained loading is also being examined.

SIMPLE BEAMS

The initial work on shear connection was described in a paper by Rao(1) who tested a variety of connectors and concluded that welded studs are likely to be the most economical. Their flexibility does however lead to slip between slab and joist which in turn affects the distribution of forces on the studs and leads to increased deflections of the beams. The experimental work has been directed mainly to examining these effects.

In addition to studies of small-scale beams, tests were carried out on 17ft span T-beams of 10in. x 4½in. @ 25 lb. R.S.J. with 72in. x 4in. concrete slabs, connected by pairs of 3/4in. studs, 3in. long and spaced at intervals of 15in. A symmetrical two point loading acting at third points of the span was applied in increments right up to failure. While the main purpose was to

observe deformations and ultimate load carrying characteristics, the opportunity was taken to examine the effects of using different stud steels and both normal and lightweight aggregate concretes. The relevant information for the first three beams (A1, A2 and A3) is given in Fig.1. Due to the predominant influence of the steel joist in flexure, the difference in concretes did not have a particularly significant effect upon the load-deflection relationship (Fig.1c) despite the low modulus of the lightweight concrete (Fig.1b). Different strengths of steel studs also had little effect; in fact the ultimate strength of the stud joist combination occurs by shearing out of the joist material below the stud.

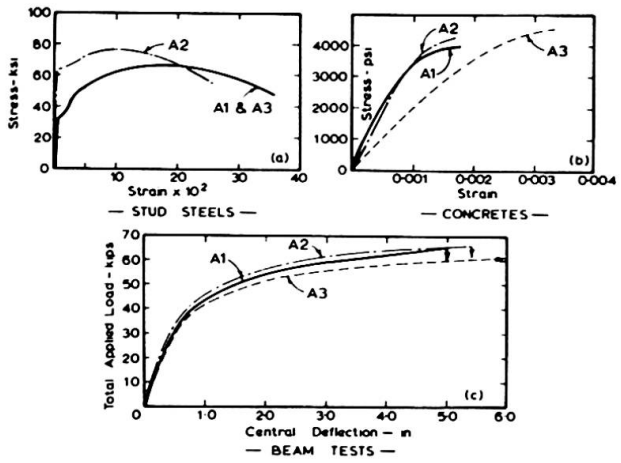

FIG. 1 LOAD DEFLECTION AND STRESS - STRAIN CURVES FOR FULL SCALE BEAM TESTS

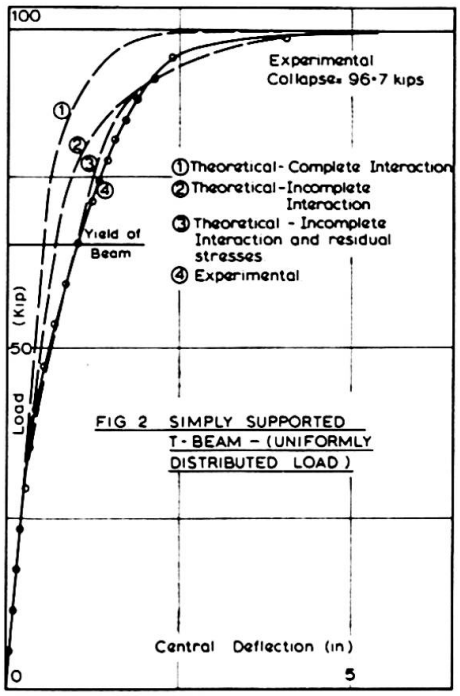

FIG 2 SIMPLY SUPPORTED T-BEAM – (UNIFORMLY DISTRIBUTED LOAD)

In Fig.2 load deflection data is given for beam A6 similar to A2 but subjected to simulated uniformly distributed loading. Curve 1 was obtained by using the Newmark(2) solution in the linear range after allowing for shear deflection; thereafter the curve depends upon an iterative plastic analysis assuming no slip and taking the stress-strain relationship for both steel and concrete to be of the form shown at (a) in Fig.3. For curve 2 the effect of slip as measured in a push-out test has been introduced into the analysis. For curve 3 a uniform distribution of residual stress of 20 kips/in.^{2} over the flange section has been assumed and taken into account in the analysis. This last solution gives better agreement with the test results.

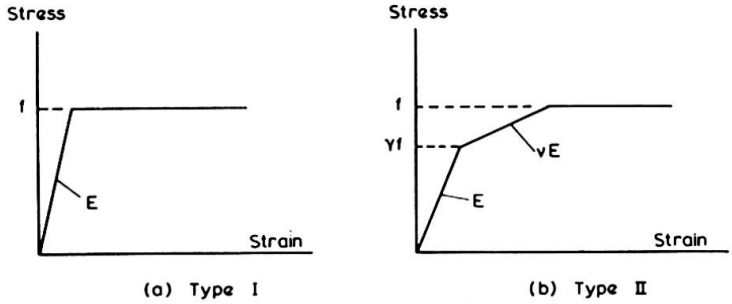

FIG. 3 ASSUMED STRESS-STRAIN RELATIONSHIPS

Repeated Loading. In order to gain understanding of the behaviour of composite beams under abnormally high repeated loading two tests were carried out on full-scale beams R1 and R2 respectively similar to A1 and A2 above. They were subjected to a programme of loading designed to produce the same maximum

stress levels on the most highly loaded pair of studs as occurred in the respective push-out tests PR5 and KR2. All loads were applied at a frequency of 30 cycles/minute and were varied from nominal zero to maximum value.

Table 1. Forces on Critical Studs for Beams R1 and R2

Max. value of repeated load on beam including selfweight (kips)	Computed force on pair of studs (kips)	
	(a) assuming rigid studs	(b) allowing for slip
8.02	11.2	10.0
10.14	14.0	12.5
12.30	17.1	15.0
14.52	20.2	17.5
16.87	23.5	20.0

Table 2. Comparison of Failure of Critical Studs - Beams R1 and R2

Condition of Stud	No. of Cycles of Load Applied x 10^{-6}							
	Beam BR1				Beam BR2			
	Stud No.				Stud No.			
	3*	4	25	26	3	4	25	26
Initial Weakening	2.33	2.33	2.33	2.33	2.45	2.45	2.35	2.24
Only Minor Stud Response	2.40	2.40	2.41	2.41	2.82	2.82	2.82	2.45
Complete Stud Failure	2.58	2.41	2.48	2.48	3.15	2.90	2.99	2.99

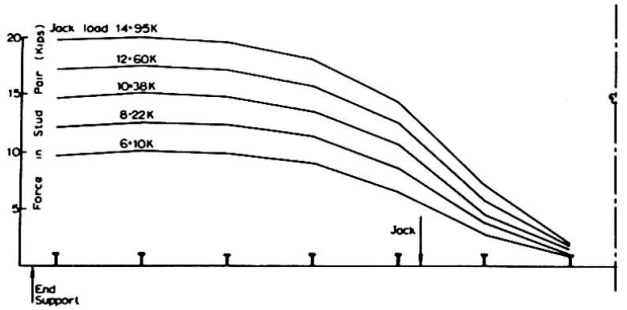

FIG 4 THEORETICAL DISTRIBUTION OF STUD FORCES FOR BEAM R1 (INCLUDING THE EFFECT OF SLIP)

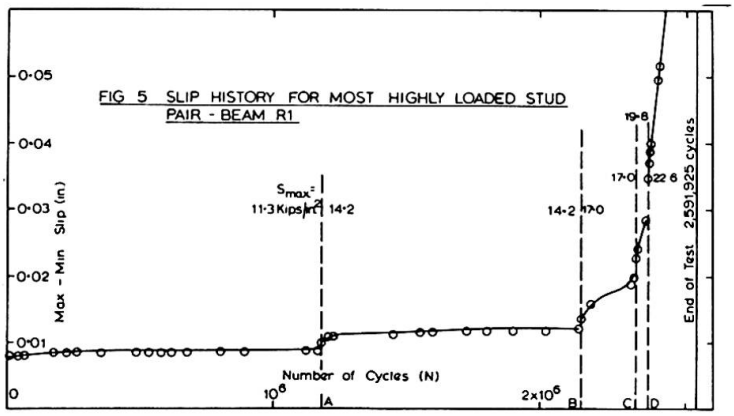

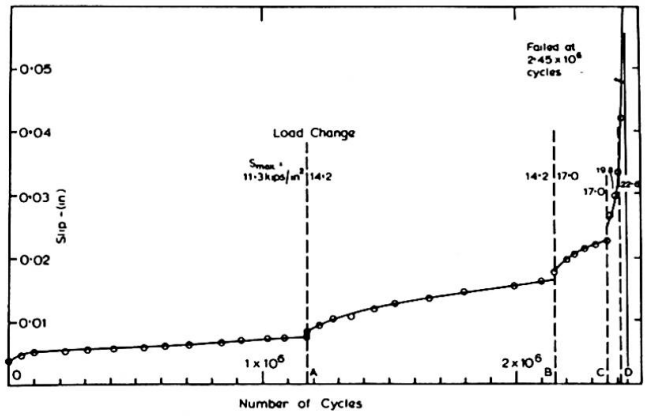

FIG 6 PUSH-OUT SPECIMEN PR5 - HISTORY OF SLIP

From accurate analysis taking account of slip, connector force distributions along the beams as shown in Fig.4 and Table 1, were evaluated. It will be seen that the maximum stud force is less than the value obtained by approximate methods assuming rigid studs. The most highly loaded pair of studs in the beams, those second from the end, were then subjected to the peak stud stresses shown in Fig.5. The slip curves for the critical studs (Fig.5) were very similar in form to those observed in the corresponding push-out tests (Fig.6). The comparison of conditions at failure for the two beams is set out in Table 2.

These tests showed that stud connected composite beams could sustain over two million applications of stresses of approximately design value, with practically no decrease in structural efficiency. Thereafter they were capable of resisting another three increments of load up to a total of twice the initial value with only a gradual deterioration of the shear connection.

CONTINUOUS BEAMS

The work on continuous beams subjected to static loading has been directed mainly to studying the behaviour in the negative moment region to provide data for use in the design of beams in rigid frame composite structures. Tests were carried out on inverted beams and small-scale continuous beams of T-section which led to the conclusion that these can confidently be designed to carry negative moments equal to the ultimate moment of resistance of the section in the positive moment region. This can be achieved by the provision of adequate reinforcement in the slab or by plating the steel section. In both cases "strain hardening" hinges of adequate rotational capacity can be developed.

Repeated Loading. A study is also being made of the behaviour of continuous beams under repeated loading of constant amplitude.

A preliminary test has been carried out on a beam of two 17ft spans and having a section composed of a 10in. x 4½in. @ 25 lb. R.S.J. and a 72in. x 4in. concrete slab with the same arrangements of studs as for beam A1. The loading consisted of central concentrated loads of 20 kips applied to each span simultaneously at 30 cycles/minute.

The elastic analysis for these tests was further refined by using three straight lines as an approximation to the observed load slip curve obtained from push-out tests. On this basis it was found from the analysis that the most heavily loaded pair of studs should carry 13.8 kips as indicated in Fig.7. A comparison of observed and theoretical deflections (Fig.8) shows good agreement.

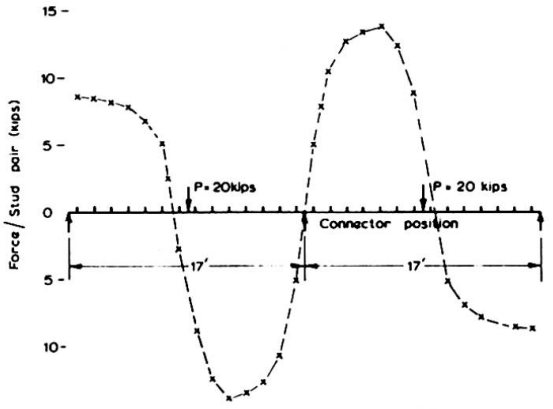

FIG. 7 DISTRIBUTION OF STUD FORCES IN CONTINUOUS BEAM USING AN ANALYTICAL METHOD ALLOWING FOR SLIP

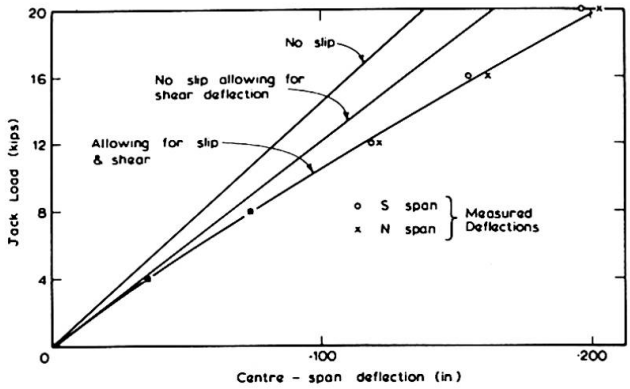

FIG 8 THEORETICAL AND EXPERIMENTAL LOAD - DEFLECTION CURVE FOR CONTINUOUS COMPOSITE BEAM

The beam loading was cycled between 0.8 and 20 kips and complete failure occurred at the first stud pair at 580,000 cycles which compared favourably with a life of 500,000 cycles as indicated by the British Code CP117(3). Sequential failure of adjacent studs then took place; at 820,000 cycles all studs had failed in one of the most heavily loaded shear spans. Final failure was brought about by the development of a fatigue crack starting at a welded bracket on the joist where the bending stress had risen to 10 kips/in.^{2}

COLUMNS

Since the completion of the early work (4) on slender pin-ended composite columns bent about their minor axes, the computerised

analysis derived for the study of these columns has been applied to cases of bending about any centroidal axis. The analysis is based upon the assumption that both steel and concrete have stress-strain relationships of the form shown in Fig.3(b) and enables the deflected form of the column to be determined for any condition of equilibrium.

Typical comparisons of experimental and theoretical results for pin-ended columns of 4in. x 3in. R.S.J. with 2in. concrete cover bent about a diagonal axis are shown in Fig.9. It will be noted that theoretically "yielding" of both the steel (SY2) and the concrete (CY2) occurs before the critical load for instability. In fact in nearly all tests this critical load was attained shortly after yielding of the steel had commenced. A summary of a whole series of tests on 7ft. long columns of this section expressed in terms of collapse load (Fig.10) would suggest that the analysis is of general application for concrete encased steel columns. It

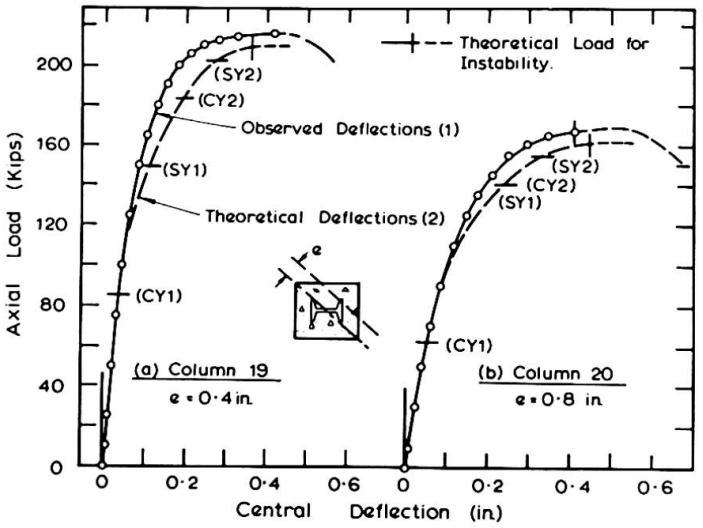

FIG. 9 LOAD - DEFLECTION RELATIONSHIPS FOR 7 FT. BENT ABOUT BOTH PRINCIPAL AXES (4"x3"RSJ(8"x7"))

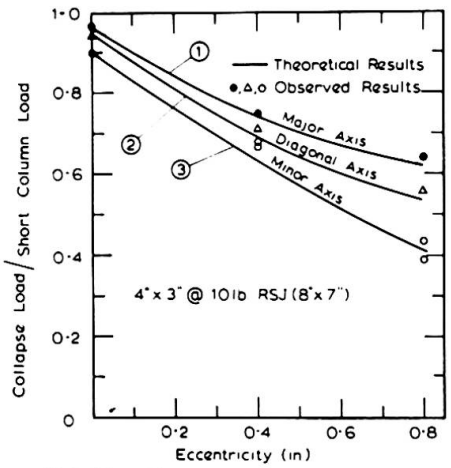

FIG. 10 RELATIONSHIP BETWEEN COLLAPSE LOAD AND ECCENTRICITY FOR 7FT COLUMNS

further demonstrates that the assumptions that (a) torsional displacements can be neglected and (b) bending displacements occur in the plane of the applied moment, are fully justified for composite columns which are roughly square in section.

Consideration has also been given to eccentrically loaded pin-ended composite battened columns. As a basic study examination has been made of columns consisting of 2/3in. x 1½in. @ 4.5 lb. channels 1 in. apart without any battens and for which reliance was placed entirely upon the plain concrete to transmit shear between the channels. Typical

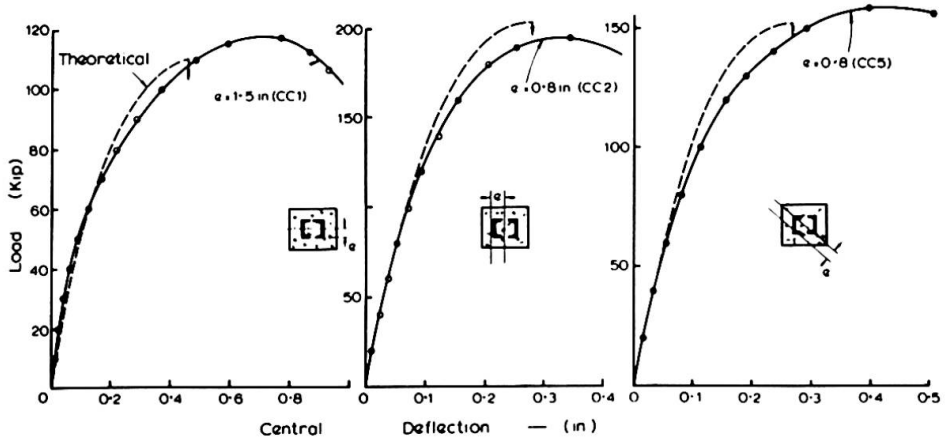

FIG 11 BATTEN COLUMNS

results together with theoretical solutions are shown in Fig.11. In all cases spalling and crushing of concrete occurred after the maximum theoretical axial load had been attained.

Pin-ended columns consisting of concrete filled tubes of 8in. x 8in. x 3/8in. section, have also been tested. Results for two specimens are given in Fig.12. Again the agreement with the theoretical solution is good.

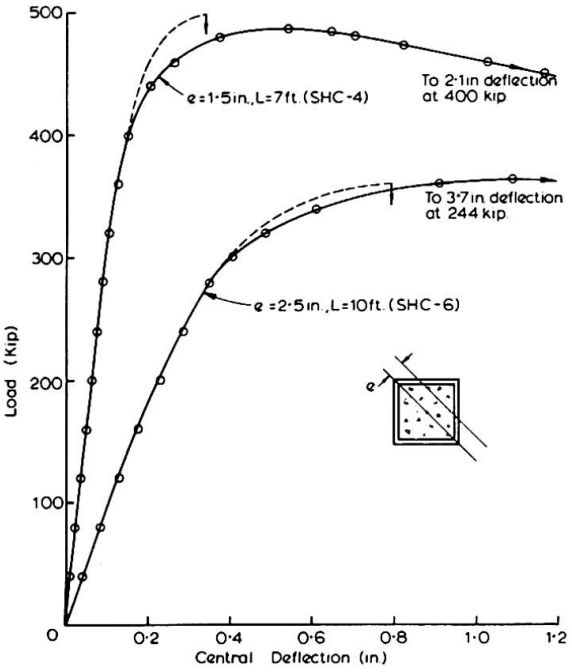

FIG 12 LOAD-CENTRAL DEFLECTION CURVES FOR COLUMNS SHC-4 AND SHC-6

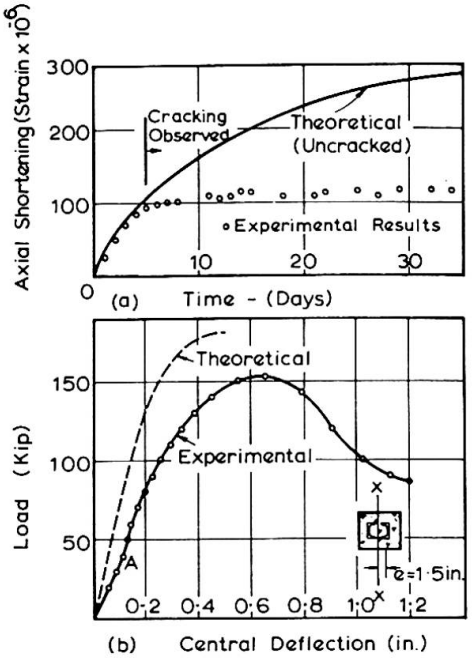

FIG.13 STRAIN DATA AND LOAD–DEFLECTION CURVES FOR COLUMN CC12.

Shrinkage and Creep of Concrete. Several aspects of the effects of shrinkage and creep of concrete on the load carrying capacity of pin-ended columns are being investigated. The test columns were all of the double channel type (Fig.11) and were 7ft. long.

Of particular interest is the case of a column subjected to large initial shrinkage stresses. For column CC12 containing an aggregate known for its high shrinkage properties, cracking commenced after 4 days drying and after some 35 days the cracking was extensive (Fig.13a). The comparison (Fig.13b) of the experimental deflections with the theoretical values assuming an uncracked section, demonstrates the effect. The portion OA of the experimental curve indicates the region where cracks on the compressive side were closing up; once point A had been reached the column acted as a normal uncracked member with somewhat higher steel stress and an increased column deflection. This extensive cracking does in fact act as a large initial imperfection which increases the central deflections and lowers the ultimate load of the column.

Column CC7 was used to examine the effect of sustained axial load applied at an eccentricity of 1.6in. about the major axis. The short term strength of this column was estimated to be 160 kips. Curves showing central deflection against time were calculated from a creep rate analysis based on control tests, and are shown in

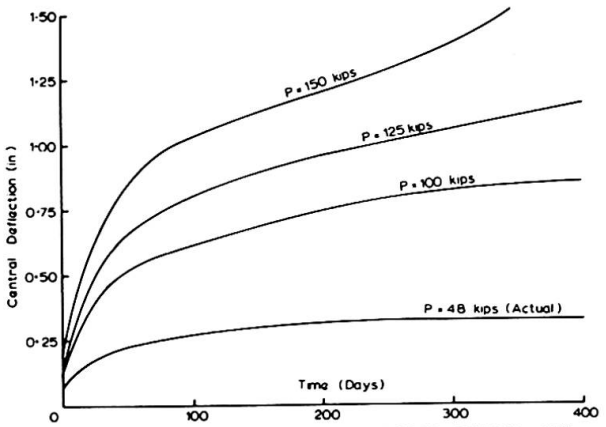

FIG 14 THEORETICAL BEHAVIOUR OF COMPOSITE COLUMN CC7 UNDER INCREASED SUSTAINED LOADS.

Fig.14. For a load of 150 kips applied for 200 days it was found that the deflection rate was still increasing with time. For 100 kips the deflection rate was always decreasing with time. It could therefore be argued that the critical load was of the order of 125 kips and less than the short term strength of 160 kips. It is of interest to note that the bare channels are themselves theoretically capable of carrying 48 kips before collapse occurs assuming provision is made for shear transmission.

CONNECTIONS

At first sight it might well be thought that in composite construction connections should be designed on the basis that both the shearing force and bending moment to be transmitted are carried entirely by the steelwork. Fortunately this is far from the truth in practice since the concrete when appropriately reinforced can assist the steel in several ways.

In the work at Sydney(5) both internal and external beam-to-column connections have been studied, though the latter has proved to be the more interesting in attempting to design connections in which the concrete around the steel connection will not disintegrate even after considerable permanent deformation has taken place. The successful connection eventually developed is shown diagrammatically in Fig.15. The steel beam is attached to the steel column by welding on top and bottom moment plates and a shear plate to the column below the beam. It will also be seen from the Figure that two of the reinforcing bars in the slab are carried around the column and another pair are turned down into the concrete encasement of the column. No other reinforcement was provided in the column. Tests on these units have shown that the concrete remained fully active right up to ultimate load.

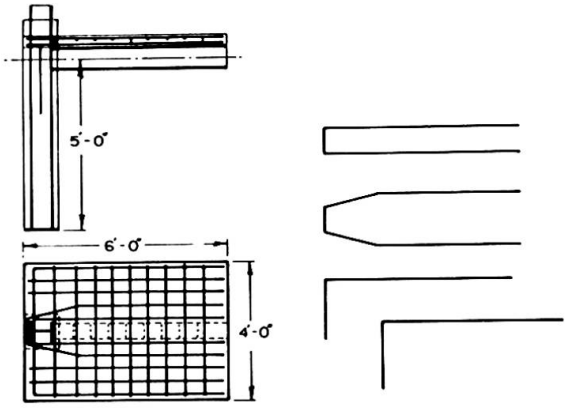

FIG 15 COMPOSITE CONNECTION REINFORCEMENT DETAILS

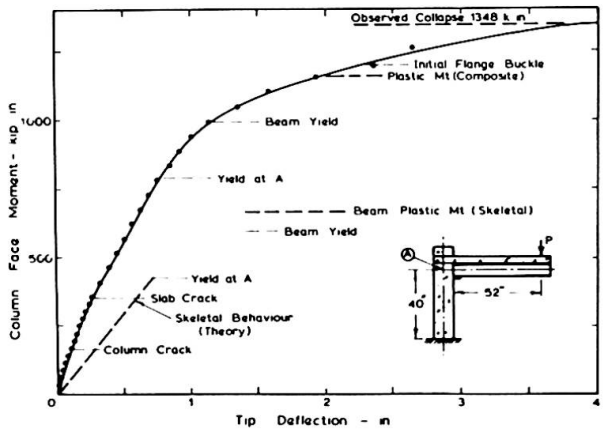

FIG 16 BEHAVIOUR OF SPECIMEN USC3

When the results of tests on bare steel units are compared with those for the corresponding composite connections, the improvment obtained with the latter is immediately obvious as may be judged from the curves in Fig.16. The upper curve relates to an 8in. x 5¼in. @ 17 lb. U.B. attached through welded studs to a 48in. x 4in. thick slab; the column consisted of an 8in. x 8in. @ 31 lb. U.C. having a 2in. cover of concrete.

The composite unit proved to be considerably stiffer than the bare steel component. The latter transmits the reactions from the beam largely by shearing action through the column web adjacent to the end of the beam. Failure occurs when the stress in this web reaches the value $1/\sqrt{3}$ times the tensile yield stress of the steel. In the composite connection the effect of the concrete between the flanges of the column is to share the shear force formerly transmitted entirely through the column web. Yielding does eventually occur in this area but again the presence of the concrete enables the connection to go on transmitting moment right up to the full plastic value of the composite T-beam.

Finally, acknowledgment is made to the present members of the Sydney group, Messrs. P.Ansourian, R.Q.Bridge and M.W.Hallam and to former members Dr. N.M.Hawkins and Dr. Y.O.Loke, all of whom contributed to the results summarised in this paper.

BIBLIOGRAPHY

1. Rao, S.N. - "Composite Construction - Tests on Small-Scale Shear Connectors". Civ.Engng Trans.Instn Engrs Aust., Vol.CE12, No.1, April 1970.

2. Newmark, N.M., Siess, C.P. & Viest, I.M. - "Tests and Analysis of Composite Beams with Incomplete Interaction". Proc.Soc.Exper.Stress Anal. Vol.9, No.1, 1951.

3. British Standard Code of Practice CP117 - "Composite Construction in Steel and Concrete". Part 2, 1967, British Standards Institution.

4. Roderick, J.W. & Rogers, D.F. - Load Carrying Capacity of Simple Composite Columns". Proc.Am.Soc.Civ.Engrs, J.Struct.Div., Vol.95, No.ST2, Feb.1969, pp.209-228.

5. Ansourian, P. - "Connections in Composite Framed Structures". Concrete Conference - Problems in Composite Structures, Instn Engrs Aust., Adelaide, Sept.1971.

SUMMARY

An account is given of the behaviour of composite steel and concrete components under the action of short and long term static loading and of repeated loading. The principal components studied were: simple and continuous composite T-beams; pin-ended composite columns made up from single and fabricated steel sections; and composite beam-to-column connections.

Steel-Reinforced Concrete Construction

Construction mixte acier-béton

Stahl-Beton Verbund-Konstruktion

TAKEO NAKA
Professor-Emeritus of the University of Tokyo, Japan

MINORU WAKABAYASHI
Professor of Kyoto University, Japan

JIRO MURATA
Professor of Tokyo Metropolitan University, Japan

Messrs. C.F. McDevitt and I.M. Viest outline very excellently the present state of the art of combining steel with concrete to form useful structural components as composite steel concrete beams, concrete encased steel beams, and steel-concrete columns. Responsing to the authors' wishes T. Naka would like to make some additional supplements to the topics described above. Since the Kanto-Earthquake occurred September 1st, 1923, almost all Japanese structural designers recognized that the composite structure having steel skeleton encased in reinforced concrete has predominantly earthquake-proof merits than any other kind of structures for multi-storeyed buildings. It behaves without serious damages under strong action of earthquake even when reinforced concrete construction shows severe cracks at columns, beam-to-column connections, shear walls, etc., which sometimes make its fatal destruction. The famous building of Nihon-Kogyo Bank, Marunouchi, Tokyo of which structure was designed by Professor Tachu Naito as steel-reinforced concrete construction with suitable shear walls showed no damages in any details of the building by the Kanto-Earthquake 1923 while in the near site Nai-Gai Building of reinforced concrete construction of about 30m height from ground level was utterly crashed down. It seems that well resistances of steel-reinforced concrete construction are due to toughness of steel skeleton after their ultimate strength of the composite structural members. Earlier papers of M. Hamada in 1929 (1) and R. Tanabashi in 1937 (2) reported that the strength and stiffeness of steel-reinforced concrete beam are almost equal to the values of reinforced concrete beam having equivalent reinforcements instead of the same area of steel skeleton. About twenty years after same results were ascertained by experimental researches of Y. Tsuboi (3), (4), T. Naito (5) and T. Naka (6), (7).

STANDARD FOR STEEL-REINFORCED CONCRETE STRUCTURE

Until 1958 there was no standard for structural calculation of steel-reinforced concrete construction and so many kinds of such composite construction were erected. This is mainly because the structural design is depending on the elastic theory and not considering the structural safety after severe deformations due to strong earthquake effects. Architectural Institute of Japan started the committee for making AIJ Standard for Structural Calculation of Steel-Reinforced Concrete Structures in 1951 to which T. Naka was the chairman and the first version of the AIJ Standard was

published in 1958. The revised edition was published in 1963 while in these years many tests were carried out and their results obtained were adopted in the revised standard of AIJ. Reports by T. Naka and his staff may be shown in (8), (9), (10), (11), (12). In 1963 Ministry of Construction indicated recommendations in which multi-storeyed buildings having seven or more floors above ground level should generally have steel skeleton which would be understood as steel-reinforced concrete construction. The current officially approved standard of the construction is that of AIJ revised one in 1963. The basic principle of the standard is as follows; the standard shall be applied to the structural calculation of steel-reinforced concrete construction used generally in Japan, the part of reinforced concrete shall be designed conforming to the AIJ Standard for Reinforced Concrete Construction and the part of steel skeleton shall be designed compling with the AIJ Standard for Steel Construction excepting the requirements for local buckling of steel members which may be ignored to the steel skeleton encased in reinforced concrete. The most special features of the standard are in the assumption that the designed maximum strength of members is simply obtained by superposition of both strength of steel skeleton and reinforced concrete construction.

For beams: The section of beams shall be determined by the following formula; allowable bending moment $M = {}_sM + {}_rM$, where ${}_sM$ is allowable bending moment of steel section only and ${}_rM$ is allowable bending moment of reinforced concrete.

For columns: The section of columns shall be determined by the following formulae assuming compression to be positive, (1) when ${}_rN_c \geq N \geq {}_rN_t$, $N = {}_rN$ and $M = {}_sM + {}_rM$ and (2) when $N > {}_rN_c$ or $N < {}_rN_t$, $N = {}_sN + {}_rN$ and $M = {}_sM$, where N and M are design axial force and bending moment respectively, ${}_sN$ and ${}_sM$ are allowable axial force and bending moment of steel skeleton respectively, ${}_rN$ and ${}_rM$ are allowable axial force and bending moment of reinforced concrete respectively, ${}_rN_c$ and ${}_rN_t$ are allowable compression and tension of reinforced concrete respectively when subjected to axial force only.

For shear: $Q = {}_sQ + {}_rQ$ where ${}_sQ$ and ${}_rQ$ are allowable shear computed for steel skeleton and allowable shear computed for web reinforcing bars or adding the effects of batten plates of steel skeleton to reinforced concrete respectively.

For bond, anchorage, beam-to-column connections, joints and column bases are deliberately described in the standard.

Although the formulae of the standard are very simple in their expression they are deduced from experimental results obtained by many researchers shown in references and verified by the ultimate strength theory which was analysed by M. Wakabayashi.

Wide Flange Section and H-shape Steel Skeleton in the Composite Structures

Steel skeleton of the composite structure is now changing gradually in form and type to welded or rolled sections such as wide flange and H-shapes to make beams, columns, etc., from traditional built-up sections of riveted angles of lattice-work. Design manual of H-shape steel for the application to the composite structure is shown in references (33) and (34). Japanese Building Law and its Enforcement approve to use welding joints and connections of steel members in 1950. Since 1959 wide flange and H-shape rolled sections have been produced in Japan, the use of them accelerates the change of form and type of steel skeleton of the composite structure.

Studies upon such type of composite structures are required and some of the results obtained are shown in references (6), (21), (22), (23), (24), (25), (26), (27), (28), (29), (30).

Elasto-Plastic Behavior

For the sake of rehabitation of big cities in Japan tall buildings of dwelling houses, apartments and hotels are recently built in the type of steel-reinforced concrete construction which requires high tensile strength steel of good weldability for the skeleton and dynamic characteristics for earthquake-proof design. Damages on reinforced concrete constructions by the Tokachioki-Earthquake occurred September 16th, 1968 and by the San Fernando-Earthquake occurred February 9th, 1971 indicate that buildings should have sufficient toughness against to the severe motion induced by any earthquake. M. Wakabayashi made experimental researches to find elasto-plastic behavior of steel-reinforced concrete columns and frames under repeated loading. Fig.1 shows the test specimen and Fig.2 shows the test set-up. Load-deflection curves obtained by the tests are shown in Fig.3. Table 1 shows the test schedule. The third revised AIJ Standard for the composite structure will be issued in this year and the fourth one will be published about four years after when dynamic characteristics of the composite structure may be clarified through the serial tests upon the problems.

In the current AIJ Standard for the composite structure two requirements to the quantity of steels are specified as follows: the ratio of the total sectional area of steel members and reinforcement in axial direction of the column to the gross area of concrete should be not less than 0.8% and the ratio of the total sectional area of principal reinforcement of the column to the gross area of concrete should not be more than 4%. Regarding the steel skeleton as reinforcement the composite structure is allowed to be calculated by the AIJ Standard for Reinforced Concrete Construction, if necessary, in the current AIJ Standard for the composite structure. This case may be useful when the steel skeleton of the composite structure has an asymmetrical section or its placement is in unbalanced situation of the gross section.

Steel-Reinforced Concrete Structures in Bridge Construction

In 1927 two bridges of Melan-type were erected in Tokyo, one is Hijiri-Bashi, Ochanomizu, Hongo and another is Yaesu-Bashi, Yaesu, Nihonbashi. The former has trussed girder using L-90x90, however its structural calculation was carried as the reinforced concrete construction. Anyhow these bridges are out of the category of steel-reinforced concrete construction above written. The first experience of the composite structure was at the approach to the Saikai-Bashi, Kyushu in 1955 and the second one was at the approach to the Wakato-O-Hashi, Kyushu in 1962 both using AIJ Standard for Structural Calculation of Steel-Reinforced Concrete Structures with some modifications on allowable stresses. The Metropolitan Expressway Corporation and the Han-Shin Expressway Corporation published recently their own Standard for the composite structure (40), (41) to which M. Wakabayashi worked as a member of the committee for making the standards. Both are very similar to the AIJ Standard in principles.

J. Murata, K. Tsuno, M. Izumi and N. Yamadera are continueing their studies on the composite structures which are used in expressway construction especially. Y. Nishino is one of their research group. (36), (37), (38), (39). The application of rolled wide flange section of heavy sizes to the composite structure of civil engineering fields is becoming a big problem. M. Kokubu and others are performing their research systems and some results are shown in references. (35).

Present Discussions and Future Problems

As the design formulae are expressed in superposition of the allowable stresses of the steel skeleton and the reinforced concrete construction of the composite structures, they can cover very wide range of the ratio of the steel skeleton and the reinforced concrete construction. On the contrary, load-deflection relationship can not be obtained from these formulae. Such deficiency in the current standard of AIJ or others should be supplemented in the succeeding revised editions. One of the most important discussion in preparing the third revised AIJ Standard for the composite structure is the design formula of shear for column where $Q = {}_{s}Q$ should be taken disregarding ${}_{r}Q$ provided minimum requirements for hoops of reinforced concrete is satisfied. This proposal seems very severe for design of the composite column, however, it is intelligible by the experimental facts that almost all damages of reinforced concrete constructions by the recent earthquakes of Tokachioki 1968 and San Fernando 1971 were due to shear cracks of the columns. On the other hand the revised Standard will take into consideration of toughness of the composite structure that has great capacity of storey-drift more than 5cm without any crack in the construction. It is another problem how to evaluate the sufficient deformability of the composite structure beyond the ultimate strength without fatal collapse.

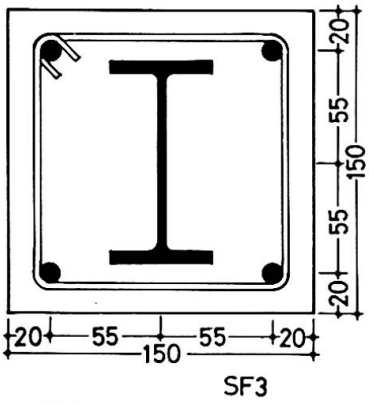

Fig. 1 Cross Section of Test Specimen

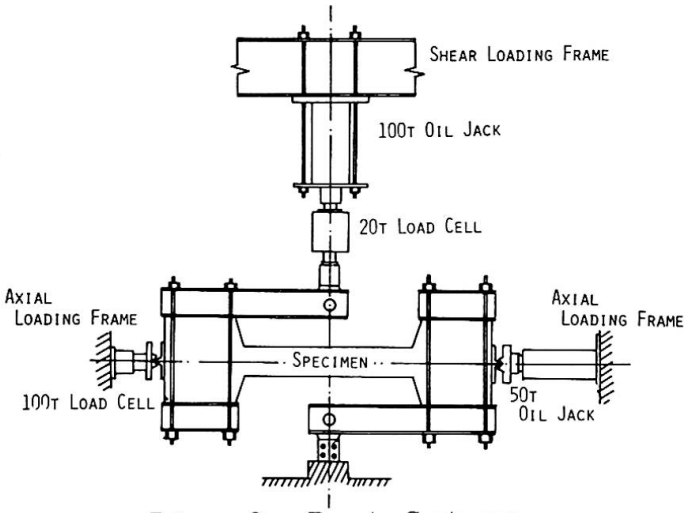

Fig. 2 Test Set-up

Table 1 Test Schedule

	Name of Specimen	Length (mm)	Main Reinforcing Bar	Shear Reinforcing Bar	Axial Force Ratio	Remarks
SRC (full-web)	BF 0 3 6	900	4-D10	3φ-50@	0,0.3,0.6	Bending Failure
	SF 0 3 6	450	4-D13	3φ-50@	0,0.3,0.6	Shearing Failure
SRC (open-web)	BO 0 3 6	900	4-D10	3φ-50@	0,0.3,0.6	Bending Failure
	SO 0 3 6	450	4-D13	3φ-50@	0,0.3,0.6	Shearing Failure
RC	BR 0 3 6	900	6-D13	3φ-25@	0,0.3,0.6	Bending Failure
	SR 0 3 6	450	8-D13	3φ-50@	0,0.3,0.6	Shearing Failure

Notes: Cross Section of Specimen; 150mm×150mm
Steel Reinforcement; Full-web Specimen; H-100×50×4×6, SS41
Open-web Specimen; Flange 2T-50×13×4×6, SS41
Web Width=15mm, Thickness=4mm, Pitch=75mm

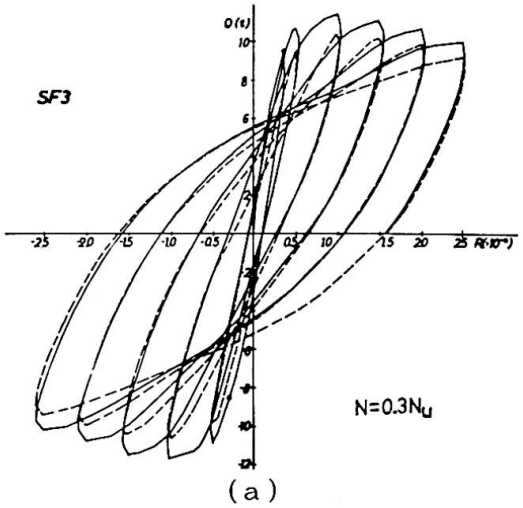

(a)

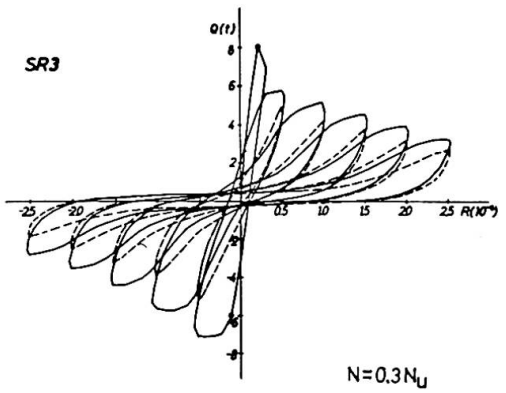

(b)

Fig. 3 Load-Deflection Curve

BIBLIOGRAPHY

1. Hamada, M., "Study on Steel-Concrete Beams," Journal, Architectural Institute, Japan, 5, 1929.
2. Tanabashi, R. and Itomi, M., "Study on Ultimate Strength of Steel-Concrete Members," Transaction No.6, Architectural Institute of Japan, 1937.
3. Tsuboi, Y. and Wakabayashi, M., "Experimental Research on Steel-Reinforced Concrete Structure," Report, Architectural Institute of Japan, 8, 1951.
4. Tsuboi, Y. and Wakabayashi, M., "Test on Steel-Reinforced Concrete Beam Subjected to Bending," Transaction No. 49, Architectural Institute of Japan, 1954.
5. Naito, T., Tsuruta, A. and Tani, S., "Test on Steel-Reinforced Concrete Beam," Report No. 21, Architectural Institute of Japan, 3, 1953.
6. Naka, T. and Takada, S., "Bending Test of Wide Flange Steel-Reinforced Concrete Beam," Report No. 21, Architectural Institute of Japan, 3, 1953.
7. Naka, T. and Ogura, K., "Study on Steel-Reinforced Concrete Construction," Report No. 26, Architectural Institute of Japan, 10, 1953.
8. Naka, T. and Takada, S., "Study on Steel-Reinforced Concrete Structures ---Tests on Shearing Strength of Beams, Part 1," Report No. 22, Architectural Institute of Japan, 5, 1953.
   Naka, T.,Takada, S. and Saito, H., dittoes, Part 2, Report No. 24, 10, 1953, Part 3, Report No. 26, 3, 1954, Part 4, Report No. 27, 5, 1954, Part 5, Report No. 28, 11, 1954, Part 6, Report No. 31, 5, 1955, Part 7, Kanto-District 19th Symposium Report, 3, 1956 and Part 8, Kanto-District 20th Symposium Report, 6, 1956, Architectural Institute of Japan.
9. Sakamoto, Y., Matsushita, K., Takada, S. and Saito, H., "Study on Steel-Reinforced Concrete Structures---Tests on Beam-to-Column Connections, Part 1," Report No. 24, Architectural Institute of Japan, 10, 1953.
   Naka, T., Matsushita, K.,Takada, S. and Saito, H., ditto, Part 2, Report No. 27, Architectural Institute of Japan, 5, 1954.
   Naka, T., Takada, S., Saito, H., Shimizu, H. and Kasajima, M., ditto, Part 3, Kanto-District 19th Symposium Report, 3, 1956.
   Naka, T., Takada, S. and Saito, H., ditto, Part 4, Kanto-District 20th Symposium Report, 6, 1956, Architectural Institute of Japan.
10. Naka, T., Wakabayashi, M., Takada, S., Saito, H. and Kamimura, K., "Study on Steel-Reinforced Light-weight Concrete Structures---Tests on Eccentrically Compressed Columns," Transaction No. 57, Architectural Institute of Japan, 1957.
11. Naka, T. and Ogura, K., "Study on Steel-Reinforced Concrete Structures ---Tests on Beams Subjected to Pure Bending," Report No. 24, Architectural Institute of Japan, 1953.
12. Naka, T., Kato, B. and Tanaka, A.,"Full-Scale Tests on Beam-to-Column Connections of Steel-Reinforced Concrete Structures---Deformation Capacity of Stiffened Joint Panels," Transaction No. 82, Architectural Institute of Japan, 1963.
    Naka, T., Kato, B., Watabe, M., Tanaka, A. and Yamada, S., "Full-Scale Tests on Beam-to-Column Connections of Steel-Reinforced Concrete Structures Subjected to the Horizontal Force," Kanto-District 34th Symposium Report, 5, 1963.
    Naka, T., Kato, B. and Tanaka, A.,"Full-Scale Tests on Beam-to-Column Connections of Steel-Reinforced Concrete Structures Subjected to the Horizontal Force," Transaction No. 89, Architectural Institute of Japan, 1963.

13. Umemura, H. and Toyofuku, T., "Study on Steel-Reinforced Concrete Structures---Tests of Eccentrically Compressed Columns," Report No. 24, Architectural Institute of Japan, 10, 1952.
14. Tsuboi, Y. and Wakabayashi, M., "Study on Steel-Reinforced Concrete Structures---Tests of Eccentrically Compressed Columns," Transaction No. 48, Architectural Institute of Japan, 3, 1954.
15. Tsuboi, Y. and Wakabayashi, M., "Study on Steel-Reinforced Concrete Structures---Tests on Beam-to-Column Connections," Transaction No. 50, Architectural Institute of Japan, 3, 1955.
16. Wakabayashi, M., "Experimental Researches on Steel-Reinforced Concrete Structures," Report of Institute of Industrial Science, University of Tokyo, Vol. 6, No. 2, 1956.
17. Tsuboi, Y., Wakabayashi, M. and Suenaga, Y., "Experimental Tests on Steel-Reinforced Concrete Columns Subjected to Axial and Shearing Forces," Transaction No. 56, Architectural Institute of Japan, 6, 1957.
18. Tsuboi, Y., Wakabayashi, M. and Suenaga, Y., "Experimental Tests on Steel-Reinforced Concrete Beams Subjected to Shearing Stresses," ditto.
19. Matsushita, K. and Takada, S., "Test on Beam-to-Column Connection of Steel-Reinforced Concrete Structures," Transaction No. 57, Architectural Institute of Japan, 1957.
20. Takada, S., "Experimental Study on Steel-Reinforced Concrete Beams Subjected to Shearing Stresses," Transaction No. 55, Architectural Institute of Japan, 2, 1957.
21. Endo, T., "Tests on Beam-to-Column Connection of Steel-Reinforced Concrete Structures," Report at Annual Assembly of Architectural Institute of Japan, 1957.
22. Fujita, T., Sotomura, K., Yajima, S. and Umemura, H., "Experimental Study on Wide Flange Steel-Reinforced Concrete Columns," Report No. 135, Architectural Institute of Japan, 1957.
23. Koreishi, I., Umemura, H., Aoyama, H. and Ito, M., "Study on Panel Zone of Beam-to-Column Connection of Steel-Reinforced Concrete Structure," Kanto-District Symposium Report, 1959 and " Tests on Beam-to-Column Connection and Column of Steel-Reinforced Concrete Structure" Report at Annual Assembly of Architectural Institute of Japan, 1959.
24. Kato, B. and Tanaka, A., "Beam-to-Column Connection of Steel-Reinforced Concrete Structure," Steel Research No. 256, Yawata Iron and Steel Co.
25. Yokoo, Y., Wakabayashi, M. and Suenaga, Y., "Study on Steel-Reinforced Concrete Structure using H shape Steel," Transaction No. 132, Architectural Institute of Japan, 2, 1967.
26. Yokoo, Y., Wakabayashi, M. and Suenaga, Y., "Study on Steel-Reinforced Concrete Structure using H-shape Steel, No. 2," Transaction No. 133, Architectural Institute of Japan, 3, 1967.
27. Yokoo, Y., Wakabayashi, M. and Suenaga, Y., "Study on Steel-Reinforced Concrete Structure using H-shape Steel, No. 3," Transaction No. 134, Architectural Institute of Japan, 4, 1967.
28. Yokoo, Y., Wakabayashi, M. and Suenaga, Y., "Study on Steel-Reinforced Concrete Structure using H-shape Steel, No. 4-1," Transaction No. 135, Architectural Institute of Japan, 5, 1967.
29. Yokoo, Y., Wakabayashi, M. and Suenaga, Y., "Study on Steel-Reinforced Concrete Structure using H-shape Steel, No. 4-2," Transaction No. 136, Architectural Institute of Japan, 6, 1967.
30. Wakabayashi, M. and Yamaguchi, T., "Elasto-Plastic Behavior of Steel-Reinforced Concrete Structures," Kinki-District Symposium Report, 5, 1971.
31. Wakabayashi, M. and Sasaki, R., "Study on Steel-Reinforced Light-weight Concrete Structures," Report at Annual Assembly of Architectural Institute of Japan, 1969.
32. AIJ Standard for Structural Calculation of Steel-Reinforced Concrete Structures, Architectural Institute of Japan, 1958 and 1963.
33. Design Manual of H-shape Steel for Structures, Yawata Steel Co. 1961.

34. Design Manual of H-shape Steel for Structures, Society of Steel Construction of Japan, 1967.
35. Osaka, Y., "Design Method of Railway Bridge with Mixed H-shape Steel-Concrete Slabs," Concrete Journal, Vol. 6, No. 3, 1968.
36. Nishino, Y., "Application of Steel-Reinforced Concrete Structures to Civil Engineering Constructions," Journal, Institute of Civil Engineerin 1967.
37. Izumi, M. and Yamadera, T., "On Piers of Steel-Reinforced Concrete Construction," Concrete Journal, Vol. 6, No. 3, 1968.
38. Murata, J., Nishino, Y. and Yamadera, T., "On the Design of Frame-Corner of Steel-Reinforced Concrete Structures," Report at the 22nd Annual Assembly of Institute of Civil Engineering, 1971.
39. Murata, J., Nishino, Y. and Izumi, M., "On the Torsion of Steel-Reinforced Concrete Members," Report at the 22nd Annual Assembly of Institute of Civil Engineering, 1971.
40. Design Standard for Steel-Reinforced Concrete Construction, Metropolitan Expressway Corporation, 1967.
41. Design Standard for Steel-Reinforced Concrete Construction, Han-Shin Expressway Corporation, 1968.

SUMMARY

The steel-reinforced concrete structures which are particularly developed in Japan are introduced as the most reliable earthquake-proof construction for multi-storeyed buildings.

AIJ Standard for the calculation of the composite structures is briefly described. That is depending on the ultimate strength theory and test results. Application of the composite structures to the civil engineering construction is very hopeful as design method in seismic zone in the world.

Summary of Full-Scale Laboratory Tests of Concrete Slabs Reinforced With Cold-Formed Steel Decking

Résumé d'essais en laboratoire sur des dalles en béton armé avec des tôles façonnées à froid

Eine Zusammenfassung von Laborversuchen an mit kaltverformten Stahlplatten armierten Betondecken

M.L. PORTER C.E. EKBERG, Jr.
Department of Civil Engineering
Engineering Research Institute
Iowa State University, Ames, Iowa, USA

INTRODUCTION

Reference is made by C. F. McDevitt and I. M. Viest[1] to the development and use of cold-formed steel decking as a form and as composite reinforcement for reinforced concrete floor slabs. The increased use of cold-formed steel-deck-reinforced concrete floor slabs stems primarily from the economic advantages including elimination of the need to install and remove formwork, ease in handling and placing the deck sheets, convenience of a working platform prior to casting, and providing the steel reinforcement for the floor slab through various shear connecting devices to give positive interaction between the steel and the concrete.

Particular reference is made by McDevitt and Viest[1] to an extensive theoretical and experimental investigation of steel decking as reinforcement for concrete slabs at Iowa State University. This investigation was initiated in 1966 under the sponsorship of the American Iron and Steel Institute to explore various aspects of the cold-formed steel-deck-reinforced floor slabs. To date 273 tests using decks from five different manufacturers have been conducted including the following types (all subjected to static loading unless otherwise indicated):

1. single span, simply supported one-way slab elements;
2. pushout specimens;
3. single span, simply supported one-way slab elements subjected to repeated loading;
4. single span, simply supported slab elements with the deck corrugations transverse to the span;
5. multiple span one-way slab elements;
6. single span slab elements containing variable welded wire fabric; and
7. full-scale two-way slabs consisting of a single span on four simply supported edges.

Extensive laboratory tests have shown that most of the one-way steel-deck-reinforced concrete slab systems exhibit a shear-bond type of failure. This is characterized by the development of a diagonal crack just before failure, followed by an observable end-slip between steel decking and concrete. An experimental linear regression relationship which permits calculation of the ultimate shear capacity of a one-way slab element was developed by Dr. R. M. Schuster[2] at Iowa State University in 1969.

This paper will focus primarily on the investigation of four full-scale slab tests, item No. 7 on the above list. The objective of this research was to develop information that would lead to improved criteria for the design of such systems. Since testing of the fourth slab of the series was only recently completed, it was not possible to reduce all the data in time for presentation. It was possible, however, to include a variety of information which describes the behavioral characteristics of each slab as it was loaded to failure in the laboratory. These characteristics include crack patterns, vertical deflections, reaction distributions, and end-slip.

DESCRIPTION OF FULL-SCALE SLAB TESTS

Figure 1 shows the general layout of the four full-scale slab tests. All four slabs had nominal out-to-out dimensions of 12 X 16 ft and were loaded with four concentrated loads located as shown in Fig. 1. The four concentrated loads were chosen to approximate the effect of a fork-lift truck, and to ascertain the load distributions encountered with concentrated loads on steel-deck-reinforced floor slabs. All slabs had the steel decking placed with its corrugations parallel to the 12 ft length as indicated in Fig. 1.

The first three slabs were constructed with steel decking, which had rolled embossments to provide a positive shear transfer between decking and concrete, whereas the fourth slab had steel decking with transverse wires spaced 3 in. apart spot-welded to the tops of the corrugations for shear transfer. Figure 2 shows a typical cross section for each deck type.

Table 1 provides data on various properties of the material for each of the four test slabs. The out-to-out slab thickness varied somewhat in each slab due to deflection of the deck under the dead weight of the wet concrete. The values of average thickness were determined from measurements taken after each slab was sawed into sections following completion of tests. The concrete strengths were obtained from tests on standard 6 X 12 in. cylinders, and the modulus of rupture values refer to 6 X 6 X 36 in. plain concrete beams.

Supplementary reinforcement in the form of welded wire fabric (WWF) was placed directly on top of the steel decking in the first and second slabs. Slab 1 contained 6 X 6 X 6/6 WWF and slab 2 contained 6 X 12 X 0/4 WWF; however, slab 3 contained no welded wire fabric. The fabric in slab 2 was placed so that the zero gage wire (on 6-in. centers) was transverse to the corrugations of the decking. Table 1 shows the steel areas and yield strengths of the steel decking and the welded wire fabric.

The four slabs were instrumented with strain gages on both the concrete and steel decking at about 17 locations with rosette gage arrangements. Deflection dials to measure vertical deflections were located at about 28 locations. Six roller transducers were placed along the south edge and 11 ball bearing transducers were placed along the west edge of the slab. These transducers were instrumented to measure only vertical reactions along the edges of the slabs. Slab 1 contained corner restraints which were instrumented to determine the vertical uplift reactions of the corners. The remaining slabs did not

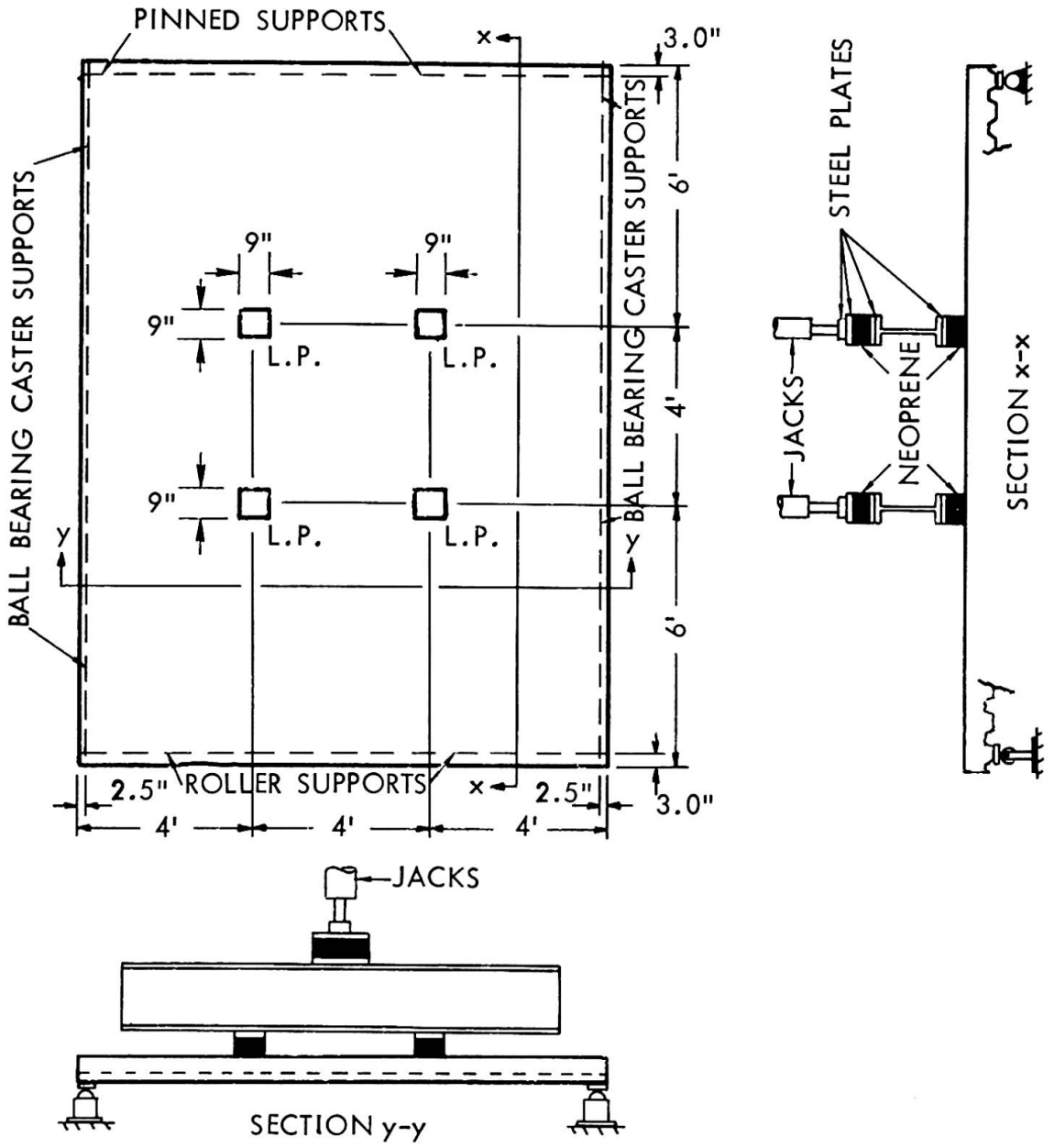

Fig. 1. General layout of full-scale slab tests indicating positions of the load points and positions of the support reactions.

contain the corner restraints and the corners were free to lift upward. The amount of the corner uplift was measured for those slabs containing no corner restraints. Figure 3 shows the transducer reaction assemblies, including the corner restraint instrumentation used in slab 1.

The overall support assemblage for the slabs is shown in Fig. 4. Also seen in Fig. 4 are the deflection dials which were supported on an independent grillage. As can be seen by the location of the deflection dials, basically only the southwest quadrant of the slab was heavily instrumented.

TEST PROCEDURE AND RESULTS OF SLAB TESTS

Loading for all four slabs was applied through the use of hydraulic jacks as shown in Fig. 5 which depicts an overall view of slab 1 immediately after

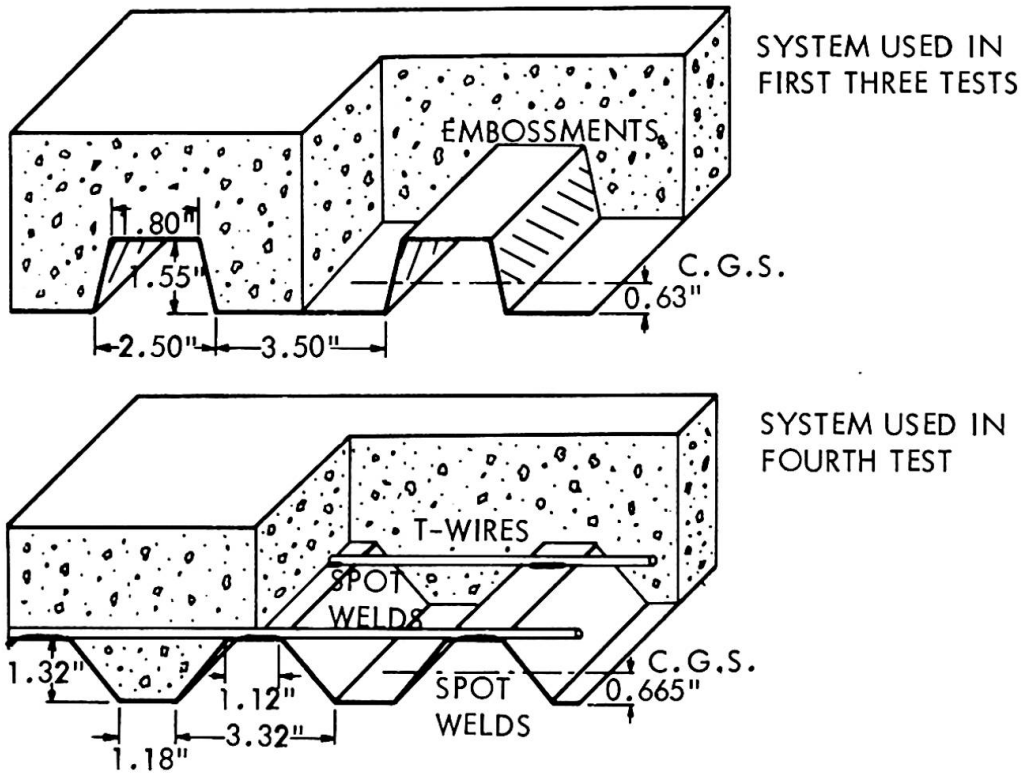

Fig. 2. Views showing types of decking used.

testing. Loading for slab 1 was applied continuously from zero to ultimate except for the time needed to take instrumentation readings.

The other three slabs were loaded continuously from zero to a designated cycling load. At this stage unloading and reloading to the cycling load occurred 10 times. After cycling, a final loading was made from zero to ultimate failure of the slab. Table 1 contains the ultimate load and cycling load for each of the four slabs. A complete view of the total crack pattern which occurred in slab 2 is shown in Fig. 6.

Figure 7 provides diagrams of the crack patterns that occurred on the top surface of the four slab tests. Indicated is the load at which essentially no top surface cracking had occurred. In each case note that the top surface cracking occurred at a fairly high percentage of the ultimate load. Except for slab 1, in which the first cracking was that across each of the corners, the first cracking of the slabs occurred as diagonal cracks along the edges of the slabs.

Figure 8 shows the edge cracking that occurred for the east edges of all the slabs. This edge cracking was typical of that which occurred on both edges of the slabs. The crack numbers in Fig. 8 indicate the order of crack development. After these edge cracks had formed, subsequent loading results in a widening of the primary cracks in each case as shown by the heavier crack lines for each edge. Ultimate failure of all four slabs was precipitated by a horizontal slippage between the steel decking and the concrete in the region between the primary edge cracks. This slippage was first detected by dial displacement gages during or just after completion of the cyclic loading for the last three slabs, but did not become significant until failure was imminent.

Table 1. Properties of component materials and test data.

	Slab 1	Slab 2	Slab 3	Slab 4
Concrete Properties				
Average cylinder strength, psi	4355	3538	3951	3816
Modulus of rupture, psi	485	470	–	521
Age of cylinder beams and slab, days	15	17	17	16
Steel Decking				
Cross-sectional area $in.^2/ft$	0.625	0.625	0.625	0.376
Yield strength at 0.2% offset, ksi	45.1	45.1	45.1	101.6
Supplementary Reinforcing (Welded wire fabric, or T-wires)				
Area of WWF parallel to deck corrugations $in.^2/ft$	0.0525	0.034	None	None
Area of WWF or T-wires transverse to deck corrugation, $in.^2/ft$	0.0575	0.144	None	0.0150
Yield strength, (0.005 strain), ksi	79.0	82.6 (#0 ga.) 84.6 (#4 ga.)	None	92.1
Composite Test Slab				
Average out-to-out thickness, in.	4.98	4.75	4.75	4.87
Corner support condition	Restrained	Free	Free	Free
Cycling load, kips/load point	None	9.4	6.4	9.4
Ultimate load, kips/load point	13.5	15.5	8.8	14.4
Equiv. ultimate uniform load, psf	300	345	196	321

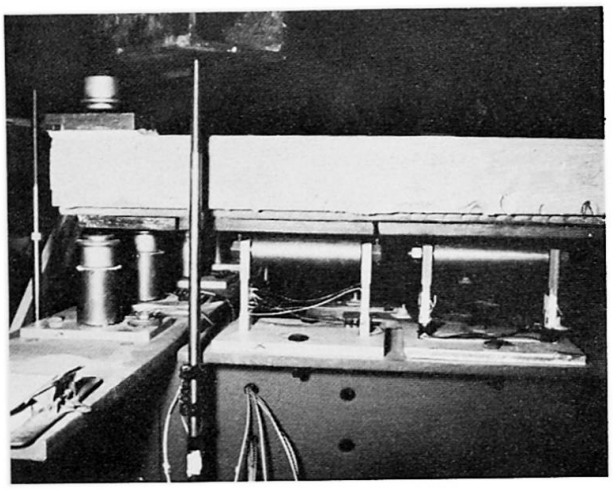

Fig. 3. Instrumentation to measure corner uplift force and vertical downward forces along the edges of slab 1.

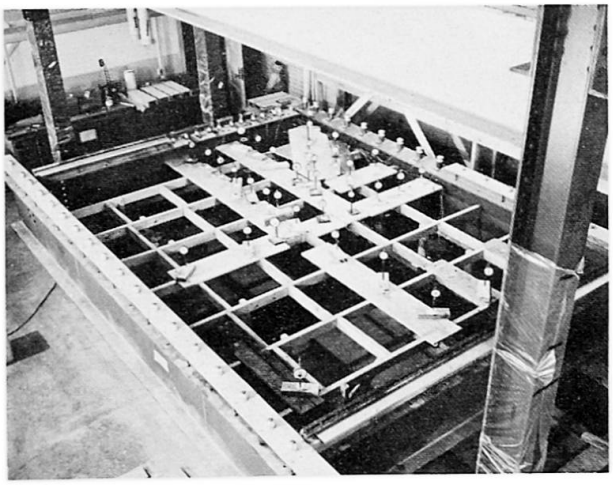

Fig. 4. Support and deflection dial arrangement for full-scale slab tests.

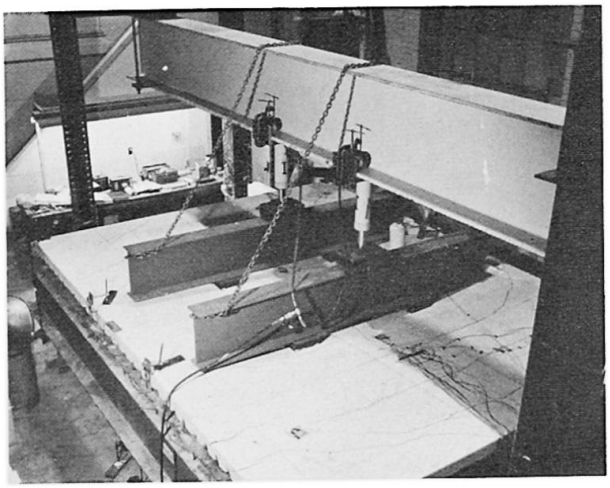

Fig. 5. View of full-scale two-way slab test.

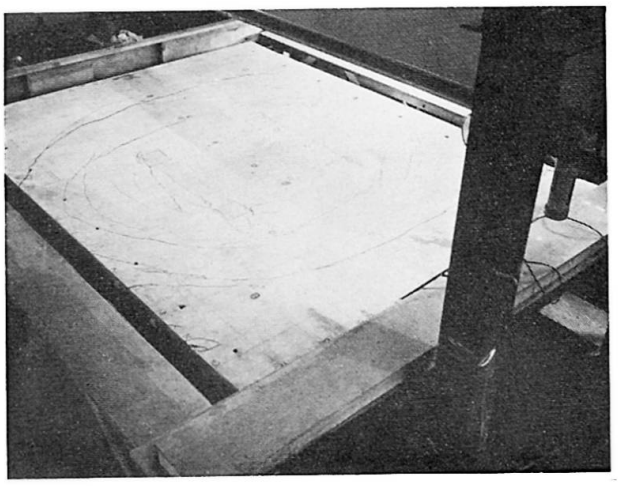

Fig. 6. Top surface of slab 2 indicating fixed crack pattern at termination of testing.

The stiffness characteristics of the four slabs can be ascertained by examining Fig. 9, which shows the load-deflection relationships for the first application of load. In the case of slab 1, the load was increased in continuously applied increments up to ultimate load. The second, third, and fourth slabs were loaded to 9.4, 6.4, and 9.4 kips per load point, respectively, during the first cycle. As previously explained, the loading on these latter three slabs was reduced to zero, and re-applied nine more times. The residual deflections following the first cycle of load, is shown to be 0.182 in., 0.101 in., and 0.265 in. for slab 2, 3, and 4, respectively. It is of interest that slab 1, with the corner tie-downs, exhibits significantly stiffer characteristics than any of the other slabs. Slab 2, which was heavily reinforced with 6 X 12 X 0/4 welded wire fabric, was somewhat stiffer than slabs 3 and 4. Slabs 3 and 4 were of about equal stiffness.

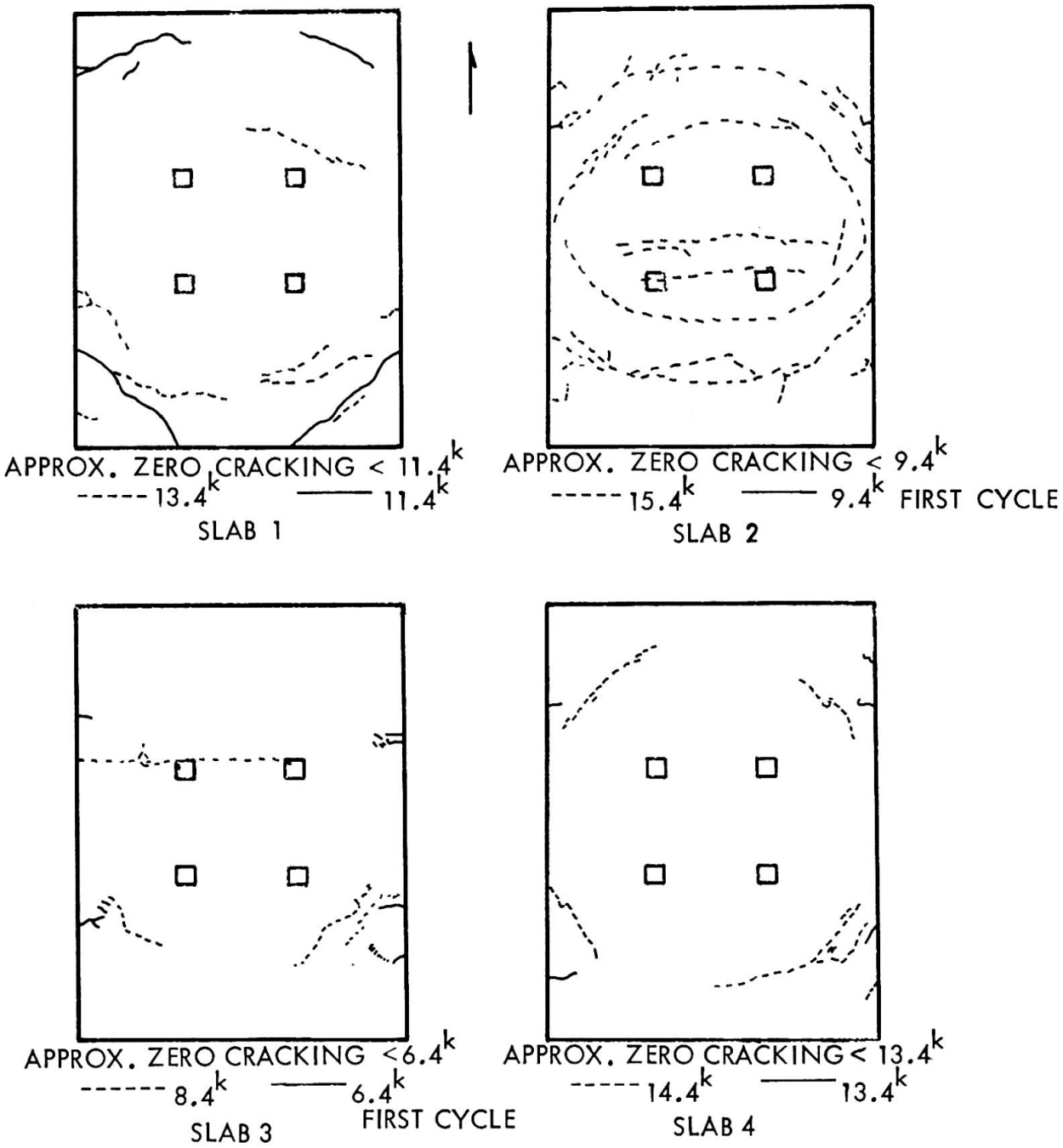

Fig. 7. Top surface cracking for the four full-scale slab tests.

Figure 10 shows the final load-defelction relationships to ultimate load for each of the four slabs. The curves for the last three slabs commence with a residual deflection corresponding to that which occurred in these slabs after 10 load cycles. These curves show that slab 2 not only carried the greatest load, but also sustained the highest ultimate deflection. This can undoubtedly be attributed to the relatively large amount of supplementary steel. Slab 3, without any additional steel, indicated the least ultimate strength as well as the least ultimate deflection. Slab 1 with the corner tie-downs and rather nominal 6 x 6 x 6/6 welded wire fabric closely approximated the behavior of slab 4, with the closely spaced welded transverse wires, neglecting the permanent deformation due to cycling.

Typical results of the measured vertical reactions along the west side may be summarized by looking at Fig. 11 for slab 1. The amount of load transmitted

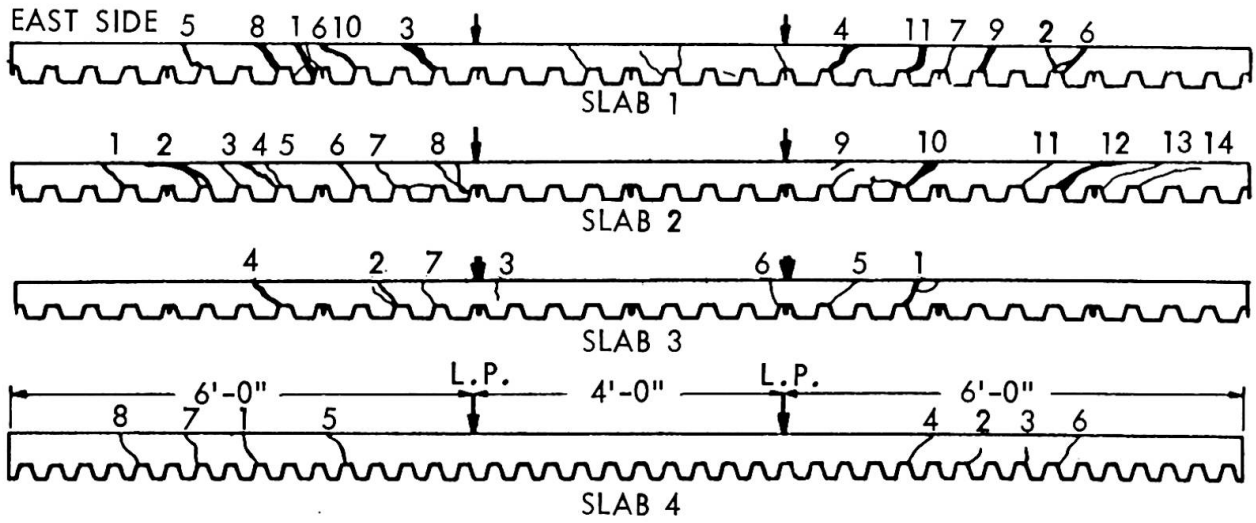

Fig. 8. Crack pattern development along the east edges of all slabs.

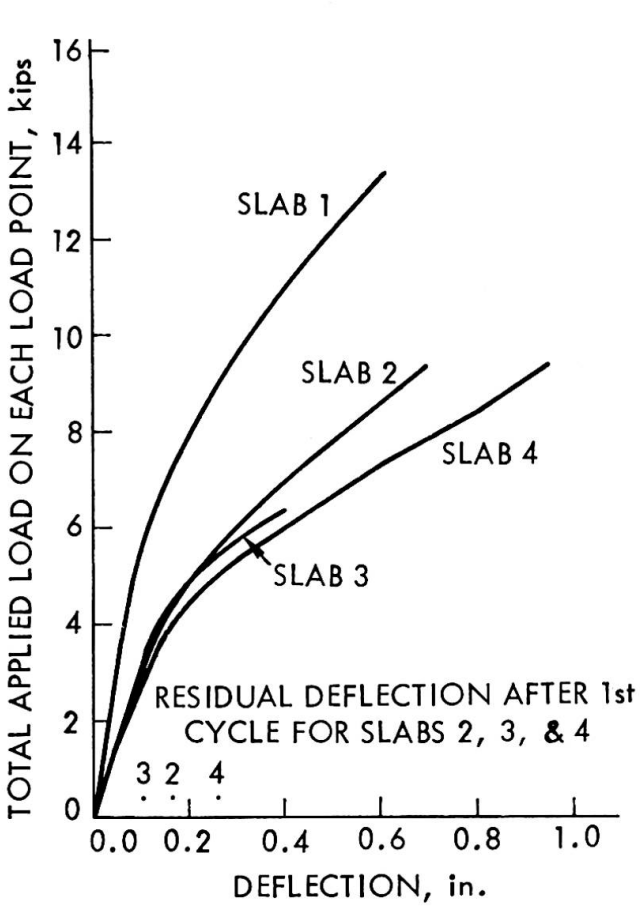

Fig. 9. Load deflection characteristics for the initial loading stages.

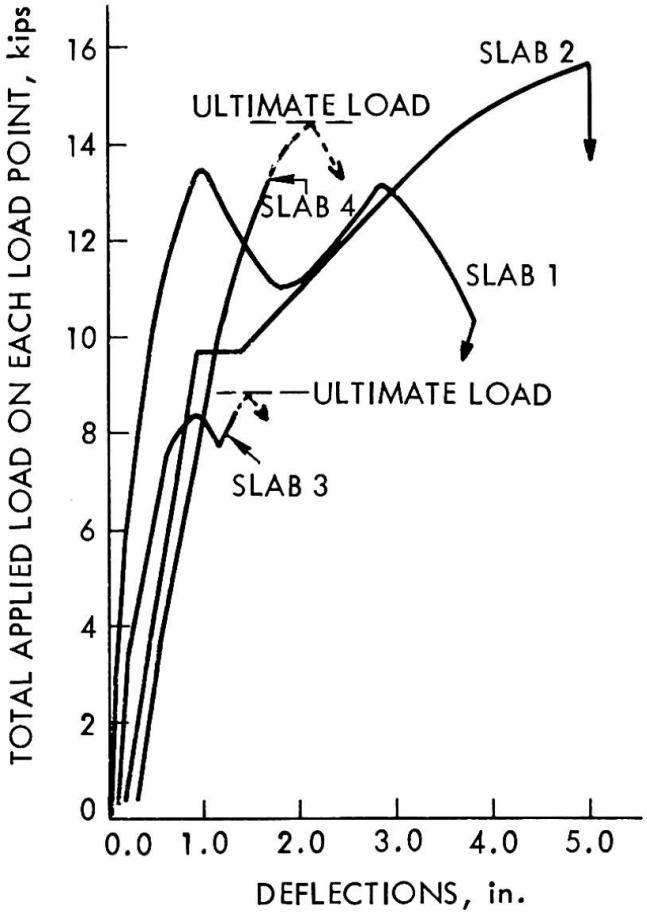

Fig. 10. Load deflection characteristics after cycling, for the final loading stages.

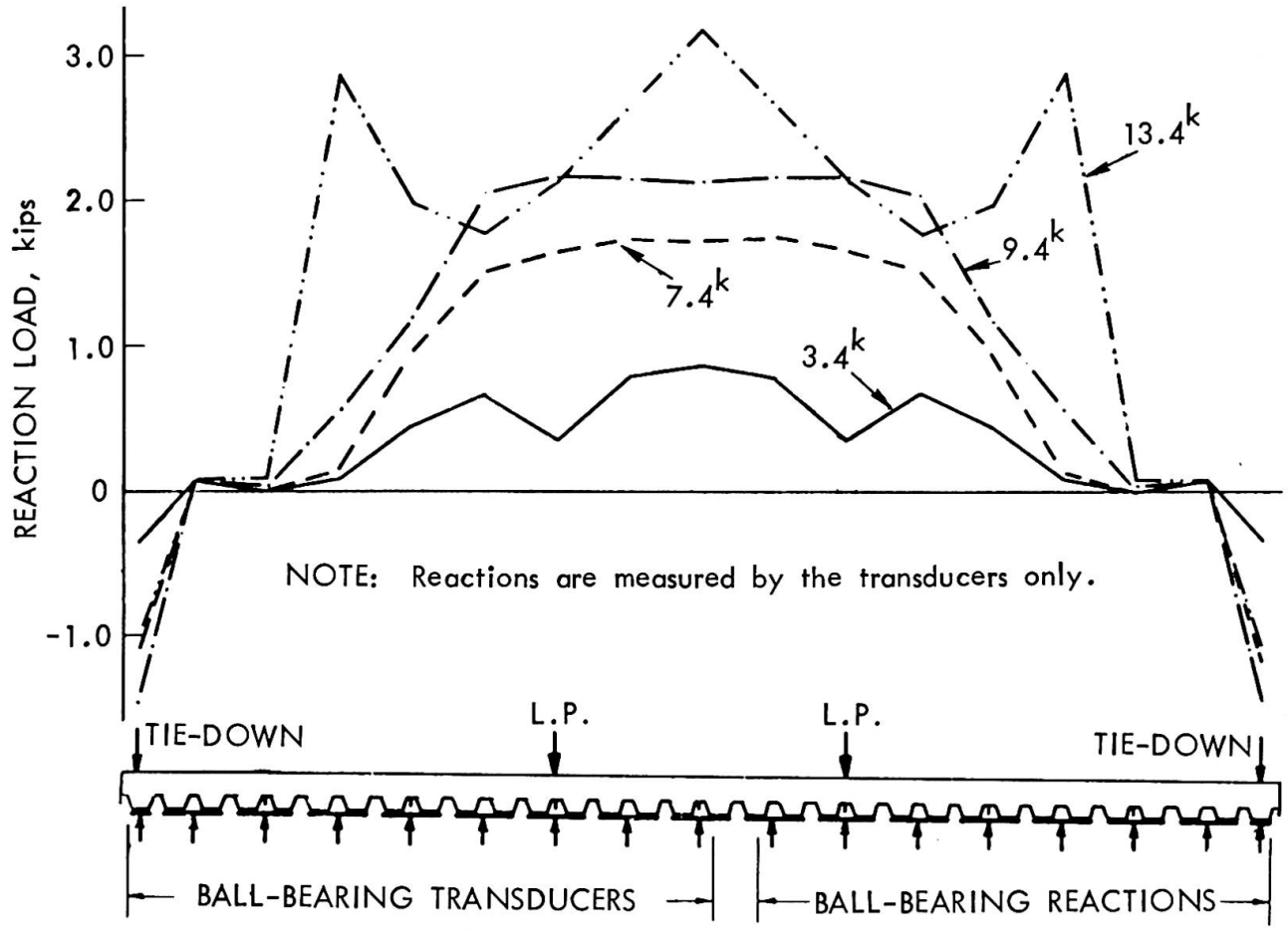

Fig. 11. Distribution of reactive forces due to the applied load along the west edge of slab 1.

in the weak direction to the south support is illustrated by the reaction distributions in Fig. 12. An indication of the percentage of load transmitted to each side as loading progressed is shown in Fig. 13. Note that the greater distribution in the direction transverse to the corrugations occurs at lower loads while the slab is essentially still elastic. The amount of distribution to south support for the other three slabs without corner tie-downs was less than that indicated by Figs. 12 and 13. In fact, for these slabs 90% or more load was transmitted to the east and west supports for all loads over 50% of ultimate.

Limitations of space prohibit presentation of reaction distributions for the other slabs. However, it was noted during testing and supported by the reactive measurements and crack patterns that for the three slabs without corner tie-downs, there appeared to be an approximate effective width of 8 ft over the central regions of the east and west support edges.

The analysis of data for each of the four slabs is still underway. Coupled with the analysis is an effort to develop a theory of failure which will provide a basis for an ultimate strength approach to design. A first attempt was to try the yield line method for predicting the ultimate strength. This method, unfortunately, gave results which were at least 22% higher than the experimental values of ultimate strength for all four slabs. This seems logical from the standpoint that the four slabs did not fail by a flexure

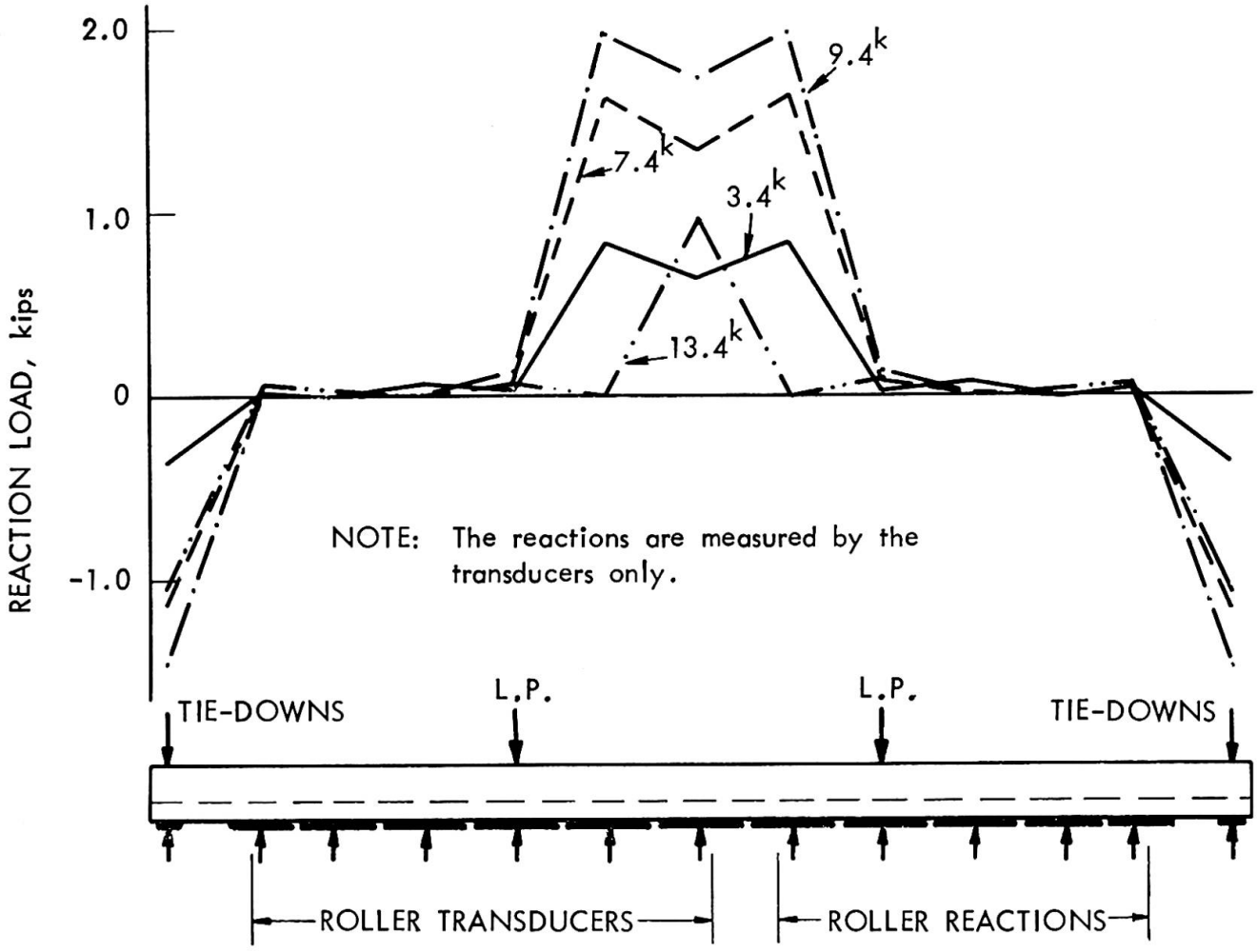

Fig. 12. Distribution of reactive forces due to the applied load along the south edge of slab 1.

action, as the yield-line method assumes, but rather by a shear-bond action involving a horizontal slippage between steel decking and the concrete.

CONCLUSIONS

1. Four full-scale slabs, of approximately identical dimensions, were loaded to failure in the laboratory. All four slabs failed by a shear-bond action which was precipitated by a horizontal slippage between steel decking and concrete.

2. Slab 2 with the largest amount of supplementary steel, in the form of welded wire fabric, sustained the largest test load. This slab also sustained the largest ultimate deflection of the four slabs.

3. Slab 1 with all four corners tied down, and with only a nominal amount of supplementary reinforcing, exhibited a significantly stiffer behavior than any of the other slabs.

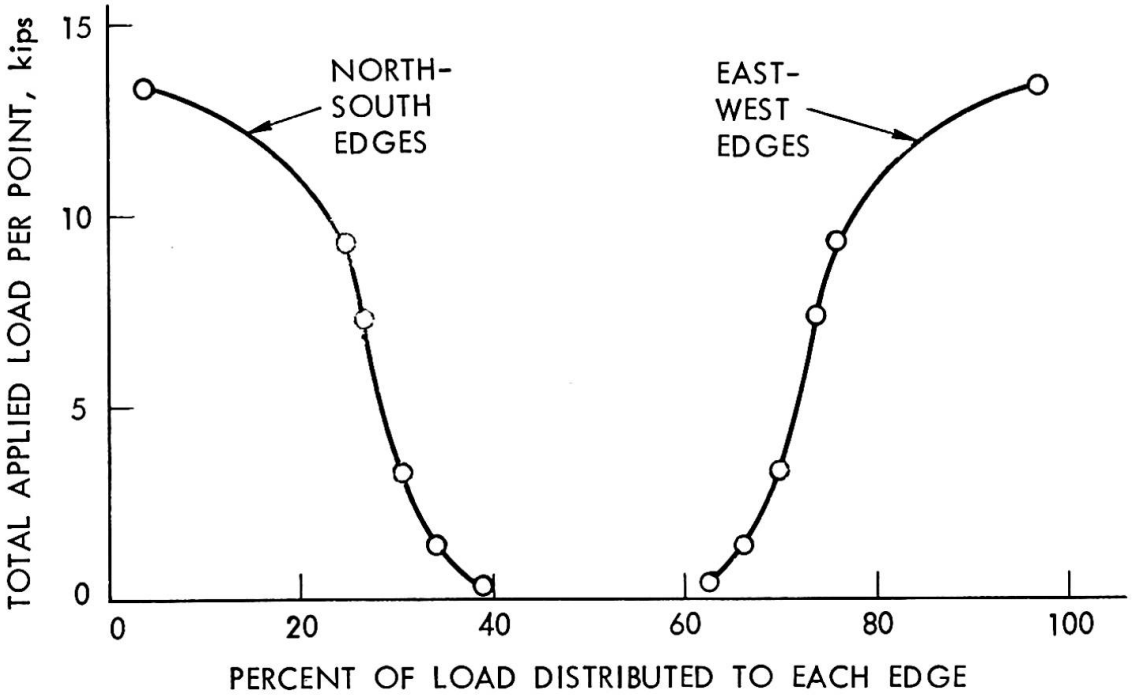

Fig. 13. Illustration of the percentage of applied load transmitted to each reaction support as loading increases for slab 1.

4. Slab 3 without any supplementary reinforcing could carry an ultimate load which was only about 57% that of slab 2. The ultimate deflection of slab was much less than that of slab 2.

5. In general, the top surface cracking behavior of all slabs was excellent. Excessive cracking did not occur until ultimate load was imminent, and even then the cracks were quite small.

REFERENCES

1. McDevitt, C. F., and Viest, I. M., "Interaction of Different Materials," Introductory Report for the Ninth Congress of IABSE-Theme IIA, May 1972, pp. 69-70.

2. Schuster, R. M., "Strength and Behavior of Cold-Rolled Steel-Deck-Reinforced Concrete Floor Slabs," PhD Thesis, Iowa State University, 1970.

SUMMARY

Four composite slabs were constructed with nominal out-to-out dimensions of 12 ft × 16 ft × 4-7/8 in. and incorporating corrugated, cold-formed steel decking as reinforcement. Two slabs had supplementary reinforcing in the form of welded wire fabric.

Laboratory tests to ultimate load on the simply supported slabs were conducted using four concentrated load points. The mode of failure was a shear-bond action precipitated by slippage between steel decking and concrete.

Leere Seite
Blank page
Page vide

Composite Steel-Deck-Reinforced Concrete Systems Failing in Shear-Bond

Ruine par défaut d'adhérence des plaques composées de tôle d'acier et de béton

Durch Stahlplatten bewehrte Betontragwerke mit Schubbruch

REINHOLD M. SCHUSTER
School of Architecture
University of Waterloo
Waterloo, Ontario, Canada

INTRODUCTION

Reference is made by Messrs. C. F. Mcdevitt and I. M. Viest[1] to the use of corrugated or ribbed panel light gage steel decks which interact with the concrete slab to form a composite floor system, often referred to as steel-deck-reinforced concrete slab construction. Mention is made by Mcdevitt and Viest of a paper authored by Ekberg and Schuster, included in the final report of the Eighth IABSE Congress[2], describing the state of the art of using steel-deck-reinforced concrete slabs in buildings. Particularly, Mcdevitt and Viest point out the more recent research conducted by Ekberg and Schuster at Iowa State University leading to the development of semi-empirical equations relating to the ultimate shear-bond strength of steel-deck-reinforced concrete systems, pointing out that laboratory tests have shown that most of these specimens exhibit a shear-bond type of failure. Since the initiation of this work in 1967, several unpublished research progress reports related to the shear-bond capacity of steel-deck-reinforced systems have resulted, including references (2), (3) and (4).

The content of this discussion, taken largely from Reference (4), is focused primarily on the development of a concept relating to the ultimate strength of steel-deck-reinforced concrete systems failing in shear-bond. This task is divided into 1. a laboratory test program and 2. an analytical ultimate strength analysis. The laboratory test program was conceived in an effort to provide the necessary experimental data for determining the ultimate shear-bond strength as obtained from a semi-rational-analytical approach, thus requiring a statistical evaluation of experimental data.

LABORATORY TEST PROGRAM

The philosophy of the test program was to involve the loading to failure of a large number of representative elements of steel-deck-reinforced concrete slabs as simple beams in order to adequately cover a full range of behavioral characteristics. Initial testing indicated that a shear type of failure would be the most predominant mode of failure in most steel-deck-reinforced systems. Based on this observation, beam testing was focused primarily on the nature of shear transfer between the steel deck and concrete.

The test program was designed in an effort to simulate, as closely as practically possible, beam elements of steel-deck-reinforced concrete slabs as found

in common construction practice. Therefore, all laboratory beam testing was conducted on simple supports and subjected to a symmetrical mode of loading, consisting of either a single concentrated line load or two concentrated line loads.

Steel decks from four different steel deck manufactures were used in the test program; however, the majority of beam tests were conducted using one particular deck profile, namely that of company I[a]. This was done in an effort to obtain a large number of test results, embodying the most logical parametric variations. To further verify the ultimate strength expressions a representative number of beam tests were conducted on composite units constructed with steel decks E, O and G.

The steel deck profiles tested were divided into two categories based on the pattern of mechanical shear connectors such as embossments, holes or welded wires. The two categories are stated as follows:

Category I - Steel deck profiles that provide horizontal shear capacity primarily by virtue of a fixed pattern of mechanical shear devices, i.e. the center to center spacing of the shear devices is constant for every steel deck thickness and depth of slab.

Category II - Steel deck profiles that have a variable spacing of mechanical shear devices, i.e. the center to center spacing of the shear devices may vary with the depth of slab and steel deck thickness.

Tests were conducted on a total of 145 steel-deck-reinforced concrete beams. All steel decks were of out-to-out depth between 1¼ and 2 in., such that the neutral axis of the composite cross section was located above the top of the steel deck. Span length, shear span, beam depth and width and steel deck thickness were varied with each of the steel-deck-reinforced systems. All beams were supported throughout during the placing and curing of the concrete, except a few selected beam specimens were shored at their ends and at mid-span during placing and curing.

The characterization of a shear-bond failure was identified by the formation of an approximate diagonal crack under or near one of the concentrated loads, resulting in a brittle type of failure at ultimate load. This failure was accompanied by end-slip between the steel deck and concrete, thus, causing the concrete shear span portion, L' (see Fig. 4 for location of L'), to become disengaged, experiencing loss of bond between steel deck and concrete. This simultaneous action of shear and bond is termed shear-bond. See Fig. 1 for typical shear-bond failure.

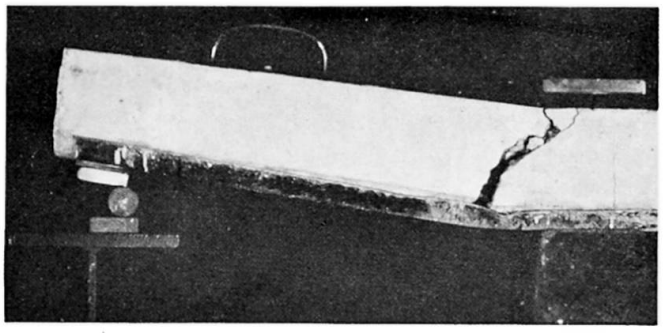

Fig. 1 - Typical shear-bond failure with end-slip of beam constructed with steel deck G

A shear-bond failure may, or may not, have been preceded by the yielding of the steel, depending on the relative values of the percentage of steel, the shear span L' and the inherent load transfer capacity of the shear transfer devices. Yielding of the steel-deck, whenever in occurrance, initiated at the extreme bottom fibers of the steel deck and in some cases progressed towards the top of the steel deck. In no case, however, did the steel deck yield over its entire depth. See Reference (4) for further detail.

[a] Letters were chosen to identify the different steel decks, thus, avoiding direct company comparison.

ANALYTICAL ANALYSIS

Based on the experimental findings, a semi-rational shear-bond concept was adopted, since a truly rational concept is complicated by the nonhomogeniety and nonisotropy of concrete. Consideration was given to beams constructed with steel decks of Category I with fixed pattern shear transfer devices and Category II where spacing of shear devices is a variable.

In some respects, a shear-bond failure regarding steel-deck-reinforced concrete slabs is similar to a shear and diagonal tension failure in conventional reinforced concrete without web reinforcement. The main similarity lies in the formation of an approximate diagonal tension failure crack, resulting from combined shear and bending. This failure crack is not always diagonal in nature, but for all practical purposes, a diagonal crack can be assumed, leading further to the assumption that this crack is caused by excessive principal tension tresses.

Category I

Based on the major variables that have been found to influence shear and diagonal tension in conventional reinforced concrete without web reinforcement, a general expression for the ultimate transverse shear may be written as follows:

$$V_{uc} = f(f'_c, L', d, b, p) \tag{1}$$

where f'_c is the compressive strength of the concrete, b is the width of the composite beam cross section, d is the effective depth from the top of concrete to the center of gravity of the steel deck and p is the percentage of steel. To arrive at an expression containing the variables of Eq. (1), it is assumed that the ultimate transverse shear, V_{uc}, neglecting dead load, is the result of the concrete and steel deck contributing independently. From Fig. 2 it can be observed, by summation of vertical force components that

$$V_{uc} = V_c + V_d \tag{2}$$

where V_c is the transverse shear carried by the concrete at ultimate load and V_d is the transverse shear carried by the steel deck at ultimate load. The maximum concrete tensile stress, below the neutral axis, is as follows:

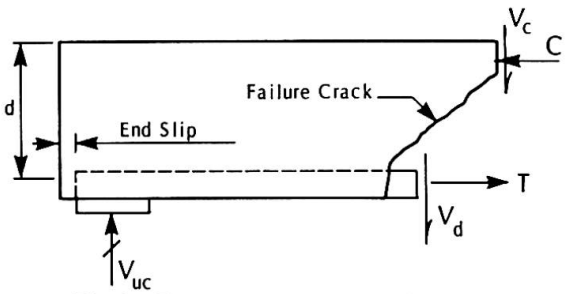

Fig. 2 - Forces at ultimate crack of typical shear-bond failure

$$\sigma_{max} = \frac{\sigma_{ct}}{2} + \sqrt{\left(\frac{\sigma_{ct}}{2}\right)^2 + v_c^2} \tag{3}$$

where σ_{ct} is the normal stress in the concrete and v_c is the vertical, or horizontal, shear stress in the concrete. The magnitude of the tensile bending stress, σ_{ct}, is influenced by the presence of tensile cracks, and may consequently be computed either from an assumed cracked or uncracked section. For this analysis, σ_{ct}, is based on the uncracked section theory. The reason for this being that cracks in the experimental beams were usually of a hairline nature even near ultimate load. It is possible then, to write

$$\sigma_{ct} = K_1 \frac{M_c}{bd^2}$$

where M_c is the moment carried by the concrete at ultimate load and K_1 is a constant as well as K_2, through K_8 to follow.

The shear stress, v_c, in the concrete is assumed to be proportional to the average intensity of shear stress on the total cross section. Thus

$$v_c = K_2 \frac{V_c}{bd} .$$

When the maximum principal stress σ_{max}, exceeds the tensile strength of concrete, f'_t, at the location of the potential diagonal failure crack, shear-bond failure is assumed to impend. The tensile strength of concrete is assumed proportional to the square root of the compressive strength, f'_c, of the concrete. Thus,

$$\sigma_{max} = K_3 \sqrt{f'_c} .$$

Substituting the above stress relationships into Eq. (3) and rearranging in terms V_c/bd results in the following:

$$\frac{V_c}{bd} \cdot \frac{1}{2K_3} = \frac{1}{\frac{K_1}{d\sqrt{f'_c}} \cdot \frac{M_c}{V_c} + \frac{1}{\sqrt{f'_c}} \sqrt{\left(\frac{K_1}{d} \cdot \frac{M_c}{V_c}\right)^2 + (2K_2)^2}}$$

Now, factoring the term $(K_1/d \cdot M_c/V_c)$ from the square root and substituting $K_4 = 2K_2/K_1$, the expression reduced to

$$\frac{V_c}{bd} \cdot \frac{1}{2K_3} = \frac{1}{\frac{K_1 M_c}{d\sqrt{f'_c}\, V_c} \left[1 + \sqrt{1 + \left(K_4 \frac{V_c d}{M_c}\right)^2}\right]} . \qquad (4)$$

A study of Eq. (4) indicates that the magnitude of the term $(K_4 dV_c/M_c)$ can be assumed to approach zero for most practical cases. Letting $K_5 = K_3/K_1$ and solving for V_c, Eq. (4) reduces to

$$V_c = \frac{K_5 bd^2 \sqrt{f'_c}\, V_c}{M_c} \qquad (5)$$

The transverse shear carried by the steel deck is assumed to be proportional to the cross-sectional area of the steel deck (A_s). Thus,

$$V_d = K_6 A_s . \qquad (6)$$

Since the concrete is placed directly over the steel deck, the transverse shear contribution can be quite appreciable, particularly when the cross-sectional area of the deck is large and the depth of the concrete is at a minimum.

Combining Eqs. (5) and (6) in accordance with Eq. (2) and expressing in terms of unit nominal ultimate shear stress, with $v_{uc} = V_{uc}/bd$, the following general equation results:

$$v_{uc} = K_5 \frac{\sqrt{f'_c}\, dV_c}{M_c} + K_6 p \qquad (7)$$

Based on actual experimental beam testing of this investigation, Eq. (7) is expressed more specifically for the special case of symmetrical concentrated loads. The terms V_c/M_c and $1/L'$ are synonymous since $M_c = V_c L'$ and

$$v_{uc} = \frac{V_{uc}}{bd} = K_5 \frac{\sqrt{f'_c}\, d}{L'} + K_6 p . \qquad (8)$$

where $p = A_s/bd$.

Equation (8) gives the parameters to be investigated and takes into account the three most important variables that affect the shear-bond strength of flexural members subjected to combined bending and shear; these are the compressive strength of concrete, ratio of reinforcement, and the ratio of external shear to the maximum moment in the shear span.

Category I

The same concept was employed in the development of a shear-bond expression for Category II as was used in Category I. However, the resulting expression now contains one additional parameter, namely, the spacing of the shear transfer devices, s.

Figure 3 shows a typical steel deck profile of Category II where the shear transfer device spacing, s, is subject to change. Summing forces between the horizontal interface of the concrete and top of the steel deck where the shear transfer devices are located, see Fig. 3, an expression that satisfies statics may be written as

$$v_{uc}bs = \frac{b}{g} m_u$$

where m_u is the ultimate load carrying capacity per weld

or,
$$\frac{V_{uc}}{bd} = \frac{1}{s} \cdot \frac{m_u}{g} = v_{uc} \cdot \qquad (9)$$

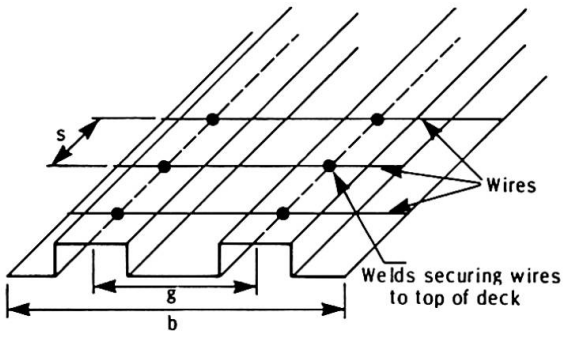

Fig. 3 - Typical steel deck profile of category II

Equation (9) indicates that the ultimate shear-bond stress, v_{uc}, is inversely proportional to the shear device spacing, s, and directly proportional to the ratio m_u/g. Since the dimension, g, of any given deck profile is constant, the ratio m_u/g can be assumed to be directly proportional to the shear-bond capacity. The following expression results

$$\frac{V_{uc}}{bd} = \frac{1}{s} \left(K_7 \frac{\sqrt{f'_c}\, d}{L'} + K_8 p\right). \qquad (10)$$

Note that K_7 and K_8 correspond to constants K_5 and K_6 of Eq. (8). The determination of these constants depends upon experimental beam test data.

TEST RESULT EVALUATION

The data resulting from the numerous beam tests was assimilated so that the ultimate shear-bond capacity could be related to the various parameters as expressed by Eqs. (8) and (10); and a statistical regression analysis was used in evaluating the respective regression constants. Equations (8) and (10), applicable to beams of Category I and II respectively, provided the necessary variables for the determination of these regression constants.

Figure 4, for example, shows a plot of ultimate strength shear-bond relationships for beams constructed with steel deck I - 22 gage. All beams were supported throughout, except three beams which were shored at midspan prior to placing of the concrete. No appreciable difference exists between beams supported throughout and those shored at midspan. Also, it can be observed that the change of width of beams produces no apparent effect on the shear-bond load carrying capacity.

Figure 5 exhibits the same linear shear-bond relationship and similar behaviorial characteristics as Fig. 4.

Figure 6 represents a plot of shear-bond relationships of beams constructed with steel deck E resulting from a combined regression analysis of tests conducted in this investigation and by company E. The reason for combining the 20 and 22 gage parameters in one regression is because the difference in steel deck thickness being very small.

Beams constructed with steel deck G are placed in Category II, and Eq. (10) applies for the shear-bond regression analysis. Figure 7 represents the ultimate shear-bond relationship for beams constructed with steel decks G-20 and 24 gage. Figure 7 reveals that the ultimate shear-bond strength of beams constructed with deck G-24 gage is greater than that of beams constructed with 20 gage decking. In the case of beams with 20-gage deck, there was a shearing action at the connectors which left the deck itself relatively intact. On the other hand, there was an actual tearing of the steel deck in the areas of the welds, with the beams constructed with 24-gage steel. This led to the conclusion that more complete

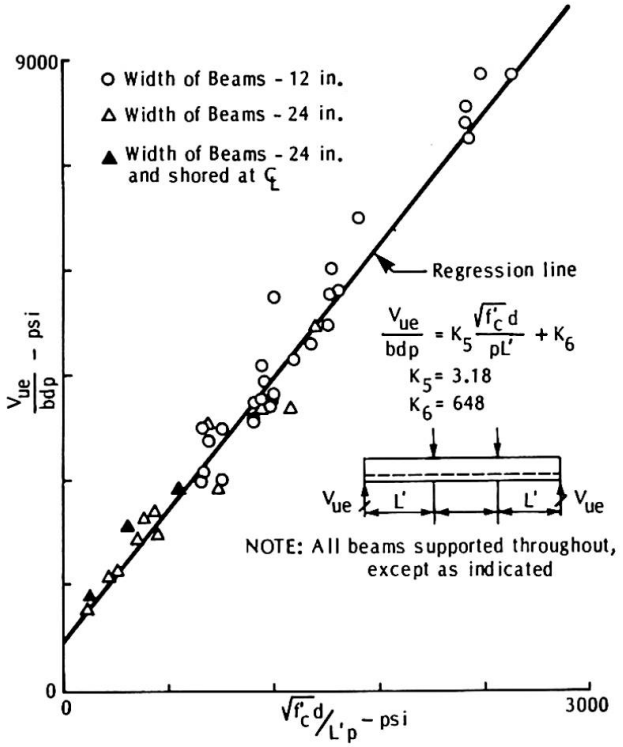

Fig. 4 - Relationship between V_{ue} / bdp and $\sqrt{f'_c}\,d$ / L'p for beams constructed with steel deck I-22 gage

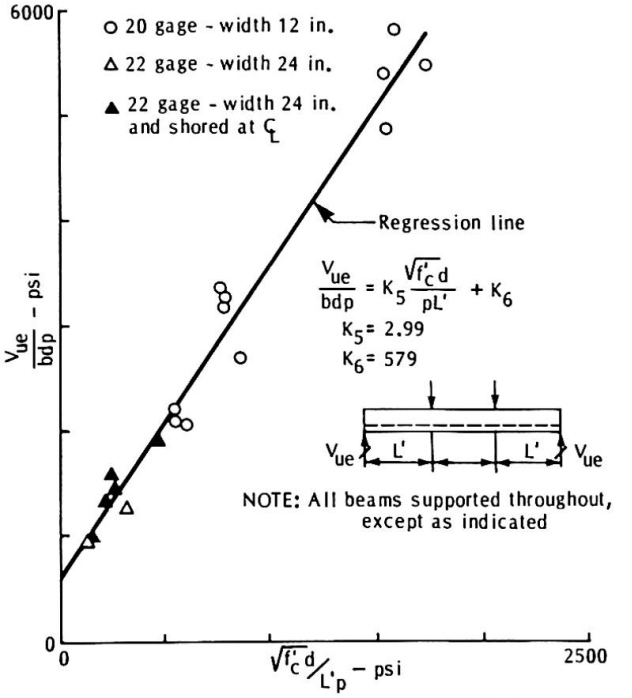

Fig. 5 - Relationship between V_{ue} / bdp and $\sqrt{f'_c}\,d$ / L'p for beams constructed with steel deck O-20 and 22 gage

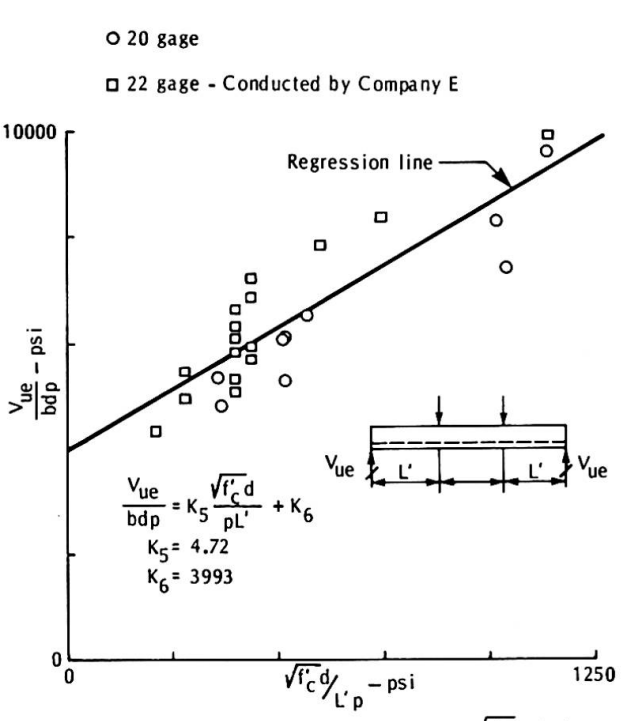

Fig. 6 - Relationship between V_{ue} / bdp and $\sqrt{f'_c}\,d$ / L'p for beams constructed with steel deck E-20 and 22 gage

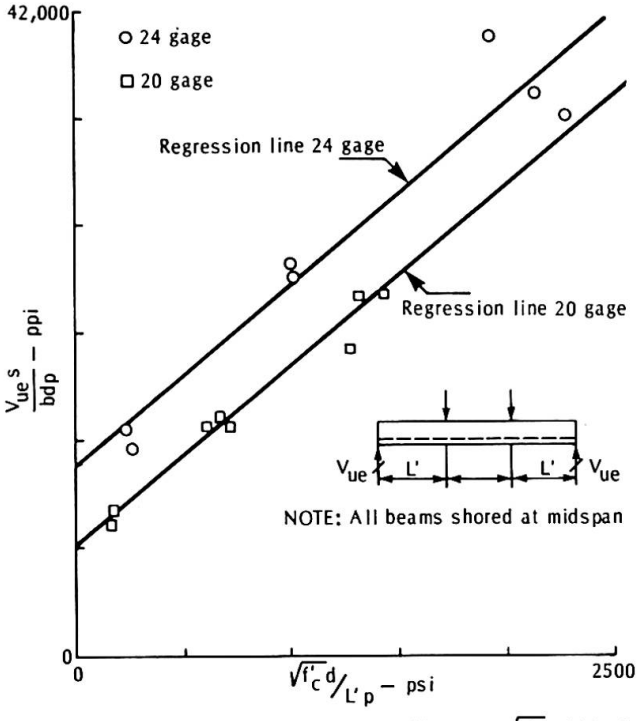

Fig. 7 - Relationship between $V_{ue}s$ / bdp and $\sqrt{f'_c}\,d$ / L'p for beams constructed with steel deck G-20 and 24 gage

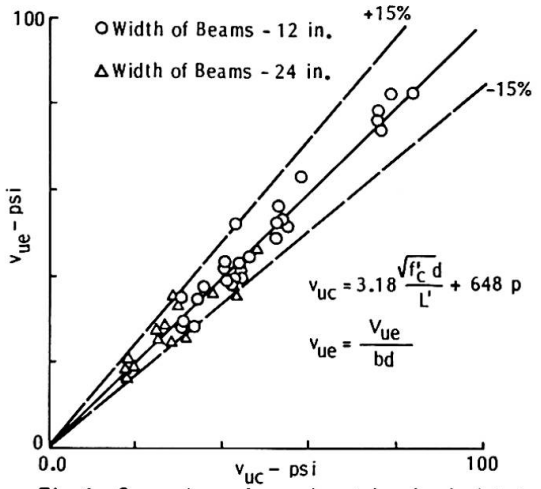

Fig. 8 - Comparison of experimental and calculated ultimate shear-bond stresses for beams constructed with steel deck I-22 gage

penetration of connector welds existed with beams of 24-gage steel decks than with those of 20-gage decking. The better penetration undoubtedly caused a greater strength at each individual weld in the case of the 24-gage decking.

Figure 8 illustrates a comparison of experimental and calculated ultimate shear-bond stresses for beam test data of Fig. 4. The calculated shear-bond stresses, v_{uc}, are obtained from Eq. (8) with constants K_5 and K_6 resulting from Fig. 4. Similar comparison curves were plotted and are recorded in Reference (4). In all cases, a maximum correlation of ±15% exists between experimental and calculated shear-bond values.

REFERENCES

1. Mcdevitt, C.F., and Viest, I.M., "Interaction of different materials", Introductory Report for the 1972 Congress of IABSE - Theme IIa.
2. Ekberg, C.E., Jr., and Schuster, R.M., "Floor Systems with Composite Form-Reinforced Concrete Slabs", International Association for Bridge and Structural Engineering Congress Proceedings 8: 385-394 (1968).
3. Mouw, K.W., and Ekberg, C.E., Jr., Fatigue Testing of Light Gage Metal Forms, Engineering Research Institute, Special Report, ERI-348, Iowa State University, Amex, (1969).
4. Schuster, R.M., "Strength and Behavior of Cold-Rolled Steel Deck-Reinforced Concrete Floor Slabs", thesis presented to Iowa State University, at Ames, Iowa, in August, 1970, in partial fulfillment of the requirements for the degree of Doctor of Philosophy.

SUMMARY

Shear-bond may be classed as a brittle type of failure and is characterized by the formation of an approximate diagonal crack, resulting in end-slip and loss of bond between the steel deck and concrete. The ultimate shear-bond capacity of steel-deck-reinforced systems is a function of the compressive strength of concrete, the depth and width of slab, the thickness of steel deck, the shear span and 2 constants to be evaluated from experimental test data. A ±15% correlation between experimental and calculated shear-bond stresses existed.

ACKNOWLEDGMENT

The work described herein was sponsored and supported by the American Iron and Steel Institute and conducted at Iowa State University under the direction of Dr. C. E. Ekberg, Jr.

Leere Seite
Blank page
Page vide

Utilisation des colles dans le béton armé
Le béton plaqué

Verwendung von Kunststoff-Klebestoffen im Stahlbetonbau
Mit Stahlblech beklebter Beton

The Use of Bonding Agents in Reinforced Concrete
Plated Concrete

ROBERT L'HERMITE
Directeur Général Scientifique et Technique de l'U.T.I.
(Union Technique Interprofessionnelle des
Fédérations Nationales du Bâtiment et des Travaux Publics)
Secrétaire Général de la R.I.L.E.M.
(Réunion Internationale des Laboratories d'Essais et de Recherches sur les Matériaux et les Constructions)
Paris, France

Les colles peuvent constituer des moyens d'assemblages efficaces et économiques. Elles ont, dans le bâtiment, de multiples emplois dès à présent, et leurs applications ne feront que prendre plus d'importance. Les collages métal sur métal ont fait l'objet de plusieurs de nos études mais la direction dans laquelle j'ai plus spécialement travaillé est le collage béton-métal et, plus particulièrement, béton-acier.

Au préalable, il a été nécessaire de reconnaître les qualités des colles : résistances, vitesses de durcissement, liaisons avec les matériaux, fluage, durée, sensibilité à l'eau et à la température. Ceci a été fait grâce à de nombreux essais effectués aussi soigneusement que possible. Finalement, les résines choisies sont de la famille des époxydes, contenant des catalyseurs appropriés et des charges inertes. Les résistances obtenues atteignent, dans le couple acier-acier, 100 bars au cisaillement et 150 bars à la traction normale. Ce qui nous donna le meilleur espoir quant à l'utilisation en béton armé vu que ces résistances étaient largement supérieures à celles d'un béton courant, et c'est ainsi que je suis arrivé au procédé du *BETON PLAQUÉ*.

On voit alors s'ouvrir deux possibilités, deux portes si j'ose dire.

La première possibilité est celle du *béton à coffrage portant* qui consiste à couler dans un coffrage servant d'armature le béton nécessaire pour assurer la résistance à la compression (fig. 1). Dans son principe, cette idée conduit à une économie de coffrage mais à condition que la liaison acier-béton soit normalement assurée sans risque de décollage et de glissement puisque les joues latérales sont destinées à résister à l'effort tranchant. Il a donc fallu sélectionner une colle propre à durcir en présence du béton frais, ce qui a été fait. Ensuite, il a été nécessaire de mettre au point le procédé de collage qui consiste, en premier lieu, à dégager de toute oxydation la surface des tôles ; ceci se fait par sablage, grenaillage ou meulage. Aussitôt, il est indispensable, pour éviter toute réoxydation rapide (on sait que l'acier s'oxyde très vite) de répandre, immédiatement après nettoyage, une couche de peinture primaire à base d'époxy qui protège la tôle d'acier pendant quelques jours. Mis en place,

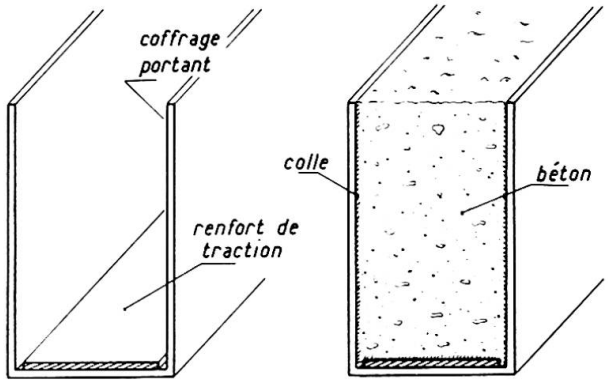

Fig. 1

le coffrage portant dont on peut maintenir provisoirement la position par des cavaliers munis d'aimants permanents est alors enduit de colle sur les surfaces destinées à entrer en contact avec le béton. Cette colle est appliquée par un moyen approprié sur une épaisseur de un à deux millimètres. Le béton coulé peut durcir naturellement ou peut être soumis à un traitement thermique, à condition que la température ne dépasse pas 80 °C. Le chauffage favorise également le durcissement de la colle et la rend moins sensible par la suite aux variations de température.

Ceci fournit une application type aux planchers de bâtiment, prise comme exemple le plus simple. Elle peut être associée aux armatures internes par exemple pour les moments négatifs ou complétée par des tôles collées après coup pour supporter des cisaillements supplémentaires, des moments négatifs et autres sollicitations.

Sans chercher à épuiser le sujet, je signale l'exécution de dalles porteuses suivant le schéma de la figure 2, réalisées en béton d'argile expansée. Le gain de poids très net provient de l'augmentation du bras de levier relatif par suppression de l'épaisseur de protection par le béton des armatures habituelles de traction. La protection contre la corrosion est faite par de la peinture généralement de même nature que la couche primaire interne.

Ultérieurement, j'ai étendu l'affaire aux coques dans lesquelles la tôle porteuse de coffrage peut être courbée à l'avance suivant la forme désirée, avec un minimum de support (fig. 3). Le béton est projeté ou coulé sur la surface courbe moyennant certaines sujétions dont j'ai étudié les principes. Il faut, pour que ce soit économique, obtenir des surfaces développables (partant d'un plan), mais les collages entre tôles, les brisures et les bordures ne sont pas exclus. J'ai, dès à présent, réalisé quelques couvertures de ce genre.

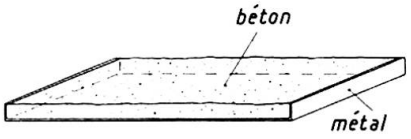

Fig. 2

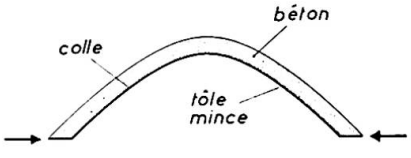

Fig. 3

Voici une illustration (fig. 4) : l'essai d'une voûte en béton plaqué sur une tôle de base circulaire.

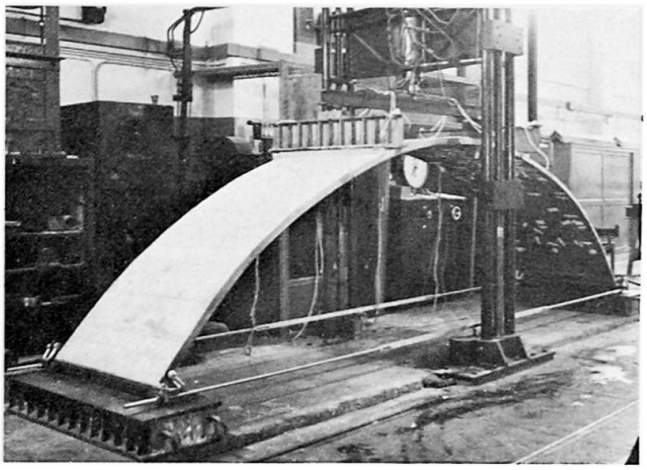

Fig. 4 - Essai d'une coque en béton plaqué. Portée 5,20 m. Flèche 1,30 m. Epaisseur 40 mm. Tôle de 2 mm.

Le *renforcement par acier plaqué* est une autre application fort intéressante du collage. Examinons le cas d'une poutre en béton armé amenée à supporter une surcharge supérieure à celle pour laquelle elle a été prévue et calculée, ou une poutre qui, par suite d'une négligence, paraît être insuffisamment armée ; lorsque l'insuffisance provient des armatures de traction, il est possible de coller sur la partie tendue de la poutre une ou plusieurs tôles de renfort (fig. 5). Lorsque la faiblesse vient d'un manque d'armature à l'effort tranchant, on vient coller des tôles sur les joues latérales que l'on retourne sur les renforcements longitudinaux. Il est souvent nécessaire d'ailleurs d'opérer un double renforcement, comme l'indique la figure 5.

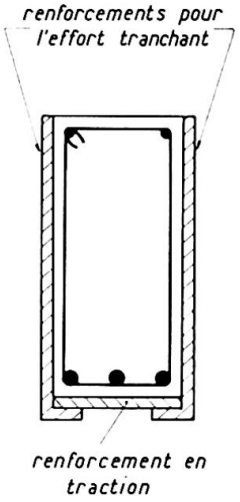

Fig. 5

La difficulté que l'on rencontre souvent se trouve dans la région des appuis, là où les barres déjà existantes supportent l'adhérence. Différents palliatifs sont possibles mais il faut porter son attention sur ce point.

Notons que pour obtenir une bonne adhérence, il faut tout d'abord que le béton soit de bonne qualité ; on peut s'en rendre compte par l'essai d'arrachement d'une pastille métallique collée (2 cm de diamètre environ). Les enduits superficiels doivent être détruits, les surfaces doivent être sablées ou meulées (la couche superficielle étant généralement de moindre résistance) afin de faire apparaître les granulats ; elle doit être dépoussiérée à la brosse et à l'aspirateur. Les surfaces dégagées doivent être aussi planes que possible pour que la tôle puisse être appliquée sans que l'épaisseur de colle dépasse 2 mm. En cas de manque de planéité, il est possible de rectifier la surface à la truelle et à la règle, à l'aide d'une couche de mortier d'époxy au sable fin.

Afin de permettre au placage de se prêter aux défauts de planéité, il est recommandé de ne pas utiliser des épaisseurs de tôle supérieures à 3 mm, quitte à coller plusieurs épaisseurs successives si nécessaire. J'ai vu des cas de décollage, dans des opérations effectuées sans mon intervention où l'on avait collé des tôles de 10 mm. La courbure qu'il avait fallu produire

pour l'application avait provoqué des tensions permanentes de flexion et des réactions de traction normales à la surface de séparation suffisantes pour dépasser la résistance de la colle. Il en est résulté un décollage sur les bordures, lequel s'est propagé sur une grande partie de la surface, rendant le renforcement illusoire. Ceci est un exemple à ne pas suivre.

Après dégagement et nettoyage de la surface de béton, il est bon d'appliquer au pistolet ou au pinceau une couche de primaire qui sert d'accrochage à la colle proprement dite, on améliore ainsi la résistance.

Une autre application du béton plaqué est celle des poutres en I élégies, à âme mince, l'âme de la poutre étant généralement armée d'étriers ou de barres relevées, surtout aux alentours des appuis. J'ai pensé remplacer l'armature de l'âme par une tôle d'épaisseur appropriée sur laquelle on colle latéralement du béton. L'essai s'est révélé très satisfaisant, c'est-à-dire que le même poids d'acier que celui des armatures d'effort tranchant mais sous forme de tôle d'acier a donné un résultat équivalent à la rupture mais le début de fissuration a été retardé. En plus, la mise en place de la tôle centrale a été plus économique que l'armature classique. Je pense même que le remplacement des armatures longitudinales hautes et basses peut être fait grâce à des profilés en cornière collés à l'âme. Je n'ai pas encore pu effectuer les essais correspondants faute de temps et de moyens. Nous retombons alors sur la charpente métallique collée et enrobée de béton.

Une autre application qui se rapproche de la charpente métallique associée au béton (construction mixte acier-béton) est le cas de planchers en béton portés par des profilés métalliques (fig. 6a). Le problème est couramment résolu en assurant la liaison acier-béton par des connecteurs soudés sur la poutre métallique. L'adhérence acier-béton étant négligeable, les liaisons devant résister au cisaillement et à la traction sont données uniquement par les connecteurs.

Dans le cas où l'on interpose entre la table supérieure des profilés et le béton une couche de colle, l'adhérence n'est plus négligeable et l'on obtient une liaison acier-béton qui est à la fois capable de résister au glissement et à la traction normale. L'avantage du collage est que les contraintes sont réparties sur toute la surface et non pas concentrées en autant de points durs qu'il y a de connecteurs. L'effort de glissement par unité de longueur est d'autant plus faible que la table supérieure est plus large. Il est possible que pour des profilés étroits la résistance au cisaillement ne donne pas un coefficient de sécurité suffisant. D'où l'idée d'interposer entre la tôle et le profilé une contre-tôle de largeur $L > \ell$ collée d'une part sur le profilé et d'autre part sur le béton (fig. 6b) qui permet de tenir compte d'une résistance au glissement plus importante.

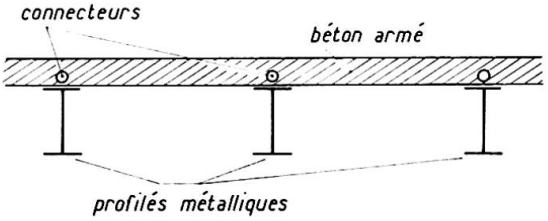

Fig. 6a

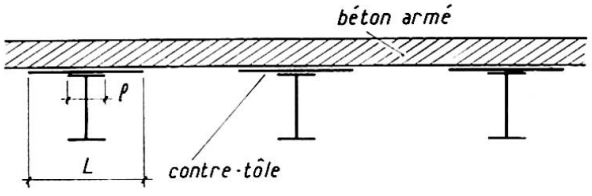

Fig. 6b

Comme application des colles au renforcement, bien que ce ne soit pas à proprement parler du béton plaqué, je citerai encore le renforcement des planchers par dalles contrecollées. Il arrive que sous l'augmentation des surcharges les dalles deviennent trop minces pour supporter les charges concentrées, ou que l'on ait besoin d'augmenter la section de la table de compression des poutres. Il faut alors dégrader la surface supérieure au jet de sable ou à la meule. On nettoie la surface nouvellement dégagée par brossage et aspiration des poussières. Une couche de colle appropriée est

alors répandue (le plus souvent au pistolet) et peu de temps après le nouveau béton est coulé sur 5 à 10 cm d'épaisseur. On dispose pour effectuer ce travail de 1 à 2 heures selon la température et la résine employée. La surcouche de béton doit être armée d'un grillage ou d'un treillis soudé léger afin, simplement, de réduire les effets du retrait. Les dalles de renforcement continues étant susceptibles de supporter des moments négatifs, il est souvent utile de placer dans la contre-couche des armatures correspondantes (chapeaux) comme l'indique la figure 7. Il ne faut surtout pas employer de béton liquide pour éviter que la laitance ait tendance à se répandre devant l'avancement du coulage et à salir la surface de colle qui n'aurait qu'une adhérence réduite. En général, on utilise un béton assez sec et une lame vibrante.

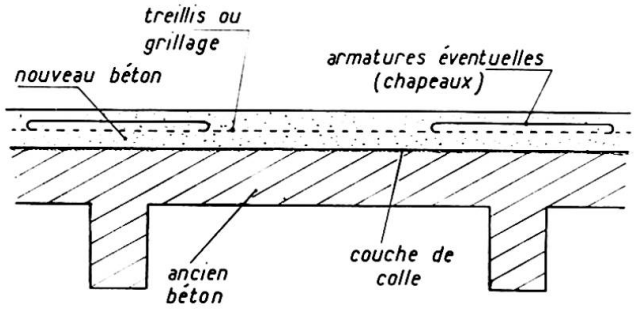

Fig. 7

On peut aussi effectuer un chauffage léger par rayonnement infrarouge pour accélérer le durcissement en ayant soin cependant de protéger le béton contre l'évaporation grâce à une membrane de plastique développée ou projetée au pistolet.

Les techniques de renforcement ne se limitent pas au béton ; elles peuvent s'étendre au bois, à la charpente et aux échafaudages pour réduire les flèches et accroître la résistance à la rupture. Elles s'appliquent même à la maçonnerie. Sur la figure 8, on voit la coupe d'un linteau en maçonnerie de briques creuses de 7 x 22 cm, collées latéralement sur une tôle de 2 mm. Sur une portée de 1,80 m, la poutre s'est rompue sous une charge de 3 800 kg tandis que sans cette armature la résistance était négligeable. On peut en faire autant avec de la pierre de taille. Ceci ouvre des possibilités de préfabrication en maçonnerie.

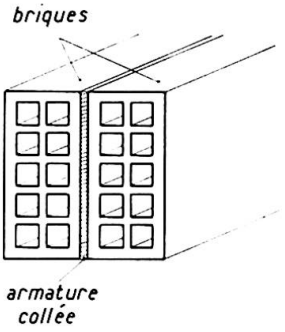

Fig. 8

Le seul inconvénient du collage est que les résines dont nous disposons actuellement s'amollissent vers 80 °C. Cependant, on peut disposer une protection efficace grâce à un isolant qui a pour effet, en cas d'incendie par exemple, de retarder le temps d'amollissement. Une protection obtenue par des plaquettes de vermiculite ou de plâtre de 5 à 6 cm d'épaisseur retarde de 1 h 30 l'apparition de la température atteignant 80 °C sous une atmosphère extérieure portée à 600 °C.

On trouvera ci-après en annexe des compléments sur le calcul et le résultat des expériences.

o
o o

ANNEXES

1 - MESURE DE L'ADHERENCE DU COLLAGE

Deux tôles T sont collées sur les deux faces opposées d'un prisme de béton de 7 x 7 x 28 cm (fig. A.1). Ces tôles sont mises en traction à leurs extrémités libres à l'aide d'une tige de traction A_1 terminée en rotule et s'appuyant sur la pièce P. Ces tôles transmettent leur effort au béton E par l'intermédiaire du collage ; la fixation à la pièce P est faite par boulonnage. Elles travaillent en traction et le prisme de béton est comprimé à l'aide de la tige A_2 et de l'étrier S qui transmet une compression par l'intermédiaire de l'appui M. Les tôles sont munies d'extensomètres à résistance de manière à mesurer la répartition de contraintes de traction sur leur longueur. On constate, ce qui correspond à l'évidence, que la répartition des contraintes dans l'acier n'est pas uniforme. Ceci peut être prévu théoriquement (d'après BRESSON) moyennant les hypothèses suivantes évidemment simplifiées :

- l'acier, le béton et la colle sont élastiques,
- la colle ne supporte que des efforts de cisaillement,
- le système est considéré comme symétrique.

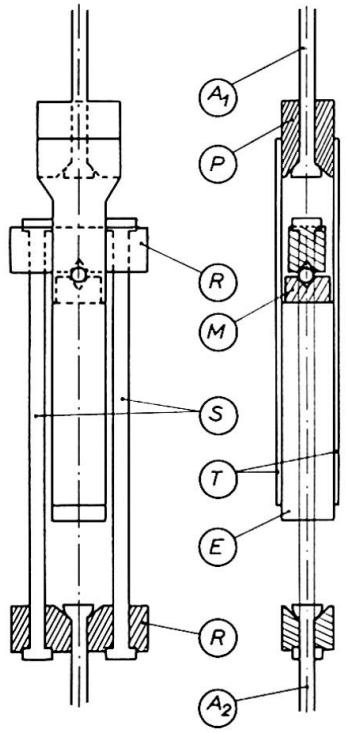

Fig. A.1

On obtient une équation :

$$\frac{d^2\tau}{dx^2} - w^2 \tau = 0$$

où τ est la contrainte de cisaillement dans la résine, x la distance depuis l'origine non chargée de la tôle, $w^2 = c\left(\frac{1}{E_1 e_1} + \frac{1}{E_2 e_2}\right)$, E_1 et E_2 les modules d'élasticité du béton et du métal, e_1 la demi épaisseur du prisme de béton et e_2 l'épaisseur de la tôle, $c = \frac{G}{d}$, G module de cisaillement de la colle d'épaisseur d.

La solution générale est alors :

$$\tau_x = P\, w\, \frac{ch\ wx}{sh\ w\ell}$$

Si ℓ est la longueur du collage :

$$\tau_{(x_o)} = 0 \qquad \tau_\ell = P\, w\, \frac{1}{tgh\ w\ell}$$

où P est la charge appliquée par unité de largeur de l'élément essayé.

La figure A.2 montre l'allure de cette courbe qui représente la variation du cisaillement dans la colle. Elle est nulle pour x = 0, extrémité libre de la tôle collée, et passe par un maximum à l'autre extrémité.

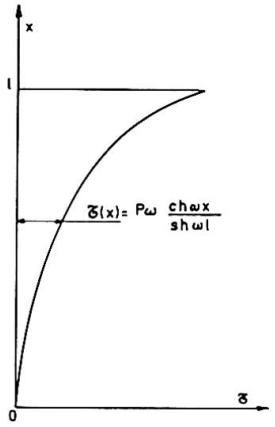

Fig. A.2

On peut encore écrire, moyennant une simplification, que la force longitudinale supportée par la tôle suit approximativement une fonction $P(x) = P\frac{sh\ wx}{sh\ w\ell}$.

Un certain nombre d'expériences ont été faites sur des collages conformément au schéma de la figure A.1. De la mesure de tension dans les lames d'acier, on tire la valeur des cisaillements $\tau_x = \frac{dP_x}{dx}$.

Pour une longueur de collage de 26 cm, la figure A.3 montre les résultats de l'essai sur une tôle de 1 mm et la figure A.4 pour une épaisseur de 4 mm. On voit que dans le premier cas une longueur de collage de 10 cm absorbe la tension appliquée tandis que dans le deuxième cas une longueur de collage de 15 cm est nécessaire. La figure A.5 montre l'élément d'essai après rupture. L'ensemble des essais est résumé dans le tableau suivant :

Numéro de l'essai	Epaisseur de la tôle (mm)	Charge de rupture (t)	Moyenne des charges de rupture (t)	τ_r moyen (bars)	σ_a (bars)
5	1	3,6	4	11	2 860
6	1	4,1			
17	1	4,5			
18	1	4			
1	2	4,1	5,8	16	2 080
2	2	5			
3	2	7,5			
19	2	6,5			
10	3	5,5	6,25	17,1	1 485
11	3	6,5			
15	3	6,5			
16	3	6,5			
8	4	8	7,9	21,8	1 400
9	4	8,5			
12	4	7,5			
20	4	7,5			
4	5	8,7	8,2	22,5	1 170
7	5	8,5			
13	5	6			
14	5	7,5			

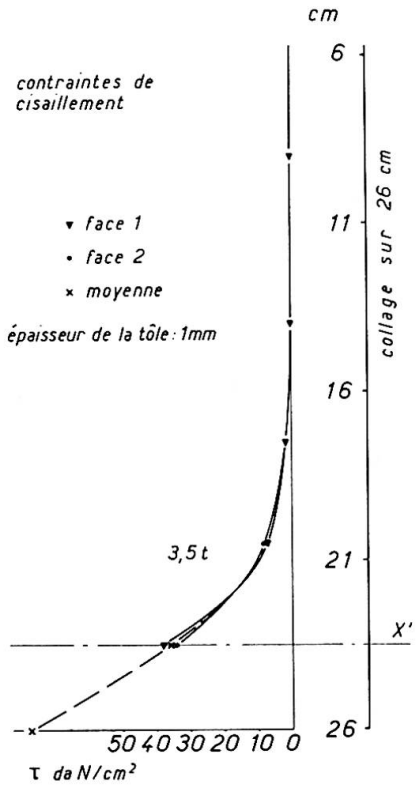

Fig. A.3

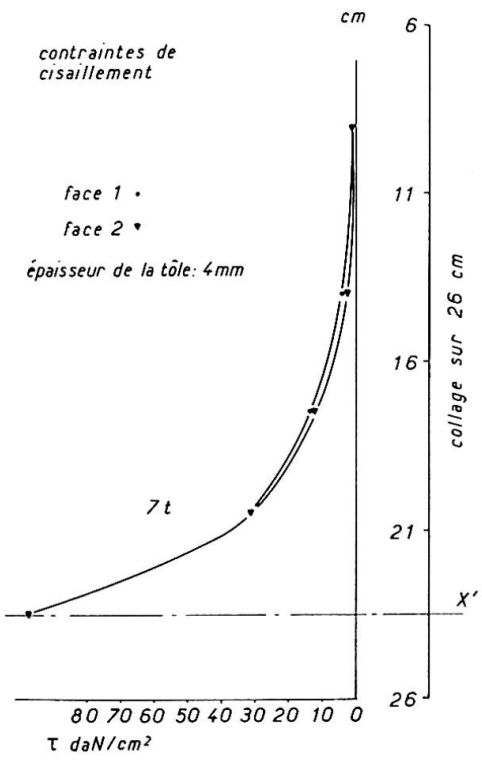

Fig. A.4

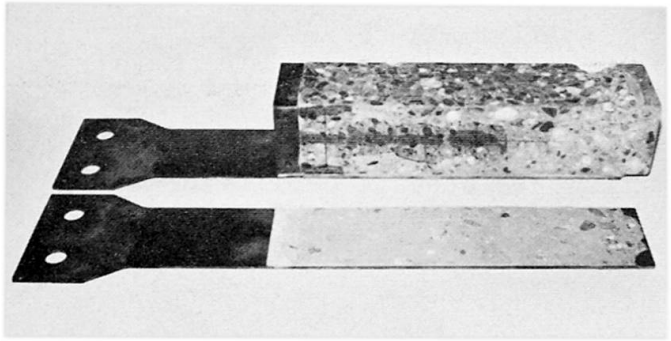

Fig. A.5

On voit que le taux de cisaillement moyen à la rupture croît avec l'épaisseur du collage tandis que le taux de travail de l'acier diminue. L'expérience montre encore que lorsque la longueur de collage dépasse 17 cm (épaisseur du collage 0,6 mm) la résistance cesse d'augmenter. Ce résultat est fort important pour les applications. On constate encore que pour des collages correctement réalisés la rupture a toujours lieu entre le béton et la colle.

2 - LIAISON ACIER-BETON DANS LA CONSTRUCTION MIXTE

J'ai parlé dans le cours du mémoire de la liaison acier-béton dans la construction mixte. Suivant la figure 6b, le cisaillement à l'interface colle-acier est, par unité de section :

$$\tau = \frac{T}{a}\,\frac{S}{I}$$

où T est l'effort tranchant, S le moment statique, I le moment d'inertie et a la largeur du contact. En accroissant a, comme l'indique la figure, par interposition d'une contre-tôle de largeur plus grande que la table, τ diminue pour atteindre une valeur admissible (fig. A.6).

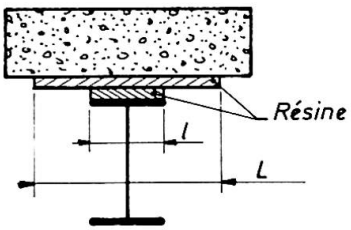

Fig. A.6

Afin de vérifier le principe théorique émis ci-dessus, J. BRESSON a effectué l'expérience définie par la figure A.7 dans laquelle les deux profilés ont été chargés en tête dans une machine de compression (fig. A.8) (la traction a été éliminée car elle aurait provoqué une rupture en traction entre BB et DD).
Sans interposition de tôle, la rupture a eu lieu à 24,7 tonnes entre la table du profilé et le béton, soit en moyenne à 20 bars (maximum 55 bars). Avec une interposition d'une tôle de 3 mm sur 0,50 m, la rupture a eu lieu à 66 tonnes entre le profilé et la tôle pour un taux de travail moyen au cisaillement de 66 bars, avec un maximum de 160 bars. C'est ce qu'il fallait démontrer (on consultera le mémoire de J. BRESSON).

La figure A.9 donne d'autres applications possibles du système.

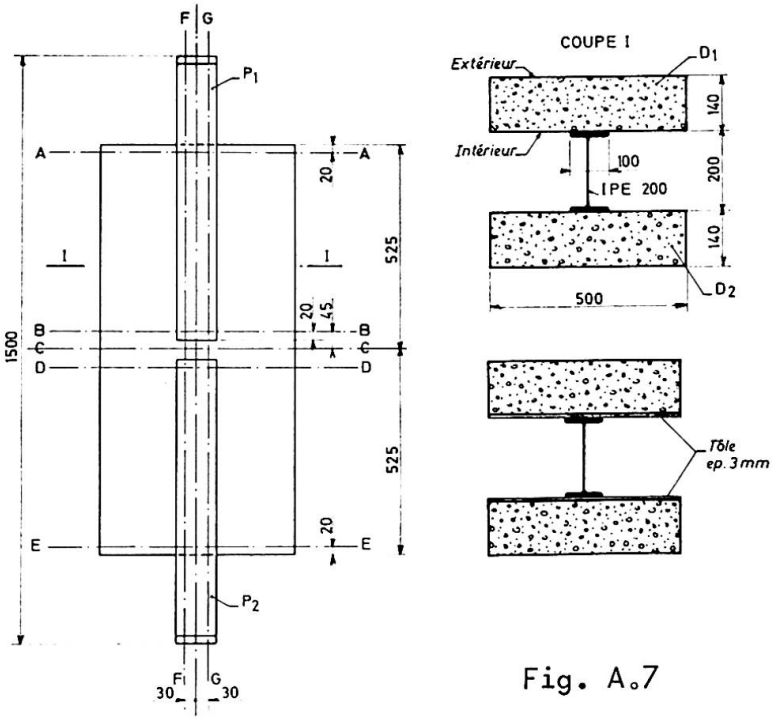

Fig. A.7

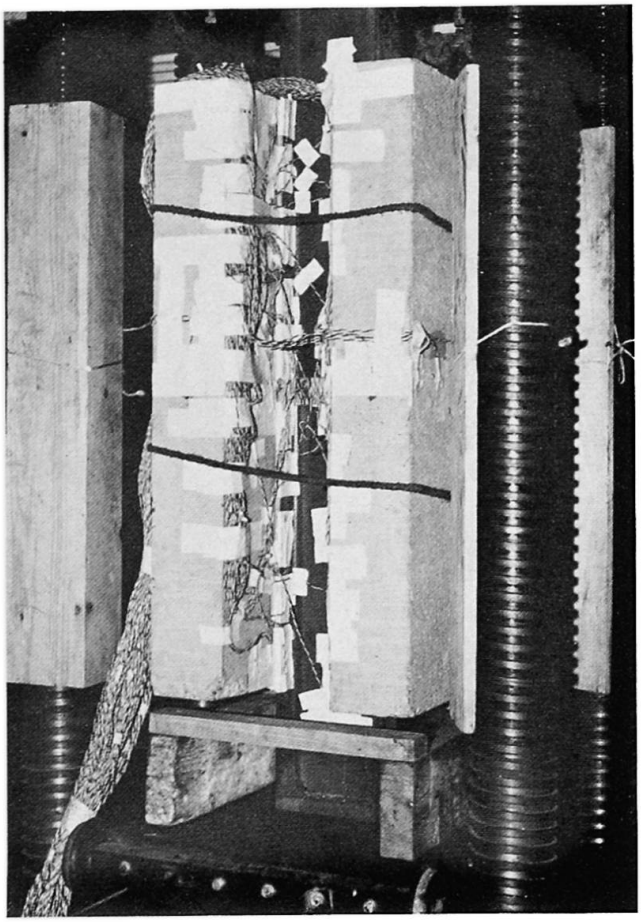

Fig. A.8

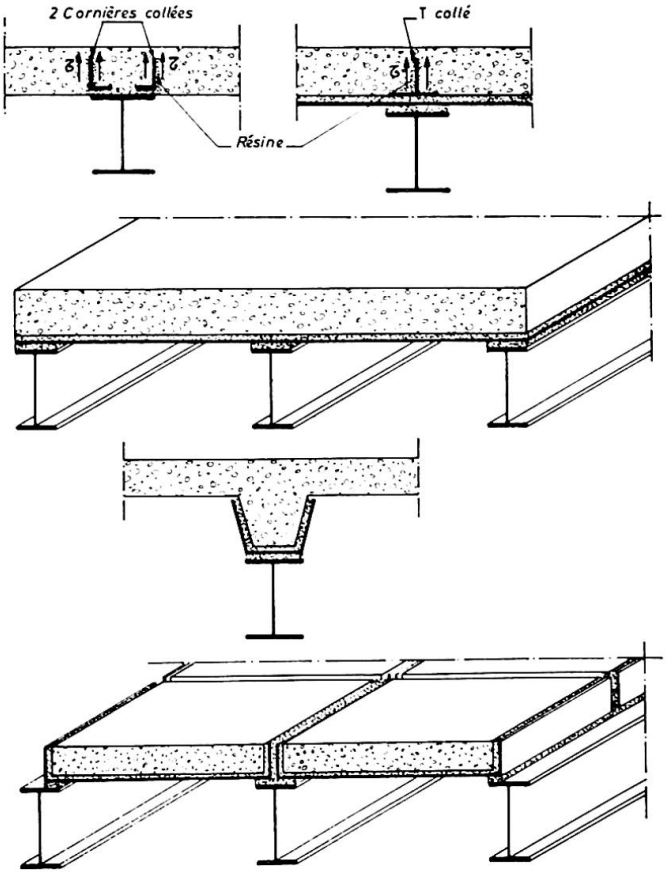

Fig. A.9

3 - VOILE MINCE

Je donne ici, sur la figure A.10, les contraintes calculées et mesurées au cours de l'essai de voûte mince illustré par la figure 4. C'est délibérément que, dans cette série d'expériences, nous n'avons pas armé les reins en traction et la rupture s'est produite dans la région correspondante. Au moment de la rupture, le béton supportait un taux de travail de - 24 bars. Cependant il est possible, et ceci a été fait, de renforcer la partie supportant un moment négatif par collage de bandes de tôle disposées suivant les directrices d'extrados, bandes qui peuvent être appliquées sur le béton encore frais ou durci. Ce renforcement permet de faire supporter à la voûte une surcharge bien plus élevée.

o
o o

Les premiers essais de collage acier-béton ont eu lieu en 1964-1965. La première application industrielle a été réalisée au début de 1966 et les suivantes sont de plus en plus nombreuses.

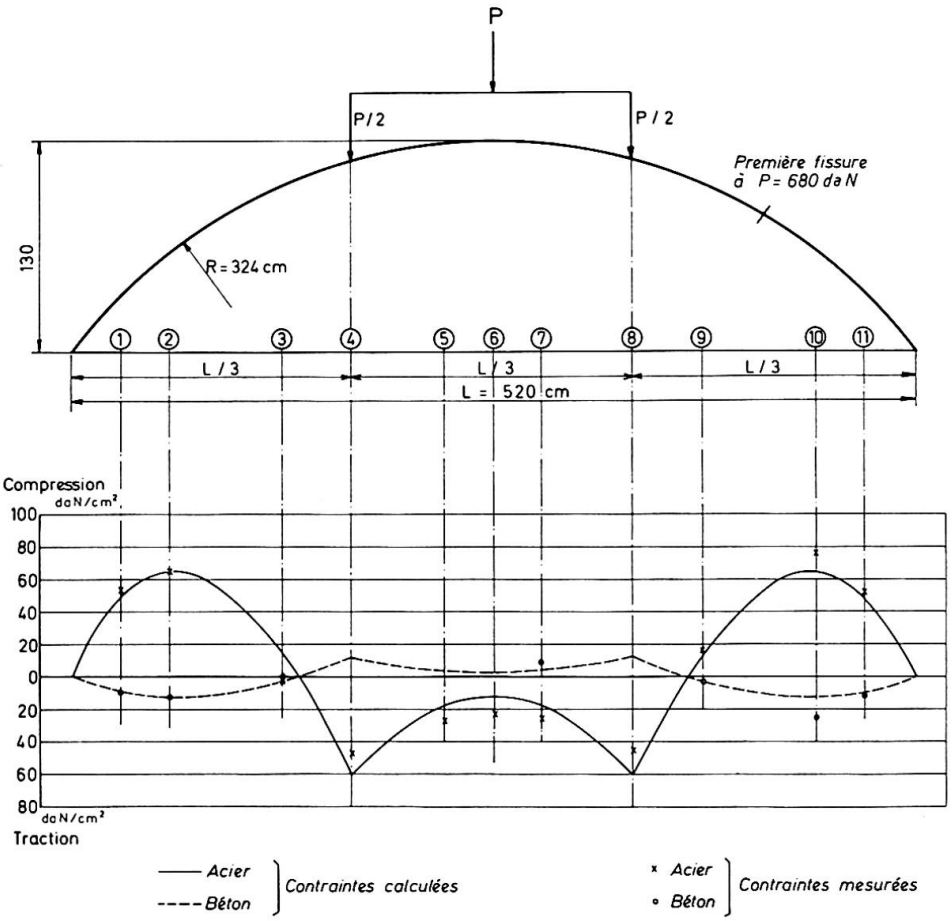

Fig. A.10

BIBLIOGRAPHIE

BRESSON (J.). - Nouvelles recherches et applications concernant l'utilisation des collages dans les structures, *Annales Inst. Techn. Bât.et T.P.*, Paris, février 1971, p. 21.

CIRODDE (R.). - Techniques d'assemblage par collage, *in* : Les résines de synthèse dans la construction, Colloque RILEM, septembre 1967, *Eyrolles*, Paris, 1971, p. 47.

L'HERMITE (R.). - L'application des colles et résines dans la construction. Le béton à coffrage portant, *Annales Inst. Techn. Bât. et T.P.*, Paris, novembre 1967, p. 1. - Les résines synthétiques dans la structure, *L'Architecture d'Aujourd'hui* , Paris, décembre 1968-janvier 1969, n° 141.

L'HERMITE (R.) et BRESSON (J.). - Béton armé par collage des armatures, *in* : Les résines de synthèse dans la construction, Colloque RILEM, septembre 1967, *Eyrolles* , Paris, 1971, p. 175.

RESUME

La mise au point, ces dernières années, de colles possédant certaines performances a rendu possible leur utilisation dans les travaux de génie civil. Ainsi a été conçu le procédé du béton plaqué qui offre deux types d'applications : le béton à coffrage portant et le renforcement par acier plaqué de structures en béton armé en particulier. On donne en annexe des compléments sur le calcul de l'adhérence acier-béton et les résultats d'expériences de laboratoire.

Prestressed Composite Hybrid Beams

Barres hybridés précontraintes et mixtes

Vorgespannte Verbund-Hybrid-Balken

GIAN MARIO BO
Prof. Ing.
Italsider S.p.A.
Associated Professor
Polytechnic of Turin, Italy

IVO DADDI
Dr. Ing.
Italsider S.p.A.
Associated Professor
University of Genoa, Italy

1. Introduction

In modern construction systems use is increasingly made of prestressing techniques with the scope to improve internal stress distribution even in the most severe operating conditions. Thus an internal bending stress can be obtained, as in the Preflex system [1], by bending Fe52 steel milled girders, with symmetrical section about the direction of bending, to form a composite concrete slab. The steel girder is submitted by external forces to a bending moment before in-situ casting of the concrete slab on the strechted flange. After curing, the externally applied stresses are relieved and the steel girder upon returning to its original conditions, causes the compression of the concrete slab.

It is thus possible to reduce the deformability of the beams and to increase operating stresses in the steel structure up to the maximum values permitted by tensile strength of the steel.

Furthermore, the oscillation of tensile stresses due to the application of load values variable in time is also reduced to the evident advantage of the endurance strength.

Finally, the concrete of the slab covering the stressed beam edge also gives fire protection.

Utilization of Fe52 steel involves, however, a rather reduced stress limit during the preliminary flexure of the girders.

Instantaneous deformation of the prestressed concrete and its subsequent increment due to creep phenomena are significantly reducing the preliminary flexure stresses. This means that the tensive strains in the concrete when submitted to the working load, may increase thus reducing the benefits obtained from the induced stresses.

Therefore we are of opinion that it would be very interesting to adopt, instead of Fe52 milled beam, a composite dissymetric welded hybrid beam [2], [3] with a high yield strength flange component, such as for instance T1 steel.

The Fe52/T1 yield strength ratio is about 0.5. This means that the elastic strain of the T1 flange component during the preliminary flexure stage will be twice as great.

The loss of tensile strength due to instantaneous compression in the concrete and in particular as a result of creep will have a lower influence rate.

2. Calculation hypothesis and findings

The internal bending stress in prestressed girders can be considered as the sum of the effects due to the preliminary bending loads applied to the steel girders and to a second load system of the same magnitude but of opposite sign. These loads are applied on the composite beam after casting and curing of the concrete slab. When indicating by s and i the two flange components, the absolute stress values found in the steel and in the concrete are obtained by the relations:

$$\frac{\sigma_s''}{\sigma_s} = 1 - \frac{W_s}{W_s'} \quad ;$$

$$\frac{\sigma_i''}{\sigma_s} = \frac{\sigma_i}{\sigma_s} - \frac{\sigma_i'}{\sigma_s} = \frac{W_s}{W_i} - \frac{W_s'}{W_i} \cdot \frac{W_s}{W_s'} \quad ; \qquad (1)$$

$$\frac{\sigma_c'}{\sigma_s} = \frac{\sigma_i'}{\sigma_s} \cdot \frac{1}{n} = \frac{W_s'}{W_i} \cdot \frac{W_s}{W_s'} \cdot \frac{1}{n}$$

In (1) letters without apex evidence the stresses during the preliminary flexure stage, discharge tension being indicated by one apex and final strains by two. W indicates the moment of resistance with regard to the Y axis.

Stresses have been calculated [4], [5] with reference to Fig. 1 taking into consideration the beam section consisting in 4 areas, with disregard of their centroid axis moment of inerzia with reference to their displacement moment.

The distance between the two flange components is assumed to be equal to the height of the girder with a very slight excess error but nearly always compensated by disregarded moment of inertia of the web, to their centroid axis.

The classical Preflex girder type is characterized by:

$$\rho = 1 \qquad \text{and} \qquad W_s = W_i$$

The hybrid girder as proposed by us is characterized by a $\rho < 1$ ratio to be calculated provided that the two flange components are reaching contemporaneously their yield point during the preliminary flexure of the bare (uncoated) girder.

Therefore we'll find that:

$$\frac{W_i}{W_s} = \frac{2\rho + c_1}{2 + c_1} = \eta \qquad (2)$$

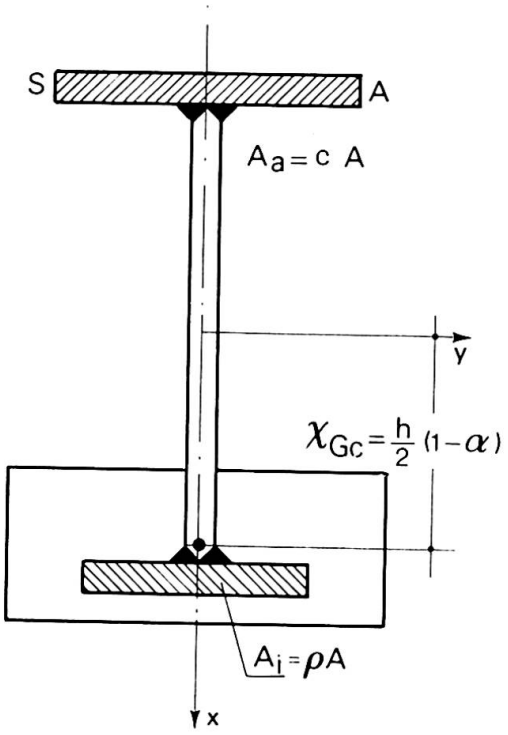

Fig. 1

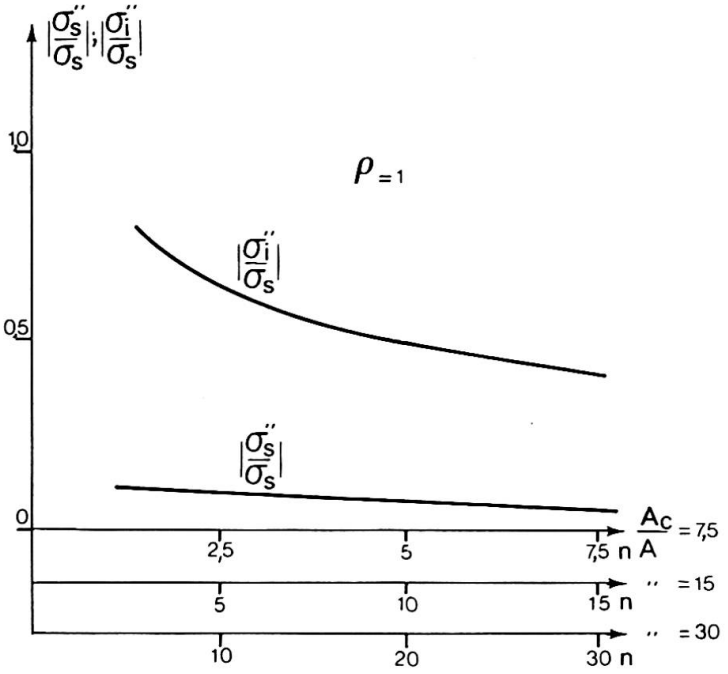

Fig. 2

η being the ratio between the yield stress values ≤ 1.
The coefficient c_1 is connected with the geometric coefficient c (see Fig. 1) of the relation:

$$c_1 = \sqrt{\eta} \cdot c \qquad (3)$$

c_1 has been found to be lower than c due to the plastic deformation of the web in vicinity of the stretched flange.

Evidently (1) are functions of n and are therefore time functions. When using Fe52 and T1 steel in the lower flange, $\eta = 0.5$ and $\frac{W_s}{W_i} = 2$ according to (2).

Figures n° 2 and n° 3 show the relationship $\frac{\sigma_i''}{\sigma_s}$, $\frac{\sigma_s''}{\sigma_s}$ calculated based upon $\rho = 1$, i.e. for a Preflex type girder and $\rho = 0.325$ obtained from (2) for a hybrid beam assuming $c = 1$ for both girders.

Based upon the third equation of (1) and on the figures it will also be possible to calculate the stresses in the concrete.

At equal maximum stresses in the concrete, the hybrid beam will require slightly higher $\frac{A_c}{A}$ ratios.

In the cases here illustrated at limited concrete stress values, $\sigma_c = 250$ Kg/cm^2 the following values have been found:

$$\rho = 1 \quad ; \quad \frac{A_c}{A} = 15$$

$$\rho = 0,325 \quad ; \quad \frac{A_c}{A} = 17$$

Creep in the concrete reduces the stresses in the stretched flange components.
Fig. 4 shows the reduction between t = 0 and t = ∞ , assuming an initial value for n = 5 and a final value n = 15. It is thus evidenced that the hybrid beam stretched flange always maintains a proportionally higher tensile strength.

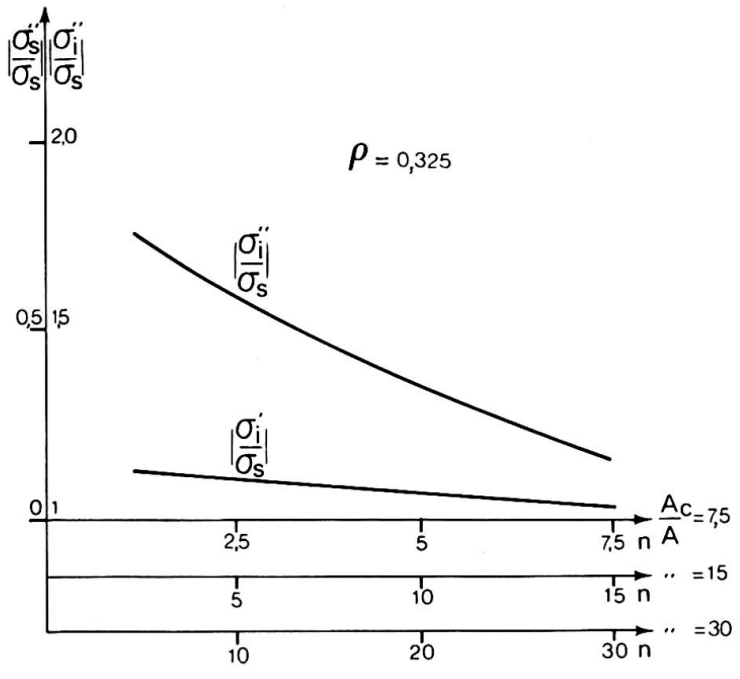

Fig. 3

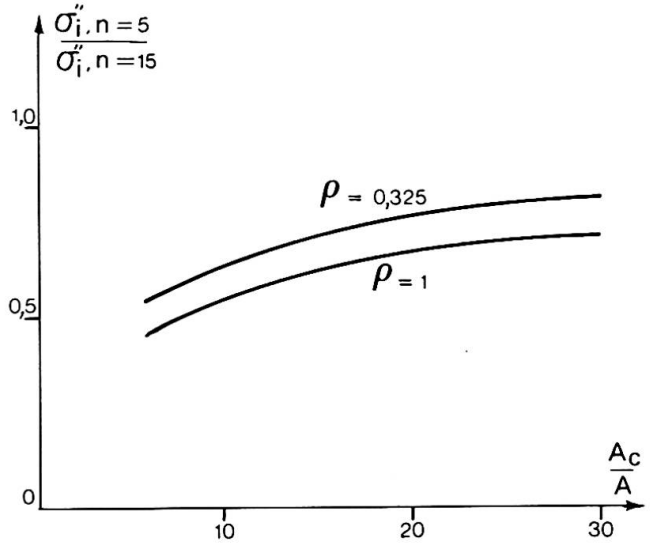

Fig. 4

3. Conclusions

The application of high tensile strength steel only for the stretched flange components and even at a reduced flange size, makes it possible to achieve higher precompression strength than can be obtained in a corresponding symmetrical girder.

This gives the possibility to use T1 steel to its maximum permissible tensile structural stress. Because of the slighter reduction due to prestressing, it will thus be possible to take complete advantage of the reduced tensive stress range in presence of variable loads.

Welding should permit plastic adaptation of less than 0.2% during the preliminary bending [6].

Welding costs can be at least partially offset by the possibility to obtain a counterflexure without particular operations, in addition of course to a greater range of applicable sections.

Bibliography

[1] Baes L., Lipski A., La poutre "Preflex", Liège, Desoer, 1954.

[2] Design of Hybrid Steel Beams, Journal of the Structural Division, ASCE, Vol. 94, N. ST6, June 1968.

[3] Daddi I., Sul dimensionamento a collasso plastico di travi a doppio T realizzate con acciai di differenti caratteristiche di resistenza, Costruzioni Metalliche, N. 3, 1968.

[4] Daddi I., Travi ibride in sistema misto presollecitate, Contributo alla discussione libera 25° Congresso Internazionale dei Centri Informazione dell'Acciaio, Salzburg, Settembre 1971.

[5] Bo G.M., Daddi I., L'impiego di travi ibride per la realizzazione di travi composte precompresse (in corso di pubblicazione).

[6] Lew H.S., Toprac A.A., The Static Strength of Hibryd Plate Girders, Report P 550 - 11, Structures Research Laboratory University of Texas, Austin, Tex., January 1968.

SUMMARY

The authors have calculated the internal stress distribution achieved by bending of a steel beam, before casting a concrete slab on the stretched flange.

A comparison is also made between the behaviour of a Fe52 milled beam and the behaviour of a Fe52 and T1 hybride welded beam. The greater stresses and strains allowable for the T1 steel permit a better prestressing of the concrete.

Leere Seite
Blank page
Page vide

Strength of Hybrid Steel Columns

Résistances de colonnes hybrides en acier

Festigkeit hybrider Stahlstützen

NEGUSSIE TEBEDGE
USA

NAGARAJ R. NADIG
India

LAMBERT TALL
USA

INTRODUCTION

The hybrid steel column is a special type of structural member built up of component plates having different grades of steel. The concept of hybrid shapes has been applied to structural members in bending, by placing a stronger material in a position where it can resist higher stresses, thus using materials according to their strength, and effecting significant material economy. This concept has been extended to columns in this study. The study provides insight also to the interesting problem of the reinforcing of old columns to carry heavier loads by adding higher strength cover plates.

This paper summarizes the analysis and results of a theoretical and experimental investigation to determine the strength of hybrid steel columns. The theoretical analysis treats hybrid shapes based on the tangent modulus and maximum strength concepts where the actual material properties, residual stresses, and initial imperfections are taken into consideration. Local buckling is also considered. The experimental study includes four different hybrid shapes fabricated from flame-cut or universal-mill plates of three different steel grades. The test program consists of tension tests, residual stress measurements, stub column tests, and pinned-end column tests.

A close correlation was shown between the theoretical predictions and experimental results. The strength of hybrid columns is defined, and some economy may be expected in their use in the lower stories of multi-story frames.

THEORETICAL ANALYSIS

Basic Column Strength

The strength of a column may be defined either by its bifurcation load or by its maximum load. For any column the strength

depends on the material properties, the magnitude and distribution of residual stresses, and on the initial out-of-straightness. A perfectly straight column with concentric load application remains straight under increasing load until the tangent modulus is reached. Real columns, however, show an initial out-of-straightness and unsymmetrical distributions in material properties and residual stresses which will cause the column to deflect immediately upon loading. The deflection will increase under increasing load up to the maximum load, as shown in Fig. 1.

In determining the strength of hybrid steel columns, the major problems are caused by the different levels in yield strength of the component materials and by the residual stresses. In this study the H-shaped hybrid column is considered consisting of higher-strength flanges and a lower-strength steel web. The material properties of the component plates are assumed to be elastic-perfectly-plastic as shown in Fig. 2.

Tangent Modulus Strength

The strength of a centrally loaded column based on the tangent modulus concept [1] may be written in the form

$$P_{tm} = \frac{\pi^2 E}{L^2} \int_A \left(\frac{E_t}{E}\right) y^2 \, dA \qquad (1)$$

where P_{tm} is the tangent modulus laod, E the elastic modulus, A the total cross-sectional area, L the effective length of the column, and E_t the effective tangent modulus of the shape. The tangent modulus load is computed based on the measured residual stresses using the computer.[2] The tangent modulus curves obtained for various shapes are shown in Fig. 3.

The tangent modulus load may also be computed based on a stub column test result as described in Ref. 3.

Maximum Strength

The calculations become more complex for maximum strength predictions even though the underlying basic concepts are rather simple. In Ref. 4 an approximate method is developed based on simplifying assumptions which is suitable for computer programming and applicable to initially straight centrally loaded columns as well as to columns with initial out-of-straightness.

The method is based on the assumption that the initial as well as deflected shape under load is described by a half-sine wave. This shape has a favorable feature since differentiation of the function twice, yields a simple relationship between the deflection δ_m and the curvature ϕ_m at the mid-height of the column as follows,

$$\phi_m = \frac{\pi^2}{L^2} \delta_m \qquad (2)$$

Thus, for any arbitrary value of δ_m the corresponding curvature ϕ_m is determined directly. The equilibrium condition at the mid-height

cross section may be written in the form

$$P_{int} = \int_A E\varepsilon \, dA = \frac{1}{\delta_m} \int_A E\varepsilon \, y dA = \frac{1}{\delta_m} M_{int} \qquad (3)$$

where ε is the strain distribution in the cross section which is a function of y. By assuming plane sections to remain plane, Eq. 3 is solved employing a numerical iterative procedure.

The maximum load is determined when the rate of resisting internal moment of the column approaches zero. Under this load the column is in a state of neutral equilibrium. The maximum strength column curves have been determined using the computer [2] and the results for columns with initial out-of-straightness e = 0 and e = L/1000 are shown in Fig. 3.

Local Buckling

In hybrid shapes, web buckling may be of some concern because the web may be partially or wholly inelastic at working load. Flange buckling can be considered without difficulty, since it will be essentially elastic. The width-thickness ratio of the web must be such that the web does not buckle even if it has yielded completely.

The buckling of plates containing residual stresses has been analyzed using the incremental flow theory and the total strain theory on the basis of the finite difference approximation of a differential equation. [5,6] Figure 4 shows the plate buckling curves for webs of welded shapes in terms of the non-dimensionalized width-thickness ratio, defined as

$$\lambda = \frac{b}{t}\sqrt{\frac{\sigma_y}{E}\,\frac{12\,(1-\mu)}{k\pi^2}} \qquad (4)$$

where μ is Poisson's ratio and k is the plate buckling coefficient.[7] According to these curves, local buckling in the plastic range is prevented when $\lambda \leq 0.62$ if the ends are fixed and $\lambda \leq 0.68$ if the plates are simply supported.

EXPERIMENTAL STUDIES

The experimental study included four hybrid shapes which were fabricated from flame-cut or universal-mill plates. The columns were not subjected to cold straightening. The tests conducted on these shapes were: tension tests, residual stress measurements, stub column tests, and pinned-end column tests. The experimental study is described in greater detail in Ref. 2.

Supplementary Tests

Supplementary tests, which included tension tests and residual stress measurements,. are conducted to determine the properties of the specimen so as to enable theoretical prediction of column strength. The mechanical properties of the shapes were obtained from tension tests conducted in accordance with the ASTM specification. The results of the tests are summarized in Table 1.

Residual stress measurements were made by the method of sectioning. The results for one quarter of each section are shown in Fig. 3

Column Tests

Stub column tests were performed in order to obtain for each cross section the average stress-strain curve which takes into account the effects of residual stresses. The proportional limit, the elastic modulus, the tangent modulus, and the average yield strength were the important data furnished by the stub column tests.

Pinned-end columns with a slenderness ratio of 65 were tested to verify the prediction of the behavior and strength of each column based on the measured residual stresses or stub column test. The test results for the stub columns and pinned-end columns are given in Table 1.

Discussion of Results

As shown in Fig. 3, there is a reasonably good agreement between the theoretical and experimental column strengths. The non-dimensionalized tangent modulus and maximum load column curves for the hybrid shapes show that the strength of these columns are much higher than that of welded homogeneous A36 steel columns. For columns with A514 steel flanges $P_m/P_{tm} \approx 1.05$ and for columns with A36 steel $P_m/P_{tm} \approx 1.25$.

PRICE-STRENGTH RELATIONSHIP

A relationship between the price and strength of columns may be established for different steel grades with the aid of column curves and cost data. Figure 5 shows comparison curves for columns of three different steel grades based on average mill price ratios of 1969.[8] A price comparison of hybrid shape No. IV with the homogeneous shape counterparts is shown in Fig. 6. This indicates that hybrid shapes may be economical for columns with low slenderness ratios. For a reliable comparison, further factors should be taken into consideration such as fabrication, transportation, and erection, any of which may change the curves shown in Figs. 5 and 6.

CONCLUSIONS

This paper summarizes the analysis and results of a theoretical and experimental investigation to determine the strength of hybrid steel columns. The theoretical analysis treats hybrid shapes based on the tangent modulus and maximum strength concepts. Local buckling is also considered. The experimental study includes four different hybrid shapes. A close correlation was shown between the theoretical prediction and the experimental results. The strength of hybrid columns is defined, and some economy may be expected in their use in the lower stories of multi-story frames.

ACKNOWLEDGEMENTS

This report is based on the research program "Hybrid Steel Columns" conducted at Fritz Engineering Laboratory, Bethlehem, Pennsylvania. The project was jointly sponsored by the Pennsylvania Department of Highways, the U.S. Department of Commerce - Bureau of Public Roads, and the Column Research Council, and was under the technical guidance of the Column Research Council Task Group 1, of which John A. Gilligan is Chairman.

REFERENCES

1. Beedle, L.S., and Tall, L.
BASIC COLUMN STRENGTH, Journ. Proc. ASCE, 86, ST7,July 1960

2. NagarajaRao, N.R.
THE STRENGTH OF HYBRID STEEL COLUMNS, PhD Dissertation, Lehigh University, April 1965; University Microfilms Inc., Ann Arbor, Michigan

3. Yu, C.K., and Tall, L.
SIGNIFICANCE OF APPLICATION OF STUB COLUMN TEST RESULTS, Journ. Proc. ASCE, 97, ST7, July 1971

4. Tall, L.
THE STRENGTH OF WELDED BUILT-UP COLUMNS, PhD Dissertation, Lehigh University, May 1961; University Microfilms Inc., Ann Arbor, Michigan

5. Ueda, Y., and Tall, L.
INELASTIC BUCKLING OF PLATES WITH RESIDUAL STRESSES, IABSE Publications, Zurich, 1967

6. Nishino, F., and Tall, L.
RESIDUAL STRESS AND LOCAL BUCKLING STRENGTH OF STEEL COLUMNS, Proc. Japan Society of Civil Engg., 172, Dec. 1969

7. Timoshenko, S., and Gere, J.M.
THEORY OF ELASTIC STABILITY, 2nd Ed.,McGraw-Hill, N.Y., 1961

8. NagarajaRao, N.R., Marek, P., and Tall, L.
HYBRID STEEL COLUMNS, Fritz Engg. Lab. Report 305.2,May 1969

Summary

The analysis and results of a theoretical and experimental investigation to determine the strength of hybrid steel columns is presented. The theoretical analysis treats hybrid shapes based on the tangent modulus and maximum strength concepts; the experimental study includes four different hybrid shapes, and a close correlation was shown between theory and experiment. Some economy may be expected in the use of hybrid columns in the lower stories of multi-story frames.

Table 1 : Summary of Test Results

SHAPE	COMPONENT PLATE	STEEL GRADE	TENSION SPECIMEN $(\sigma_y)_{Ten.}$ (N/mm²)	TENSION SPECIMEN σ_{ult} (N/mm²)	STUB COLUMN P_y (N)	STUB COLUMN $\frac{(\sigma_y)_{stub}}{(\sigma_y)_{Ten.}}$	PINNED-END COLUMN (L/r = 65) δ_o (mm)	PINNED-END COLUMN P_{max} (N)	PINNED-END COLUMN $\frac{P_{max}}{P_y}$	PINNED-END COLUMN $\frac{P_{max}}{P_{theory}}$
I	Flange	A441 (UM)	345	550	1750	1.01	1.5	1260	0.72	0.96
	Web	A36	269	461						
II	Flange	A441	361	575	1780	1.02	0.5	1480	0.83	1.05
	Web	A36	260	455						
III	Flange	A514	760	843	3440	1.03	1.5	2580	0.75	1.01
	Web	A36	275	461						
IV	Flange	A514	740	810	3450	1.04	2.5	2570	0.75	1.01
	Web	A441	338	490						

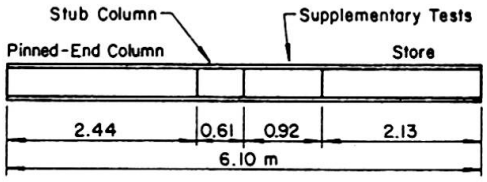

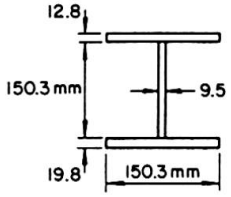

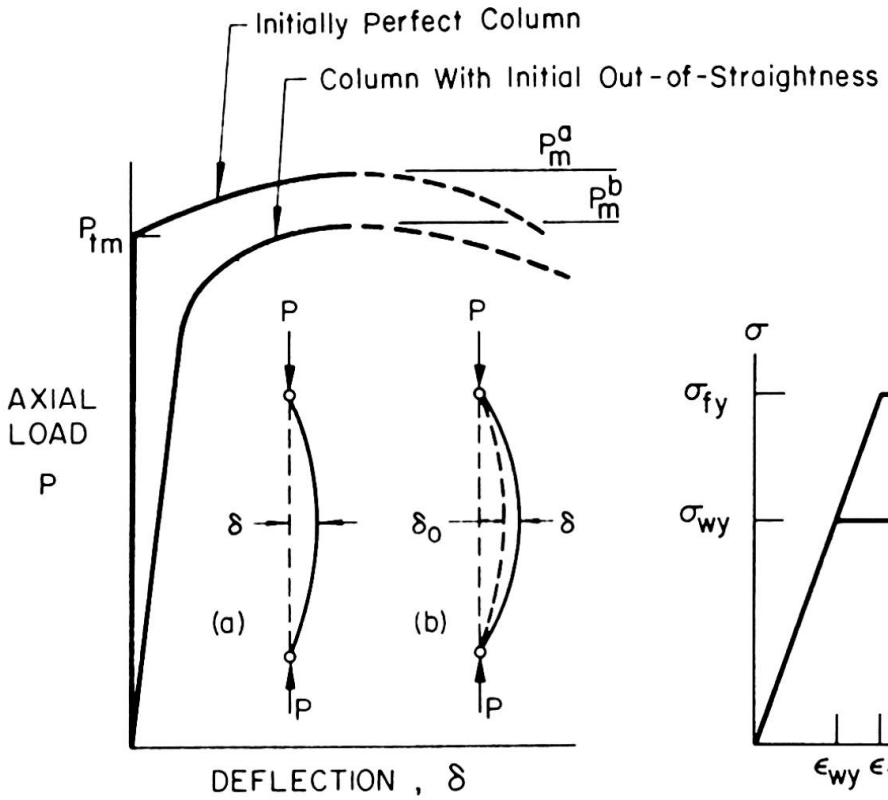

Fig. 1

Load - Deflection Curve for a Centrally Loaded Column

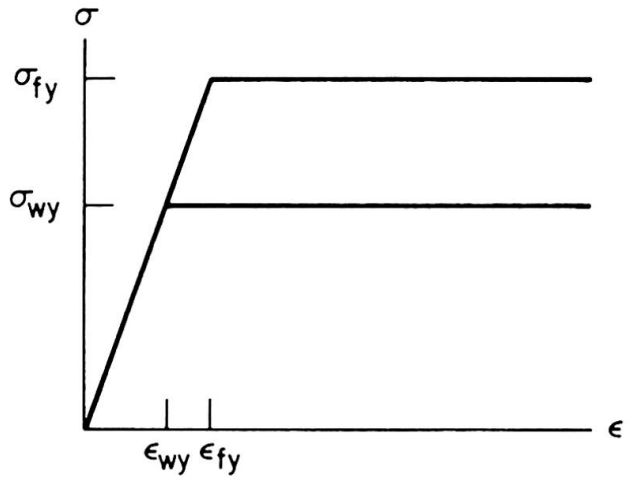

Fig. 2

Idealized Stress-Strain Curves

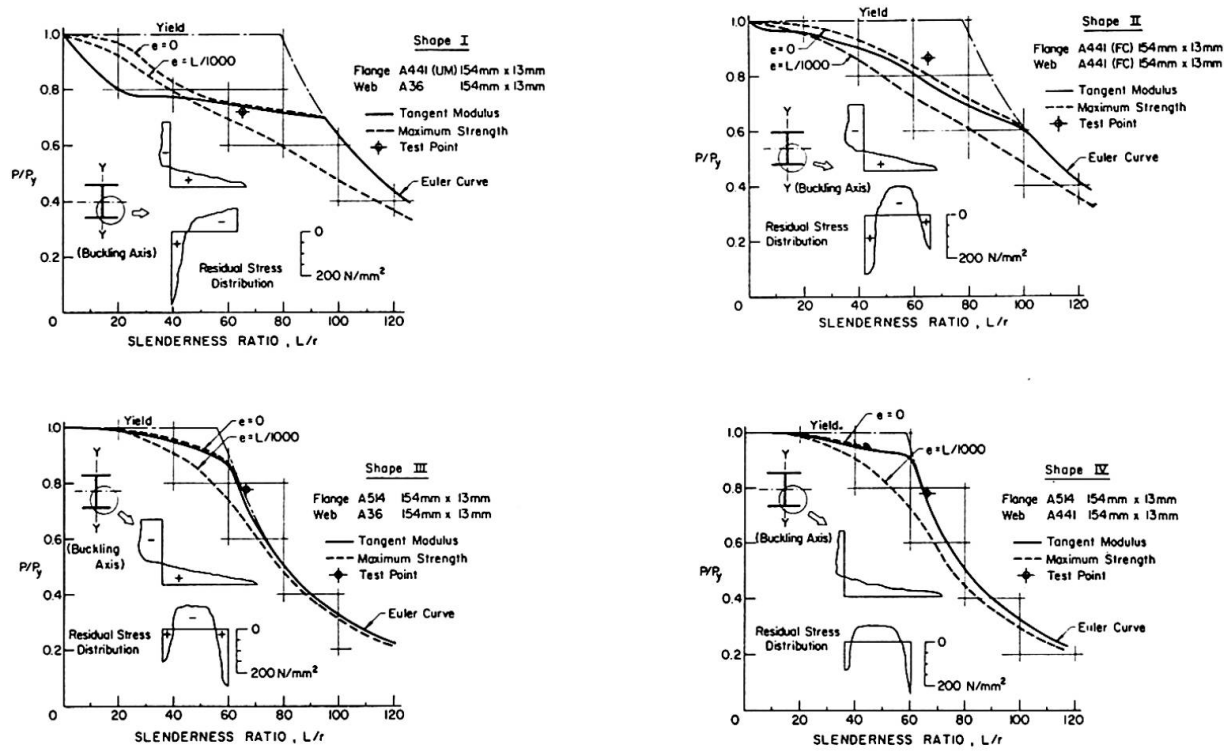

Fig. 3 Tangent Modulus and Maximum Strength Column Curves

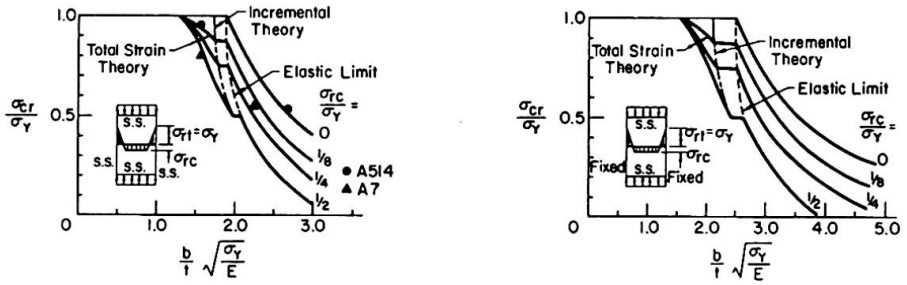

Fig. 4 Plate Buckling Curves

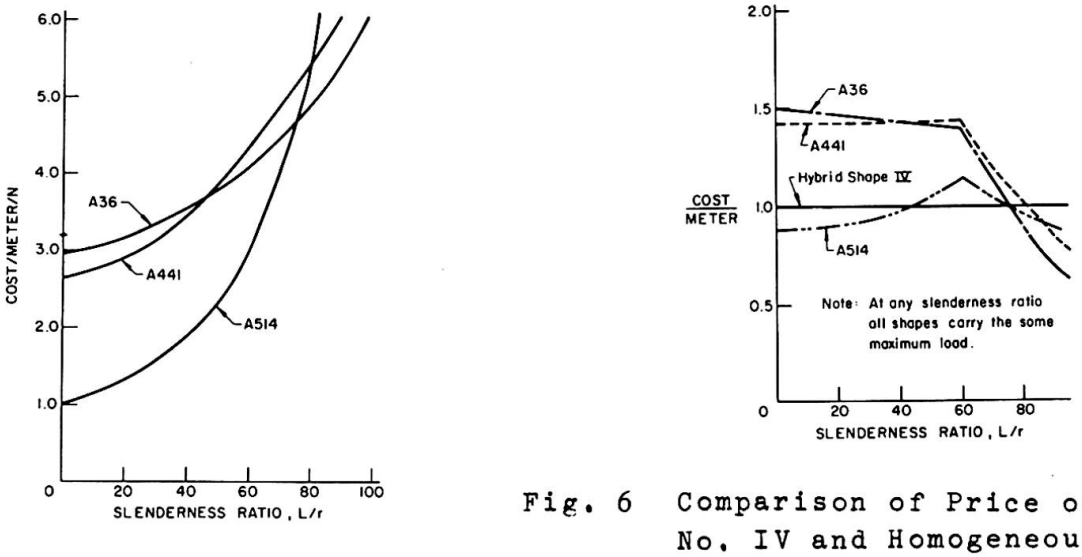

Fig. 5 Relative Cost vs. Slenderness Ratio of Homogeneous Shapes

Fig. 6 Comparison of Price of Hybrid Shape No. IV and Homogeneous Shapes

Leere Seite
Blank page
Page vide

Czechoslovak Research in the Area of Prestressed Metallic Structures

Recherches tchécoslovaques dans le domaine des constructions métalliques précontraintes

Tschechoslowakische Forschung auf dem Gebiete der vorgespannten Metallkonstruktionen

MILOSLAV TOCHÁČEK BOHUSLAV ROSENKRANZ
Building Research Institute of the Czech Technical University, Prague, CSSR

PAVEL FERJENČÍK
Civil Engineering College of the Slovak Technical University, Bratislava, CSSR

1. COORDINATED SCIENTIFIC AND RESEARCH ACTIVITIES

In the Czechoslovak Socialist Republic it is predominantly the Building Research Institute of the Czech Technical University in Prague (formerly a part of the Institute of Theoretical and Applied Mechanics of the Czechoslovak Academy of Sciences) and the Chair of Metal and Timber Structures of the Slovak Technical University in Bratislava that have been systematically engaged in the research of prestressed metallic structures (PMS). Since 1960 the state scientific and research programs for prestressed steel structures (PSS) have been regularly elaborated, each for the period of five years. The mentioned two institutions have mutually coordinated the scientific and research activities in the area of PSS in the state-wide scale.

The purpose of the first research period (1961-1965) especially was to prepare, in the cooperation with other working units, the Czechoslovak specification for the designs of PSS /7/. Hence, most activities were aimed towards that goal. Theoretical and experimental investigations pertained to the problems of designing, proportioning, constructing, economy, execution and verification of the actual behavior of the basic, most common types of web-plate structures and trusses /2,4,12,20,31,33-35,40,45-47,51,55,58/.

Rather rich outcomes of the first research period enabled Czechoslovakia not only to partake significantly in the success of the 1st International Conference on PSS, Dresden (German Democratic Republic) 1963 /12/, but even to organize the 2nd International Conference, Tale (Czechoslovakia) 1966 /13/, and to demonstrate there the Czechoslovakian achievements in the area of PMS until that time. Also the first Czechoslovakian monograph on PMS /4/ appeared, making the engineering public acquainted with the then state of knowledge in the area and providing a deeper exposition of the contents of the specification /7/.

The specification /7/ for designing PSS is one of the first codes in the world. It concerns mainly the structures prestressed by high-strength tendons and is based on the Limit States (Load

Factor) Concept /79,81/. The appropriate constructional materials are therein recommended, the principal organization -, transport -, and technological hints and data are provided. The attention is paid specifically to the construction and economical design of prestressed web-plate girders, queen post trusses and open-web trusses.

During the second research period (1966-1970), reflected mainly by the publications /63,65,66,68,70,72,74,75,82,84-86,89, 91,94/, more involved problems were studied. They pertained, for instance, to the perfected economical proportioning of prestressed plate girders, and that also in the elasto-plastic state, composite girders, trussed beams, spatial roof-trusses, etc. Experimental investigations were performed to confirm theoretical results from the both periods. Some Czechoslovak achievements from the second research period were given publicity also at the 3rd International Conference on PMS, Leningrad (USSR) 1971 /15/. The second research period was concluded by the monograph /11/.

The objective of the third scientific and research period (1971-1975) is to deepen further the theory of PMS and, in addition to that, to solve also a number of technological problems. Consideration should be given, inter alia, to more complex systems prestressed by tendons; systems prestressed by other means; reconstructions and strengthening of structures through prestressing; dynamics and fatigue of PMS; modern design methods, especially those using the mathematical programming; special problems.

The specification /7/ for designing the basic types of PMS will be revised. Numerous remarkable findings have been acquired during the past research periods also in other fields than in that of web-plate structures and trusses - e.g., in the areas of prestressed suspended roofs /1,3,4,11-15,27,29,36,38,41,42,48,49,52, 54,64,69,77,78,90/; suspended bridges /4,11-13,15,23,39,88); guyed masts /4,5,11,30,44,73/; pressure vessels /4,19,24,37/; exploitation or removing of residual stresses /4,11,18,32,56,61/, etc. Nonetheless, no regulations for these disciplines will be incorporated in the revised specification /7/ as it is felt that these disciplines merit their own codes. They would certainly deserve a broader treatment in this paper, too. However, the shortage of space hinders that.

At present, a new specification is being prepared for the executions of PSS. A part of the scientific and research groundworks has been already accomplished /9,11/. During the first and second research periods, also many experimental investigations of the technological nature were performed, especially on the high-strength rods, strands and ropes, and on their anchorages /6,10, 12-15,21,22,25,26,28,43,50,67,71,76,80,87,92,93/, with the aim to exploit the results for the specification. Among other things, the elasticity moduli both of virgin and prestretched elements, their actual bearing strength, as well as the state of strain of the zinc-poured sockets were observed.

At least a selection of some Czechoslovak findings is briefly dealt with in the sequel.

2. TRUSSES

Trusses prestressed by high-strength tendons are statically indeterminate systems even when supported in a statically determinate

manner. If their geometry is given or preselected, these structures can be economically designed by an inverse method /4,11,34,40,59, 63,70/:

The optimal total tendon forces are found, e.g., by the use of a linear programming technique, with the theoretical weight of the truss employed as the decision function. For these forces and the considered external loads, the truss members can be easily proportioned. After the sections have been picked up, the redundant forces in tendons are calculated, e.g. by the force method. The necessary prestressing forces are specified by the differences between the optimal total forces and the statically indeterminate forces in tendons. - In the reality, the design appears to be a little more involved, because of several intervening load combinations, differentiated prestress accuracy factors and some other coefficients not known in advance.

Much simpler is the design of those trusses, where the distinct tension members are prestressed independently, by the coaxial tendons. Each tendon influences only one member. The design of prestressed tension members is treated in /4,7,11,55/. The non-prestressed truss members are designed as in a structure without tendons.

The most complicated optimization problems are those where the system geometry is to be varied. In /60,68/, the variable parameters were: the amount of panels, the depth and the distance of plane roof trusses with parallel chords, the distance and the type of purlins, the type and the size of the used profiles, the configuration of the prestressing tendons and the magnitude of prestressing. The involved analytical expressions were solved numerically for the selected characteristic cases. In Fig.1, the theoretical steel consumption over the ground plan of 24m x 48m is correlated with the distance of the roof trusses which have the depth of 2,9m.

The results of the theoretical investigations were utilized in a typification study of the roof trusses /4,31/. A roofing using tubular ∇ - trusses, Fig.2a,b, proved to be very economical. Prestressing of trusses with the chords of constant cross-sections and the spans of 24; 30; 36m by two polygonal wire-ropes economizes 20 through 22% or 14 through 16% of steel, at the heavy cladding (240 kg/m^2) or at the light cladding (60 kg/m^2), respectively. The top truss web consist of purlins only, being connected for torsion with the concrete cladding slabs; during the erection, the crossed prestressed strands are employed as the temporary diagonals.

Prestressed open-web structures of a special character are the transmission and television masts /4,5,11,30,44,73/.

3. WEB-PLATE STRUCTURES

A good deal of attention has been paid to the economical design of a plate girder prestressed by a straight high-strength tendon near the tension flange /4,7,8,11,33,46,47,51,62,65,66,72, 75,82,89,91,94/. The highest economy can be achieved in a girder with the optimal asymmetry when the both girder flanges in the critical sections and the tendon along the entire length are fully stressed. Problems of the optimum design were solved for the case of a tendon of the optimum length as well as of the length equal-

ing the girder span; for various positions of the tendon with respect to the tension flange; for equal or differentiated design stresses of the flanges; for flanges with limited or unlimited cross-section areas. Four distinct decision functions were considered, the simplest being that of preselected tension flange parameter φ_2, Fig.3, or that of maximum bearing capacity at the constant volume. In a research program, conducted by one of the authors during his stay abroad, also the optimum design of a prestressed composite (steel - concrete) girder was studied, besides other topics /82/. In the case of the prestressed steel resp. composite girder, numerous intervening expressions and variables were replaced, through the analytical manipulations, by one resp. two equations only, for two resp. three unknowns, governed by one decision function. Because of their complexity, the expressions were solved numerically (by the use of a computer) for a representative selection of situations. The appropriate aids, as that one in Fig.3, can be worked out to facilitate the practical design.

The economical proportioning of prestressed steel plate girders was investigated both in elastic and elasto-plastic ranges, Fig.4 /65,75/. However, the buckling problems entangle the exploitation of the plastic reserve so far that not too much additional economy can be gained from the plastic design.

Another research topic was the prestressed deep trussed beam, i.e. a beam supported by posts and a polygonal tendon, Fig.5 /7,11, 74/. When the structure geometry is known, the design can be realized also by an inverse method similar to that for trusses. The optimum tendon force follows from the requirement that the critical sections of the beam should be fully stressed. The redundant tendon force can be readily calculated with the aid of the chart in Fig.5.

An inverse design technique combined with the linear programming was elaborated also for continuous beams prestressed by the enforced deformations of redundant constraints, e.g., by the intentional displacements of redundant supports /70,86/.

4. CLOSURE

The endavour of designers to economize maximally steel, without reducing the safety of structures, attracts the interest always more to PMS - as testified, e.g., by the themes of the contemporaneous international congresses (Leningrad 1971, Amsterdam 1972, Dresden 1974). The state of stress can be modified efficiently through prestressing structures in such a way that the internal effects are redistributed to the less utilized sections or section fibres, and the structural elements can be better and more evenly exploited.

It is our pleasure to conclude that Czechoslovakia belongs among the countries having recognized early the hopefulness and importance of PMS, so that the Czechoslovakian specialists have been able to contribute significantly to the scientific and engineering progress in this field.

5. BIBLIOGRAPHY +

If not stated otherwise, references are in Czech or Slovak

+ For the shortage of space, the bibliography by far cannot be complete. Just with a few exceptions, especially research reports and dissertations are not cited. For a more complete list see /16,17/.

/1/ SOBOTKA,Z.: Suspended Roofs. Prague, SNTL 1962. Moscow,Stroiizdat 1964 (in Russian)

/2/ SCHUN, J. - FERJENČIK, P. - DUTKO, P.: Steel Structures II. Bratislava, SVTL 1963

/3/ BIELEK, M.: Suspended Roof Structures. Bratislava, SVTL 1964

/4/ FERJENČÍK, P. - TOCHAČEK, M.: Prestressed Metal Structures. Bratislava SVTL 1966

/5/ KOZÁK, J.: Steel Masts. Prague, SNTL 1966

/6/ RABAS, E.: Catalog of Steel Strands and Wire Ropes. Prague, ŽD Bohumín 1966

/7/ TOCHÁČEK, M. - FERJENČÍK, P. et al.: Branch Specification ON 73 1405 Instructions for Designs of Prestressed Steel Structures. Prague, ÚNM 1967

/8/ FERJENČÍK, P. et al.: Metal Structures II. Bratislava, SVTL 1968

/9/ VOVES, B.: Foundations for Branch Specification ON 73 14 .. Instructions for Executions of Prestressed Steel Structures in the Area of the Prestressing Technique. Prague, SvF ČVUT 1970. Research Report.

/10/ SPAL, L.: Steel Strands and Wire Ropes in the Civil Engineering Structures. Prague, SNTL 1971

/11/ FERJENČÍK, P. - TOCHÁČEK, M.: Vorgespannte Stahlkonstruktionen. (Working title, in German.) Bauingenieur-Praxis, Heft 38. Berlin, W.Ernst (submitted for press)

Conference Proceedings

/12/ Internationale Fachtagung "Vorgespannte Stahlkonstruktionen". Dresden 1963 (in German). = In: Wissenschaftliche Veröffentlichungen aus der Fakultät für Bauwesen der Technischen Universität Dresden 1964, B - Reihe, No 30

/13/ International Conference on Prestressed Metal Structures, Tále 1966. Proceedings (in four languages). Prague, Building Research Institute 1966

/14/ Seminar on Suspended Roof Structures. Reports. Bratislava 1970. Bratislava, Dom techniky 1971

/15/ Third International Conference on Prestressed Metal Structures. Reports (in four languages). Leningrad 1971

Bibliographical Booklets

/16/ TOCHÁČEK, M. - FERJENČÍK, P.: Prestressed Metal Structures. Selected bibliography. With a supplement - Bibliographical leaflet No 13, coauthor ROSENKRANZ, B.. Prague STK 1965 and 1966

/17/ FERJENČÍK, P.: Prestressed Metal Structures. Bibliographical compendium ... Bratislava,SVŠT 1971

Papers, Chapters

/18/ PUCHNER, O.: Schwellfestigkeit geschweisster Knotenblechanschlüsse und ihre Erhöhung durch örtliche Glühung (in German) = "Schweisstechnik 1956/4

/19/ VALENTA, J.: Strip-Wound Vessels. = Rozpravy ČSAV" 1957/4

/20/ KRCHOV,J.: Steel Structures with Prestressing. = In:Súčasný stav predpätého betonu v ČSR. Bratislava, N SAV 1957

/21/ HEJDA, O.: Prestressing of Reinforcements by Electroheating. = "Stavivo" 1960/3

/22/ RABAS, E.: Steel Wire Ropes in Civil Engineering Structures. = "Inženýrské Stavby" 1960/10

/23/ TESÁR, A.: Suspended Pipeline Bridges. = In: Sborník vedeckých prác SvF SVŠT. Bratislava. SVTL 1961

/24/ VALENTA, J.: The Elasto-Plastic State of Multilayer Vessels (in English). = "Rév.Mécan.Appl., Bucarest" 1961/3

/25/ RABAS, E.: Possibilities and Ways of Fixing the Wire Rope Ends. = "Inž. Stavby" 1962/ 10

/26/ KAUCKÝ, Z.: Prestress Loss from Wire Slips in an Anchor. = "Inž. Stavby" 1963/5

/27/ PIRNER, M.: Model Measurements of Deformations of Prestressed Suspended Roofs with Static and Dynamic Loadings. = "Inž.Stavby" 1963/9

/28/ KOZÁK, J.: Safety of Wire Ropes in Civil Engineering Structures. = Inž. Stavby" 1964/1

/29/ BÁRTLOVÁ, A.: A Solution for a Prestressed Unloaded Wire Rope Network. = "Staveb.Čas." 1964/4. Also in: /14, 15/

/30/ VOŘÍŠEK, V.: Actual Behavior of Prestressed Guyed Masts for an Extra-High Voltage Transmission Line. = "Inž. Stavby" 1964/7

/31/ TOCHÁČEK, M. - ROSENKRANZ, B.: Spatial Tubular Roof Trusses Prestressed by Wire Ropes. = "Inž.Stavby" 1964/11

/32/ DUTKO, P.: Effect of Residual Stresses on the Instability of Centrally Compressed Struts with I-Sections and Possibilities of Increasing Their Load--Carrying Capacity. = In: Sborník vedeckých prác SvF SVŠT v Bratislave. Bratislava, SVTL 1964

/33/ FERJENČÍK, P.: Economies Reached in Some Types of Prestressed Metal Structures. = In: Sborník vedeckých prác SvF SVŠT v Bratislave. Bratislava, SVTL 1964

/34/ TOCHÁČEK, M.: Analysis of Prestressed Metal Structures According to the Limit States. = In: Teória výpočtov stavebných konštrukcií a základov podla medzných stavov. Bratislava, V SAV 1964

/35/ FERJENČÍK, P.: Einige Bemerkungen zu den vorgespannten Stahlkonstruktionen (in German). = In: /13/

/36/ HORÁK, V.: Beitrag zur nichtlinearen Theorie der Hängedachkonstruktionen (in German). = In: /13/

/37/ PANC, V.: Die Berechnung der kreiszylindrischen, durch elastische Ringe vorgespannten Druckbehälter (in German). = In: /13/

/38/ PIRNER, M.: Dynamic Properties of Prestressed Cable Roofs (in English) = = In: /13/

/39/ TESÁR, A.: Berechnung und Ausführung einer vorgespannten Rohrleitungsbrücke in der ČSSR (in German). = In: /13/

/40/ TOCHÁČEK, M.: Der Entwurf optimaler vorgespannter Fachwerke (in German). = In: /13/

/41/ BŘEZINA, V.: Statical Analysis of Wire Rope Roofs. = "Staveb.Čas." 1965/3

/42/ KOZÁK, J.: Statics of a One-Span / Continuous Wire Rope Subjected to a Vertical Load. = "Inž.Stavby" 1965/4, 8

/43/ KRCHOV, J.: Fabrication Checks of Prestressing Force. = "Inž.Stavby"

/44/ SPAL, L.: Utilization of a Computer for the Analysis of a Mast Guyed in Three Directions. = "Staveb.Čas." 1965/5

/45/ TOCHÁČEK, M. - FERJENČÍK, P.: Prestressed Metal Structures in Czechoslovakia and Their Design. = "Staveb.Čas." 1965/6

/46/ TOCHÁČEK, M.: A Web-Plate Girder Prestressed by a Straight Tendon. = In: Práce ČVUT, series I, 1965/7. Prague, SPN 1965

/47/ HLAVÁČEK, V. - TOCHÁČEK, M.: Prestressed Steel Craneways. Ibid.

/48/ FERJENČÍK, P. - TOCHÁČEK, M.: Cladding-Bearing Structure of Prestressed Wires. = "Inž.Stavby" 1965/9

/49/ PIRNER, M.: Berechnung von vorgespannter Seilnetzen (in German). = Bauplan-Bautechn." 1965/11

/50/ VOVES, B.: A New Prestressing Reinforcement. = "Pozemní Stavby" 1965/11

/51/ TOCHÁČEK, M. - FERJENČÍK, P.: Design of Prestressed Metal Structures (in Italian). = "Costruz.Metall." 1966/1

/52/ BŘEZINA, V.: Theory of Lens-Shaped Cable Roof Anchored in a Plane Ring (in English). = "Rozpravy ČSAV, series TV" 1966/2

/53/ FERJENČÍK, P. - TOCHÁČEK, M.: Anchorage, Prestressing and Force-Measurements in Tendons of Prestressed Metal Structures. = "Pozem.Stavby" 1966/3

/54/ STUDNIČKA, J. - ZMRHAL, V.: Model Measurements of a Prestressed Suspended Roof Being Loaded Statically. = "Inž.Stavby" 1966/11

/55/ FERJENČÍK, P.: Prestressed Metal Tension Members. = In: Sborník vedeckých prác SvF SVŠT v Bratislave. Bratislava, SVTL 1966. Also in: /13/

/56/ FALTUS, F.: Special Cases of Utilization of the Initial State of Stress in Metallic Structures (in English). = In: /13/

/57/ FERJENČÍK, P.: Contributions of Czechoslovakia in the Area of Prestressed Metal Structures. = In: /13/

/58/ LEDERER, F.: Metal Structures Prestressed by High-Strength Tendons (in English). = In: /13/

/59/ PIRAS, Z. - TOCHÁČEK, M.: Introduction to the Econometrics of Prestressed Metal Structures (in English). = In: /13/

/60/ ROSENKRANZ, B.: Optimum Heights of Prestressed Steel Parallel Chord Trusses (in English). = In: /13/

/61/ TESÁR, A.: Special Cases of Utilization or Elimination of Initial Stresses in Metal Structures (in English). = In: /13/

/62/ TOCHÁČEK, M.: Contributions of the Building Research Institute of the Czech Technical University to the Development of the Theory of Prestressed Metal Structures. - Prestressed Web-Plate Structures. - Prestressed Trusses. = In: /13/

/63/ PIRAS, Z. - TOCHÁČEK, M.: Introduction to the Econometrics of Prestressed Metallic Structures (in English). = In: Acta Polytechnica - Práce ČVUT v Praze, series I. Prague, SPN 1967/1

/64/ SOBOTKA, Z.: Statics of Annular Suspended Roofs with a Single Bearing System. = "Staveb.Čas." 1967/1

/65/ TOCHÁČEK, M. - ROSENKRANZ, B.: Optimum Design of a Simply Supported Plate Girder Prestressed by a Straight Tendon, Within the Elasto-Plastic Range. = "Staveb.Čas." 1967/4-5

/66/ FERJENČÍK, P.: On Some Problems of Prestressed Steel Plate Girders. = In: Sborník vedeckých prác SvF SVŠT v Bratislave. Bratislava, SVTL 1967

/67/ ROSENKRANZ, B. - FERJENČÍK, P. - TOCHÁČEK, M.: Tendons of Prestressed Metal Structures, Their Material and Protection. = "Pozem.Stavby" 1968/1

/68/ ROSENKRANZ, B.: Contribution to the Weight-Optimization of Trusses (in Italian). "Costr.Metall." 1968/5. Also in: "Inž.Stavby" 1966/12

/69/ KOLÁŘ, V.: Nichtlineare Gleichungssysteme der Seilnetze und ihre numerische Behandlung (in German). = "ZAMM" 1968/8

/70/ PIRAS, Z. - TOCHÁČEK, M.: Use of Econometrics in Designs of Metal Structures. = "Staveb.Čas." 1968/8

/71/ ROSENKRANZ, B. - SPAL, L.: On Problems of End Fittings of Steel Wire Ropes. = "Inž.Stavby" 1968/9

/72/ VASILKOV, F.V. et al.: Plate Girders Prestressed by a High-Strength Tendon. = In: Sborník vedeckých prác SvF SVŠT v Bratislave. Bratislava, Alfa 1968

/73/ KOZÁK, J.: Einige Bemerkungen zur Projektierung verankerten Fernsehrohrmasten (in German). = "Stahlbau" 1969/6

/74/ TOCHÁČEK, M. - FERJENČÍK, P.: Prestressed Trussed Beams (in Italian). = "Costruz.Metall." 1970/5. Also in: Zborník vedeckých prác SvF SVŠT v Bratislave. Bratislava, Alfa 1969

/75/ ROSENKRANZ, B. - TOCHÁČEK, M.: Economy of Prestressed Steel Plate Girders in the Elasto-Plastic State. = "Pozem.Stavby" 1970/8

/76/ SPAL, L.: Calculated Elasticity Moduli of Wire Ropes. = "Pozem.Stavby" 1970/8

/77/ FERJENČÍK, P. et al.: Straight Prestressed Strings in Roof Structures. = In: /14/

/78/ KADLČÁK, J.: Statical Analysis of Elastic Wire Rope Networks. = In: /14/

/79/ TOCHÁČEK, M. - AMRHEIN, F.G.: Which Design Concept for Prestressed Steel? (in English). = "Engng J., AISC" 1971/1

/80/ SPAL, L.: Zinc-Poured Sockets for Wire Rope Structural Members. = "Pozem. Stavby" 1971/3,4

/81/ TOCHÁČEK, M. - AMRHEIN, F.G.: Design of Prestressed Steel Structures According to the Limit States (in English). = In: Conference on Applications of Statistics & Probability to Soil & Structural Engineering, Proceedings. Hong Kong, University of Hong Kong 1971

/82/ MEHTA, C.L. (advisor TOCHÁČEK, M.): Optimum Design of Prestressed Plate Girders and Prestressed Composite Girders. Stillwater (USA), Oklahoma State Univ. 1971. Ph.D. - Dissertation (in English)

/83/ AGÓCS, Z.: Results of Investigations into the Theoretical and Actual Behaviour of Prestressed Wire Rope Systems (in Russian). = In: /15/

/84/ FERJENČÍK, P.: On Optimal Parameters of Prestressed Steel Plate Girders with the Given Bottom Chord Area (in Russian). = In: /15/

/85/ HORÁK, V.: Employment of Inverse Variational Principles of Mechanics in the Investigations into Prestressed Rigid Bodies (in Russian). = In: /15/

/86/ PIRAS, Z.: Optimization of Prestressed Metal Structures with One/Several Critical Loads (in Russian). = In: /15/

/87/ ROSENKRANZ, B.: Beitrag zum Elastizitätsmodul von Stahlseilen (in German). = In: /15/

/88/ TESÁR, A.: Die Vorspannung von Balkenbrücken inbs. Schrägseilbrücken durch planmässige Abstützungsbewegung im Zuge der Montage (in German). = In: /15/

/89/ TOCHÁČEK, M.: Economic Design of a Prestressed Plate Girder, under More General Conditions (in English). = In: /15/

/90/ AGÓCS, Z.: Some Characteristics of Wire Ropes Used in Suspended Load--Carrying Systems. = In: Zborník vedeckých prác SvF SVŠT v Bratislave. Bratislava, Alfa 1971

/91/FERJENČÍK, P.: Optimal Parameters of a Prestressed Steel Plate Girder. Optimization within the Elastic State. Ibid.

/92/ ROSENKRANZ, B.: Elasticity Modulus of Strands with a Locked Construction. = "Pozem.Stavby" 1971/7,8. Also in: /14/

/93/ ROSENKRANZ, B.: Effect of Wire Rope Prestretching on the Magnitude of the Elasticity Modulus. Ibid, in press

/94/ TOCHÁČEK, M. - MEHTA, C.L.: Economical Design of a Prestressed Plate Girder (in English). = "J.Struct.Div.,ASCE", in press

6. SUMMARY

Since 1960, the Czechoslovakian research in the area of prestressed metallic structures has been organized and planned for five-year periods. Achievements from the two periods are described, when mainly the basic structural types have been investigated. The specification for the designs of prestressed steel structures has been published and the specification for the executions of prestressed steel structures is in preparation. To illustrate some results of the accomplished scientific and research activities, problems of the economical design of prestressed steel trusses and web-plate structures are briefly treated.

7. ILLUSTRATIONS

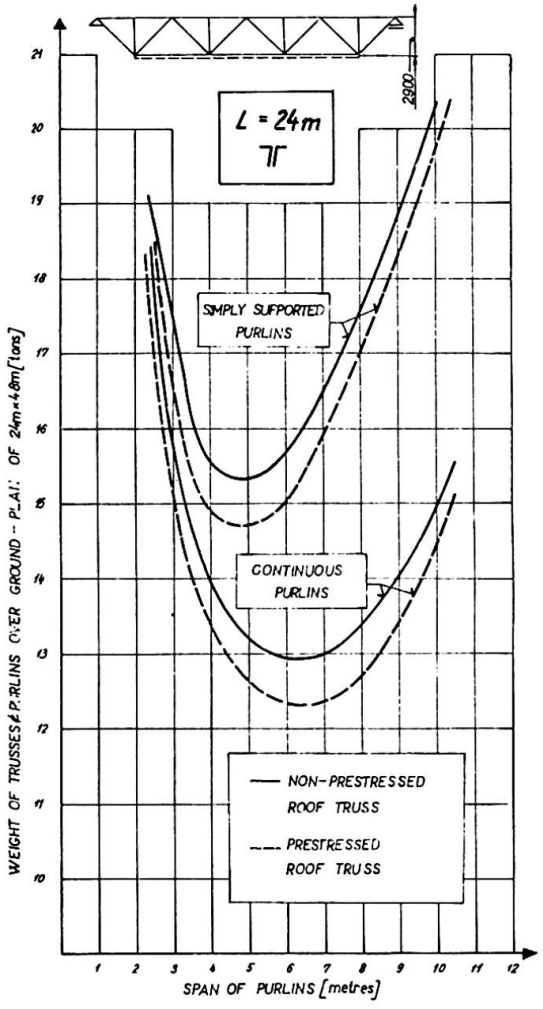

Fig. 1
Weight of a steel roof as affected by truss distance

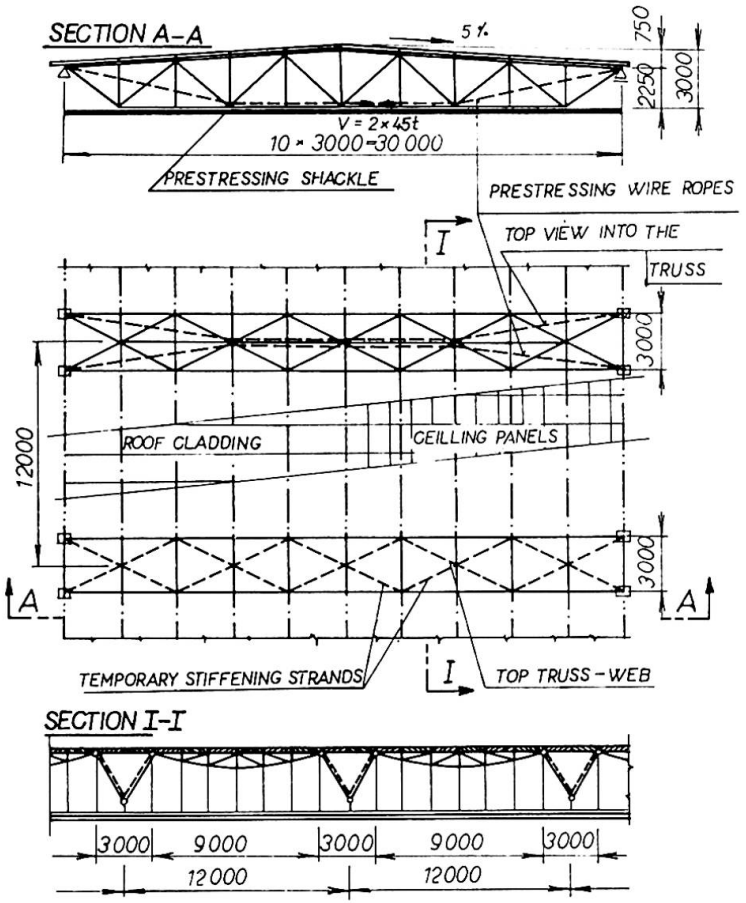

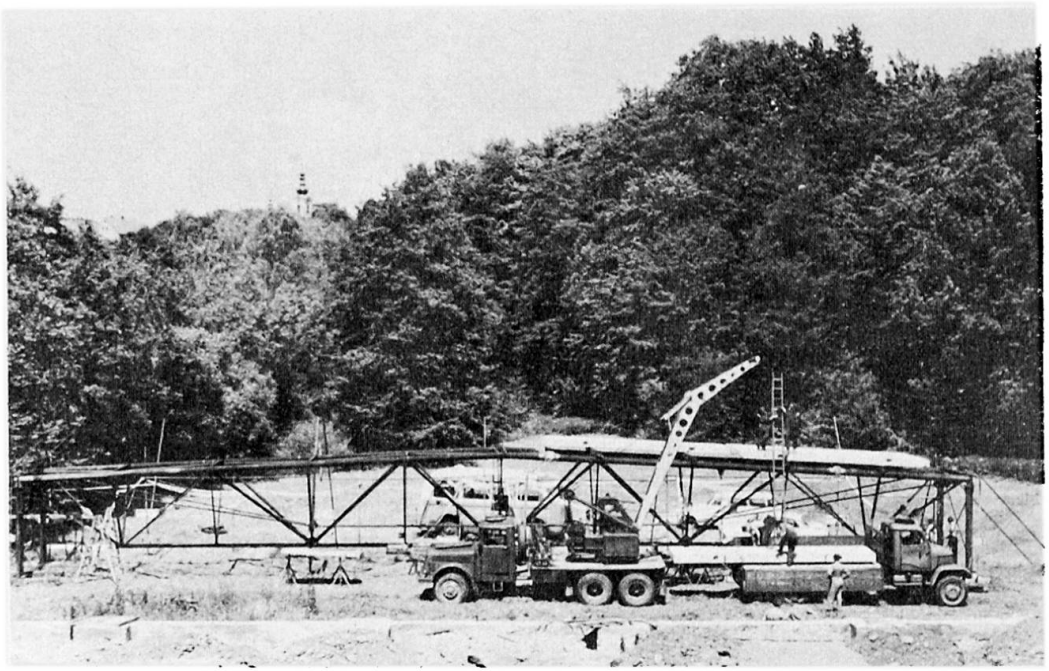

Fig. 2 Tubular roof truss prestressed by two polygonal tendons

(a) General layout

(b) Experimental investigations

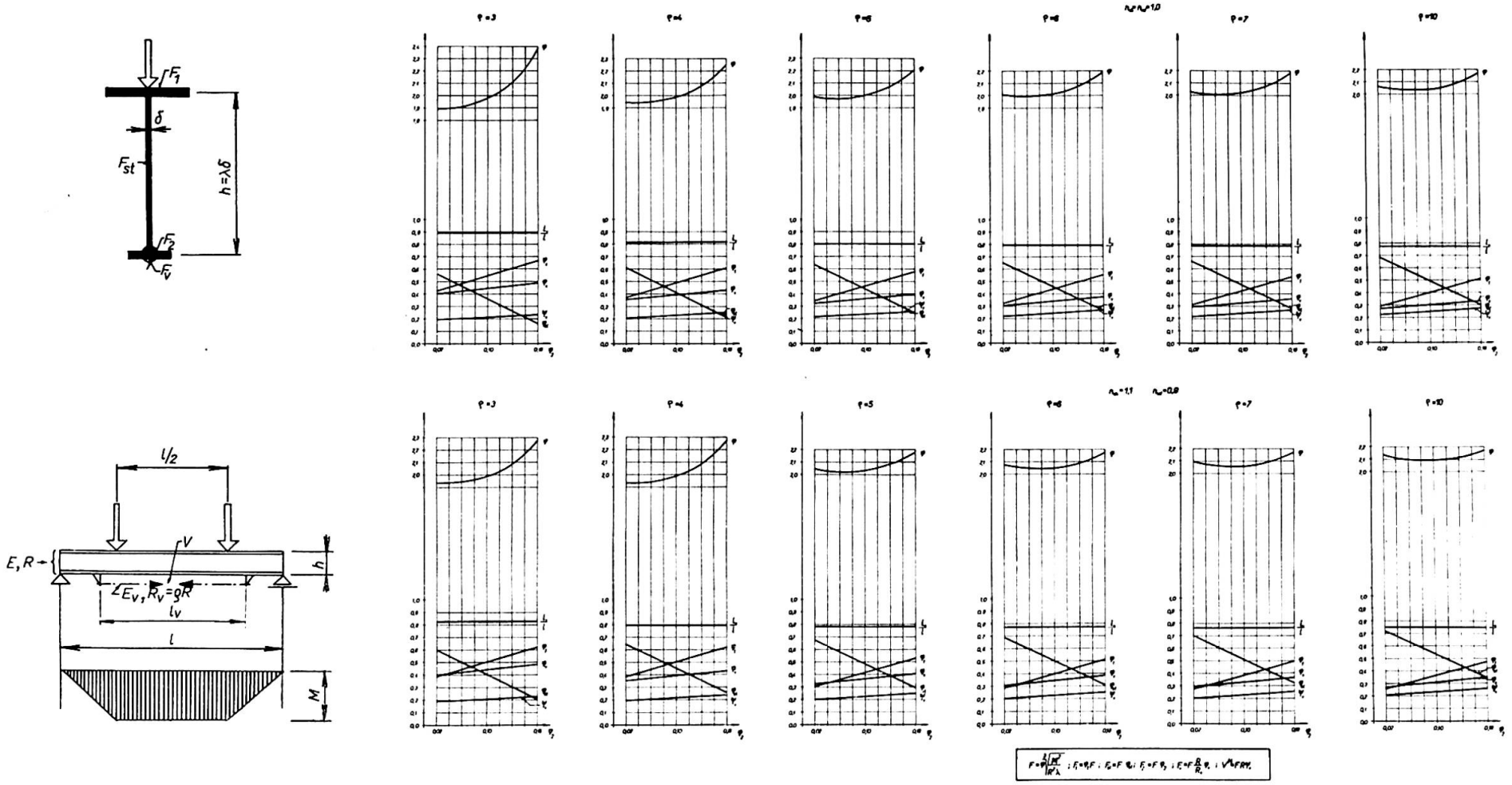

Fig. 3 Formulas and coefficients for a straightforward proportioning of a prestressed plate girder

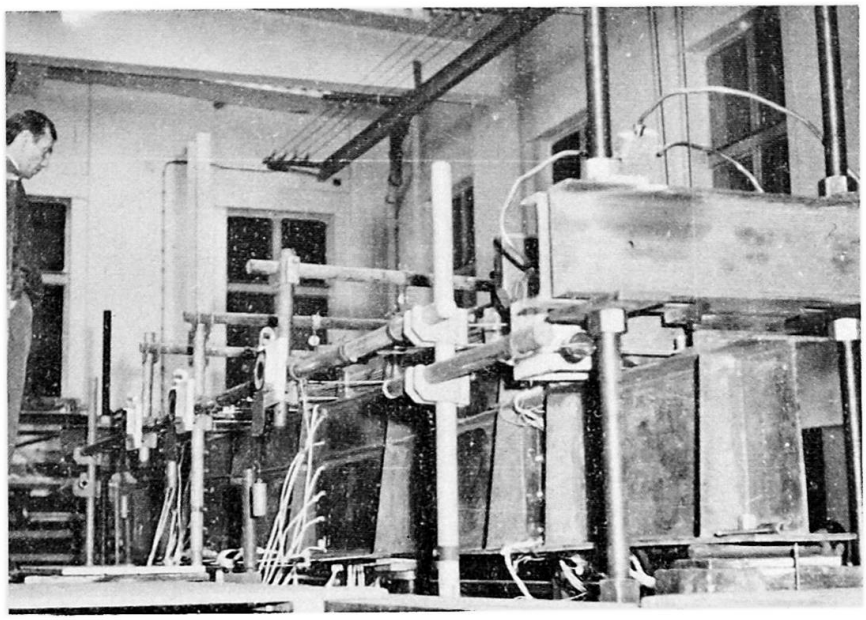

Fig. 4 Tests of plate girders in which prestressing exerted the elasto-plastic state

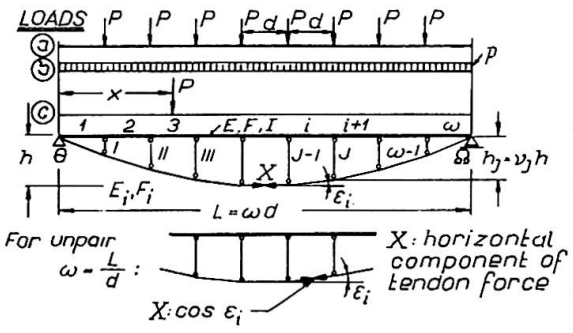

$$X = \frac{\max M_0}{K_Z K_T h}$$

$\max M_0$ - max bending moment of simply supported beam

K_Z - from table below, for respective load

$$K_T = 1 + \frac{I}{h^2 \lambda^3}\left(\frac{\alpha}{F}\lambda^3 + \frac{\beta}{F_s} + \frac{E}{E_t}\frac{\gamma}{F_t}\right)$$

$\lambda = \frac{L}{h}$; coefficient α, β, γ from table below

For posts with unequal areas: $\frac{1}{F_s} = \sum_{J-1}^{\Omega-1} \frac{\nu_J}{F_{sJ}}$

NO OF PANELS ω	LOAD a	LOAD b	LOAD c	LOAD a	LOAD b	LOAD c	COEFFICIENTS FOR CALCULATING SHAPE FACTOR K_T α	β	γ	δ	RELATIVE LENGTHS OF POSTS I Ω-I	II Ω-II	III Ω-III
	BENDING MOMENTS max M_0/PL	M_0/pL^2	$M_0/P(L-x)$	LOAD COEFFICIENTS K_Z									
2	0,25			0,8			3	48	$3(\lambda^2+4)^{1,5}$	0,25	1		
3	0,333			1,023			1,8	32,4	$1,2[(\lambda^2+9)^{1,5}+0,5\lambda^3]$	0,19	1		
4	0,5			0,9485			2,087	20,87	$1,043[(\lambda^2+9)^{1,5}+(\lambda^2+1)^{1,5}]$	0,21	0,75	1	
5	0,6			1,007			1,849	17,12	$0,7397[(\lambda^2+11,11)^{1,5}+(\lambda^2+2,777)^{1,5}+0,5\lambda^3]$	0,19	0,66̇	1	
6	0,75	0,125	1	1	0,977		1,965	13,58	$0,6550[(\lambda^2+11,11)^{1,5}+(\lambda^2+4)^{1,5}+(\lambda^2+0,444)^{1,5}]$	0,20	0,55̇	0,88̇	1
7	0,8571				1,004	$\approx \frac{x(L-x)}{\delta L^2 \sin\frac{\pi x}{L}}$	1,862	11,83	$0,5320[(\lambda^2+12,25)^{1,5}+(\lambda^2+5,444)^{1,5}+(\lambda^2+1,361)^{1,5}+0,5\lambda^3]$	0,19	0,5	0,83̇	1
8	1				0,987		1,925	10,11	$0,4812[(\lambda^2+12,25)^{1,5}+(\lambda^2+6,25)^{1,5}+(\lambda^2+2,25)^{1,5}+(\lambda^2+0,25)^{1,5}]$	0,20	0,437	0,75	0,937
9	1,111				1,002		1,867	9,075	$0,4140[(\lambda^2+12,96)^{1,5}+(\lambda^2+7,29)^{1,5}+(\lambda^2+3,24)^{1,5}+(\lambda^2+0,81)^{1,5}+0,5\lambda^3]$	0,20	0,4	0,7	0,9
10 & more	$0,125\frac{\omega^2-1}{\omega^2}$				1		1,875	$120\left[\frac{\omega}{\omega^2-1}\right]^2 \nu_J$	$1,875(\lambda^3+8\lambda+19,2\lambda^{-1})$	0,20	μ_J		

General formulas for coefficients

$\omega = \frac{L}{d}$ No. of panels

Superscripts a, b, ... - kind of loads

$$\alpha = \frac{6\omega}{\sum_{J-1}^{\Omega-1} \nu_J(\nu_{J-1}+4\nu_J+\nu_{J+1})}; \qquad \nu_J = \frac{h_J}{h};$$

$$\beta = \alpha\left(\frac{PL}{\max M_0^a}\right)^2 \sum_{J-1}^{\Omega-1} \nu_J; \qquad K_Z^b = \frac{6\omega}{\alpha \sum_{J-1}^{\Omega-1} \nu_J\left[\mu_{J-1}+4\left(\mu_J+\frac{1}{\omega^2}\right)+\mu_{J+1}\right]};$$

$$\gamma = \frac{\alpha}{\omega}\sum_{J-1}^{\Omega-1} \sec^3\varepsilon_i; \qquad \mu_J = \frac{M_{QJ}^a}{\max M_0^a}$$

Fig. 5 Formulas for the redundant force X in the tendon of a trussed beam

Tschechoslowakische Realisationen auf dem Gebiete vorgespannter Metallkonstruktionen

Réalisations tchécoslovaques dans le domaine de constructions métalliques précontraintes

Czechoslovakian Realizations in the Domain of Prestressed Metal Constructions

PAVEL FERJENČÍK
Dipl. Ing., CSc.
Fakultät für Bauwesen der TH
Bratislava, ČSSR

MILOSLAV TOCHÁČEK
Dipl. Ing., CSc.
Bauinstitut der TH
Praha, ČSSR

Im Beitrag widmen wir die Aufmerksamkeit einigen wichtigen Realisationen und Patenten auf dem Gebiete vorgespannter Metallkonstruktionen in der Tschechoslowakischen Sozialistischen Republik. Auf ähnliche Arbeiten, die über diese Problematik handeln, machen wir auf /1, 6--17/ und /19/ aufmerksam.

I. Hochbaukonstruktionen

Vorgespannte Metallkonstruktionen haben bei uns eine reiche Vergangenheit. So z.B.wurde Bedřich Schnirch /1791--1868/ als erstem auf der Welt /nach bisherigen Angaben/, schon im Jahre 1826 das Patent für eiserne Dachstühle - Hängedächer /1, 14, 18--21/ erteilt.

B.Schnirch entwarf nach seinem Patent z.B.zwei Hängedächer in Banská Bystrica, von denen die Originalpläne erhalten geblieben sind /Bild 1, Bild 2/. Auf dem Bild 1 ist das erste Dach, angefertigt im Jahre 1826, das bis heute in Benützung ist. Das Gebäude hat die Ausmasse 13, 4x26, 4 m. Statt Seilen sind Tragelemente benützt worden, die aus vier gelenkig angeschlossenen Eisenbändern ⌀ 10 x 40 mm bestehen. Die 26 Tragelemente der Dachkonstruktion sind in einer cca 47 cm Entfernung und sind durch gemauerte Bogenkonstruktionen unterstützt - Bild 1, die die Stützen bilden und gut im Dachraum zu sehen sind; am Bild 3 ist der mittlere gemauerte Bogen, der die Hauptstütze der Dachkonstruktion bildet.

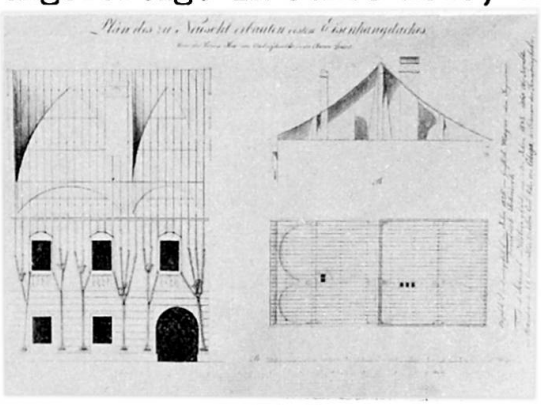

Bild 1

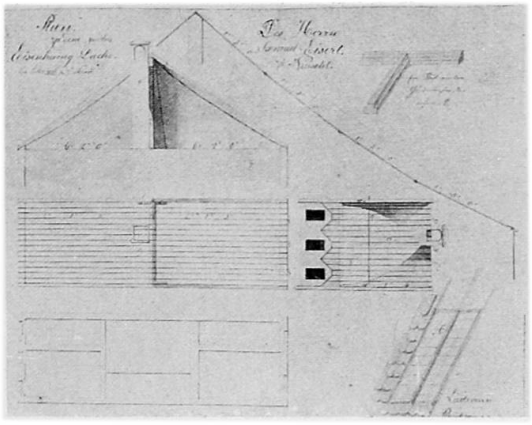

Bild 2

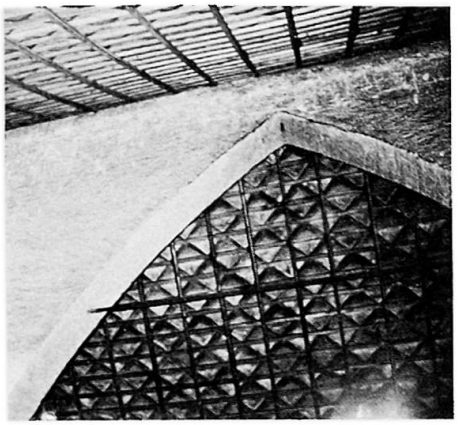

Bild 3

In den letzten Jahren erreichten in der ČSSR besonders die vorgespannten Hängedächer eine bedeutende Entfaltung /5/. Durch Vorspannung kann man das Verformen verringern und das Anheben oder Schwingen unter Windbelastung verhindern. Man realisierte mehrere Vorspanndächer über einen allgemeinen Grundriss, und das bei Objekten, die besonders für Sport- und Kulturzwecke bestimmt waren. Seit 1958 realisierte man über 80 Hängedächer von einer Gesamtfläche von 70000 m^2. Hier kann man auch die interessante Lösung einstöckiger Kreisgaragen einrechnen /Bild 4/, die in Bratislava unter der Ausnützung des Prinzips nach tschechoslowakischem Patent /22/ realisiert wurden.

Das mit seinen Abmessungen grösste Seildach, und zwar die Überdachung des Winterstadions in Prešov, hat die Ausmasse 92,00 x 77,64 m - Bild 5.

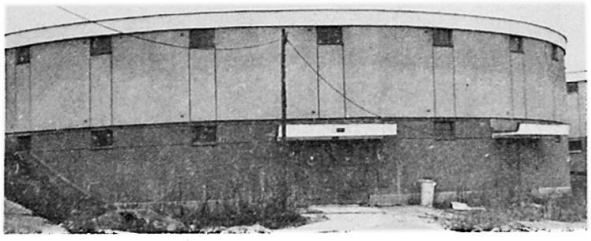

Bild 4

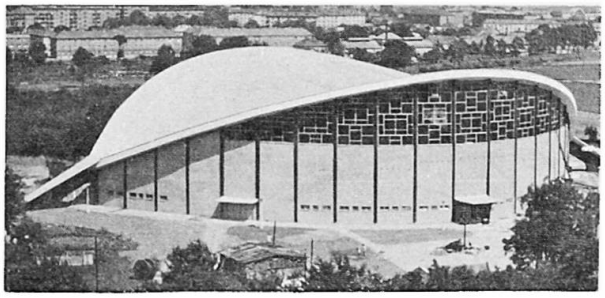

Bild 5

Am Bild 6 ist die Aula der Fakultät für Maschinenbau in Bratislava mit den Abmessungen 30 x 40 m. Am Bild 7 ist die Turnhalle in Bratislava, mit den Ausmassen 25 x 40 m. Die Überdachung des Sommertheaters in Praha mit den Ausmassen 44 x 38 m ist am Bild 8.

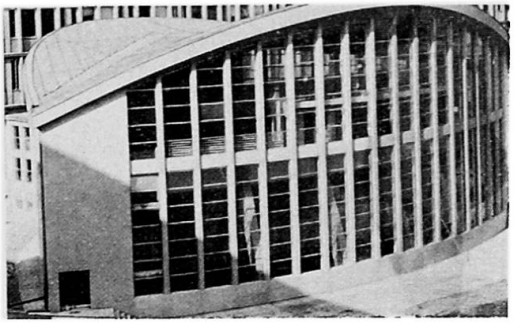

Bild 6

Bild 7

Von den tschechoslowakischen Patenten auf diesem Gebiet machen wir auf das Dach für eine grossräumige Gebäudeüberdachung aufmerksam /23/. Hierher können wir auch das tschechoslowakische Patent /24/ der vorgespannten Dachhaut zählen.

Ausser den bis jetzt angeführten Seilsystemen erschienen in der letzten Zeit auch vorgespannte Drahtkonstruktionen /1, 19, 25, 26/. Am Bild 9 ist eine Überdachungskonstruktion der Autobusstation in Banská Bystrica ersichtlich.

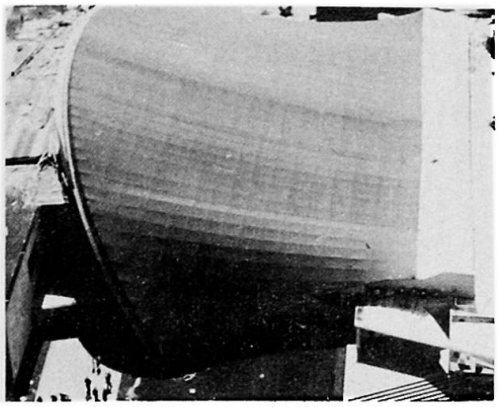

Bild 8

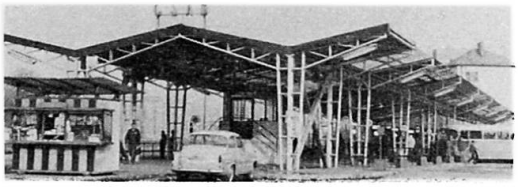

Bild 9

Am Bild 10 ist die Überdachungskonstruktion einer Zollstation bei Bratislava, von einer Gesamtlänge 66 m. Das Bild 11 zeigt eine Perronüberdachung der Eisenbahnstation in Svit. In allen Fällen wird die Welldachdeckung durch vorgespannte Zwillingsdrähte getragen.

Bild 10

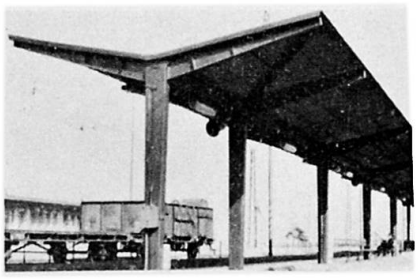

Bild 11

Eine weitere vorgespannte Konstruktion ist die Überdachung des Winterstadions in Bratislava - Bild 12 /27/. Die ursprüngliche Eisenbetonkonstruktion der Tribünen des Stadions wurde durch einen horizontalen Stahlfachwerkkranz zusammengehalten. Diese geschlossene Stahlkonstruktion übernimmt die Horizontalkräfte aus 6 vollwandigen Stahlzweigelenkrahmen von 52,3 m Spannweite. Dieses System ergab sich aus der Bedingung, dass die ursprüngliche Eisenbetonstützkonstruktion durch Horizontalkräfte nicht belastet werden konnte. Die Hauptträger des rhombischen Fachwerkkranzes wurden mit einer Überhöhung so vorgefertigt, dass nach der Montage alle Rahmen gleich wirken konnten. Die Schliessung des Systems und das Gewährleisten seines gewünschten Spannungszustandes, erreichte man mittels zwei 100 Mp Pressen, die so in Aktion gesetzt wurden, wie es am Schema /Bild 13/ aufgezeichnet ist.

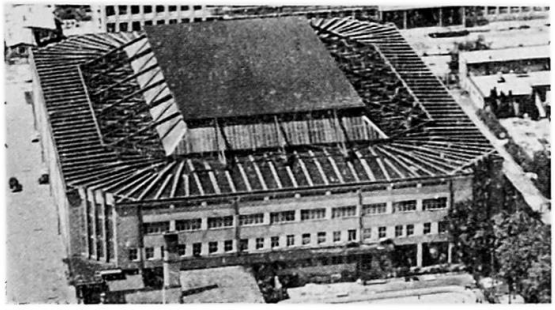

Bild 12

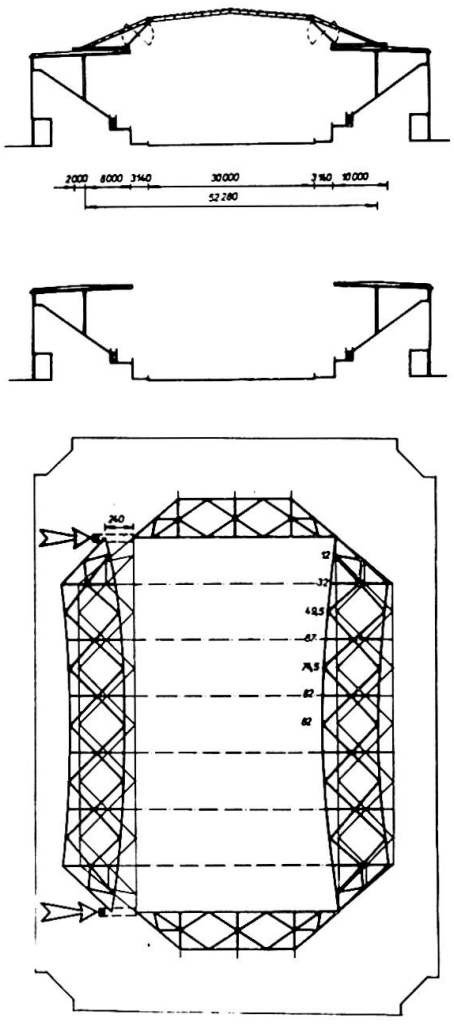

Bild 13

Am Bild 14 ist das Prinzip des tschechoslowakischen Patentes /28/ angedeutet, das für die Vorspannung und für die Spannungsregulierung der Dachkonstruktionen grosser Spannweite benützt wird. Die Tragkonstruktion besteht aus zwei Tragsystemen, die sich gegenseitig spannen /29/.

In letzter Zeit widmete man in der ČSSR Aufmerksamkeit auch der Vorspannung von Fachwerkdachplatten, die mittels günstig situierter Seilsprengwerksystemen vorgespannt sind /30, 31/. Die Vorspannung ermöglicht die Benützung von Standartdachelementen für vergrösserte Plattenspannweiten.

Ein weiteres tschechoslowakisches Patent /32/ betrifft die Vorspannung von Zweischichtträgern; eine Schicht wird elektrisch erwärmt und zur nicht erwärmten Schicht angeschweisst. Nach dem Auskühlen der erwärmten Schicht entsteht im Träger Vorspannung /33/. In grösserer Menge wurden diese Träger als Decken- und Dachträger der Feuerwehrstation in Praha /Bild 15/ benützt.

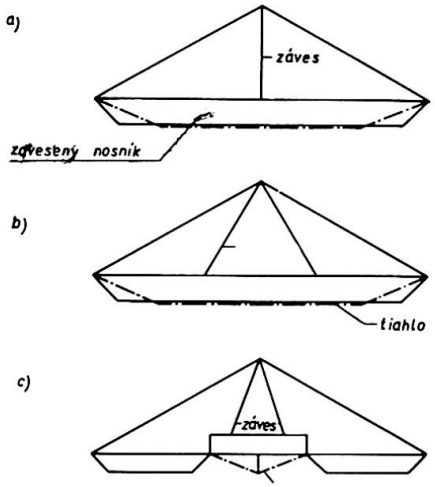

Bild 14

Bild 15

II. Brückenkonstruktionen

II.1 Eisenbahn- und Strassenbahnbrücken

Zuerst ein Beispiel aus der Geschichte. Bild 16 zeigt eine Brücke des Schiffkornsystems /1, 34, 35/. Es geht um ein zerlegbares Eisenbahnprovisorium. Die Vorspannung erzeugte man mittels Muttern an den Vertikalen, wodurch in Diagonalen Druck, in den Gurten Zug entstand. Es waren 163 solche Brücken gebaut; die erste im Jahre 1858.

Im Jahre 1962 wurde unweit von Ostrava eine Eisenbahnbrücke aus Duraluminium gebaut, Bild 17, 18 /1, 19/. Das Zugband aus bainitischem Stahl wurde mittels Erwärmung - durch Azetylbrenner - vorgespannt.

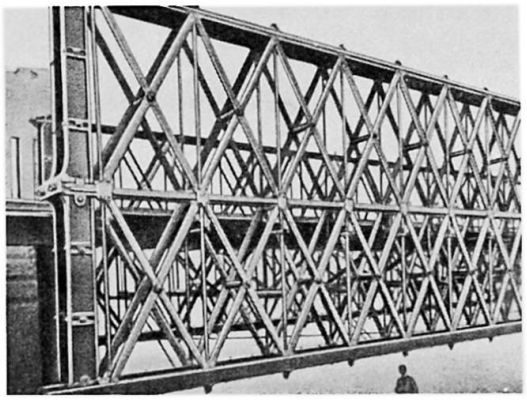

Bild 16

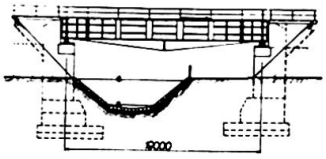

Bild 17

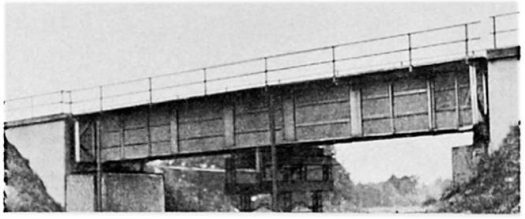

Bild 18

Bild 19

Bild 20

In Ostrava wurde durch Vorspannung eine Eisenbahnbrücke - Bild 19 - verstärkt /36/. Die Verstärkung erreichte man mittels vorgespannter Sprengwerke aus Stahl 37, die von der Aussenseite der Hauptträger angeordnet waren.

Die Vorspannung eines anderen Typs wurde bei einer Eisenbahnbrücke benützt, die VŽKG Ostrava - Vítkovice für den Export nach Irak lieferten, Bild 20 /1/. Es geht um die Fachwerkbrücke mit vorgespanntem Mittelfeld; im Mittelfeld waren die Knotenpunkte so mächtig, dass ihre tatsächliche Wirkung weit von der vorausgesetzten theoretischen Gelenkwirkung war. Die Nebenbiegespannungen in den Knotenpunkten aus der Verkehrslast kompensierte man mittels einer Vorbiegung, die bei der Montage durch Zwängung während der Stabusammenfügung entstand. Die Stäbe hatten zu diesem Zweck Fertigungsabweichungen von einer "genauen" geometrischen Form.

Eine der bedeutendsten vorgespannten Konstruktionen der letzten Zeit ist die Donaustrassenbrücke in Bratislava /37, 38, 39/. Es geht um unsymmetrisch aufgehängte Brückenbalken mit einem 303 m langem Mittelfeld. Die realisierte Konstruktion ist aus Stahl 11 523 und 11 483 ganz geschweisst. Die Kabel sind aus parallelen geschlossenen Seilen /jedes Ø 70,3 mm/ gebildet. Durch einen Montagevorgang erreichte man den gewünschten Vorspannzustand.

II.2 Stege, Rohr- und Transportbrücken

Am Wasserkraftwerk Vyšné Opatské wurde gemäss eines tschechoslowakischen Patentes /40/ ein vorgespannter Bedienungssteg gebaut /Bild 21/. Einzelne Vollwandbrückenbalken sind auf selbständigen Lagern dicht an den Pfeilerrändern aufgesetzt. Bei der Montage werden die Balken der Nachbarfelder über den Pfeilern, mittels Bänder, verbunden, wobei das angeschlossene Ende des neu montierten Balkens an den Lagern aufliegt, das andere Ende aber nicht. Infolge der Vorspannung werden die Biegemomente und die Balkendurchbiegungen deutlich verkleinert.

Weiter führen wir ein Beispiel an, wie ein havarierter Zustand eines Bedienungssteges durch Vorspannung rekonstruiert wurde /41, 42/. Es geht um eine Konstruktion von 36 m Spannweite

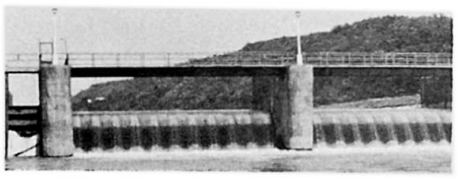

Bild 21

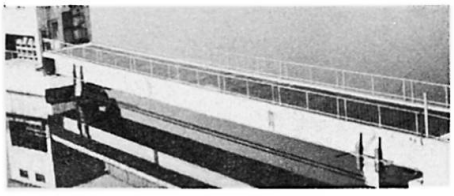

Bild 22

die als eine Verbundkonstruktion entworfen ist, um als Zugang zum Einlassturm des Wasserkraftwerkes auf dem Fluss Váh zu dienen /Bild 22/. Nachdem Auflegen der Hauptträger und der Prefabrikate verlor die Montagestütze ihre Funktion, setzte sich. Die Montageüberhöhung, die zum Verbund bei der Rekonstruktion notwendig war, erreichte man durch Vorspannung. So befestigte man am Untergurt der Hauptträger die Ankerkonsolen mit hochfesten Schrauben. Jeder der Hauptträger ist mit 2 Kabeln aus 24 Ø P 7 vorgespannt /Bild 23/. Die Vorspannkraft im Zugband beträgt 190 Mp.

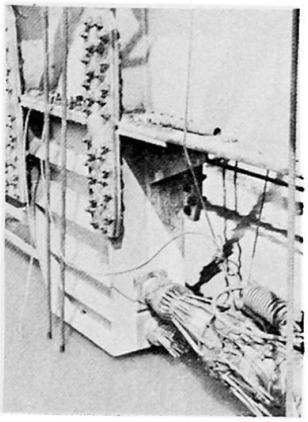

Bild 23

Bild 24

Am Bild 24 ist die Ansicht auf den vorgespannten Fussgängersteg über den Fluss Orava in Dolný Kubín /43/ dargestellt. Es geht um eine vorgespannte räumliche Hängekonstruktion mit den Feldweiten von 25 + 100 + 25 m. Die Vorspannung erreicht man durch Anspannen der Windseile; die Horizontalkomponente der Vorspannkraft beträgt 103 Mp.

Am Bild 25 ist eine vorgespannte Rohrbrücke über den Fluss Ohře /44/. Es geht um einen dreieckigen ganzgeschweissten Fachwerkträger, bei dem der Kraftverlauf durch Vorspannung voteilhaft mittels eines Betonballastes an den Konsolen geregelt ist.

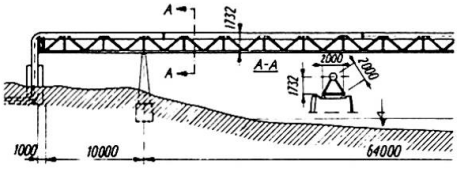

Bild 25

Über den Fluss Nitrica realisierte man eine Gasleitung, als einfaches vorgespanntes Sprengwerk - Bild 26 /1, 19/.

Nach einem tschechoslowakischen Patent /45/ wurden mehrere vorgespannte Rohrbrücken gebaut; die erste Konstruktion baute man über der Vltava bei Kralupy /46-48/. Es geht um ein Seilfaltwerk, dessen Steifigkeit durch Vorspannung gewährleistet ist. Die Spannweite, dieses Hängesystems beträgt 160 x 2 x 40 m. Das System ist durch Tragseile /4 Ø 60 mm/ und durch zwei unter 45° geneigten Windseilen /Ø 60 mm/ /Bild 27/ ausgebildet. Eine weitere solche Konstruktion wurde über den Fluss Labe bei Neratovice gebaut /Bild 28/; eine dritte Brücke wird gerade in Ústí vollendet.

Ein weiterer Typ einer Rohrbrücke als eine vorgespannte Seilkonstruktion /Bild 29/ wurde über den Fluss Váh in Rybárpole gebaut /1, 19, 49/. Die Brückenspannweite beträgt 75,9 m. Die V-förmigen Pylone tragen die Tragseile, welche durch die im Pylonfunda-

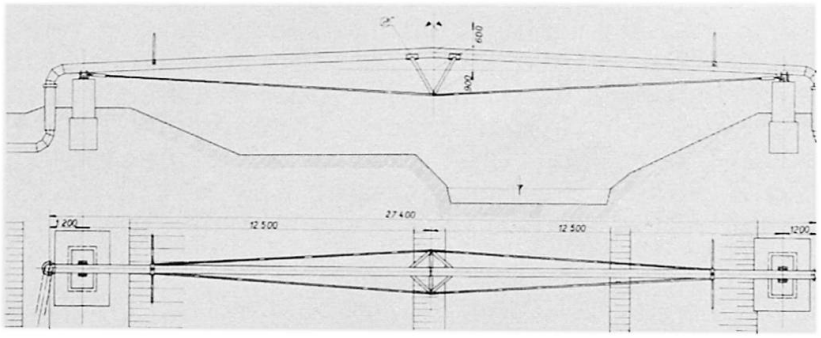

Bild 26

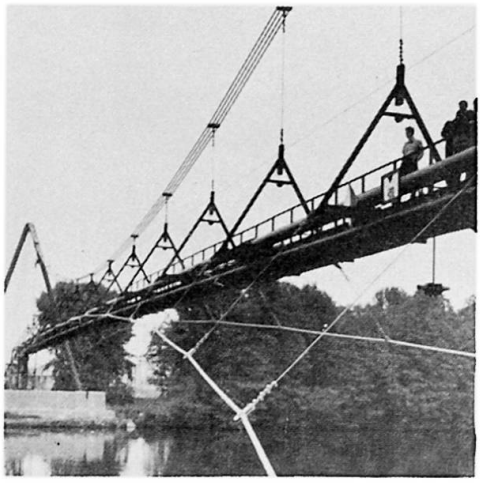

Bild 27

ment verankerten Spannseilen vorgespannt sind. Die Tragseile sind in selbständigen Ankerblöcken verankert. Am Bild 30 ist ein Detail von der Vorspannung eines Seiles der erwähnten Konstruktion sichtbar.

Am Bild 31 ist eine vorgespannte Schlackenleitungskonstruktion zu sehen /50/. Das System ist für jedes Feld separat stabilisiert. Die Vorspannung ist durch Rektifikationselemente gesichert, die am Seilende angeordnet sind.

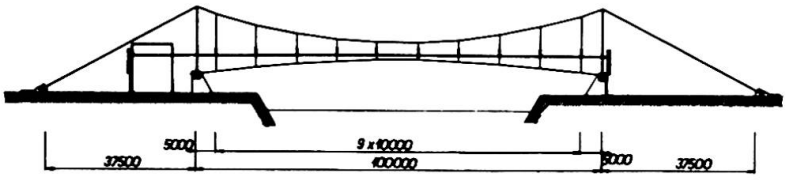

Bild 28

Am Bild 32 ist eine verstärkte sprengwerkartige Transportfachwerkbrücke in Ostrava /36/ zu sehen. Verstärkt wurden die beiden Felder und zwar mittels Vorspannseilen unter dem Untergurt und mittels Nebendiagonalen, die zwischen den ursprünglichen Mittelgurt und den Untergurt gelegt wurden.

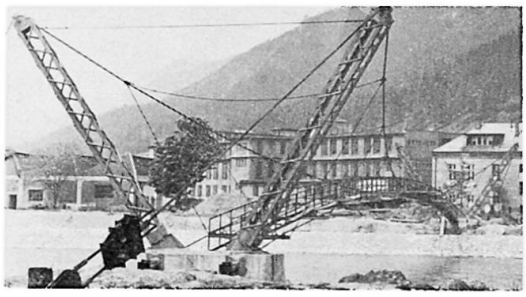

Bild 29

Bild 30

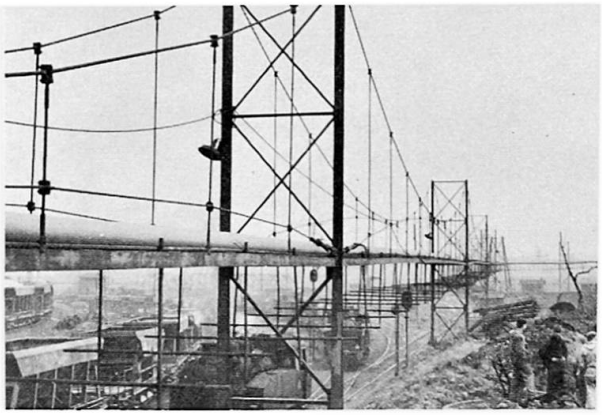

Bild 31

III. Konstruktionen besonderen Typs

Ein vorgespanntes Rammgerät nach dem tschechoslowakischen Patent /51/ ist am Bild 33 abgebildet. Der Riegel des Rammgerätes ist dauernd mit Seilen vorgespannt. Diese Seile haben an einem Ende eine Spannvorrichtung, am anderen Ende den Schwingarm. Ein eigentliches Vorspannen erreichte man mittels einer Last, die um 25 % gegenüber dem Gewicht der Birne vergrössert ist, so dass beim Aufhängen im Spannzustand die Spreizen zwischen dem Zugband und dem Riegel eingelegt werden. Der unterstützte Riegel erfährt nach einer schnellen Entlastung der Birne nur kleine Verformungen und geringe Schwingungen. So ist am Bild 33 das erste ausgeführte vorgespannte Rammgerät von 31,6 m Spannweite, 29 m Höhe und cca 25 m Hubhöhe dargestellt.

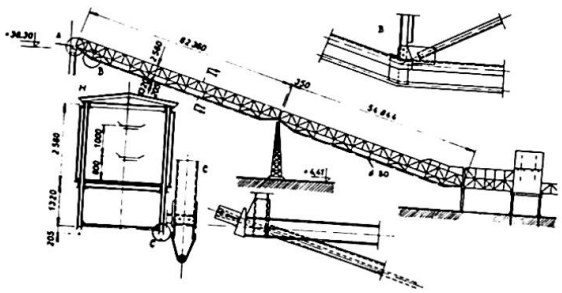

Bild 32

Vorgelegt wurden auch mehrere Entwürfe von Transportstahlkonstruktionen und Hebeeinrichtungen /52, 53/, bei denen mit Erfolg die Vorspannung benützt wurde. Mehrere von ihnen wurden in der ČSSR patentiert /54/.

In grösserer Menge waren in der ČSSR vorgespannte Stahlkonstruktionen des Masttyps verwendet /55/. Die Untersuchung der tatsächlichen Wirkung des Mastes des ersten Types - Bild 34/a - zeigte ausser anderem, dass die Vorspannung bis cca 7 Mp die Maximalkräfte im Mast nicht ungünstig

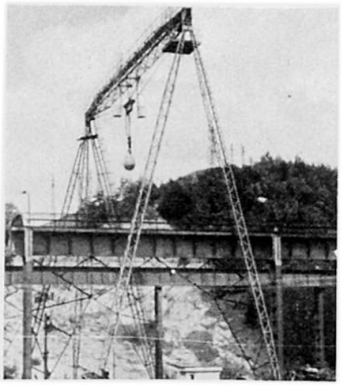

Bild 33

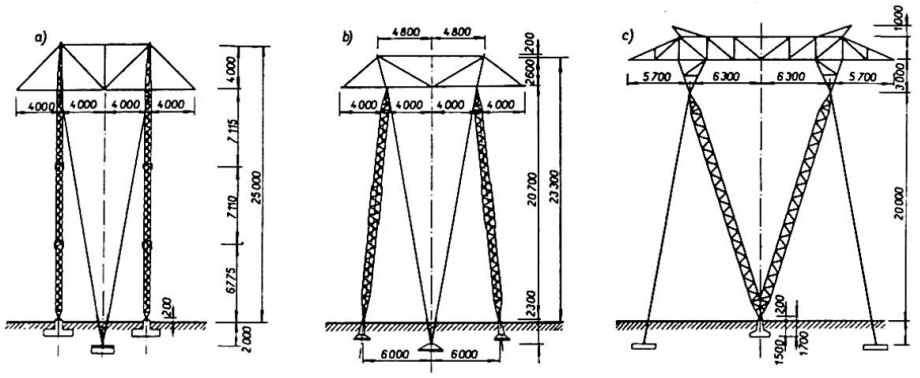

Bild 34

beeinflusst und seine Steifigkeit bedeutend vergrössert. Nach erworbenen Erfahrungen wurde ein verbesserter Typ gefertigt - Bild 34/b. Den zweiten Typ - vorgespannter verankerter Mast der Form V - sehen wir am Bild 34/c. Es zeigte sich, dass bei diesem Typ die Vorspannung bis 5 Mp die Steifigkeit der Konstruktion erhöht. Der Prototyp wurde nach Bemerkungen verbessert. Er wurde in einer Menge von einigen hundert Stücken benützt. Von den tschechoslowakischen Patenten auf diesem Gebiet führen wir eines an - Bild 35 /56/.

Der weitere Typ des vorgespannten zerlegbaren und transportablen Mastes - Bild 36 - wurde in der ČSSR für Zwecke metheorologischer Messungen verwendet.

IV. Schlussbemerkung

Schon aus dem kurzen Überblick sieht man, dass in der ČSSR auf dem Gebiete vorgespannter Metallkonstruktionen ein bestimmter Schritt vorwärts getan wurde. Wegen Platzmangel konnten wir uns mit den Zielen und Prinzipien der Vorspannung bei den einzelnen Objekten eingehend nicht befassen und auch nicht mehr von den technologischen Angaben und Einzelheiten anführen.

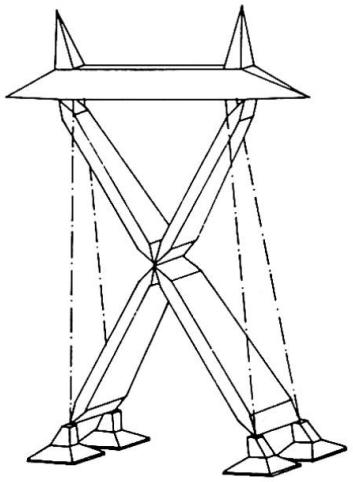

Bild 35

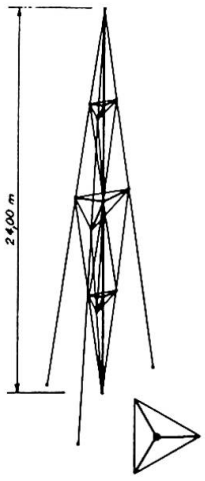

Bild 36

Literaturverzeichnis:

/1/ Ferjenčík P. - Tocháček M.: Predpäté kovové konštrukcie, Bratislava, SVTL 1966

/2/ Internationale Fachtagung "Vorgespannte Stahlkonstruktionen", Dresden 1963. Wissenschaftliche Veröffentlichungen aus der Fakultät für Bauwesen der Technischen Universität Dresden 1964, B-Reihe,No 30

/3/ Sborník II.mezinárodní konference o předpjatých kovových konstrukcích, Tále - Mýto pod Ďumbierom 1966. Praha SÚ ČVUT 1966

/4/ III.meždunarodnaja konferencija po predvariteľno naprjažennym metalličeskim Konstrukcijam. Doklady. Leningrad 1971

/5/ Zborník prednášok zo seminára o visutých strešných konštrukciách. Dom techniky SVTS, Bratislava 1971

/6/ Ferjenčík P.: Einige Bemerkungen zu den vorgespannten Stahlkonstruktionen in der ČSSR. In: /2/

/7/ Ferjenčík P.: Predvariteľno naprjažennyje staľnyje konstrukciji v Čechoslovakiji. Premyšlennoje stroiteľstvo 1964, No 9

/8/ Ferjenčík P.: Feszített Fémszerkezetek Csehszlovákiában. Mélyépítéstudományi Szemle 1965, szám 3

/9/ Ferjenčík P.: Stato attuale e posibilita futura delle strutture di acciaio presollecitate in Cecoslovacchia. Costr.metalliche 1965, N.3.

/10/ Ferjenčík P.: Razrabotka i primenenie predvariteľno naprjažennych staľnych konstrukcij v Čechoslovakiji Izvestija VUZ, Stroiteľstvo i architektura 1965, No 10

/11/ Tocháček M. - Ferjenčík P.: Predpjaté oceľové konstrukce v ČSSR a jejich navhrhování. Stav.časopis SAV 1965, č.6

/12/ Ferjenčík P. - Tocháček M.: Sprężone mosty metalove w ČSRS. Inż.i budownictwo 1965, NR 11

/13/ Ferjenčík P.: Predpäté kovové konštrukcie. In: Zborník vedeckých prác SvF SVŠT v Bratislave 1965. Bratislava SVTL, 1965

/14/ Ferjenčík P.: Niektoré z realizovaných predpätých kovových konštrukcií v ČSSR, In: /3/

/15/ Ferjenčík P.- Tocháček M.: Ossature métalliques précontraintes pour batiments en Tchécoslovaquie. Acier-Stahl-Steel 1967, 10

/16/ Ferjenčík P. - Tocháček M.: Esijännitetyistä teräskonstruktioista Tshekkoslovakiassa. Rakennustekniikka 1968, 10

/17/ Tocháček M.: Předpjaté kovové konstrukce průmyslových staveb. Poz.stavby 1963, č.12

/18/ Wasmuths Lexikon der Baukunst, zweiter Band C bis Gyp. Verlag Ernst Wasmuth, A. - G.Berlin 1930, S.321

/19/ Ferjenčík P.: Predpäté kovové plnostenné konštrukcie; časť I.-IV. Bratislava, KKDK SvF SVŠT, 1965

/20/ -K-: Prvá železná strecha sveta na Slovensku. Revue slovenskej architektúry, Projekt, 1970, č.3

/21/ Ferjenčík P.: Príspevok k historii visutých strešných konštrukcií. In: /5/

/22/ Poštulka J.: Lanová strecha s kruhovým pôdorysom. Patentný spis č.102985; Praha ÚPV 1962
/23/ Koloušek V.: Střecha pro zastřešení budov s rozsáhlym prostorem. Patentní spis č.103485; Praha 1962
/24/ Horák V. - Tocháček M.: Nosná a současne krycí konstrukce. Petentový spis č.117313; Praha 1966, ÚPV
/25/ Ferjenčík P. - Tocháček M.: Nosná konštrukcia krytiny z predpätých drôtov. Inž.stavby 1965, č.9
/26/ Ferjenčík P. - Dutko P. - Agocs Z. - Tocháček M.: Priame predpäté vlákna v konštrukciách striech. In: /5/
/27/ Tesár A.: Prestrešenie zimného štadiona v Bratislave. Inž.stavby 1959, č.3
/28/ Dundr J.: Nosná konstrukce. Patentový spis 127746; Praha ÚPV 1968
/29/ Dundr J.: Trám vystužený trojkloubovým nosníkem. In: /3/
/30/ Russ J.: Predvaritelʹno naprjažennaja pravilʹno uporjadočennaja prostranstvennaja steržnevaja konstrukcija. In: /4/
/31/ Veselý V.: Krovelʹnaja prostranstvennaja rešetčataja konstrukcija, kombinirovannaja s trosovymi elementami. In: /4/
/32/ Šindler V.: Způsob výroby predpjatého vrstveného nosníku, po prípade vrstvené desky. Patentový spis 121156; Praha ÚPV 1966
/33/ Šindler V.: Predpínání ocelových nosníků. In: /3/
/34/ Kolář J.: Mostní stavitelství I., II., III. Praha 1923, 1925, 1926
/35/ Velflík A.V.: Hlavní trámové příhradové nosníky. In: Velflík A.V., Stavitelství mostní II., Praha, ČMT 1905
/36/ Bustín J.: Erhöhung der Tragfähigkeit von Stahlbauwerken durch Vorspannung. In: /2/
/37/ Tesár A.: Il nuovo ponte sul Danubio a Bratislava. Costr. metalliche 1966, N.5
/38/ Tesár A.: Projekt mosta čerez Dunaj v Bratislave. In: Materialy po metalličeskim konstrukcijam, vyp.12. Moskva 1967
/39/ Tesár A.: Das Projekt der neuen Strassenbrücke über die Donau in Bratislava, ČSSR. Bauingenieur 1968, H.6
/40/ Rusina B.: Spôsob predpnutia mostných členov skriňového prierezu, ÚPV 1961
/41/ Veríšek V. - Ferjenčík P. - Agócs Z.: Rekonštrukcia oceľovej lávky pomocou predpínania. Inž.stavby 1968, č.11
/42/ Vasiľkov V.V.- Voříšek V. - Ferjenčík P. - Agócs Z.: Plnostenné nosníky predpäté vysokopevnostným ťahadlom. In: Sborník vedeckých prác SvF SVŠT Bratislava 1968; Bratislava ALFA 1968
/43/ Agócs Z.: Rezuľtaty issledovannija teoretičeskoj i dejstviteľnej raboty vantových predvariteľno naprjažennych sistem. In: /4/
/44/ Pařížek F.: Ocelové konstrukce pro převádění plynového potrubí pres prírodní prekážku. Inž.stavby 1964, č.4
/45/ Tesár A.: Visutý potrubní most. Patentový spis 114163; Praha ÚPV 1965
/46/ Tesár A.: Potrubné visuté mosty. In: Sborník vedeckých

prác SvF SVŠT v Bratislave 1961, zv.1; Bratislava, SVTL 1961
/47/ Tesár A.: Prvý predpätý visutý most v ČSSR. Inž.stavby 1963, č.10
/48/ Tesár A.: Berechnung und Ausführung einer vorgespannten Rohrleitungsbrücke in der ČSSR. In: /2/
/49/ Ferjenčík P. - Dutko P.: Predpínanie visutého potrubného mosta. In: Sborník vedeckých prác SvF SVŠT v Bratislave 1966; Bratislava, SVTL 1966
/50/ Kozák J.: Lanová konštrukcia troskovodu. Inž.stavby 1965, č.12
/51/ Paučík J.: Beranidlo. Patentový spis 114081; Praha ÚPV, 1965
/52/ Paučík J.: Predpiate oceľové konštrukcie dopravných a zdvíhacích zariadení. In: /3/
/53/ Stránsky I.: Dopravníkový pás krytý tenkostenným prútom predpätým samonapätím vzniklým pomocou vzpínadla. In: /3/
/54/ Paučík J.: Žlabový dopravník pro dopravu kulatiny nebo jiného kusového zboží. Patentový spis 126285; Praha ÚPV, 1968
/55/ Voříšek V.: Skutočné pôsobenie predpätých kotvených stožiarov elektrického vedenia veľmi vysokého napätia. Inž. stavby 1964, č .7.
/56/ Bojsa M.: Nosný stožiar pre elektirické vedenia. Patentový spis 121439; Praha ÚPV 1966

Zusammenfassung

Zur Darstellung der breiten und praktischen Tätigkeit auf dem Gebiete vorgespannter Metallkonstruktionen in der ČSSR werden die namhaften Beispiele von Realisationen und Patenten angeführt. Die Beispiele sind in drei Gruppen geteilt: Hochbau, Brückenbau und Spezialkonstruktionen. Die ČSSR hat auf diesem Gebiete eine reiche Tradition mit Objekten, die 150 Jahre alt sind. Gegenwärtig behauptet sich die Vorspannung hauptsächlich bei Hängedächern und Brücken.

Leere Seite
Blank page
Page vide

Schrägkabelbrücke mit drei Fahrbahnen übereinander

Diagonal Cable Bridge with three Superposed Roadways

Pont à haubans inclinés avec trois tabliers superposés

O. STEINHARDT
Prof. Dr.-Ing., Dr. sc. techn. h.c. (ETH)
Karlsruhe, BRD

1. Vorbemerkung

Aufgrund der verkehrstechnischen Neuordnung der Großstadt W u p p e r t a l wurde vom städtischen Tiefbauamt, neben den bereits vorhandenen und geplanten Ost-West-Straßenverbindungen, eine leistungsfähige Querverbindung in Süd-Nord-Richtung projektiert. Da die Bundesbahn gleichzeitig eine S-Bahnlinie vom Bahnhof Wuppertal-Elberfeld in Richtung Essen plante, erschien es sinnvoll und naheliegend, beide Verkehrswege zu einer gemeinsamen Trasse zu vereinigen.

Ausgehend von den Voruntersuchungen des Ing.-Büro H. Berger (Stuttgart) über Tunnel und freie Strecke wurde im folgenden als optisch wirkungsvollstes Kernstück innerhalb der Gesamtplanung eine H o c h b r ü c k e als eine mögliche Lösung der Talüberquerung von Straße und Eisenbahn aufgezeigt.

2. Tragsystem

Die kostenmäßig deutlich überwiegenden Anteile weiterer Bauwerke im Rahmen des Gesamtbauvorhabens - wie z.B. Tunnelbauten, Einschnitte, Dämme, niveaufreie Straßenentflechtungen, und auch die Berücksichtigung örtlicher Gegebenheiten, wie mögliche Pfeilerstandorte und Unterführung der Schwebebahn - ergaben Zwangsbedingungen, die durch den vorliegenden Entwurf einer durch "Rautenträger versteiften Schrägkabelbrücke" nach Bild 1 in optimaler Weise respektiert werden konnten.

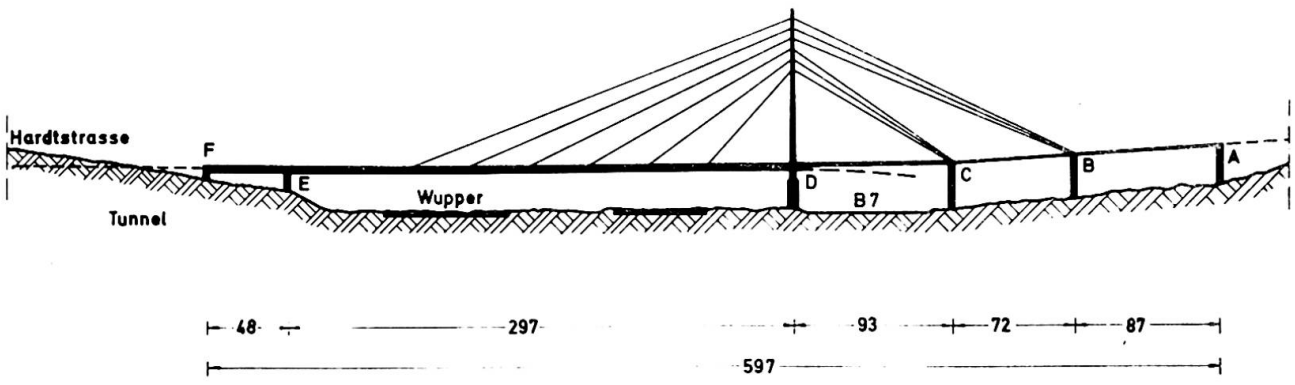

Bild 1: Vorstudie "HOCHBRÜCKE WUPPERTAL" - System -

Bekanntlich sind in den letzten Jahren in der BRD zahlreiche kabelüberspannte Brückenkonstruktionen entstanden, im vorliegenden Entwurf wird jedoch erstmalig für eine maximale Spannweite von nahezu 3oo m nicht nur eine zweigleisige Eisenbahn (mit dem Lastenzug S 195o) in einer mittleren Höhe von ca. 2o m über den Stadtteil Elberfeld geführt, sondern es werden zusätzlich zwei übereinander angeordnete Fahrbahnen (mit richtungsgebundenem Straßenverkehr, nach DIN 1o72 für SLW 6o) von denselben Versteifungsträgern aufgenommen.- Im Bereich des Pylons (Pkt.D) spaltet sich die Eisenbahnlinie in einer Kurve vom Haupttragwerk ab; die hieraus resultierenden Nachteile infolge der stark unterschiedlichen Trägheitsmomente der Felder werden jedoch zum Teil durch die besondere Anordnung der Schrägkabel kompensiert.

Die für die Hauptöffnung gewählte "Fächerform" für die Schrägkabel ergibt neben einer wirksamen Begrenzung der Durchbiegungen auch die Möglichkeit, den Gradientenverlauf der "Fahrbahn-Oberkanten" durch planmäßige und nachrichtbare Überhöhungen unter der ständigen Last so abzustimmen, daß z.B. für die Eisenbahn (Feld EF) nur Steigungen bis zu 4o% des zul. Wertes (=3o‰) infrage kommen, bzw. daß beim täglichen "Regelverkehr" (d.h. bei etwa 6o% Auslastung gegenüber dem Eisenbahnlastenzug und bei etwa 2o% Straßenbelastung) praktisch nur 1o% der Grenzsteigung, d.h. im allgemeinen nur eine solche von ca. 3,1‰ erreicht wird.- Um dem System die für Eisenbahnbrücken erforderliche Steifigkeit zu geben, erfolgt die Rückverankerung in die Seitenöffnungen durch "sternförmige" Zusammenführung der Kabel zu den Pfeilern B und C hin.

3. Tragwerk

Der Brückenquerschnitt nach Bild 2, mit den drei übereinander liegenden Fahrbahnen, ergab sich - außer aus statischen Gründen - als sinnvolle Fortführung der für den Tunnel optimalen Querschnittslösung nach Bild 3.

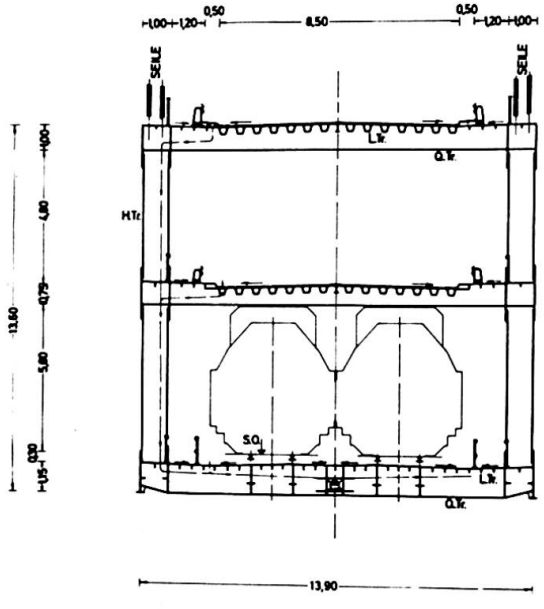

Bild 2: Brückenquerschnitt (3-Stockform)

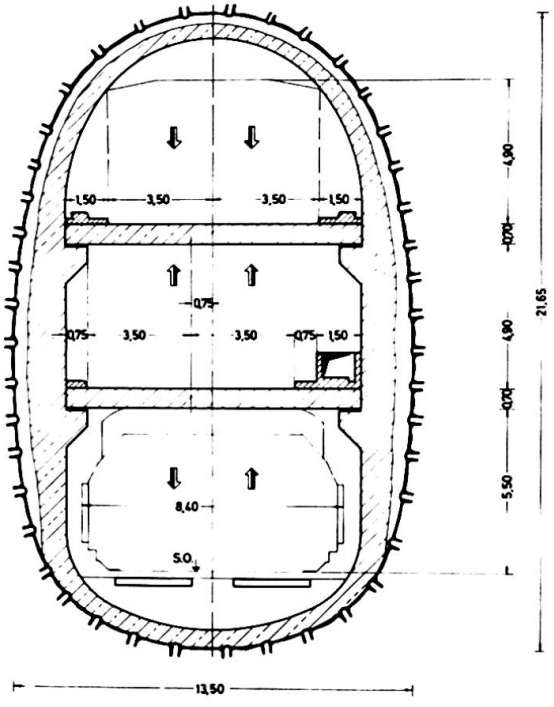

Bild 3: Tunnelquerschnitt (Vorschlag E des Ing.-Büro Berger)

Unter Berücksichtigung der lichten Durchfahrtshöhen und der Spurbreiten erhält man eine Bauhöhe von ca. 13,6o m, bei einer Gesamtbreite von 13,9o m.- Der bis auf die Montagestöße als Schweißkonstruktion vorgesehene Brückenquerschnitt setzt sich aus zwei seitlichen Hauptträgern zusammen, die im Bereich der kombinierten Straßen- und Eisenbahnbrücke (von D bis F) als rautenförmiges Fachwerk und bei der Straßenbrücke allein (von A bis D) als einfaches Strebenfachwerk ausgebildet sind. Die kastenförmigen Ober- und Untergurte werden jeweils durch die "mittragende Breite" der äußeren Fahrbahntafeln verstärkt.- Alle drei Fahrbahntafeln sind als orthotrope Platten aus Fahrbahnblech, Längsträger und Querträger ausgebildet.-

Die Krafteinleitungspunkte bzw. die Kabelverankerungen in den Hauptträgern wurden planmäßig in obere (vollwandige) "Dreiecksscheiben" gelegt, wodurch die aus den Kabeln resultierenden Horizontalkräfte - statisch günstig - den beiden "oberen" Fahrbahntafeln zugewiesen werden konnten; Kraftumlenkungen infolge des Querschnittssprunges am Pylon werden dadurch vermieden.

Vorteilhaft erscheint es auch, daß der etwa quadratische Querschnitt durch seine Torsionssteifigkeit der im Regelfall einseitigen Eisenbahnlast, und auch der meist einseitigen Strassenbelastung, besonders gut widersteht. Außerdem wird durch die Anordnung von zwei Seilebenen die mögliche Schrägstellung der Gleise auf ein Mindestmaß reduziert.

Der alternativ in Bild 4 dargestellte Querschnitt mit n e b e n e i n a n d e r l i e g e n d e n Straßenspuren und einer Mittel-Seilebene würde gegenüber der 3-Stocklösung keine wesentlichen Vorteile mehr erbringen.

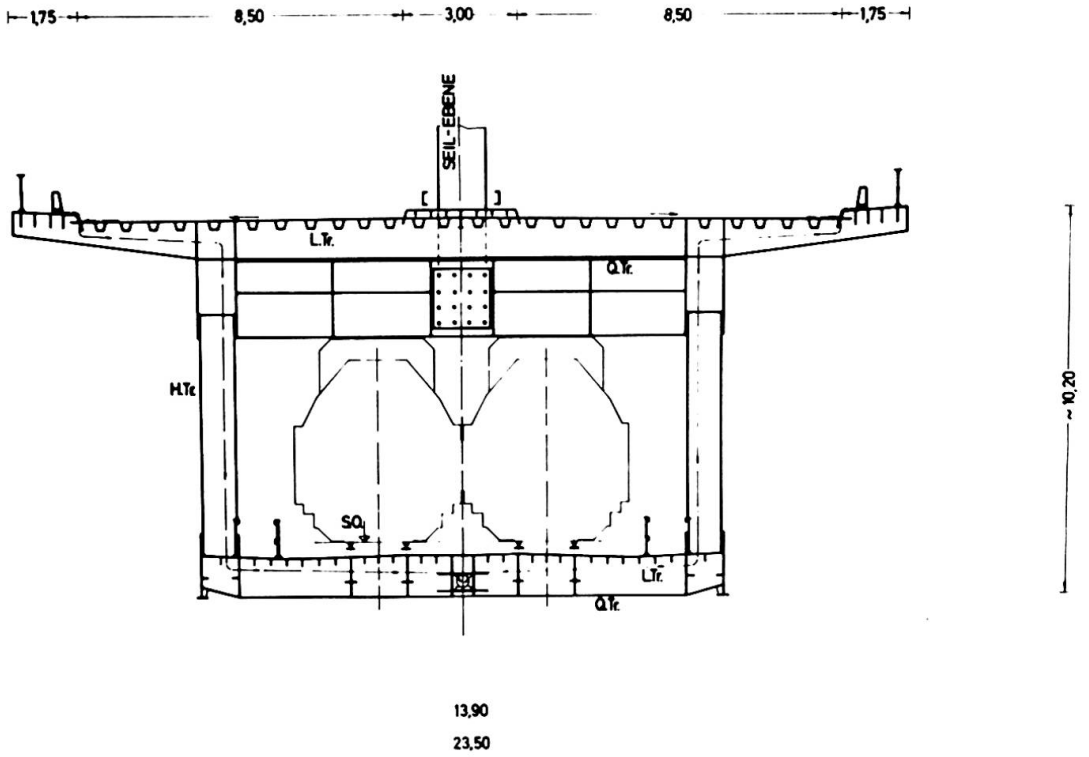

Bild 4: Brückenquerschnitt mit nebeneinanderliegenden Fahrspuren

Besondere Aufmerksamkeit ist im vorliegenden Fall der Verminderung des Lärms (Stoßdämpfung und Schalldämmung) durch die Schienenfahrzeuge zu widmen; hier sind neuere Erfahrungen an elastisch gelagerten Schienen und neueste Versuchsergebnisse z.B. gemäß [1] bei der Ausführung zu berücksichtigen.

4. Pylon und Seile

Der ursprünglich in A-Form geplante Pylon erbrachte - wegen der bei einseitiger Verkehrsbelastung entstehenden horizontalen Abtriebskräfte quer zur obersten orthotropen Platte - gegenüber der in Bild 5 dargestellten Form einige technischen Nachteile, wie auch rein optisch die Überschneidungen bei (räumlichen) Schrägkabeln aus der "Stadtperspektive" sich als nicht ganz befriedigend erweisen würden. Der neue Pylon mit zwei in den Stahlbetonpfeiler eingespannten Stielen und oberem Querriegel hat eine Höhe von etwa 93 m bis zur obersten Kabellagerung.

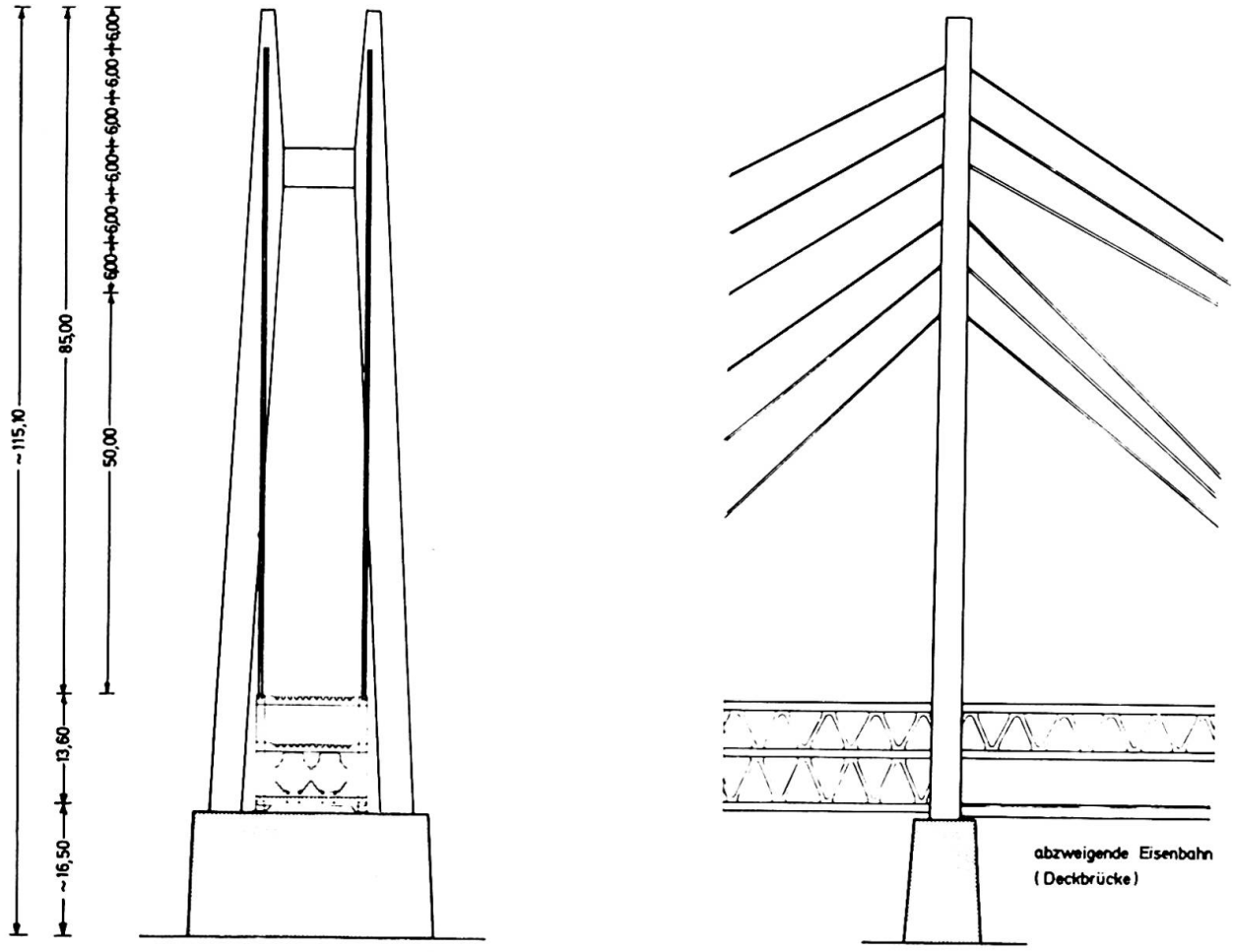

Bild 5: Pylon

Die Schrägkabel, bestehend aus jeweils vier paralleldrähtigen Einzelseilen, die am oberen Rand zentrisch gelagert (Hammerkopf gegen Schotte abgestützt) und am unteren Ende zusätzlich vorspannbar sind, werden in parallelen Ebenen zu den - oben schon erwähnten - scheibenartig ausgesteiften Rautenfeldern der Hauptträger hingeführt und dort mit max. Einzelkräften bis zu ca. 650 Mp je Seil angespannt.

Schrifttum:

[1] VDI-Berichte, Nr. 17o - Lärmminderung im Schienenverkehr
VDI-Verlag GmbH, Düsseldorf

6. Zusammenfassung

Anhand eines ausschreibungsreifen Hochbrücken-Entwurfs wird gezeigt, daß seilverspannte Konstruktionen, selbst über dichtbebauten Stadtgebieten und bei einheitlicher Überführung von drei übereinander angeordneten Verkehrsebenen, sehr geeignete technische Lösungen darstellen können. Bei einer maximalen Stützweite von nahezu 3oo m, und bei Anordnung eines über 93 m hohen zweistieligen Pylons, ergeben die rautenförmig ausgefachten, 13,5 m hohen Versteifungsträger bei der Verwendung von z.T. vorgespannten Schrägkabeln einen sehr günstigen Gradientenverlauf unter Regelverkehr.

Leere Seite
Blank page
Page vide

Schrägseilbrücken

Cable-Stayed Bridges

Ponts à câbles inclinés

HERIBERT THUL
Bundesverkehrsministerium Bonn, BRD

1. Geschichtliches

Herr Professor Leonhardt hat im Einführungsbericht das Wesentliche zu den Seilkonstruktionen und ihrer Anwendung in der Bundesrepublik Deutschland gesagt. Mit meinem Beitrag kann ich daher nur noch einige den Brückenbau betreffende Ergänzungen vortragen.

Die Schrägseilbrücke ist keine Erfindung unserer Zeit. Schon im Jahre 1617 stellte der venezianische Ingenieur Verantius eine Brücke mit mehreren parallelen schrägen Ketten dar, und im Jahre 1784 beschrieb der deutsche Imanuel Löcher eine hölzerne Brücke, die bereits alle Merkmale einer Schrägseilbrücke aufwies. Dieser neuartige konstruktive Gedanke wurde in England im Jahre 1817 mit der 1. eisernen Schrägseilbrücke für Fußgänger (Spannweite 34 m) wieder aufgegriffen. Auch in Frankreich entwarf Poyet 4 Jahre später eine hölzerne Balkenbrücke, die mit geraden Eisenstäben an hohen Masten aufgehängt werden sollte. Schließlich war es nochmals England, wo Hartley im Jahre 1840 das Projekt einer Brücke mit zueinander parallelen Abspannungen vorlegte. Von weiteren Versuchen mit diesem damals bereits über 2 Jahrhunderte alten Konstruktionsprinzip ist nichts überliefert worden.

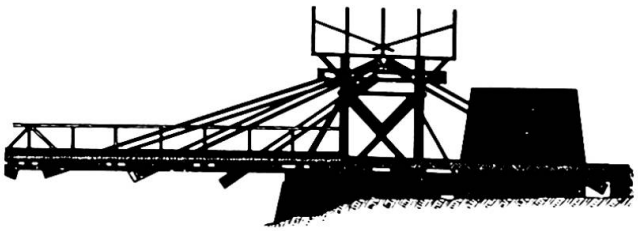

Bild 1: Alte Holzbrücke 1784:
Bauart Löscher

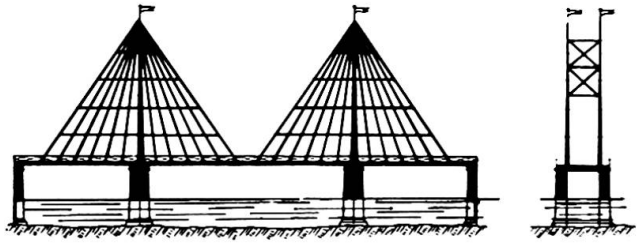

Bild 2: Brücke von 1821
Bauart Poyet

Bild 3: Kettenbrücke von 1840
Bauart Hatley

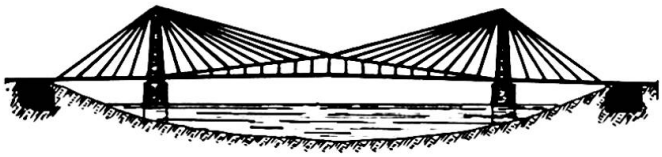

Bild 4: Schrägseilbrücke
Bauart Gisclard-
Anodin

Im modernen Brückenbau gewann die Seilkonstruktion erst wieder an Bedeutung, nachdem Material hoher Festigkeit zur Verfügung stand und das Kräftespiel der hochgradig statisch unbestimmten Systeme sowie eine wirtschaftliche Montage beherrscht wurden.

2. Systeme der Schrägseilbrücken

Grundsätzlich ist zwischen 1- und 2-wandigen Systemen zu unterscheiden.

Die Tragebene 1-wandiger Systeme liegt in der Regel über der Mittellinie des Bauwerkes. Der Versteifungsträger ist dabei als Hohlkasten ausgebildet, über den die aus der Exzentrizität der Lasten herrührenden Torsionsmomente abgetragen werden. Von besonderem Vorteil ist hierbei die Möglichkeit, die Abmessungen der Pfeiler klein zu halten.

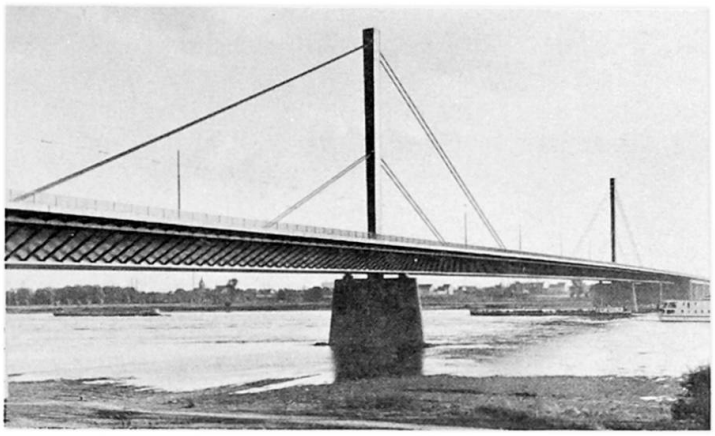

Bild 5: Rheinbrücke Leverkusen;
einwandige Schrägseilbrücke

Bei den 2-wandigen Systemen können die Seiltragwände entweder innerhalb oder außerhalb der Geländer angeordnet werden. Im ersten Falle ist ein größerer Brückenquerschnitt, im zweiten Falle sind aufwendigere Konstruktionen für Verankerung und Pfeiler erforderlich. Die Seilebenen können senkrecht oder gegeneinander geneigt gewählt werden.

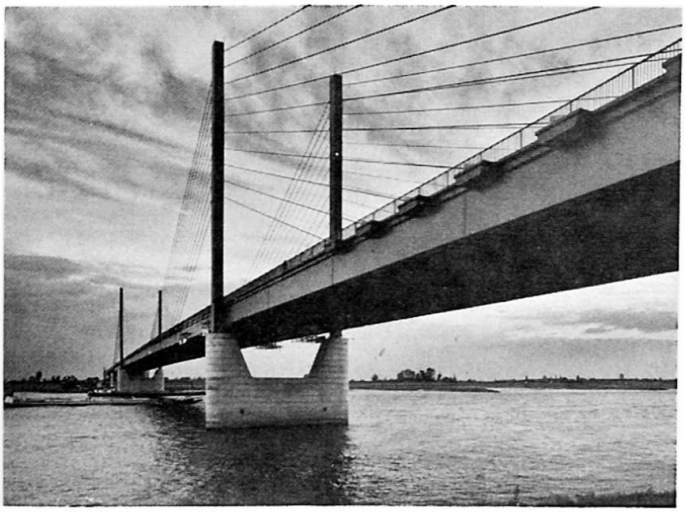

Bild 6: Rheinbrücke Rees;
zweiwandige Schrägseilbrücke

Beide Systeme, ein- und zweiwandige, können sich hinsichtlich der Zahl und Anordnung der Seile voneinander unterscheiden.

Ist die Brücke nur an wenigen Seilen aufgehängt, so wird deren Verankerung in Anbetracht der großen Kraftkonzentration schwierig. Erhebliche Verstärkungen der Hauptträger an den Einleitungspunkten sind dann nicht zu vermeiden. Demgegenüber kann beim Vielseilsystem mit Annäherung ein kontinuierlich unterstützter Träger auf elastischer Bettung angenommen werden, wobei die Gesamtheit der Tragglieder einer Kabelebene durch eine elastische Wand ersetzt wird.

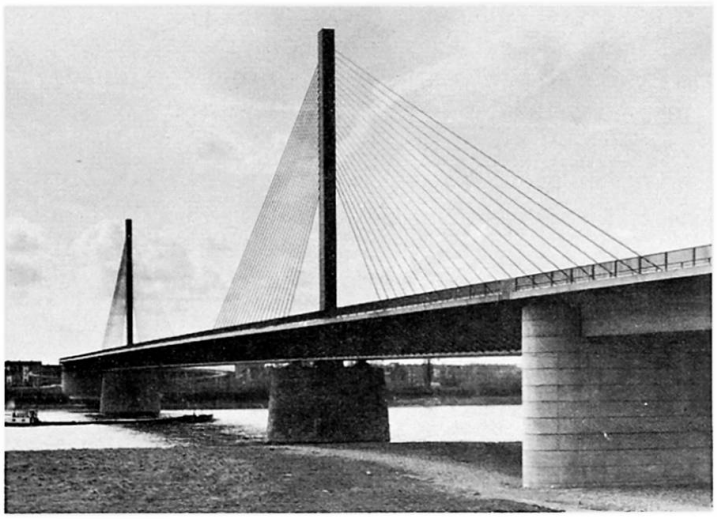

Bild 7: Friedrich-Ebert-Brücke über den Rhein in Bonn/Nord

Die Seiltragwände lassen sich in ein- oder zweihüftiger (symmetrischer) Bauweise ausführen, wobei die Seile in Büschel- oder Harfenform angeordnet werden können. Die einhüftige Ausführung erfordert zwar mehr Stahl, doch wird sie oft mit Rücksicht auf die vorgegebene Stellung der Pfeiler oder aber auch aus gestalterischen Gründen zu wählen sein.

Im allgemeinen werden die Seile im Pylonenkopf fest verankert; hierdurch wird eine große Steifigkeit des Systems erreicht. Die Seile können aber auch über Sattellager geführt werden. Die Entscheidung darüber, welche dieser beiden Konstruktionsarten vorzuziehen ist, hängt einmal von einem Wirtschaftlichkeitsvergleich ab, wird aber auch in starkem Maße von der ästhetischen Wirkung mitbestimmt.

Insgesamt stehen also eine Vielzahl von Variationsmöglichkeiten zur Verfügung, mit denen sowohl allen technischen Erfordernissen durch sachgemäße konstruktive Ausbildung wie auch allen Wünschen nach einer ansprechenden architektonischen Gestaltung Rechnung getragen werden kann.

3. Die Seile

In den vergangenen Jahren sind fast ausschließlich v e r s c h l o s s e n e S e i l e angewandt worden.

Diese haben gegenüber den aus Runddrähten zusammengesetzten Spiralseilen folgende Vorteile:

- Besserer Korrosionsschutz
- Größere Materialdichte (90% gegenüber 70% beim Normalseil)
- Höherer Elastizitätsmodul; dieser erreicht bereits nach wenigen Lastspielen im Verkehrslastbereich einen Wert von 1 700 Mp/cm^2. Das entspricht etwa dem Mittelwert der Elastizitätsmodulen, die für einfache Seile einerseits und normale Baustahlprofile andererseits gelten. Die für Umlenkungen notwendige Biegsamkeit bleibt bei verschlossenen Seilen trotz der hohen Steifigkeit aufgrund des spiralförmigen Aufbaues erhalten.
- Größere Unempfindlichkeit gegen Querpressung, weil sich die einzelnen Profildrahtlagen flächenhaft und nicht linienförmig wie bei normalen Seilen gegeneinander abstützen.

Nach der einschlägigen DIN-Vorschrift (Entwurf) dürfen verschlossene Seile mit 42% der rechnerischen Bruchlast beansprucht werden. Die Sicherheit, bezogen auf die wirkliche Bruchlast, die bis zu 8% unter die rechnerische Bruchlast sinken kann, beträgt dann wie bei Baustählen $\nu = 2{,}2$ während sich als Sicherheit gegenüber der technischen Streckgrenze der Wert $\nu = 1{,}5$ ergibt.

Aus zahlreichen Dauerschwingversuchen wurde deutlich, daß bei einer Oberlast von 35% der Bruchlast eine Schwingbreite von 1 500 kp/cm^2 und bei einer Unterlast von 0 kp/cm^2 eine Schwingbreite von 2 000 kp/cm^2 zugelassen werden kann.

Demzufolge gilt in der Bundesrepublik Deutschland folgendes:

- Für eine Oberspannung von 42% der rechnerischen Bruchlast ist eine Schwingbreite von 1 500 kp/cm^2, für die Ursprungfestigkeit eine solche von 2 000 kp/cm^2 zugelassen. Eine Zusammenstellung der auftretenden Seilkräfte bei einer repräsentativen Anzahl gebauter sowie geplanter Seilbrücken wie Hängebrücken, Zügelgurtbrücken und Schrägseilbrücken hat ergeben, daß mindestens 40% der rechnerischen Verkehrslast angesetzt werden können, ohne daß die Dauerfestigkeit für die Bemessung der Seilquerschnitte maßgebend wird.

- Eine zusätzliche Querpressung führt nicht zu einer Abminderung der Dauerfestigkeit verschlossener Seile, wenn die Größe der Querpressung auf 1 Mp/cm begrenzt wird bei Seilen, die direkt auf Stahl aufliegen, und auf 2,5 Mp/cm, wenn zwischen Seil und Stahl eine Weichmetalleinlage von mindestens 1 mm Dicke liegt.

Die Steifigkeit einer Schrägseilbrücke hängt ganz wesentlich von der Steifigkeit der Schrägseile ab.

Der Einfluß des Durchhanges auf den E-Modul wurde im Einführungsbericht behandelt.

Durch Zwischenunterstützungen oder Aufhängungen kann eine Änderung des Seildurchhanges sehr langer Seile verhindert werden. In diesem Falle können auch Schrägseilsysteme mit sehr großen Seillängen wirtschaftlich sein und für Hängebrücken eine echte Konkurrenz werden. Gestalterische Probleme, die durch derartige Hilfskonstruktionen entstehen, lassen sich befriedigend lösen; die Kräfte, die in diesen Hilfsseilen auftreten, betragen nämlich nur etwa 4% der Kräfte in den Hauptseilen, so daß die Durchmesser der Hilfsseile verhältnismäßig klein gehalten werden können.

Es ist jedoch m.E. sehr optimistisch anzunehmen, daß es auch mit Schrägseilbrücken möglich werden könnte, größte Spannweiten zu überbrücken. Diese werden vorerst den Hängebrücken vorbehalten bleiben, zumal beachtliche Schwierigkeiten bei der Montage im Freivorbau sowie aus der Druckbeanspruchung des Versteifungsträgers zu erwarten sind, für die sich gute Lösungen z.Zt. nur schwer finden lassen.

Eine weitere Möglichkeit wirtschaftlicher Anwendung von Schrägseilsystemen bietet sich bei der Verwendung von P a r a l l e l d r a h t b ü n d e l n . Die Vorteile parallel geführter Drähte sind folgende:

- Der E-Modul - ohne Berücksichtigung des Durchhanges - kann mit 2 000 Mp/cm^2 (gegenüber 1 700 Mp/cm^2) angesetzt werden.

- Die Dauerfestigkeitswerte liegen mit 2 000 Mp/cm^2 (gegenüber 1 500 Mp/cm^2) bzw. 2 500 Mp/cm^2 (gegenüber 2000 Mp/cm^2)

höher als bei Spiralseilen.

- Ein Unterschied zwischen wirklicher und rechnerischer Bruchlast ist kaum feststellbar.
  Die in Bearbeitung befindliche Vorschrift sieht daher vor, die zul. Spannung auf 45% der Nennfestigkeit festzusetzen, gegenüber 42% bei verschlossenen Seilen.

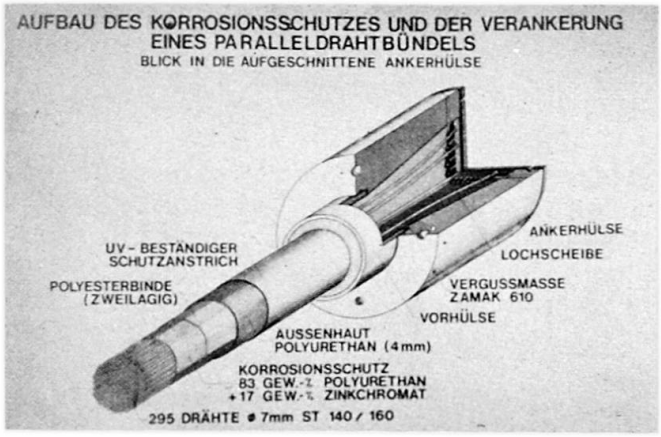

Bild 8: Beispiel für den Korrosionsschutz von Parallelseilen

Schwieriger gegenüber den verschlossenen Seilen sind jedoch der Korrosionsschutz sowie die Montage wegen der Empfindlichkeit gegen Biegung.

Neuartig sind Zugglieder in der Form b e t o n u m - m a n t e l t e r S p a n n s t a h l b ü n d e l , wie sie erst kürzlich erstmalig bei uns angewandt worden sind. Hier ist die Gefahr der Korrosion weitgehend gebannt, besonders dann, wenn das Spannstahlbündel durch eine Stahlhülse geschützt wird.

Bei der erwähnten erstmaligen Anwendung handelt es sich um eine seilverspannte Spannbeton-Brücke für kombinierten Eisenbahn- und Straßenverkehr. Die Seilbündel wurden an Ort und Stelle hergestellt, die Spannstähle für das Eigengewicht des Überbaues vorgespannt. Durch die nachträglich hergestellte Betonumhüllung wird ein Verbund zwischen den Spannstählen und der relativ stark dimensionierten Stahlhülse hergestellt. Gleichzeitig wird die Stahlhülse derart im Beton des Überbaues und des Pylonen verankert, daß alle weiteren Lasten nur noch über die nunmehr mittragende Stahlhülse in das Zugglied eingetragen werden. Dadurch wird erreicht, daß die Verkehrslasten vom gesamten Verbundquerschnitt des Seiles aufgenommen werden, während die einbetonierten Spannstähle zusätzlich das Eigengewicht der Konstruktion allein tragen.

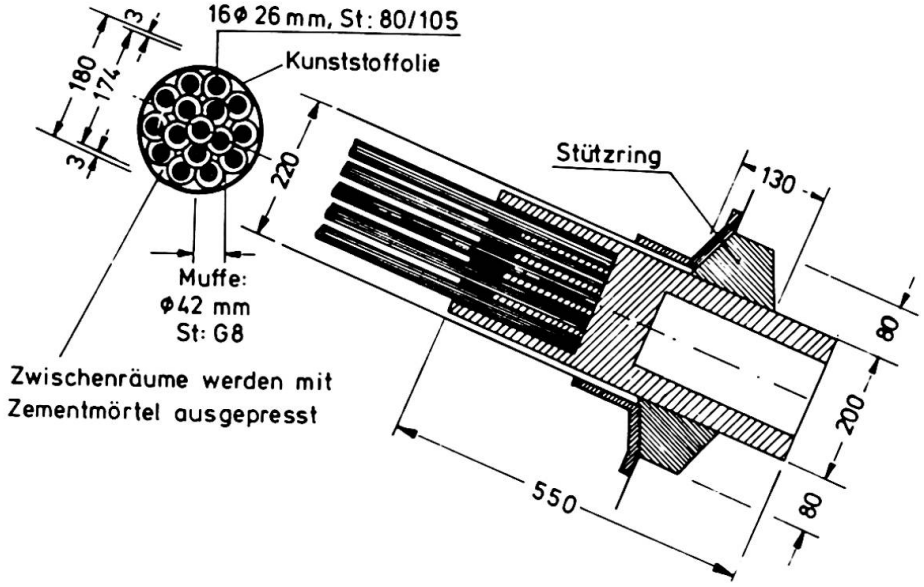

Bild 9: Betonummanteltes Spannstahlbündel

Da die Betonumhüllung von der allseits geschlossenen Stahlhülse geschützt wird, ist die Zugbeanspruchung des Betons im Hinblick auf den Korrosionsschutz der Spannstähle ohne Bedeutung. Die Einleitung der Verkehrslasten in den Verbundquerschnitt wurde durch Dauerschwingversuche geprüft. Es konnten hierbei keinerlei Schäden festgestellt werden. Allerdings muß mit Nachdruck darauf hingewiesen werden, daß es zwar schwierig, aber unbedingt erforderlich ist, den Spannstahl bis zur Fertigstellung der Betonumhüllung einwandfrei vor jedem Rost zu schützen. Daß es sich hierbei durchaus um längere Zeiträume handeln kann, läßt sich leider nicht ausschließen.

4. Seilkopfverguß

Im allgemeinen werden die Seilköpfe mit Feinzink (450° C) vergossen. Die Folge ist eine Abminderung der Dauerfestigkeit der Seile bzw. das Auftreten von Brüchen im oder in der Nähe des Seilkopfes. Um derartige Schäden zu vermeiden, haben wir beim Bau der Rheinbrücke Mannheim-Nord bei einigen Paralleldrahtbündeln erstmals einen Kaltverguß aus Stahlkugeln und einem Zinkstaub-Epoxydharzgemisch angewandt, wie er im Einleitungsbericht beschrieben ist.

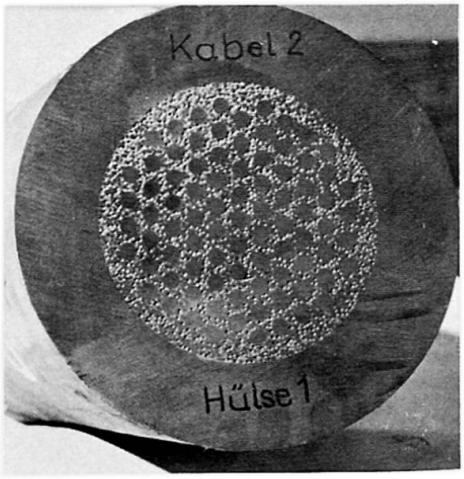

Bild 10: Querschnitt durch eine Ankerbrücke mit Kunststoff, Zinkstaub und Stahlkugeln

Warm- und Kaltverguß wurden in Laborversuchen einander gegenübergestellt.

Im Zerreißversuch wurden bei den warmvergossenen Seilköpfen im Mittel etwa 11 mm Schlupf, bei den kaltvergossenen Seilköpfen dagegen nur 2,5 mm gemessen.

Auch im Dauerschwing- und Dauerstandsversuch wurden bei Kaltverguß bessere Ergebnisse erzielt. Drahtbrüche wurden nicht festgestellt. Die während des Dauerschwingversuches gemessene Schlupfzunahme von 0,3 mm bis auf 1,0 mm ist praktisch unbedeutend.

Bei der Dauerstandsbelastung kam der Schlupf schon nach wenigen Tagen zum Stillstand, so daß der Kriechvorgang nur mit einem geringen und für die Sicherheit des Bauwerkes unbedeutenden Endkriechwert in Rechnung zu stellen ist.

Über die Alterungsbeständigkeit des Kunststoffvergusses kann aber leider zur Zeit noch nichts Endgültiges ausgesagt werden.

5. Seilschäden

Abschließend sei noch ein Hinweis auf Seilschäden gestattet.

Verschiedentlich festgestellte Brüche von verzinkten Profildrähten in den äußeren Lagen von verschlossenen Seilen gaben Anlaß, den Ursachen dieser Schäden nachzugehen. Wir waren der Meinung, daß diese Bruchschäden auf die elektrolytische Verzinkung zurückzuführen seien, da wir hier die meisten Ausfälle hatten.

Im Grunde ist der Bruch eines einzelnen Drahtes nicht besonders gefährlich, da das Seil im Abstand von etwa 2 bis 3 Schlaglängen bereits wieder seine volle Tragkraft hat. Zudem lassen sich Bruchstellen meist sehr einfach zusammenlöten.

Die gerissenen Drähte zeigten ungewöhnlich rauhe Kanten, von denen die Brüche ausgegangen waren, sowie eine krokodilhautartige, narbige Oberfläche. Diese beiden Erscheinungen können jedoch nicht als alleinige Ursachen für die Brüche betrachtet werden.

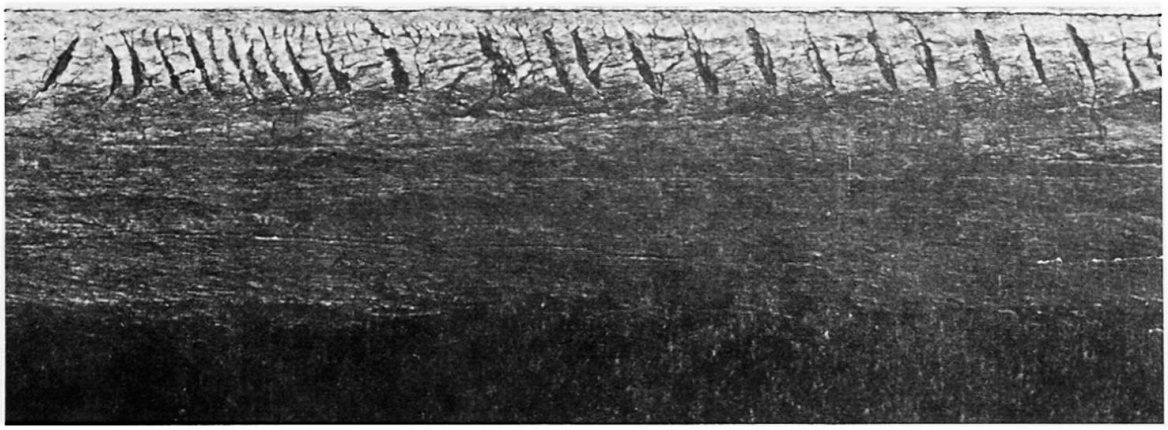

Bild 11: Verzinkter Draht mit örtlichen Aufreißungen

An der Drahtoberfläche wurden dann auch zusätzlich schräg verlaufende Zerreißungen festgestellt, die große Ähnlichkeit mit den in der Fachliteratur bereits beschriebenen Erscheinungen am Walzdraht haben. Ungewöhnlich aber ist, daß von diesen Zerreißungen fast senkrecht zur Drahtoberfläche verlaufende ausgezackte Risse ausgingen.

Diese charakteristischen Beobachtungen könnten darauf hinweisen, daß Wasserstoff bei der Bildung der Risse mitgewirkt hat. Auch die Tatsache, daß die Drahtbrüche erst nach dem Verseilen, z.T. erst auf der Baustelle, gefunden wurden, läßt darauf schließen, daß eine Beziehung zu den verzögerten Brüchen durch Wasserstoff besteht.

Zur Klärung dieser Fragen haben wir in verschiedenen Versuchen die mechanischen Eigenschaften und Dauerfestig-

keitswerte von blanken, galvanisch verzinkten und feuerverzinkten Profildrähten - jeweils gezogen und gewalzt - einander gegenübergestellt. Diese Versuche sind noch nicht abgeschlossen, so daß eine definitive Beurteilung derzeit noch nicht möglich ist.

Aus den bisherigen Untersuchungsergebnissen läßt sich jedoch folgendes schließen:

1.) Hinsichtlich der Dauerfestigkeit besteht kaum ein Unterschied zwischen den beiden Drahtsorten und Verzinkungsarten. Die Dauerhaftigkeit dürfte somit kaum ein Kriterium für die Bewertung sein.

2.) Unterschiede sind in der Biege- und Verwindungsfähigkeit vorhanden, die im wesentlichen von der Drahtsorte, weniger aber von der Verzinkungsart abhängen. Gezogene Stähle zeigten sowohl in blanker als auch in verzinkter Form Vorteile.

3.) Die Frage, ob die elektrolytische Verzinkung die Gefahr der Wasserstoffversprödung in sich birgt, ist noch nicht zu beantworten.

6. Zusammenfassung

Schrägseilbrücken haben in den letzten Jahren mehr und mehr Eingang im Brückenbau gefunden. Durch entsprechende konstruktive Maßnahmen gelingt es, große Spannweiten zu überbrücken.

Neben verschlossenen Seilen werden zukünftig auch Paralleldrahtbündel und betonummantelte Spannstahlbündel häufiger zur Ausführung kommen. Gleiches gilt für die kaltvergossenen Ankerköpfe. Besondere Sorgfalt ist weiterhin auf den Korrosionsschutz und die Seilschäden zu legen.